Thèse

présentée pour obtenir le grade de docteur

de l'École Nationale Supérieure des Télécommunications

Spécialité : Electronique et Communications

Irfan Ghauri

TRAITEMENT DU SIGNAL POUR LES SYSTÈMES D'ACCÈS MULTIPLE PAR RÉPARTITION EN CODES UTILISANT LA MÉTHODE DE SÉQUENCE DIRECTE

Soutenue le lundi 31 janvier 2000 devant le jury composé de

Claude Gueguen (ENST, Paris)	Président
Marc Moonen (K.U.Leuven, Belgium) Robert Vallet (ENST, Paris)	Rapporteurs
Pierre Comon (I3S, Sophia Antipolis) Giuseppe Caire (EURECOM)	Examinateurs
Dirk Slock (EURECOM)	Directeur de Thèse

École Nationale Supérieure des Télécommunications

Acknowledgments

I would like to express my profound gratitude towards Prof. Dirk Slock for having welcomed me to the Mobile Communications Department of Eurécom as a PhD student and having let me choose my area of research (I insisted) - an area which was not even his expertise at that point in time. It was days when in France very few groups were involved in research on CDMA receivers and I remember that we started our work amidst criticism that nothing original was possible any more in this area. It gives me great pleasure and satisfaction that Dirk and I managed to lay the foundation of what is now a large *CDMA* group at Eurécom, handling most signal processing aspects of CDMA communications. Even if, I at times was frustrated at the way research progressed, slowly and painstakingly, Dirk always kept faith and things picked up fast once we started seeing relationships between his existing work and our problem. Dirk was an absolute wizard at identifying these relationships and turned out to be an awesome PhD advisor. As I always maintain, the sad part of working for him is that one is almost sure of never ever meeting someone equipped with such an arsenal of mathematical prowess, research intuition, and general signal processing culture. Outside of work, he is a wonderful person and in him, over these years, I reckon to have made a good friend. I wish him continued success in his professional activities and all the happiness in his personal life.

I would like to acknowledge MOST's unfailing financial support during my first five french years. Thanks also to the *gang*. Due to them my stay in this lovely region was memorable with those great parties and *sortie*s all over the place. We sure did have our fill. When I landed in this region, Sandro Mazziotta and the Roselière crowd made my integration possible within the group. I am very thankful to them. I would also like to thank Karim Maouche for having been a reliable friend, and Raymond Knopp, Christian Blum, Neda Nikaein, Sergio Loureiro and David Tremouillac, to name a few, for a number of things ranging from those great mountain specials to interesting technical discussions and a couple of fireside drinks. My very special thanks go to Jean-Luc Dugelay, who, long ago, in a place far away, advised me to apply for a doctoral position at Eurécom, and to Prof. Pierre Humblet and Giuseppe Caire, who I worked for as a teaching assistant and who helped clear up many confusions in my head regarding technical matters. I'd also like to thank all others at Eurécom for their cooperation.

It was a great pleasure to work side by side (sometimes through white nights) with my friend and colleague Giuseppe Montalbano who always shared my enthusiasm for new ideas and with whom we managed to do very rewarding work on spatio-temporal downlink processing for CDMA systems. I am indebted to him for putting in a lot of effort in joint work which is included in this thesis as chapters V, VI and VII. My thoughts also go to Perrine Delacourt, among others, for having helped me with the french translations.

Finally and most importantly, it is to Fred that I owe a great deal for having stood by me through some of the toughest and the most trying times of my life, and to my parents who loved us so and made so many sacrifices for the future of their kids, among which this ultimate one, in the shape of bearing with my absence for these long years. It is to them that I dedicate this thesis.

Abstract

The last decade of twentieth century witnessed explosive growth in wireless cellular mobile and fixed systems, and the continuing interest in this area suggests that most future communication systems will be untethered networks. With the advent of digital wireless cellular systems like GSM and IS-95, the concept of reliable global coverage in nomadic communications has for the first time seemed possible. However, these systems were representatives of the second generation of wireless communications and the target market was voice. Even though the quality still leaves much to be desired, voice communication in cellular radio is already considered to be a second generation (2G) issue - solved, and thus a deployment issue, and of little interest in terms of future growth.

In today's wireless communication forums, experts therefore dare to speak of networks capable of handling high-speed data over mobile and wireless channels for multimedia applications. GSM is hoping to smoothly evolve a part of itself into EDGE, a new version, capable of handling higher (approaching 384 kb/s) data rates at the cost of mobility/coverage. GPRS, another variant, is the packet-switched service of GSM already at the brink of seeing its market debut. It is said to be capable of handling rates approaching 144 kb/s under low system loading conditions. Third generation systems like the Universal Mobile Telecommunication System (UMTS) or its North American counterpart, the CDMA-2000 are both aiming at rates approaching 2 megabits per second for cellular systems. It seems, however, that third generation (3G) systems will be based, to start with, upon a second generation backbone and the two will co-exist for long years before the natural death of the latter.

Lessons learned from 2G systems and attempts to develop high-rate versions of them, however, suggest that the network must be a hybrid structure. This is motivated by the fact that all rates and all applications are never required by all customers in all situations and communication scenarios. Consequently, a major core of any network will need to support voice and relatively low-rate data at all mobile speeds and locations, ensuring global reliable connectivity, with advanced services provided wherever and whenever the need arises. The third generation of wireless networks basically aims at the following target performances:

- Full coverage and mobility for 144 kb/s at first, and 384 kb/s later
- Limited coverage and mobility for 2 Mb/s
- High spectrum efficiency compared to 2G systems
- Higher flexibility to incorporate new services
- Backward compatibility to 2G systems

In order to satisfy some of these highly demanding requirements, a high performance physical layer needs to be designed, incorporating sophisticated signal processing techniques to mitigate the distortion

caused by radio propagation phenomena. For DS-CDMA systems which constitute the core multiple-access technology in future wireless systems, the traditionally used receiver technique is the RAKE receiver. This receiver is an anti-multipath device, but is known to operate in environments where the delay spread of the propagation channel is short relative to the symbol duration. Furthermore, strict power control needs to be exercised in order to keep the interference level down for the proper functioning of this receiver. If these conditions are not satisfied, when for example, transmission rates require the symbol duration to be short, thus resulting in a small processing gain, or when power cannot be controlled efficiently, more sophisticated interference cancelation algorithms need to be designed to either replace or supplement the RAKE receiver. This is the driving force behind the major portion of the work carried out in thesis where *advanced* receiver algorithms for multipath radio channels are proposed as alternatives to the traditionally used RAKE receiver.

A related and even more critical issue is that of parameter estimation which implies identification of channel parameters or its impulse response. Naturally, this estimate needs to be relatively accurate in order to build any reasonable receiver. This thesis also deals with channel identification issues and techniques through various methods. The usual method for channel identification is the use of known training data. Bandwidth efficiency lost to training data or pilot channels is another of the undesirable phenomenon in a system; to get around this problem, we propose *blind* methods (without the use of training information) for channel identification and also explore hybrid *semi-blind* channel identification and receiver algorithms.

A crucial observation pertaining to advanced receivers is that the interference canceling capability for a given receiver comes about due to *diversity* techniques, which refers to the reception of the signal through several independent channels. These channels can be created by employing one of the well-known methods e.g., fractional oversampling or several reception antennas. This issue is discussed in detail in this thesis and spatio-temporal interference cancelation schemes are presented for both the forward and reverse link problems. Emphasis is also laid on the of exploitation of side information in the problem, like training information, transmitter filter characteristics, structure of the channel, and the knowledge of spreading sequences of DS-CDMA users, in order to derive improved and low-complexity receivers. From the same motivation, the uplink and downlink problems are treated separately, since although the latter can be made to look like the former and handled in the same fashion, appreciable gains can be achieved by considering it from a different angle while exploiting the very particular structure of the forward link.

A new dimension where interference can be cancelled, and which has attracted much interest in recent years is the space dimension. Joint spatio-temporal signal processing techniques, also known in the literature as *smart antenna* processing, offer a significant advantage over pure beamforming strategy for forward link transmission. This is another area addressed in this thesis. We treat the problem of performing optimum spatio-temporal processing while using antenna arrays at the base-station for multiuser downlink transmission. The two transmission modes discussed are the Time-Division Duplex (TDD) and the Frequency-Division Duplex (FDD), in which varying degrees of information about the downlink channel is available at the base-station from the uplink channel estimate. It is this information that is exploited to design spatio-temporal filters at the base-station to attempt to separate users in space/time and to improve downlink performance while reducing mobile station complexity. The TDD and FDD problems are discussed separately and solutions are proposed for both. The effect of scrambling on the structure of the problem are also discussed and solutions for this case are also presented.

Résumé

Le récepteur RAKE est le récepteur traditionnellement utilisé dans les systèmes d'accès multiple par répartition en codes (AMRC) utilisant la méthode de séquence directe. Ce récepteur est un filtre adapté à la cascade du canal et à la séquence d'étalement de l'utilisateur considéré. C'est un appareil qui combine les différents trajets générés par le canal de propagation de façon cohérente et qui exploite ainsi la diversité des fréquences. Le récepteur considère les interférences créées par les utilisateurs concurrents comme du bruit non corrélé. Ceci est dû à l'étalement des symboles des différents utilisateurs par les séquences qui sont faiblement inter-corrélées. Par ailleurs, la quasi-orthogonalité des séquences d'étalement est détruite par le canal de propagation et par l'arrivée asynchrone des symboles des utilisateurs. Par conséquent, le contrôle de puissance est nécessaire au bon fonctionnement de ce récepteur et permet de diminuer les contributions d'interférences à la sortie du filtre adapté. La situation peut être encore aggravée lorsque les paramètres de transmission sont tels que le signal reçu est caractérisé par une importante interférence entre symboles. Dans le cadre de cette thèse, nous traitons le problème d'annulation d'interférences dans les systèmes AMRC et nous proposons comme alternative les récepteurs linéaires avancés.

L'annulation d'interférences est étudiée dans un contexte multi-voie. Ce contexte se présente par exemple lorsqu'on utilise plusieurs antennes à la réception ou lorsqu'on sur-échantillonne le signal reçu par rapport à la cadence des symboles transmis (fonctionnement normal des systèmes AMRC par séquences directes) ou par rapport à la cadence des bribes. L'identification aveugle d'un modèle multi-voie est désormais rendue possible grâce à l'exploitation des statistiques du second ordre portant sur la sortie vectorielle stationnaire d'un canal à entrées et sorties multiples (MIMO).

Nous proposons un récepteur linéaire à forçage à zéro, minimisant l'erreur quadratique moyenne (MMSE-ZF), pour annuler les interférences du point de vue de l'utilisateur considéré. Ce récepteur est adapté de manière aveugle et décentralisée. Il possède de plus l'avantage d'être résistant aux fortes puissances reçues en présence d'utilisateurs interférants. Nous démontrons qu'une estimation du canal de l'utilisateur considéré peut également être obtenue par cet algorithme. Cette estimation est relativement robuste à la sur-détermination de l'ordre du canal. Cependant, même si l'estimation est relativement bonne, la performance du récepteur reste insuffisante pour être utilisé dans la plupart des cas. Nous démontrons alors que les performances peuvent être améliorées en utilisant l'information apportée par la séquence d'apprentissage en conjonction avec l'information aveugle. On parle alors d'un algorithme semi-aveugle. Nous démontrons que dans un tel contexte, un nombre important d'utilisateurs interférants peut être supprimé grâce au grand nombre de degrés de liberté inhérents à la largeur de bande d'un tel système. Un récepteur aveugle linéaire maximisant le rapport signal-à-interférence-plus-bruit (RSIB) est aussi proposé pour le cas particulier de la liaison descendante dans les systèmes AMRC.

Enfin, nous nous intéressons aux performances de la liaison descendante lorsque des antennes adaptatives sont utilisées à la station de base. L'emploi de telles antennes permet un traitement spatio-

temporel conjoint qui présente un avantage significatif par rapport à la technique classique de formation de voies. Finalement, nous appliquons ce principe aux systèmes AMRC basés sur les modes duplex de division en fréquence (DDF) et duplex de division en temps (DDT).

Contents

List of Figures

Mathematical Notation

a	Variable scalar
$\boldsymbol{a}$	Variable vector
$\boldsymbol{A}$	Variable matrix
a	Constant scalar
a	Constant vector
A	Constant matrix
$a(t)$, $a(\tau)$	Continous-time function of the temporal variable t or τ
$a(n)$	Discrete-time function $a(n) = a(nT)$ for a given T
a_n	Discrete-time function $a_n = a(nT)$ for a given T
$A(z)$	z-transform of $a(n)$
$A(z_r)$	z-transform of $a(n/r)$ for integer r
$\boldsymbol{A}^\dagger(z) = \boldsymbol{A}^H(1/z^*)$	
$\boldsymbol{I}_m$	$m \times m$ dimensional identity matrix
$(\cdot)^*$	Complex conjugate
$(\cdot)^T$	Transpose
$(\cdot)^t$	Block transpose
$(\cdot)^H$	Hermitian transpose
$(\cdot)^+$	Moore-Penrose pseudo-inverse
$\otimes$	Kronecker product
$\odot$	Schur Hadamard product
$*$	Convolution product
$\|\cdot\|_p$	p norm
P_X	$\boldsymbol{X}(\boldsymbol{X}^H\boldsymbol{X})^{-1}\boldsymbol{X}^H$: Projection on the column space of $\boldsymbol{X}$
$P_X^\perp$	$\boldsymbol{I} - P_X$: Projection on the left null-space of $\boldsymbol{X}$
$\lambda_{\max}(\boldsymbol{A}, \boldsymbol{B})$	Maximum generalized eigenvalue of $(\boldsymbol{A}, \boldsymbol{B})$
$\lambda_{\min}(\boldsymbol{A}, \boldsymbol{B})$	Minimum generalized eigenvalue of $(\boldsymbol{A}, \boldsymbol{B})$
$V_{\max}(\boldsymbol{A}, \boldsymbol{B})$	Eigenvector associated to the maximum generalized eigenvalue of $(\boldsymbol{A}, \boldsymbol{B})$
$V_{\min}(\boldsymbol{A}, \boldsymbol{B})$	Eigenvector associated to the minimum generalized eigenvalue of $(\boldsymbol{A}, \boldsymbol{B})$
$\mathrm{E}\{\cdot\}$	Expectation operator
$\mathrm{tr}\{\cdot\}$	Trace operator
$\mathrm{cnst.}$	Constant
$\lceil x \rceil$	smallest integer $> x$
$\lfloor x \rfloor$	largest integer $< x$
$\triangleq$	By definition equals
δ_{ij}	Kronecker delta
$\ln(.)$	Natural logarithm

Acronyms and Abbreviations

AMRC	*Accès multiple par répartition en codes*
APS	Aperiodic Spreading Sequences
AWGN	Additive White Gaussian Noise
BER	Bit Error Rate
BFA	*Borne de filtre adapté*
BPSK	Binary Phase Shift Keying
CDF	Cumulative Density Function
CDMA	Code-Division Multiple Access
CW	Continuous Wave
DF	Decision Feedback
DML	Deterministic Maximum–Likelihood
DOA	Direction of Arrival
DS-CDMA	Direct-Sequence CDMA
EDGE	Enhanced Data-rates for GSM Evolution
FDD	Frequency-Division Duplex
FER	Frame Error Rate
GML	Gaussian Maximum–Likelihood
GPRS	General Packet Radio Service
GSC	Generalized Side-lobe Canceler
GSM	Global System for Mobile Communications
i.i.d.	independent & identically distributed
IAM	*Interférence accès multiples*
IC	Interference Canceler or Interference Cancelation
ICRR	Interference Canceling Rake Receiver
IES	*Interférence entre symboles*
IIR	Infinite Impulse Response
IIU	*Interférence entre utilisateurs*
INR	Interference-to-Noise Ratio
IS-95	Interim Standard-95
IPI	Inter-Path Interference
ISI	Inter-Symbol Interference
IUI	Inter-User Interference
LCMV	Linearly Constrained Minimum Variance
LF	Loading Fraction
LMS	Least Mean Squares

NLMS	Normalized LMS
LOS	Line of Sight
LPF	Low Pass Filter
LS	Least Squares
MAI	Multiple Access Interference
MFB	Matched Filter Bound
MIMO	Multi-Input Multi-Output
MLSE	Maximum-Likelihood Sequence Estimator or Estimation
MSE	Mean Square Error
MMSE	Minimum MSE
MOE	Minimum Output Energy
MRC	Maximum Ratio Combining or Combiner
MUD	Multiuser Detection or Detector
MVDR	Minimum Variance Distortionless Response
NMSE	Normalized MSE
OVSF	Orthogonal Variable Spreading Factor
PDF	Probability Density Function
PIC	Parallel Interference Cancelation
PCS	Personal Communications Services
PSS	Periodic Spreading Sequences
QPSK	Quarternary Phase Shift Keying
RMS (rms)	Root Mean Squared
RC	Raised Cosine
RRC	Root-Raised Cosine
RSB	*Rapport signal à bruit*
RSI	*Rapport signal à interférence*
RSIB	*Rapport signal à interférence plus bruit*
RX	Receiver
SDMA	Space-Division Multiple Access
SIC	Serial Interference Cancelation
SIMO	Single-Input Multi-Output
SINR	Signal-to-Interference plus Noise Ratio
SIR	Signal-to-Interference Ratio
SNR	Signal-to-Noise Ratio
SOS	Second-Order Statistics
SSMA	Spread-Spectrum Multiple Access
s.t.	subject to
SVD	Singular Value Decomposition
TDD	Time-Division Duplex
TDMA	Time-Division Multiple Access
TSLP	Two-Sided Linear Prediction
TS	Training Sequence(s)
TX	Transmitter
UMTS	Universal Mobile Telecommunication System
WMF	Whitened Matched Filter
WSS	Wide Sense Stationary
w.r.t	with respect to
ZF	Zero-Forcing

Chapter I

Introduction

I.1 Digital Mobile Cellular Communications

In digital cellular mobile radio, the problem of multiple access has received considerable attention in recent years. These ways of accessing the channel, namely FDMA (*Frequency Division Multiple Access*), TDMA (*Time Division Multiple Access*), and CDMA (*Code Division Multiple Access*) or SSMA (*Spread-Spectrum Multiple Access*) have been known for quite some time now [Rap96] and these methods or their combinations have been successfully used in the design of digital mobile radio systems to accommodate a given number of users. The goal of all these schemes is to split time, frequency, or the signal space into concurrent users by allocating them separate time slots, frequency slots, or distinct signature waveforms respectively. In practical systems, a combination of the above three multiple access schemes is usually employed (taken two at a time traditionally). An example is the European Global System for Mobile Communications (GSM) [ETS95] or the North American IS-54 standard that are both based upon a combination of FDMA and TDMA multiple access strategies. Another example, Qualcomm Inc.'s IS-95 [TIA93], is a direct-sequence (DS) CDMA based mobile cellular system, with users assigned distinct, psudorandom (PN) spreading sequences in an otherwise frequency split system. The goal is to make different user signals look as noise-like for each other as possible. Other methods of spreading spectrum like frequency-hopping (FH) CDMA [Pro95] never really became very popular for wireless systems. IS-95 was the first instance of a cellular wireless system based upon spread-spectrum technology, which was traditionally applied in military applications, carrying the great advantage of hiding the signal in background noise and rendering the probability of interception low.

Perhaps the foremost concern in the successful implementation of future cellular networks is *capacity*, and can be defined as the number of concurrent users that can be supported for a given total bandwidth. Consequently, a number of comparisons between the above multiple access methods have been carried out (e.g., [GJ$^+$91] [JBS93]) in recent years in order to establish the superiority of one over the other in terms of system capacity. However, no practical examples are available to make one believe that one system is better than the other. In terms of market success of second generation systems, GSM has had the better of the North American direct sequence CDMA based standard IS-95. The major reasons for its success however were a European will to invest in second generation of wireless communications and accords among system operators making the system coverage more global (roaming) and seamless in some sense, and thus of interest for the subscriber. What can be said of second generation systems is that they basically targeted the voice market (data being considered too high rate to handle in those days) and all customer level comparisons of the two second generation rival systems *vis-à vis* the voice quality are never actually a direct measure of the technical superiority of a system

for all other applications.

The comparisons dealing with other system issues, however, do show that a mobile cellular network employing DS-CDMA as the multiple access scheme would have its advantages. The hand-off[1], for example, in the existing mobile systems is known to be fragile since back and forth relaying between the two base stations and mobile is involved. The proposed CDMA systems get the better of this problem by maintaining contact to the two stations during hand-off until the mobile is sure of the proximity of one of them. This is called "soft hand-off".

Another statement frequently made is that performance of a CDMA network degrades relatively *gracefully* [PMS82] *vis-à-vis* the interference. A network splitting time and frequency among users can support no more than K users, if K time-frequency slots are available. A CDMA based network is said to have *soft capacity* in the sense that if a slightly degraded performance is tolerable during certain periods, more users can be supported.

Second generation systems had no direct handle on interference. Multiple access schemes tend to split-up the bandwidth among active users so that some sort of orthogonality is maintained, either in time and frequency (GSM) or in terms of the signal subspace spanned by user waveforms (DS-CDMA). Single user algorithms are then employed to estimate the parameters (channel impulse responses), and to detect the user of interest. However, the capacity of these systems is interference limited e.g., co-channel interference in GSM, and multiple access interference (MAI) in DS-CDMA systems. In TDMA/FDMA based systems, like the former, the problem is not so critical, since co-channel interference is kept to a minimum by using the technique of frequency planning, where the same frequency band is allocated to cells far apart from each other. Frequency re-use factors of 3 and 7 are common for GSM. In DS-CDMA based systems, there is no clear notion of cell boundaries, emanating from the frequency re-use factor of unity. Thus, interference needs to to kept down by employing strict power control. This situation arises, of course, when users' spreading sequences are non-orthogonal upon reception at the base-station, which usually is the case when user signals arrive with different delays, and when the propagation environment leads to multipath propagation [Rap96]. Nevertheless, spread-spectrum is traditionally a well known technique [Skl97] for multipath mitigation and the system performance may still be acceptable with single user detection techniques – such is the case in IS-95, and all the more the reason why third generation wireless communication systems like the UMTS are based upon CDMA technology [ETS97a, PO98] and the RAKE receiver as the standard reception technique. The RAKE receiver however operates under low loading fractions[2], and advanced techniques to reduce or cancel interference will need to be employed for increased data-rate applications or increased loading fractions.

I.2 Characterization of the Propagation Channel

There are three basic phenomena that influence radio propagation in wireless communication systems. These are

- *reflection*, which occurs when a propagating electromagnetic wave impinges on a smooth surface with a dimension several times larger than the wavelength (λ),
- *diffraction*, arising when a dense obstructing body of dimension larger than λ lies in the path between the transmitter and receiver; the electromagnetic wave rolls around the body and can

[1] transferring control to the closest base-station as mobile traverses cell boundaries
[2] defined as number of users per processing gain

reach the receiver even when there is no direct line-of-sight path, and

- *scattering*, which happens when the wave strikes a rough surface or a body whose dimensions are lesser than or of the order of λ, thus causing the reflected energy to scatter all over.

Depending upon the type of environment, i.e., urban, rural etc., one or several of these phenomena might occur. Therefore, channel models have been developed for particular environments [COS89] that take into account the effects of these mechanisms, and translate them to signal distortions like time-spreading and loss in signal-to-noise ratio (due to multipath components). The transmitted signal can therefore be considered to be passing through a channel which has a certain impulse response, so that the actual electromagnetics remain transparent to the systems engineer.

A further concern is the time-variations of the channels, in terms of the power arriving at the receiver, referred to as *fading*, and of which the two major types are as follows.

- *Large-scale* fading, defined as the average signal power attenuation due to motion over large areas, occurring due to major contours (hills, buildings etc.) between the transmitter and the receiver. The receiver is said to be shadowed by these imposing obstacles. Shadowing is statistically characterized as a log-normally distributed random variable. If P is the power transmitted to the kth mobile situated at a distance d_k from the base-station, then the received power is given by $P_{k,\mathrm{dB}} = P_{\mathrm{dB}} - L_{k,\mathrm{dB}}$; $L_{k,\mathrm{dB}} = L_k(d_0)_{\mathrm{dB}} + 10\log_{10}(\frac{d_k}{d_0})^n + G_\sigma$ where, G_σ denotes a zero-mean Gaussian random variable (in dB) with standard deviation, σ (also in dB, $\approx$6-10 dB). The large-scale fading mechanism is surroundings and distance dependent, i.e., even for vehicles moving at high speeds, the variation over time is rather slow. $L_k(d_0)_{\mathrm{dB}}$ is the free-space path-loss at a reference distance d_0 somewhere close to the transmitting antenna [Hat80]. Hence the estimate of the total path loss (in dB) including the mean path-loss (nth power loss with distance) and the variations about the mean accounting for shadowing, can be obtained. $n = 2$ for free space. It can be smaller in the presence of guided wave phenomenon in urban streets and larger when obstacles are present, e.g., when the mobile station is situated indoors.

- *Small-scale* fading manifests itself as rapid changes in amplitude and phase of the received signal. These variations are the result of a large number of multipath components with uniformly distributed phases adding up over time. When the received signal is composed of multiple reflected rays plus a significant line-of-sight (non-faded) component, the envelope amplitude due to small-scale fading has a Rician pdf. The fading in this instance is called *Rician fading*. As the amplitude of the non-faded component goes to zero, the Rician pdf approaches a Rayleigh pdf, given as [Rap96]

$$p(r) = \begin{cases} \dfrac{r}{\sigma^2} e^{-\frac{r^2}{2\sigma^2}} & \text{for } r \geq 0 \\ 0 & \text{otherwise} \end{cases} \tag{I.2.1}$$

  where, r is the envelope amplitude of the received signal, and $2\sigma^2$ is the mean power of the received signal. Rayleigh fading is considered to occur in most urban channels.

  The worst case variations can be of the order of 20-30 dB. Of course, these variations are carrier frequency dependent and their rapidity, for the system under consideration, depends upon the transmission rate and relative speeds (Doppler effect) of the transmitter and the mobile unit. The fading rapidity classifies channels as either *fast* or *slow* fading channels.

To sum up, a mobile moving over a large area receives signals that experience both types of fading; the resultant fading undergone can therefore be considered to be small-scale fading superimposed over large-scale fading.

I.2.1 Wide-Sense Stationary Uncorrelated Scattering (WSSUS) Model

The notion of WSSUS ([PZE+95] and references therein) stems from modeling the signal variations arriving with different delays as uncorrelated. It has been shown that such a channel is effectively WSS in both time and frequency domains. The model is very general, and is applicable to all frequencies and all time delays. There are four functions that make up the model, and serve as benchmarks for the characterization of a channel as seen by the signal propagating through it. These four functions [Skl97] are shown in fig. I.1. In the following, we shall examine these functions and shall discuss their impact on system design in terms of transmission parameters and receiver structure.

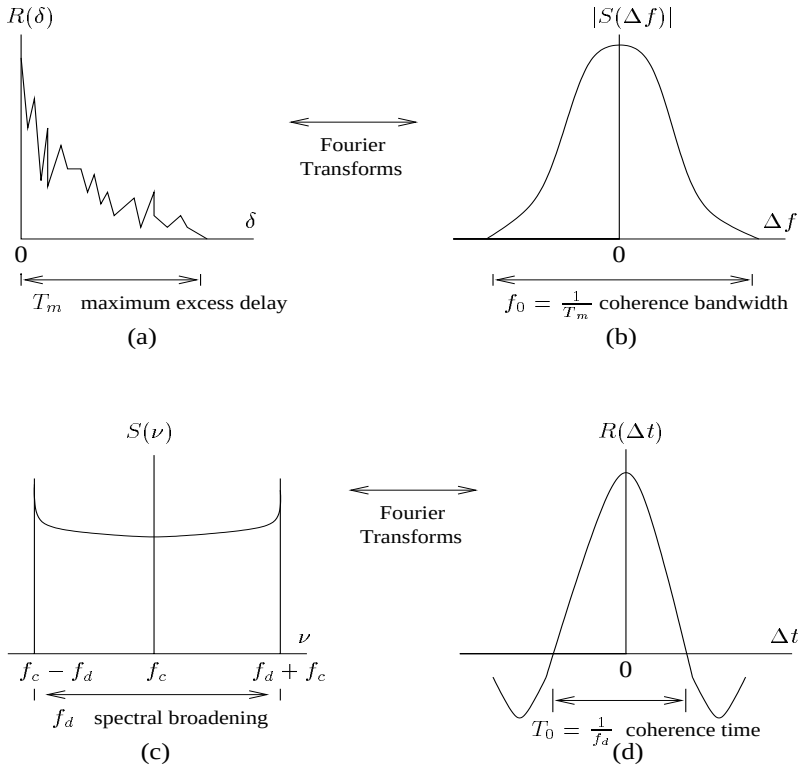

Figure I.1: (a) Multipath intensity profile, (b) spaced frequency correlation, (c) Doppler power spectrum, and (d) spaced-time correlation function of the channel.

I.2.1.1 Multipath Propagation

Fig. I.1a shows the multipath intensity profile $R(\delta)$ as a function of the delay, δ. Most wireless radio channels consist of multiple echoes (discrete paths). The multipath intensity profile defines the *maximum excess delay*, T_m, as the time elapsed between the first and the last (significant) received copies of the transmitted single impulse. For the most part, the last received copy would be selected by fixing some power threshold. A good measure for this threshold could be 10-20 dB below the strongest

component. Note that for an ideal system (with no multipath), $R(\delta)$ would be an ideal impulse with weight corresponding to the total average received signal power.

Let us denote by T, the symbol time of the transmitted signal. If $T_m > T$, the channel is said to exhibit *frequency selective fading*, thus inducing *intersymbol interference* (ISI) in the received signal. Note however, that the transmission pulse, which usually is a band-limited pulse, also induces some kind of ISI in the signal before transmission over the channel. However this is a system design parameter and can be undone at the receiver. The ISI introduced by the channel needs to be removed by the equalizer (channel equalization), for the purpose of which, the channel impulse response needs to be estimated.

On the contrary if $T_m < T$, the channel is referred to as *flat fading*. In this case all multipath components of a symbol arrive within the time duration of that symbol, and thus are unresolvable in time if symbol level resolution (sampling rate $\approx \frac{1}{T}$) is considered at the receiver. No equalization is required in this case. However, a loss in SNR can occur due to adding up of different multipath phasors destructively.

An alternative way of characterizing multipath propagation is to look at the spaced-frequency correlation function shown in fig. I.1b, which is the Fourier transform of $R(\delta)$. $|S(\Delta f)|$ represents the correlation between the channel's response to two signals as a function of the frequency difference between the two signals. It can be thought of as the channel's frequency transfer function. The coherence bandwidth, f_0, is a statistical measure of the range of frequencies over which the channel passes all spectral components with approximately equal gain and linear phase. Note that

$$f_o \approx \frac{1}{T_m}, \tag{I.2.2}$$

However, the approximation is not appropriate in statistical terms, since different channels with the same T_m can have very different profiles, $R(\delta)$, over the delay span. We can write the relation in a more apt manner as

$$f_o \approx \frac{1}{\gamma \sigma_\delta}, \tag{I.2.3}$$

where,

$$\sigma_\delta = \sqrt{\overline{\delta^2} - \bar{\delta}^2}, \tag{I.2.4}$$

is the RMS delay spread and $\bar{\delta}$ is the mean excess delay. $\bar{\delta}^2$ is the mean squared and $\overline{\delta^2}$ is the second moment of $R(\delta)$. Then, σ_δ is the square-root of the second moment of $R(\delta)$ [Rap96]. γ in (I.2.3) is a number which is actually based upon system requirements and measurements [Lee89], e.g., if coherence bandwidth is defined as the frequency interval over which the channel's complex frequency transfer function has a correlation of at least 0.9, then $\gamma = 50$. A more popular approximation of f_0, corresponding to a bandwidth interval having a correlation of at least 0.5, is $\gamma = 5$.

A channel is referred to as frequency-selective if $f_0 < \frac{1}{T} \approx W$, where the symbol rate, $1/T$ is nominally taken to be equal to the signal bandwidth W. Frequency-selective fading distortion occurs whenever a signal's spectral components are not all affected equally by the channel. Frequency-nonselective or flat fading degradation occurs whenever $f_0 > W$. Hence, all of the signal's spectral components will be affected by the channel in a similar manner. Flat-fading does not introduce channel-induced ISI distortion, but as previously stated, performance degradation can still be expected due to loss in SNR

whenever the signal is fading. In order to avoid channel-induced ISI distortion, the channel is required to exhibit flat fading by ensuring that

$$f_0 > W \approx \frac{1}{T}. \tag{I.2.5}$$

Hence, the channel coherence bandwidth f_0 sets an upper limit on the transmission rate that can be used without incorporating an equalizer in the receiver. To sum up, excess signal dispersion time and coherence bandwidth are the parameters that describe the channel's time-spreading properties.

A cellular mobile communication system like GSM with a signal bandwidth of 200 kHz. is an example where the channel coherence bandwidth is lesser than the signal bandwidth, or as viewed in the time domain $T_m > T$, leading to significant ISI. The GSM channel is therefore sufficiently frequency selective to require the use of an equalizer at the receiver [ETS95]. A Viterbi equalizer [For72] is used in GSM systems. In a typical DS-CDMA based system, like IS-95, on the other hand, $T_m \ll T$, and therefore no equalization is deemed necessary. The spread-spectrum signal bandwidth is approximately equal to $1/T_c$, where T_c is the chip duration; hence, the normalized coherence bandwidth $f_0 T_c$ of approximately unity implies that the coherence bandwidth is about equal to the spread-spectrum signal bandwidth. This describes a channel that can be called frequency-nonselective or very slightly frequency-selective. A RAKE receiver [PG58] [SOSL94] is employed to provide multipath diversity. We shall discuss the operation mechanism and particularities of the RAKE receiver for DS-CDMA systems in more detail in a subsequent section.

I.2.1.2 Time-Variance of the Channel

Multipath propagation is a phenomenon that characterizes the received signal in a fixed area. It does not offer information about the time-varying nature of the channel caused by relative motion between a transmitter and receiver, or by movement of objects within the channel. In practical mobile radio applications, the channel is time-variant because motion between the transmitter and receiver results in propagation path changes. Thus, for a transmitted continuous wave (CW) signal, as a result of such motion, the radio receiver sees variations in the signal's amplitude and phase. Assuming that all scatterers making up the channel are stationary, whenever motion ceases, the amplitude and phase of the received signal remains constant; that is, the channel appears to be time-invariant.

The WSSUS model describes equally well the time-variation of the channel in terms of transmitted signal parameters and relative motion of the transmitter and the receiver. For example, fig. I.1d shows the function $R(\Delta t)$, designated the spaced-time correlation function; it is the autocorrelation function of the channel's response to a sinusoid. This function specifies the extent to which there is correlation between the channel's response to a sinusoid sent at time t_1 and the response to a similar sinusoid sent at time t_2, where $\Delta t = t_2 - t_1$. The *coherence time*, T_0, is a measure of the expected time duration over which the channel's response is essentially invariant. Note that for an ideal time-invariant channel (e.g., a mobile radio exhibiting no motion at all), the channel's response would be highly correlated for all values of Δt, and $R(\Delta t)$ would be a constant function.

A completely analogous characterization of the time-variant nature of the channel can be given in the Doppler shift (frequency) domain. Fig. I.1c shows a Doppler power spectral density, $S(\nu)$, plotted as a function of Doppler-frequency shift, ν. Usually, the Doppler spectrum, for the case of the dense-scatterer model, a vertical receive antenna with constant azimuthal gain, a uniform distribution of signals arriving at all arrival angles throughout the range $(0, 2\pi)$, and an unmodulated CW signal, is

defined as [Rap96]

$$S_\nu = \frac{1}{\pi f_d \sqrt{1 - \left(\frac{\nu}{f_d}\right)^2}}. \tag{I.2.6}$$

A detailed description of the reasons for this bowl-shaped spectrum can be found in [Jak74]. The largest magnitude (infinite) of $S(\nu)$ occurs when the scatterer is directly ahead of the moving antenna platform or directly behind it. In that case the magnitude of the frequency shift is given by

$$f_d = \frac{V}{\lambda}, \tag{I.2.7}$$

where, V is relative velocity, and λ is the signal wavelength. It can be seen that f_d is positive when the transmitter and receiver move toward each other, and negative when moving away from each other.

Knowledge of $S(\nu)$ allows us to learn how much spectral broadening is imposed on the signal as a function of the rate of change in the channel state. The width of the Doppler power spectrum is referred to as the spectral broadening or Doppler spread, denoted by f_d, and is sometimes called the fading bandwidth of the channel. Note that the Doppler spread, f_d, and the coherence time, T_0, are reciprocally related (within a multiplicative constant). Therefore, we show the approximate relationship between the two parameters as

$$T_0 \approx \frac{1}{f_d}. \tag{I.2.8}$$

Hence, the Doppler spread f_d or $1/T_0$ is regarded as the typical fading rate of the channel. Like in the relationship between rms delay spread and coherence bandwidth, there is no strict relationship between the coherence time and Doppler bandwidth, unless one defines a measure; e.g., one may define channel time coherence of T_0 as the maximum time delay between the transmission of two sinusoids one after the other so that they have a correlation of β. Usually, for $\beta = 0.5$ [Skl97]

$$T_0 \approx \frac{9}{16\pi f_d}. \tag{I.2.9}$$

Other ways of defining T_0 also exist [Lee89]. The time-variant nature of the channel or fading rapidity mechanism can be viewed in terms of two degradation categories: *fast* fading and *slow* fading. The former is used to describe channels in which $T_0 < T$ ($1/T$ approximately equal to the signaling rate or bandwidth W), i.e., the fading rate is greater than the signaling rate. Fast fading describes a condition where the time duration in which the channel behaves in a correlated manner is short compared to the time duration of a symbol. Therefore, it can be expected that the fading character of the channel will change several times while a symbol is propagating, leading to distortion of the baseband pulse shape. Since the pulse shape is not known any longer, a matched filter at the receiver cannot be defined. Consequently, synchronization problems, among others, will arise.

A channel is generally referred to as introducing slow fading if $T_0 > T$ (signaling rate is greater than the fading rate). Here, the time duration during which the channel behaves in a correlated manner is long compared to the time duration of a transmitted symbol. Thus, one can expect the channel state to virtually remain unchanged during the time in which a symbol is transmitted, i.e.,

$$W > f_d, \qquad \text{or} \qquad T < T_0. \tag{I.2.10}$$

In section § I.2.1.1, it was indicated that due to signal dispersion, the coherence bandwidth, f_0, sets an upper limit on the signaling rate which can be used without suffering frequency-selective distortion. Similarly, (I.2.10) shows that due to Doppler spreading, the channel fading rate, f_d, sets a lower limit on the signaling rate that can be used without suffering fast fading distortion.

In the IS-95, the transmission rate is such that the symbol duration, T, is much smaller as compared to the coherence time, T_0 of the channel ($\approx 5ms.$ at 75 mph. for a mobile user at a carrier frequency of 900 MHz). The variations of the channel are therefore slow as compared to the symbol rate (typically of the order of 10 kilosymbols/sec.) and we can classify the fading process as slow fading. The fading rate of the channel gives a measure of how often power control needs to be exercised or how often the channel impulse response needs to be re-estimated (and the receiver adapted). In GSM, bursty communication is adopted and it is considered that the coherence time of the channel is longer than the burst duration. Training symbols are placed in the middle of the burst to have a good correlation of the estimated channel impulse response with the actual channel impulse responses for signal on both sides of the training sequence up to the edges.

In summary, practical systems avoid the pitfall of fast fading by having a reasonably high signaling rate satisfying (I.2.10). Other ways of combating fast fading are the use of error-correcting codes and interleaving [Rap96]. The effects of frequency selective fading can be mitigated by the use of equalization, or by spreading the signal over a sufficiently large bandwidth (DS/SS systems).

I.3 DS-CDMA Signal Model

Section § I.2 gives a fairly comprehensive description of the mobile radio channel, laying the groundwork for the assumptions and hypotheses put to work in the following part of this document. Unless otherwise stated, for the course of this work, we shall consider a slow fading frequency selective multipath channel, so that the channel coherence time is very long compared to the symbol duration. The multipath channel under consideration is described by a set of delayed echos [COS89]; the channel is therefore akin to a tapped-delay line, and can be considered finite-impulse response (FIR) for all practical purposes. If there are very few (significant) taps, and their exact positions w.r.t. some reference are known, then the channel will be referred to as a *sparse* channel.

I.3.1 Definitions, Notations, and Hypotheses

We shall start by setting up a few notations and hypotheses for the signal model that will be carried through this dissertation.

I.3.1.1 Equivalent Baseband Description of the DS-CDMA Signal

We denote by T, the common symbol duration, and T_c, the chip duration of the DS-CDMA signal. The ratio $P = \frac{T}{T_c}$ is known as the *processing gain*, *spreading factor* or bandwidth expansion factor in the literature [Vit95]. Let us consider that the kth user transmits a symbol sequence $\{a_k(n)\}$ belonging to a finite alphabet, Ω. The symbol sequences is first spread by the kth user's periodic[3] spreading sequence $c_k(p), \quad p \in \{1, \ldots, P-1\}$, and later scrambled by a *long* [TIA93] pseudo-noise (PN) sequence, $s_k(l)$. The *chips* of the spreader and the scrambler belong to a finite alphabet, Θ.

[3] periodic from symbol to symbol

We shall exclusively consider linear modulations [Pro95]. The case of some non-linear modulations has also been taken up [Tri99] by approximating them as linear modulations. The continuous-time baseband signal (or the complex envelope) at the output of the linear modulator can be written as

$$x_k(t) = \sum_{l=-\infty}^{+\infty} p(t - lT_c) b_k(l). \tag{I.3.1}$$

$p(t)$ is the pulse shaping filter, assumed to have strictly limited (one-sided) bandwidth, $W/2$ [Pro95], and is usually a raised cosine (RC), or a root-raised cosine (RRC) pulse. It is clear that W also is the effective bandwidth of the kth user's signal. In spread spectrum systems, $W \approx \frac{1}{T_c}$. The spread and scrambled chip sequence $b_k(l)$ is an *i.i.d.* sequence.

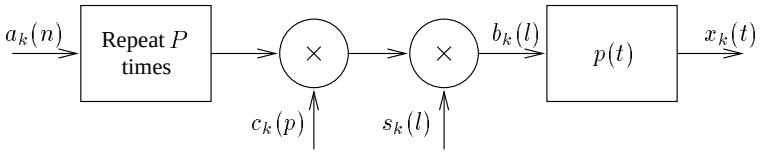

Figure I.2: Spread signal for kth user.

In the above model, the spread signal is referred to as *aperiodic* since the scrambler removes the periodicity introduced by the sequences $c_k(p)$. We can also write (I.3.1), in the absence of scrambler as

$$x_k(t) = \sum_{n=-\infty}^{+\infty} \psi_k(t - nT) a_k(n), \tag{I.3.2}$$

where,

$$\psi_k(t) = \sum_{i=0}^{P-1} p(t - iT_c) c_k(i), \tag{I.3.3}$$

is the spreading waveform for the kth user in the absence of scrambling. If the scrambler is active, then $\psi_k(t)$ can be replaced by $\psi_{k,n}(t)$ in (I.3.2) and (I.3.3) to express its dependence on the symbol index, n.

I.3.1.2 Multipath Channel

The propagation channel is characterized by a $K \times M$ matrix with elements, $\phi_{k,m}, \quad (1 \leq k \geq K;\ 1 \leq m \geq M)$, having K inputs (number of users) and M outputs (number of sensors or antennas at the receiver). This model is a linear model owing to the assumption that the principle of superposition of signals from different users holds in this case. As discussed in section I.2, the multipath propagation environment can be approximated by a small number of delayed and phase-shifted copies of the transmitted signal. Under these assumptions, the channel for the kth user, as seen from the mth sensor can be written as

$$\phi_{k,m}(t) = \sum_{q=0}^{Q-1} \delta(t - \tilde{\tau}_{q,km}) \widetilde{\phi}_{k,m}(q), \tag{I.3.4}$$

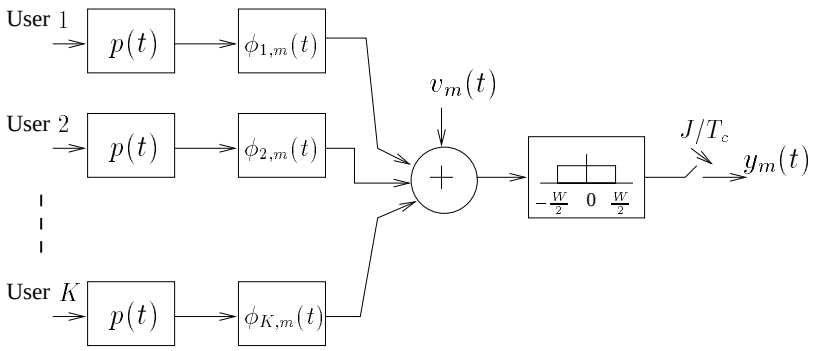

Figure I.3: Baseband signal model for the RX signal at mth sensor.

where, Q is the number of paths (assumed without loss of generality to be the same for all users), $\widetilde{\phi}_{k,m}(q)$ and $\tilde{\tau}_{q,km}$ are the qth path gain (complex) and delay for the kth user and the mth sensor respectively. The latter depends on the angle of arrival and the geometry of the antenna/sensor. The values of these delays depend on the propagation environment (rural, urban, etc.) [Rap96]. In a multiuser context, there will be a uniformly distributed mutual arrival delay between signals of different users, rendering them mutually asynchronous. We shall refer to this delay as τ_k, for the kth user with respect to some reference.

I.3.1.3 Reception Filter and Discrete Time Channel

Consider the signal model shown in fig. I.3. The causal low-pass filtered channel as seen from the mth sensor is

$$h_{k,m}(t) = \int_0^{\Delta T_c} p(t-\tau)\phi_{k,m}(\tau)d\tau, \tag{I.3.5}$$

where, $p(t)$ is the combined TX/RX filter[4](assumed to be the same for all K users), and $\phi_{k,m}(t)$ is the continuous time propagation channel impulse response between the kth user and the mth sensor given by (I.3.4). T_c denotes the chip period, and ΔT_c is the maximum duration of the $\phi_{k,m}(t)$, i.e., the delay spread of the propagation channel. Δ is a positive integer. The TX filter, $p(t)$ is a band-limited pulse shaping filter (e.g., a root-raised cosine, with an excess bandwidth α as shown in fig. I.4), while the RX is an anti-aliasing, ideal low-pass filter with a cut-off frequency corresponding to the sampling frequency, W. Hence, to satisfy the anti-aliasing condition imposed by the well-known sampling theorem [Vai93], the bandwidth W, of the low-pass RX filter can lie anywhere beyond $f_{\text{nq.}} = (1+\alpha)/T_c$, which is the Nyquist frequency, and corresponds to critically sampling the received signal to avoid aliasing.

Let us consider sampling at a rate W. The oversampled discrete representation for the overall channel can now be written as

$$h_{k,m}(t) = \sum_{l=0}^{L-1} p(t - \frac{l}{W})\phi_{k,m}(l). \tag{I.3.6}$$

[4]the RX filter is just an anti-aliasing low-pass filter, hence the convolution of the TX and RX filters is just the TX pulse-shaping filter

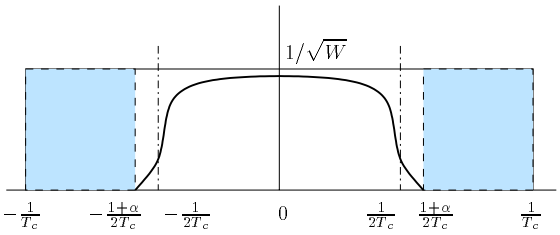

Figure I.4: RX filter with cut-off frequency $\frac{1}{T_c}$, and $\frac{1+\alpha}{2T_c}$.

The $\phi_{k,m}(l)$ are the discrete representation of $\phi_{k,m}(t)$, corresponding to a sampled version (at rate W) of an ideally low-pass filtered version of $\phi_{k,m}(t)$. It must be noted that in principle, if $W > f_{\text{nq.}}$ as shown in fig. I.4, the discrete time representation, $\phi_{k,m}(l)$, of the propagation channel is not unique. One can essentially add any signal to it that lies within the shaded portion (between $f_{\text{nq.}}$ and W) to alter the coefficients $\phi_{k,m}(l)$, since the components corresponding to those frequencies will be removed by the TX filter. This reflects the redundancy introduced in the sampled channel coefficients due to excessive oversampling. Alternatively, one can adjust the sampling frequency W to have the cut-off arbitrarily close to the TX pulse bandwidth. This can be achieved

- either by oversampling by a factor β and then downsampling by a factor γ, with $\beta > \gamma$, so that $\frac{\beta}{\gamma} \rightarrow 1+\alpha$ (this results in a uniformly sampled signal)
- or by non-uniform sampling, in the event of which one still needs to satisfy the following extension to the sampling theorem (see e.g. [Mar87])

Theorem 1
A signal with limited spectral support can be reconstructed from its non-uniform samples as long as the average sampling rate exceeds the Nyquist rate.

Furthermore, the representation of the overall channel in terms of sampled versions of TX/RX filter and the actual channel is justified by the following result.

Theorem 2
The sampled version of the convolution of two band-limited signals can be represented by the convolution of the sampled versions of the two signals, once the sampling rate equals or exceeds the Nyquist rate for at least one of the two signals.

It must be mentioned that in the instance of a sparse channel, as is the case of several mobile communication scenarios, only a few of the $\phi_{k,m}(l)$ are non-zero. The overall channel in (I.3.6) can now be sampled at any rate J/T_c to obtain

$$h_{k,m}(nT_c + j\frac{T_c}{J}) = \sum_{l=0}^{L-1} p(nT_c + j\frac{T_c}{J} - \frac{l}{W})\phi_{k,m}(l), \tag{I.3.7}$$

where, $j = 1, \cdots, J$, and $n = 0, 1, \cdots, \Psi$, where, $\Psi = \Delta + \Phi$, and Φ, the *effective* duration of the chip pulse shaping filter $p(t)$. The above equation can be written as

$$h_{k,m}(nT_c + j\frac{T_c}{J}) = \boldsymbol{p}_j^T(n)\overline{\boldsymbol{\phi}}_{k,m}, \tag{I.3.8}$$

and where,

$$\boldsymbol{p}_j(n) = \left[p(nT_c + j\frac{T_c}{J}), \ldots, p(nT_c + j\frac{T_c}{J} - \frac{L-1}{W})\right]^T,$$

and, $\overline{\boldsymbol{\phi}}_{k,m} = [\phi_{k,m}(0), \ldots, \phi_{k,m}(L-1)]^T$, where, L is the effective FIR length of the low-pass filtered and sampled channel impulse response.

Now, the overall chip-rate channel for the kth user and the mth sensor can be written as

$$\begin{aligned}\overline{\boldsymbol{h}}_{k,m} \triangleq \Big[&h_{k,m}(0), h_{k,m}(\tfrac{T_c}{J}), \ldots, h_{k,m}(\tfrac{(J-1)T_c}{J}),\\ &h_{k,m}(T_c), h_{k,m}(T_c + \tfrac{T_c}{J}), \ldots h_{k,m}(\Psi T_c + \tfrac{(J-1)T_c}{J})\Big]^T,\end{aligned} \tag{I.3.9}$$

and,

$$\overline{\boldsymbol{h}}_k \triangleq \left[\overline{\boldsymbol{h}}_{k,1}^T, \overline{\boldsymbol{h}}_{k,2}^T, \ldots, \overline{\boldsymbol{h}}_{k,M}^T\right]^T$$

is the $MJ\Psi \times 1$ overall channel vector as seen by the M sensors.

$$\widetilde{\boldsymbol{P}} = \left[\boldsymbol{p}_0(0), \boldsymbol{p}_1(0), \ldots, \boldsymbol{p}_{J-1}(0), \boldsymbol{p}_0(1), \ldots, \boldsymbol{p}_{J-1}(\Psi - 1)\right]^T \tag{I.3.10}$$

is the $J\Psi \times L$ pulse shaping matrix. We can now write the overall channel as

$$\overline{\boldsymbol{h}}_k = \left(\boldsymbol{I}_M \otimes \widetilde{\boldsymbol{P}}\right)\overline{\boldsymbol{\phi}}_k, \tag{I.3.11}$$

where, $\overline{\boldsymbol{\phi}}_k = \left[\overline{\boldsymbol{\phi}}_{k,1}^T, \ldots, \overline{\boldsymbol{\phi}}_{k,M}^T\right]^T$.

If the front-end low-pass filter (and thus the sampling rate W is known) along with the discrete path delays, $\tilde{\tau}_{q,km}$, then one can consider the substitution [CM99],

$$\overline{\boldsymbol{\phi}}_k = (\boldsymbol{I}_M \otimes \boldsymbol{\Pi})\,\bar{\widetilde{\boldsymbol{\phi}}}_k, \tag{I.3.12}$$

where, $\boldsymbol{\Pi}$ is a $L \times Q$ matrix of sampled sinc functions[5], corresponding to the front-end LPF at the M sensors, and $\bar{\widetilde{\boldsymbol{\phi}}}_k^T = [\widetilde{\boldsymbol{\phi}}_{k,1}, \ldots, \widetilde{\boldsymbol{\phi}}_{k,M}]$ is the $1 \times MQ$ vector of discrete paths of the propagation channel. We can write the overall channel as

$$\overline{\boldsymbol{h}}_k = \left(\boldsymbol{I}_M \otimes \widetilde{\boldsymbol{P}}\boldsymbol{\Pi}\right)\bar{\widetilde{\boldsymbol{\phi}}}_k. \tag{I.3.13}$$

Alternatively, one could write the overall channel vector as

$$\begin{aligned}\boldsymbol{h}_k \triangleq \Big[&h_{k,1}(0), h_{k,1}(\tfrac{T_c}{J}), \ldots, h_{k,1}(\tfrac{(J-1)T_c}{J}), h_{k,2}(0), h_{k,2}(\tfrac{T_c}{J}) \ldots, h_{k,M}(\tfrac{(J-1)T_c}{J}), h_{k,1}(T_c), \ldots,\\ &h_{k,1}(T_c + \tfrac{(J-1)T_c}{J}), \ldots, h_{k,M}(T_c), \ldots, h_{k,M}(T_c + \tfrac{(J-1)T_c}{J}), \ldots, h_{k,1}(\Psi T_c), \ldots, h_{k,M}(\Psi T_c + \tfrac{(J-1)T_c}{J})\Big]^T,\end{aligned}$$

in which case, we can write as

$$\boldsymbol{h}_k = \underline{\widetilde{\boldsymbol{P}}}\boldsymbol{\phi}_k, \tag{I.3.14}$$

[5] $\mathrm{sinc}(x) = \frac{\sin(\pi x)}{\pi x}$

where, $\boldsymbol{\phi}_k = \left[\boldsymbol{\phi}_k^T(1), \ldots, \boldsymbol{\phi}_k^T(L-1)\right]^T$, and $\boldsymbol{\phi}_k^T(i) = [\phi_{k,1}(i), \ldots \phi_{k,M}(i)]$, with $i \in \{0, 1, \ldots, L-1\}$, and

$$\underline{\widetilde{\boldsymbol{P}}} = \begin{bmatrix} \boldsymbol{I}_M \otimes \widetilde{\boldsymbol{P}}_{1:J} \\ \boldsymbol{I}_M \otimes \widetilde{\boldsymbol{P}}_{J+1:2J} \\ \vdots \\ \boldsymbol{I}_M \otimes \widetilde{\boldsymbol{P}}_{(\Psi-1)J+1:\Psi J} \end{bmatrix},$$

with $\widetilde{\boldsymbol{P}}_{1:j}$ representing rows 1 to j of the pulse shaping matrix, $\widetilde{\boldsymbol{P}}$. Note that $\boldsymbol{h}_k$ is just a permuted version of $\overline{\boldsymbol{h}}_k$. Including the sparseness in the channel, we can write as

$$\boldsymbol{h}_k = \underline{\widetilde{\boldsymbol{P}}}\, \underline{\boldsymbol{\Pi}} \widetilde{\boldsymbol{\phi}}_k, \tag{I.3.15}$$

where, $\underline{\boldsymbol{\Pi}}$ is an appropriately permuted version of $(\boldsymbol{I}_M \otimes \boldsymbol{\Pi})$, and the rearranged vector of discrete paths of the propagation channel is $\widetilde{\boldsymbol{\phi}}_k = [\widetilde{\phi}_{k,1}(0), \ldots, \widetilde{\phi}_{k,M}(0), \ldots, \widetilde{\phi}_{k,1}(Q-1), \ldots, \widetilde{\phi}_{k,M}(Q-1)]^T$.

The above model gives a complete description of the equivalent baseband, discrete time, chip-rate channel as seen by the receiver, including the TX/RX filters and the channel output sampling rate. It becomes clear from the above discussion, that the specular radio channel (a few echoes) will yield a different set of coefficients depending upon the ideal RX filter bandwidth, and thus the sampling rate. Similar treatment of the channel modeling problem has been introduced in [NCP]. There is also a definite link with the case of *canonical coordinates* as introduced in [SA99, OSV99], where the authors argue that the representation of the discrete-time channel up to infinite precision is not necessary and that a set of basis functions (canonical coordinates) suffice to represent the channel. Signal processing within this basis can be performed to build the desired receiver, ensuring avoidance of unnecessary complexity incurred by processing in inactive coordinates. Of course, the number of these basis functions does relate to precision, especially in numerical evaluations.

I.3.1.4 Diversity Reception

If the M sensors are located sufficiently far apart (mutually), we obtain M delayed and phase-shifted copies of the received signal, leading to spatial diversity. The case for $M = 2$ is shown in fig. I.5. Two physical diversity channels are thereby created. Alternatively, oversampling the signal received at each sensor with a rate $\frac{J}{T_c}$ also leads to artificially created diversity [Ung76]. This mechanism is depicted in fig. I.6 for the case of $J = 2$. The sub-channels $\boldsymbol{H}_1$ and $\boldsymbol{H}_2$ in this case are polyphase components of the oversampled channel [PRS97]. The model obtained by either of the two methods creates sub-channels and is thus referred to as *multichannel* model in the literature. Referring back to

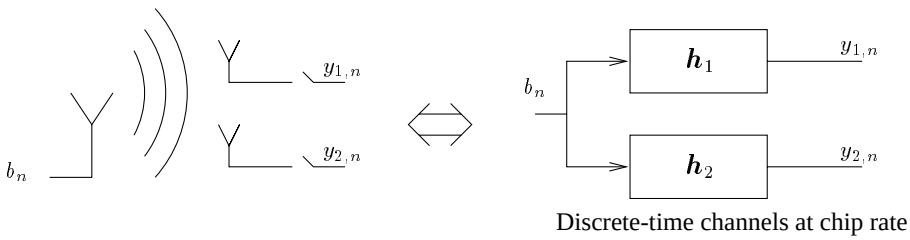

Figure I.5: Multiple sensor diversity at the receiver.

section I.3.1.3, let us suppose that the kth user's signal received at the mth antenna at time $nT_c + jT_c/J$

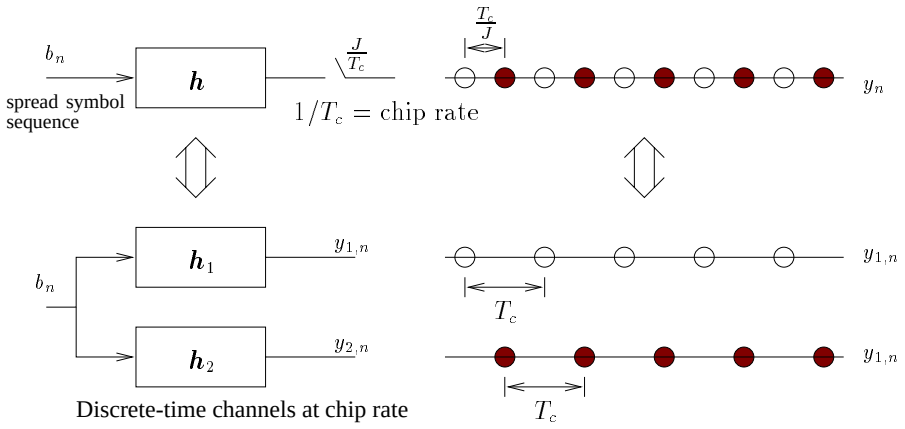

Figure I.6: Oversampling of the received signal.

is $y_{k,m}(nT_c + jT_c/J)$. Stacking together the oversampled signal in a vector we can write the nth instant received signal as

$$\boldsymbol{y}_{k,m}(n) = \left[y_{k,m}(nT_c), y_{k,m}(nT_c + \frac{T_c}{J}), \ldots\ldots, y_{k,m}(nT_c + (J-1)\frac{T_c}{J}) \right]^T . \tag{I.3.16}$$

Stacking together the samples on all M sensors, we have,

$$\boldsymbol{y}_k(n) = \left[\boldsymbol{y}_{k,1}^T(n), \boldsymbol{y}_{k,2}^T(n) \ldots\ldots, \boldsymbol{y}_{k,M}^T(n) \right]^T , \tag{I.3.17}$$

as the overall (diversity) signal for the kth user at the nth instant. As mentioned in [Slo93], there are limits to the oversampling factor, J, that can be employed in practical systems, for there may not be enough excess bandwidth in most cases to exceed $J = 2$.

Other forms of diversity also exist, namely polarization diversity, transmit diversity [Win98, ETS97a], and smarter methods where real and imaginary components of a real constellation (BPSK, for instance) are exploited to create virtual sub-channels [Tri99]. Unless stated otherwise, we shall stick to multiple sensors/oversampling at the receiver, during the course of this document.

I.3.1.5 Additive Channel Noise

The thermal noise, $v(t)$ is added at the sensors, at the front-end of the receiver. It is modeled as a white Gaussian circular random variable with zero mean and a variance of $\mathcal{N}_0$. If the sensors are more than $\lambda/2$ apart in space, where λ is the wavelength, then the noise can be considered as spatially white. The noise power will be equally distributed across the M sensors if they were identical. The spectrum of white noise is very large (theoretically infinite) and is considered flat over all finite signal bandwidths.

Most existing literature (see survey in [Mos96]) considers a chip-matched filter baseband front end, followed by chip-rate sampling without explicit timing reference. However, chip-rate sampling in the case of a band-limited TX pulse with non-zeros excess bandwidth, does not constitute sufficient statistics [Kay93] for detection purposes unless the exact timing epoch is available. The noise also gets colored at the output of the chip-matched filter. To get around these difficulties, we consider a low-pass front end, leading to a sampled version of noise that remains white.

Consider the case of one sensor, $M = 1$. $\frac{\mathcal{N}_0}{2}$ is the power spectral density of the real (or imaginary) part of the additive noise, $v(t)$. The RX filter, as stated in section I.3.1.4 is an ideal low-pass filter: $\Pi(t) = \frac{1}{\sqrt{W}}\mathrm{sinc}(tW)$. At the output of this filter, we shall have

$$v_o(t) = v(t) * \Pi(t) = \int_{-\infty}^{+\infty} \Pi(\tau) v(t-\tau) d\tau, \tag{I.3.18}$$

which will be sampled at instants $t = j\frac{T_c}{J}$, $j \in \mathbb{Z}$, leading to $v_o(j\frac{T_c}{J}) = \int_{-\infty}^{+\infty} \Pi(\tau) v(j\frac{T_c}{J} - \tau) d\tau$. Upon evaluation of the auto-correlation of the output noise [Tri99], we realize that the noise remains white but it is amplified by a factor of J: $\sigma^2_{vo} = J\mathcal{N}_0$.

I.3.2 Received Discrete Time Signal

Fig. I.7 shows the equivalent baseband received signal model. The K users are assumed to transmit linearly modulated signals over a linear multipath channel with additive Gaussian noise. It is assumed that the receiver employs M sensors to receive the mixture of signals from all users. The receiver front-end is an anti-aliasing low-pass filter. The continuous-time signal received at the mth sensor can

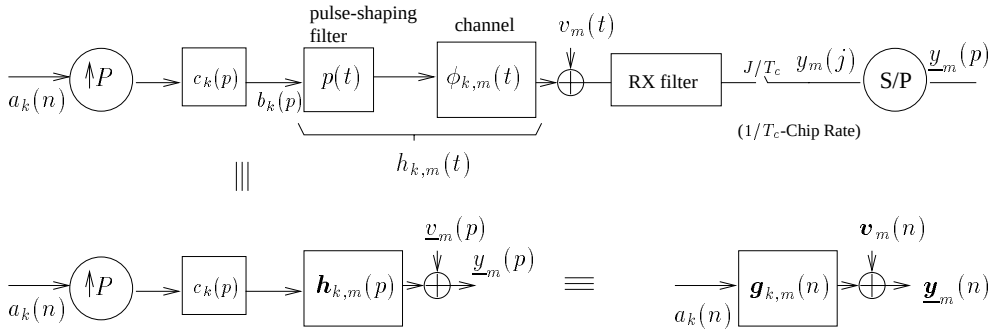

Figure I.7: Signal model in continuous and discrete time, showing only the contribution from one (kth) user.

be written in baseband notation as

$$y_m(t) = \sum_{k=1}^{K} \sum_{n} a_k(n) g_{k,m}(t - nT) + v_m(t), \tag{I.3.19}$$

where the $a_k(n)$ are the transmitted symbols from user k, T is the common symbol period, $g_{k,m}(t)$ is the overall channel impulse response (including the spreading sequence, and the transmit and receive filters) for the kth user's signal at the mth sensor, and $\{v_m(t)\}$ is the complex circularly symmetric AWGN with power spectral density $\mathcal{N}_0$. Assuming the $\{a_k(n)\}$ and $\{v_m(t)\}$ to be jointly wide-sense stationary, the process $\{y_m(t)\}$ is wide-sense cyclostationary with period T. The overall channel impulse response $g_{k,m}(t)$, is the convolution of the spreading code c_k and $h_{k,m}(t)$, itself the convolution of the chip pulse shape, the receiver filter, and the actual channel representing the multipath environment (see sections § I.3.1). This can be expressed as

$$g_{k,m}(t) = \sum_{p=0}^{P-1} c_k(p) h_{k,m}(t - pT_c), \tag{I.3.20}$$

where T_c is the chip duration. The symbol and chip periods are related through the processing gain, P: $T = PT_c$. S/P in fig I.7 denotes serial to parallel conversion (vectorization) with downsampling with factor J. Sampling the received signal at J (oversampling factor) times the chip rate, we obtain the wide-sense stationary $PJ \times 1$ vector signal $\underline{\boldsymbol{y}}_m(n)$ at the symbol rate. It is to be noted that the oversampling aspect (with respect to the symbol rate, $\frac{1}{T}$) is inherent to DS-CDMA systems by their very nature, due to the large (extra) bandwidth and the need to acquire chip-level resolution. This aspect directly translates into temporal diversity and explains the interference cancelation capability of these systems.

We consider the FIR channel, $\boldsymbol{h}_k$, between the kth user and all of the M sensors to be of length $\Psi_k T_c$. Let $n_k \in \{0, 1, \cdots P-1\}$ be the chip-delay index for the kth user: $\boldsymbol{h}_{k,m}(n_k)$ is the first non-zero $J \times 1$ chip-rate sample of $\boldsymbol{h}_{k,m}(p)$. Let us denote by N_k, the FIR duration of $g_{k,m}(t)$ in symbol periods. It is a function of Ψ_k, n_k, and P. We nominate the user 1 as the user of interest and assume that $n_1 = 0$ (synchronization to user 1). The symbol sequences for other users are relabeled (delayed or advanced), so that their relative delay with respect to user 1 falls in $[0, T)$.

Let $N = \sum_{k=1}^{K} N_k$. The vectorized oversampled signals at M sensors lead to a discrete-time $PMJ \times 1$ vector signal at the symbol rate that can be expressed as

$$\boldsymbol{y}(n) = \sum_{k=1}^{K} \sum_{i=0}^{N_k-1} \boldsymbol{g}_k(i) a_k(n-i) + \boldsymbol{v}(n) = \sum_{k=1}^{K} \boldsymbol{G}_{k,N_k} A_{k,N_k}(n) + \boldsymbol{v}(n) = \boldsymbol{G}_N \boldsymbol{A}_N(n) + \boldsymbol{v}(n), \tag{I.3.21}$$

where,
$$\boldsymbol{y}(n) = \begin{bmatrix} \boldsymbol{y}_1(n) \\ \vdots \\ \boldsymbol{y}_P(n) \end{bmatrix}, \boldsymbol{y}_p(n) = \begin{bmatrix} \boldsymbol{y}_{p,1}(n) \\ \vdots \\ \boldsymbol{y}_{p,M}(n) \end{bmatrix}, \boldsymbol{y}_{p,m}(n) = \begin{bmatrix} y_{p,1m}(n) \\ \vdots \\ y_{p,Jm}(n) \end{bmatrix}$$

$$\begin{aligned} \boldsymbol{G}_{k,N_k} &= [\boldsymbol{g}_k(N_k-1) \ldots \boldsymbol{g}_k(0)] \ , \boldsymbol{G}_N = [\boldsymbol{G}_{1,N_1} \ldots \boldsymbol{G}_{K,N_K}] \\ A_{k,N_k}(n) &= [a_k(n-N_k+1) \ldots a_k(n)]^T \ , \boldsymbol{A}_N(n) = \left[A_{1,N_1}^T(n) \ldots A_{K,N_K}^T(n)\right]^T, \end{aligned} \tag{I.3.22}$$

and the superscript ^{T} denotes transpose. For the user of interest (user 1), $\boldsymbol{g}_1(i) = (\boldsymbol{C}_1(i) \otimes I_{MJ})\, \boldsymbol{h}_1$, where, $\boldsymbol{h}_1$ is the $MJ\Psi_1 \times 1$ propagation channel vector given in (I.3.14) (I.3.14) and can be written as

$$\boldsymbol{h}_1 = \begin{bmatrix} \boldsymbol{h}_{1,1} \\ \vdots \\ \boldsymbol{h}_{1,\Psi_1} \end{bmatrix}, \boldsymbol{h}_{1,i} = \begin{bmatrix} \boldsymbol{h}_{1,i1} \\ \vdots \\ \boldsymbol{h}_{1,iM} \end{bmatrix}, \boldsymbol{h}_{1,im} = \begin{bmatrix} h_{1,im}(1) \\ \vdots \\ h_{1,im}(J) \end{bmatrix} \ ,$$

$\otimes$ denotes the Kronecker product, and the Toeplitz matrices $\boldsymbol{C}_1(i)$ are shown in fig. I.8, where the band consists of the spreading code $[c_0 \ \ldots \ c_{P-1}]^T$ shifted successively to the right and down by one position. For the interfering users, we have a similar setup except that owing to asynchrony, the band in fig. I.8 is shifted down n_k chip periods and is no longer coincident with the top left edge of the box. We denote by $\boldsymbol{C}_1$, the concatenation of the code matrices given above for user 1: $\boldsymbol{C}_1 = [\boldsymbol{C}_1^T(0) \ \ldots \ \boldsymbol{C}_1^T(N_1-1)]^T$.

From (I.3.14) and (I.3.15), we can see that $\boldsymbol{h}_1$ can be split up as a product of the pulse shaping filter, the RX filter and the actual discrete tap propagation channel. Then we can write as

$$\boldsymbol{g}_1(i) = \{\boldsymbol{C}_1(i) \otimes I_{MJ}\}\, \boldsymbol{h}_1 = \widetilde{\boldsymbol{C}}_1(i)\, \boldsymbol{\phi}_1 = \widetilde{\widetilde{\boldsymbol{C}}}_1(i)\, \widetilde{\boldsymbol{\phi}}_1, \tag{I.3.23}$$

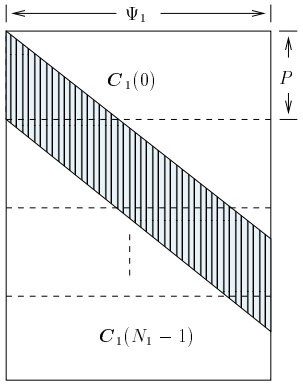

Figure I.8: The Code Convolution Matrix C_1.

where,

$$\widetilde{\boldsymbol{C}}_1(i) = \{\boldsymbol{C}_1(i) \otimes I_{MJ}\}\,\underline{\widetilde{\boldsymbol{P}}}, \quad \text{and,} \quad \widetilde{\widetilde{\boldsymbol{C}}}_1(i) = \{\boldsymbol{C}_1(i) \otimes I_{MJ}\}\,\underline{\widetilde{\boldsymbol{P}}}\,\underline{\boldsymbol{\Pi}}. \tag{I.3.24}$$

In all cases it will be assumed that $PMJ > K$, a condition which holds even if the loading fraction[6] exceeds 1.

I.3.2.1 Periodic Spreading Sequences and Frequency Domain Formulation

Usually two modes of transmission are considered in communication system, namely the *burst* mode, where packets are transmitted independently of each other[7], and the *continuous* mode, where adaptive receivers can be designed to track the slowly fading characteristics of the channel. If the packet size is very long, and the edge effects are negligible, the two modes can be considered equivalent in a time-invariant channel. This time-invariant, asymptotic scenario, with periodic spreading sequences allows us to formulate the problem in the frequency domain.

For the purpose of these developments, we introduce the delay operator, q^{-1} (corresponding to z^{-1} in the z-transform domain). Then, in the noiseless case ($v(t) \equiv 0$), we can write (I.3.21) as

$$\boldsymbol{y}(n) = \sum_{k=1}^{K} \mathbf{G}_k(q) a_k(n) = \sum_{k=1}^{K} \left(\sum_{i=0}^{N_k-1} \boldsymbol{g}_k(i) q^{-i} \right) a_k(n) = \sum_{k=1}^{K} \sum_{i=0}^{N_k-1} \boldsymbol{g}_k(i) a_k(n-i). \tag{I.3.25}$$

We can write the system model concisely in the frequency domain as a MIMO system with K inputs (users) and PMJ outputs. Considering $N_1 = N_2 = \ldots = N_K = N_c$,

$$\boldsymbol{y}(n) = \mathbf{G}(q)\,\boldsymbol{A}(n) + \boldsymbol{v}(n) = \sum_{i=0}^{N_c-1} \boldsymbol{g}(i)\,\boldsymbol{A}(n-i), \tag{I.3.26}$$

with, $\mathbf{G}(q) = \begin{bmatrix} \mathbf{G}_1(q) & \cdots & \mathbf{G}_K(q) \end{bmatrix}$, and $\boldsymbol{A}(n) = \begin{bmatrix} a_1(n) & \cdots & a_K(n) \end{bmatrix}^T$.

The power spectral density matrix of the above vector stationary process can be written as

$$\mathbf{S}_{\mathrm{yy}}(z) = \mathbf{G}(z)\mathbf{S}_{aa}(z)\mathbf{G}^{\dagger}(z) + \mathbf{S}_{\mathrm{vv}}(z). \tag{I.3.27}$$

Note that the signal part (contributions of K users) is low rank if $K < PMJ$.

[6] loading fraction is defined as, $\mathrm{LF} = \frac{K}{P}$

[7] most often in TDMA based systems to benefit from burst length duration $<$ coherence time

I.3.2.2 Cyclostationarity of the Received Signal

In the instance of a time-invariant channel and periodic spreading sequences (PSC), the received signal is cyclostationary at the symbol rate, i.e.,

$$\boldsymbol{R}_{yy}(n,\tau) = E\{\boldsymbol{y}(n)\boldsymbol{y}^H(n-\tau\} \tag{I.3.28}$$

is cyclic in n with period PMJ. Thus the $PMJ \times 1$, $\boldsymbol{y}(n)$ is a stationary vector signal. The model holds for both the periodic uplink and the downlink of a DS-CDMA based system.

On the contrary if aperiodic scrambling is active (see fig. I.2), so that symbol-to-symbol spreading is aperiodic, then the received signal is cyclostationary in n with period MJ. Chip-rate cyclostationarity of this kind holds for a single user's signal in the aperiodic downlink. However, if the scrambler is the same for all downlink users (cell dependent) [ETS97a], then the sum signal received at the mobile station is still symbol rate cyclostationary.

I.3.3 Structure of the ISI

Let us stack L successive $\boldsymbol{y}(n)$ vectors in a super vector

$$\boldsymbol{Y}_L(n) = \mathcal{T}_L(\boldsymbol{G}_N)\,\boldsymbol{A}_{N+K(L-1)}(n) + \boldsymbol{V}_L(n), \tag{I.3.29}$$

where,

$$\mathcal{T}_L(\boldsymbol{G}_N) = [\mathcal{T}_L(\boldsymbol{G}_{1,N_1}),\ \ldots\ ,\mathcal{T}_L(\boldsymbol{G}_{K,N_K})]\,,$$

and $\mathcal{T}_L(\boldsymbol{x})$ is a banded block Toeplitz matrix with L block rows and $\begin{bmatrix}\boldsymbol{x} & \boldsymbol{0}_{p\times(L-1)}\end{bmatrix}$ as first block row (p is the number of rows in $\boldsymbol{x}$), and $\boldsymbol{A}_{N+K(L-1)}(n)$ is the concatenation of user data vectors ordered as $[A^T_{1,N_1+L-1}(n), A^T_{2,N_2+L-1}(n),\ \ldots\ , A^T_{K,N_K+L-1}(n)]^T$. $\boldsymbol{V}_L(n)$ is the additive noise vector. We shall refer to $\mathcal{T}_L(\boldsymbol{G}_{k,N_k})$ as the *channel convolution matrix* for the kth user. Consider the noiseless received

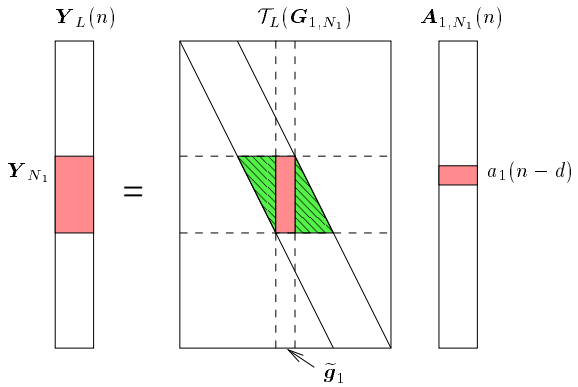

Figure I.9: ISI for the desired user.

signal shown in fig. I.9 for the contribution of user 1 (without loss of generality, the desired user). The desired symbol at the nth instant, $a_1(n-d)$, multiplies the column $\widetilde{\boldsymbol{g}}_1$ of the channel convolution matrix, $\mathcal{T}_L(\boldsymbol{G}_{1,N_1})$.

Due to the limited delay spread, the effect of a particular symbol, $a_1(n-d)$, influences N_1 symbol periods, rendering the channel a moving average (MA) process of order $N_1 - 1$ [Slo94b]. We are

interested in estimating the symbol $a_1(n-d)$ from the received data vector $\boldsymbol{Y}_L(n)$. One can notice that $a_1(n-d)$ appears in the portion $\boldsymbol{Y}_{N_1}$ of $\boldsymbol{Y}_L(n)$. The shaded triangles constitute the ISI, i.e., the effect of neighboring symbols on $\boldsymbol{Y}_{N_1}$. The contributions from the other (interfering) users to the received data vector have a similar structure. Note that to handle ISI and MAI, it may be advantageous to consider the longer received data vector $\boldsymbol{Y}_L(n)$.

I.4 Parameter Estimation in DS-CDMA

In this section we briefly review the channel (and therefore the receiver) identification problem in a historical perspective.

I.4.1 Training and Blind Philosophies

In order to determine a receiver structure, parameters like asynchronous delay, τ_k and the (multipath) channel impulse response $\boldsymbol{h}_k$ of the user in question needs to be obtained. Traditional single user channel estimation (and equalization) techniques were based on training, where the sender transmits a training sequence (TS) known at the receiver and which is used to estimate the channel coefficients or to directly estimate the equalizer. In GSM, for instance [Ste92], the data is organized and transmitted in bursts. Each normal burst contains a midamble training sequence used to estimate the channel, considered as time–invariant over the duration of a burst. In the single user in white noise case, least squares channels estimation corresponds to ML. However, TS based methods also carry a major disadvantage: including TS decreases bandwidth efficiency; in GSM, for example, 20% symbols of a burst are used for training. In multiuser scenarios, to make matters worse, single user least-squares estimation leads to a biased estimate. Joint LS is one solution to the multiuser case, for which users must operate (quasi-)synchronously.

The concept of *blind* equalization emerged with the work of Sato [Sat75]. The philosophy of blind estimation and equalization techniques is to estimate the channel or the equalizer based only on the received signal without any training symbols. Later, the introduction of multichannels, or SIMO models where a single input symbol stream is transmitted through multiple linear channels, gave birth to a new approach to blind estimation techniques: when the received signal is oversampled at a rate higher than the symbol rate, the resulting sampled signal is cyclostationary with the symbol rate. Gardner [Gar91], Tong, Xu and Kailath [TXK91] proved that, due to spectral redundancy properties, both the amplitude and the phase function of the channel can be identified from the Second–Order Statistics (SOS) of the data. This temporally oversampled model was shown to be equivalent to a spatially oversampled model where the signal is received through multiple sensors [TXK93].

In the multiuser context (MIMO model), however, channels can only be identified up to a mixture of users [Slo94b, Gor97]. The properties of this mixture depends on the relative lengths (orders) of the individual user channels. Consequently, other properties of the signal like the higher-order statistics need to be put to work to resolve this mixture. The general MIMO case in the SOS context is therefore a problem with no practical scope. In the DS-CDMA multiuser problem, however, we can estimate the channels of users from SOS up to a scalar phase factor as in the SIMO case [TX97a]. This issue will be discussed in more detail in subsequent chapters, notably chapter II, where we shall present a SOS based channel identification algorithm.

I.4.2 Channel Estimation by Training Sequences and Sparse Channels

Let us consider the problem of channel identification for K synchronous users in a DS-CDMA system by training chip sequences. Let us continue with the channel model developed in section § I.3.1.3, and consider the transmission of a chip sequence of length Ψ by the kth user written as

$$\boldsymbol{b}_k(n) = [b_k(n), b_k(n-1), \ldots, b_k(n-\Psi+1)]^T$$

is the chip sequence vector for the kth user at chip period n. Since $\Psi - 1$ is the overall delay spread including the effect of the TX/RX filter and the actual propagation channel $\phi_{k,m}(t)$, we need to consider a total of $N_{\rm ts}$ training chips per user, leading to $N = N_{\rm ts} - \Psi + 1$ chips of the known received signal. Stacking kth user's training chips in a $N \times \Psi$ Hankel matrix, $\boldsymbol{B}_k = [\boldsymbol{b}_k(\Psi), \boldsymbol{b}_k(\Psi+1), \ldots, \boldsymbol{b}_k(N_{\rm ts})]^T$, and assuming that all users have the same channel length, Δ, we can write the $MNJ \times 1$ discrete time received signal (sampled at rate J/T_c) corresponding to the training duration at the M sensors as

$$\boldsymbol{Y}_{\rm ts} = \{\boldsymbol{I}_M \otimes (\boldsymbol{B}_{\rm ts} \otimes \boldsymbol{I}_J)\}\,\overline{\boldsymbol{h}} + \boldsymbol{V}_{\rm ts} = \{\boldsymbol{I}_M \otimes (\boldsymbol{B}_{\rm ts} \otimes \boldsymbol{I}_J)\,\mathcal{P}\}\,\overline{\boldsymbol{\phi}} + \boldsymbol{V}_{\rm ts}, \tag{I.4.1}$$

where, $\boldsymbol{B}_{\rm ts} = [\boldsymbol{B}_1, \cdots, \boldsymbol{B}_K]$ is the $N \times K\Psi$ training chip sequence matrix, $\mathcal{P} = \boldsymbol{I}_K \otimes \widetilde{\boldsymbol{P}}$ is a $JK\Psi \times KL$ matrix, $\overline{\boldsymbol{\phi}} = \left[\overline{\boldsymbol{\phi}}_1^T, \cdots, \overline{\boldsymbol{\phi}}_K^T\right]^T$ is the $KLM \times 1$ concatenation of channel vectors of the K users, and $\overline{\boldsymbol{h}} = \{\boldsymbol{I}_M \otimes \mathcal{P}\}\,\overline{\boldsymbol{\phi}}$ is the $JKM\Psi \times 1$ overall channel vector for all K users and across all M sensors. Let us further denote $\boldsymbol{B}_{\rm ts} \otimes \boldsymbol{I}_J$ by $\mathcal{B}$ in order to simplify notation. $\boldsymbol{V}_{\rm ts}$ represents the vector of the additive white channel noise.

I.4.2.1 Structured Channel Estimation

Let $N_{\rm ts} \geq 2\Psi - 1$ be the number of training chips per user. The unstructured least-squares estimate of the multiuser channel $\overline{\boldsymbol{h}}$ can be obtained as the solution to the problem

$$\widehat{\overline{\boldsymbol{h}}} = \arg \min_{\overline{\boldsymbol{h}}} |\boldsymbol{Y}_{\rm ts} - (\boldsymbol{I}_M \otimes \mathcal{B})\,\overline{\boldsymbol{h}}|^2, \tag{I.4.2}$$

resulting in

$$\widehat{\overline{\boldsymbol{h}}} = \left\{(\boldsymbol{I}_M \otimes \mathcal{B})^H (\boldsymbol{I}_M \otimes \mathcal{B})\right\}^{-1} (\boldsymbol{I}_M \otimes \mathcal{B})^H \boldsymbol{Y}_{\rm ts}. \tag{I.4.3}$$

Alternatively, taking into account the structure of the problem in terms of the knowledge of the pulse shaping matrix $\widetilde{\boldsymbol{P}}$, we can obtain an estimate of the propagation channel as

$$\widehat{\overline{\boldsymbol{\phi}}} = \arg \min_{\tilde{c}} |\boldsymbol{Y}_{\rm ts} - (\boldsymbol{I}_M \otimes \mathcal{B}\mathcal{P})\,\overline{\boldsymbol{\phi}}|^2, \tag{I.4.4}$$

giving, as solution

$$\begin{aligned} \widehat{\overline{\boldsymbol{\phi}}} &= \left\{\boldsymbol{I}_M \otimes \left(\mathcal{P}^H \mathcal{B}^H \mathcal{B}\mathcal{P}\right)\right\}^{-1} (\boldsymbol{I}_M \otimes \mathcal{B}\mathcal{P})^H \boldsymbol{Y}_{\rm ts} \\ &= \left\{\boldsymbol{I}_M \otimes \left(\mathcal{P}^H \left(\boldsymbol{B}_{\rm ts}^H \boldsymbol{B}_{\rm ts} \otimes \boldsymbol{I}_J\right) \mathcal{P}\right)^{-1}\right\} (\boldsymbol{I}_M \otimes \mathcal{B}\mathcal{P})^H \boldsymbol{Y}_{\rm ts} \end{aligned} \tag{I.4.5}$$

Rank Deficiency in the Pulse Shaping Matrix :

As pointed out in [NCP97], if the sampling rate for the channel, i.e., W is large, then, so is L, the FIR length of the channel impulse response (fine temporal resolution). Under these conditions the pulse shaping matrix, $\mathcal{P}$ can be fat rather than tall, and $\mathcal{P}^H(\boldsymbol{B}_{\rm ts}^H\boldsymbol{B}_{\rm ts}\otimes\boldsymbol{I}_J)\mathcal{P}$ becomes rank deficient. The solution proposed in [NCP97] comprises of computing the SVD of $\widetilde{\boldsymbol{P}}$ as $\widetilde{\boldsymbol{P}}=\boldsymbol{U}\boldsymbol{\Sigma}\boldsymbol{V}^H$, where the $J\Psi\times q$ matrix $\boldsymbol{U}$ consists of the left orthonormal singular vectors, $\boldsymbol{\Sigma}$ is the diagonal matrix of q positive singular values, and $\boldsymbol{V}$ is the $q\times L$ matrix of right orthonormal singular vectors (q is the *effective* rank of $\widetilde{\boldsymbol{P}}$), and replacing $\mathcal{P}$ by $\widetilde{\boldsymbol{U}}$ (where, $\widetilde{\boldsymbol{U}}=\boldsymbol{I}_K\otimes\boldsymbol{U}$) in (I.4.5), whenever $\mathcal{P}$ is numerically ill-conditioned. The column span of $\boldsymbol{U}$ is the same as that of $\widetilde{\boldsymbol{P}}$. Therefore, we can write $\overline{\boldsymbol{h}}=(\boldsymbol{I}_M\otimes\mathcal{P})\overline{\boldsymbol{\phi}}=(\boldsymbol{I}_M\otimes\widetilde{\boldsymbol{U}})\widetilde{\boldsymbol{g}}$, where, $\widetilde{\boldsymbol{g}}=\left\{\boldsymbol{I}_M\otimes(\boldsymbol{I}_K\otimes\boldsymbol{\Sigma}\boldsymbol{V}^H)\right\}\overline{\boldsymbol{\phi}}$, resulting in

$$\widehat{\widetilde{\boldsymbol{g}}}=\left\{\boldsymbol{I}_M\otimes\left(\widetilde{\boldsymbol{U}}^H\left(\boldsymbol{B}_{\rm ts}^H\boldsymbol{B}_{\rm ts}\otimes\boldsymbol{I}_J\right)\widetilde{\boldsymbol{U}}\right)^{-1}\right\}\left(\boldsymbol{I}_M\otimes\mathcal{B}\widetilde{\boldsymbol{U}}\right)^H\boldsymbol{Y}_{\rm ts} \tag{I.4.6}$$

Fig. I.10 shows an example of the singular value spread of the matrix $\widetilde{\boldsymbol{P}}$, with a channel sampling rate of $W=2/T_c$, as shown in fig. I.4, with $J=2$ samples per chip, and a channel with $\Delta=24$, so that L is quite large. It can be seen that there is a large concentration of singular values at the two limits.

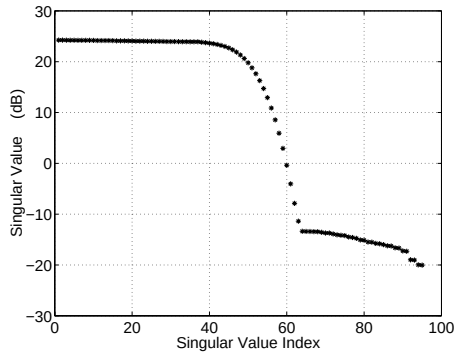

Figure I.10: Singular value distribution of $\widetilde{\boldsymbol{P}}$ with $W=2/T_c$.

However, there is no clear transition point in between (quite a few singular values are smeared out in the transition region), with the result that there is no clear selection criterion for q.

One more drawback of the above approach is that in the case of sparse channels, i.e., when very few of the $c_{k,m}(l)$ are non-zero, the SVD destroys the locality property in the matrix $\widetilde{\boldsymbol{P}}$, i.e., while each column of $\widetilde{\boldsymbol{P}}$ was associated with a particular $\phi_{k,m}(l)$ (of which very few are non-zero), the singular vectors in $\boldsymbol{U}$ are not, with the consequence that a certain delay contributes in all positions in addition to its own position. In other words, $\widetilde{\boldsymbol{P}}$ and $\mathcal{P}$ are banded (so that $\overline{\boldsymbol{h}}_k$ is sparse if $\overline{\boldsymbol{\phi}}_k$ is), while $\boldsymbol{U}$ is not. No gains can therefore be obtained if the channel is known to have a sparse rather than a full FIR impulse response.

Estimation of the Fractionally Sampled Channel :

Alternatively, W can be made to approach the Nyquist frequency, $f_{\rm nq.}$ as closely as possible (in one of the two ways as discussed above), in the event of which the $c_{k,m}(l)$ become unique and L is smaller than the case of integer sampling, i.e., $W=n/T_c$, $n=2,3,\ldots$. As mentioned before, sampling at $W=(1+\alpha)/T_c$, $\alpha=1/\sigma$, $\sigma=1,2,3,\ldots$ is realizable by non-uniform sampling, e.g., with an initial

sampling rate of $W_i = 2/T_c$, by taking all odd samples and one out of σ (periodically) of the even samples. As can be verified, the average sampling rate still satisfies the Nyquist rate, even though some of the temporal resolution is lost. Sparseness can now be integrated in the model as the deletion of the columns of $\mathcal{P}$ (corresponding to fractional down-sampling), that multiply the insignificant (nearly zero) elements in $\overline{\phi}$.

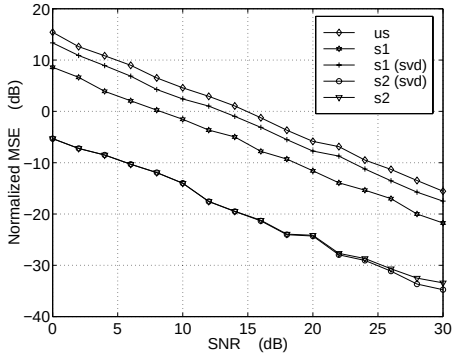

Figure I.11: Normalized mean square estimation error (MSE) for structured and unstructured channel estimation methods.

As an example, we consider $K = 16$ users in a quasi-synchronous system where the users are block synchronous with a timing misalignment of up to a quarter of a chip. This scenario corresponds to 100% loading ($K =$ processing gain) on the uplink of the TDD version of the UMTS proposal [ETS97b] for third generation cellular systems. The transmitted block is assumed to contain a mid-amble of $N_{\text{ts.}} = 256$ training chips. For the maximum channel lengths (ISI) presumed in the third generation systems, this number of training chips is insufficient to accommodate more than 8 uplink users. However, we consider scenarios where this number suffices for estimation of all K channels in the unstructured fashion. Fig. I.11 shows the normalized mean-square error (NMSE) of the channel estimation algorithms based upon SVD and the fractionally spaced sampling. us refers to unstructured, s_1 to the case where only the channel delay spread Δ is assumed to be known, and s_2 to the case where timing delays of the few physical multipath components, i.e., $\widetilde{\phi}_k$'s are known (estimated separately). As seen in this figure, there is no difference between the performance of the two s_2 methods, since the sparseness is taken into account by both SVD based and fractionally spaced methods. However, there is a significant performance gap between the two methods in the s_1 case when the channel is sampled at an integer rate ($W = 2/T_c$ here) followed by SVD, and the fractionally spaced sampling with sparseness exploited. Here, the TX pulse is a root-raised cosine with an excess bandwidth of $\alpha = 0.22$, and the sampling rate is $1.25/T_c$.

For the s_1 SVD based method, the ratio of the maximum singular value to the qth one is taken to be 30 dB. As stated above (fig. I.10), there is no clear selection criterion for q. Simulations show that there is a marked performance difference in setting the threshold to 10^2 as opposed to e.g., 35 dB, for which the NMSE essentially becomes the same level as for the unstructured case. The same phenomenon is observable if too few of the singular vectors constitute $\boldsymbol{U}$.

There is a slight flooring effect in all cases (understandably, more for the case of fractional sampling) due to numerical approximations, e.g., the fact that the pulse shaping matrix and the RX filter are both time-limited (and are hence only approximately band-limited).

I.4.3 Deterministic and Gaussian Data Models

Referring to the signal model described in section § I.3.2, we can consider ourselves to be in the deterministic framework [Kay93] if both input symbols and channel coefficients are assumed to be deterministic quantities. Consider the sample covariance matrix of the received signal $\boldsymbol{Y}_L$ (I.3.29), and its expected value (w.r.t. the noise only, as $\boldsymbol{A}$ is deterministic):

$$\boldsymbol{R}_{YY} = \mathcal{T}_L(G_N) \left[\sum_{n=0}^{M-L-1} A_L(n) A_L^H(n) \right] \mathcal{T}_L^H(\boldsymbol{G}_N) + \sigma_v^2 I, \tag{I.4.7}$$

where M is the length of the averaging window.

Deterministic methods are based on structural properties of the received signal and especially on the low–rank property of $\mathcal{T}(\boldsymbol{G}_N)$. For an irreducible channel [PRS97] and under certain conditions on the burst length and input symbols, the channel can indeed be determined uniquely (up to a scale factor) from the column space of $\mathcal{T}(\boldsymbol{G}_N)$, which is referred to as the *signal subspace* or from its orthogonal complement called the *noise subspace*.

In the Gaussian model, the input symbols are considered to be *i.i.d.* Gaussian random variables with mean 0 and variance σ_a^2. This model may appear inappropriate as the input symbols are in fact discrete-valued.

The purpose of the Gaussian model is to take into account first and second–order moments of the data, which appear to play a predominant role in the multichannel context. In the blind case, the mean is zero and the second–order moment is:

$$\boldsymbol{R}_{YY}(\theta) = \sigma_a^2 \mathcal{T}(\boldsymbol{G}_N) \mathcal{T}^H(\boldsymbol{G}_N) + \sigma_v^2 \boldsymbol{I}\,. \tag{I.4.8}$$

Unlike the deterministic case, the input symbols in the Gaussian model are no longer nuisance parameters for the estimation of $\boldsymbol{g}_1$. The parameters to be jointly estimated are the channel coefficients and the noise variance. The channel is identifiable up to a phase factor and Gaussian methods should be solved using a phase constraint.

Already existing blind methods which base channel estimation on the second–order moments of the data, and in which the input symbols are considered *i.i.d.* random variables, can be classified into the Gaussian category. The Gaussian distribution is the simplest distribution, leading to simple derivations and allowing to incorporate the first and second-order moments of the data: $\boldsymbol{Y} \sim \mathcal{N}(m_Y(\theta), R_{YY}(\theta))$, where θ is the parameter vector; the Gaussian hypothesis for the symbols leads to a Gaussian distribution for $\boldsymbol{Y}$.

I.4.3.1 Subspace Fitting Methods

The eigendecomposition of $\boldsymbol{R}_{YY}$ is:

$$\boldsymbol{R}_{YY} = V_{\mathcal{S}} \Lambda_{\mathcal{S}} V_{\mathcal{S}}^H + V_{\mathcal{N}} \Lambda_{\mathcal{N}} V_{\mathcal{N}}^H. \tag{I.4.9}$$

where the columns of $V_{\mathcal{S}}$ span the signal subspace and the columns of $V_{\mathcal{N}}$ the noise subspace, $\Lambda_{\mathcal{N}} = \sigma_v^2 I$. Let $\widehat{V}_{\mathcal{S}}$ et $\widehat{V}_{\mathcal{N}}$ be estimates of the signal and noise eigenvectors obtained from the sample covariance matrix.

The signal subspace fitting (SSF) tries to fit the column space of $\mathcal{T}_L(\boldsymbol{G}_N)$ to its estimates through the quadratic criterion:

$$\min_{\|h_1\|^2=1} \|P_{\widehat{\mathcal{V}}_N} \boldsymbol{C}_1 \boldsymbol{h}_1\|^2. \tag{I.4.10}$$

The criterion is quadratic in $\widetilde{\boldsymbol{g}}_1$, but the method require an eigendecomposition, which can be costly. Another variant of the subspace method called the noise subspace fitting (NSF) [AS97] is also frequently used.

Several other methods, like the sub-channel response matching SRM [AS97], which is also called Cross-Relation (CR) method [XLTK95], and is based on a linear parameterization of the noise subspace can also be employed to obtain the desired user's channel estimate. Note that in all these methods, distinction between user's channels is possible because of the partial knowledge and the distinctness of the desired user's spreading signature (pulse shape), which is not the case with usual multiuser scenarios (co-channel interfereres in TDMA systems all have the same TX/RX filters).

I.4.3.2 Blocking equalizers determined by linear prediction

A minimum parameterization $\overline{\boldsymbol{P}}$ of the noise subspace can be found in terms of prediction quantities [Slo94a, Slo94b, SP95]: $\overline{\boldsymbol{P}}$ can be obtained from the prediction filters or through the SRM-like criterion $\min_{\overline{P}} \|\mathcal{T}(\overline{\boldsymbol{P}})\boldsymbol{Y}\|^2$ with specific constraints on several coefficients of $\overline{\boldsymbol{P}}$ [dCDS98] [GS97]. The channel is then determined uniquely by the subspace fitting criterion: $\min_{\|h_1\|^2=1} \|\overline{\boldsymbol{P}}\boldsymbol{C}_1\boldsymbol{h}_1\|^2$.

I.4.3.3 Deterministic Maximum–Likelihood (DML)

Consider a signal user situation, $K = 1$, and suppress the subscripts k in (I.3.29). The DML criterion corresponds to the maximization of $f(\boldsymbol{Y}|\boldsymbol{g})$, the Gaussian conditional probability density function of the received data $\boldsymbol{Y}$, given the channel $\boldsymbol{g}$ in white noise, and can be reduced to the least-squares criterion

$$\min_{\boldsymbol{A},\|\boldsymbol{g}\|=1} \|\boldsymbol{Y} - \mathcal{T}(\boldsymbol{G}_N)\boldsymbol{A}\|^2 . \tag{I.4.11}$$

This criterion can be solved directly in this form by minimizing alternatively w.r.t. $\boldsymbol{A}$ and $\boldsymbol{g}$ [PD98].

Another way of solving (I.4.11) is to eliminate $\boldsymbol{A}$ (by minimizing w.r.t. $\boldsymbol{A}$ and substituting its expression in (I.4.11)) to get a DML criterion in $\boldsymbol{g}$:

$$\min_{\boldsymbol{g}} \boldsymbol{Y}^H P^{\perp}_{\mathcal{T}(\boldsymbol{G}_N)} \boldsymbol{Y} . \tag{I.4.12}$$

Computationally less intensive solutions to solve this criterion are based on a linear parameterization of the noise subspace. Using the parameterization $\mathbf{G}^{\perp}(z)$:

$$(I.4.12) \Rightarrow \min_{\boldsymbol{g}} \boldsymbol{Y}^H \mathcal{T}^H(\boldsymbol{g}^{\perp}) \left[\mathcal{T}(\boldsymbol{g}^{\perp})\mathcal{T}^H(\boldsymbol{g}^{\perp})\right]^{+} \mathcal{T}(\boldsymbol{g}^{\perp})\boldsymbol{Y} . \tag{I.4.13}$$

The Iterative Quadratic Maximum–Likelihood (IQML) method was proposed in [Hua96]: at each iteration, the denominator $\mathcal{T}(\boldsymbol{g}^{\perp})\mathcal{T}^H(\boldsymbol{g}^{\perp})$ is considered constant, evaluated from the previous iteration, so that the DML criterion becomes quadratic. In [Slo94a, dCS96], the IQML strategy was also proposed based on the blocking equalizers. At low SNR, IQML is biased and performs poorly: SRM used to

initialize IQML in [Hua96] performs in fact better at low SNR conditions. DML is the most powerful method among all the deterministic methods, as shown in [dC99]. This method however stays single user. Any multiuser parameterization of $\mathbf{G}^{\perp}(z)$ will necessarily require knowledge of channel parameters of all users from the previous iteration. The DML therefore stays rather impractical for the DS-CDMA problem and also for the general multiuser problem.

I.4.3.4 Gaussian Maximum–Likelihood

Again, we choose to stay in a single user case. As $\boldsymbol{Y} \sim \mathcal{N}(0, R_{YY}(\theta))$, the GML criterion is:

$$\min_{\theta=[\boldsymbol{g},\sigma_v^2]} \ln\det \boldsymbol{R}_{YY}(\theta) \; + \boldsymbol{Y}^H \boldsymbol{R}_{YY}^{-1}(\theta)\boldsymbol{Y} \; . \tag{I.4.14}$$

The Gaussian hypothesis is only used to build the GML criterion, which is solved using the true symbol distribution. A semi–blind ML method based on this model was proposed in [dC99] and shown to give better performance than ML based on the deterministic model. The Gaussian hypothesis for the sources is also well known in in antenna array processing and direction of arrival finding [VON95] and the associated ML is proven to give better performance than the deterministic ML methods [OVSN93]. It was essentially introduced to solve the problem of inconsistency of joint parameter estimation resulting from DML. Blind channel identification by GML was first introduced in [Bap96].

I.4.4 The Semi–Blind Idea

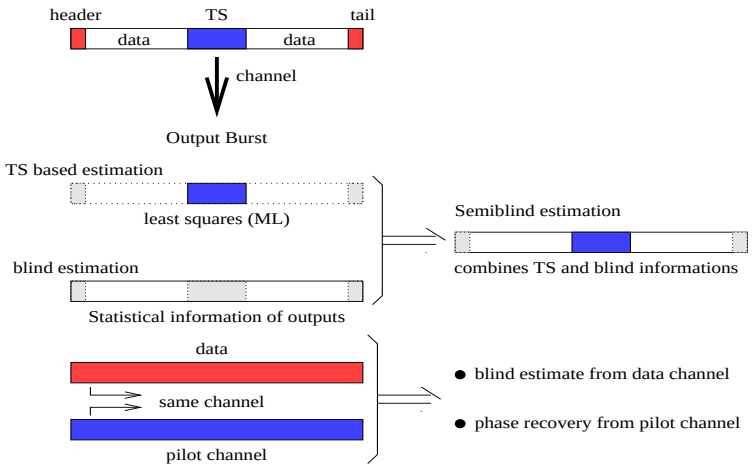

Figure I.12: Semi–Blind Principle: TS and pilot channels.

Recent work on single user blind channel identification [dC99] is based on the argument that these approaches suffers from lack of robustness in various scenarios like channel order over-estimation and proposes that SOS blind techniques should not be used alone but with some form of additional information. Likewise, TS based methods are also non-robust when the sequence is too short to estimate the channel impulse response. The use of *semi–blind* techniques is therefore advocated to get around these problems. We shall briefly describe the semi-blind idea in its raw form here while emphasizing that in the CDMA problems, blind channel identification is robust to a great degree. Receiver adaptation is however a different ball game [GS99a], and training information can be of utility to improve its estimation. This issue will be discussed in chapter III.

Assume that the data is transmitted either in burst mode or continuously. We assume that known symbols are present in the burst in the form of a training sequence aimed at estimating the channel or simply some known symbols used for synchronization or as guard intervals, like in the GSM or DECT burst. The continuous transmission has a parallel channel originating from the same source, like the downlink situation in IS-95, where mutually orthogonal codes are assigned to the pilot and the active users. In this latter case, it suffices to *search* over the time-field of interest, by correlating the received signal with the pilot sequence, for delayed multipath signals. As soon as delays are available, phases and amplitudes can be recovered by a correlation version of the LS approach. Note that the mechanism banks heavily on power control, and is called the *searcher* based or *correlation* based channel estimation.

Training sequence methods base the parameter estimation only on the received signal containing only known symbols, and all the other observations, containing (some) unknown symbols, are ignored. On the other hand, blind methods are based on the whole received signal, containing known and unknown symbols, possibly using hypotheses on the statistics of the input symbols, like the fact that they are *i.i.d.* for example. No training information is integrated in the criterion. The purpose of semi–blind methods is to combine both training sequence and blind information (see figure I.12).

In short, semi–blind techniques, because they incorporate the information of known symbols, can help avoid the possible pitfalls of blind methods (in whichever circumstances they occur). A thorough discussion of the use of semi-blind methods for channel identification is given in [dC99]. There, the problem was to improve the quality of channel estimate, or to identify channels otherwise non-identifiable. We shall emphasize that training data can be useful for a variety of operations depending upon the type of problem addressed [GS98a].

I.5 Matched Filter Bound, Signal-to-Interference-plus-Noise Ratio and Probability of Error

In the case of a single user in the AWGN channel, the probability of error depends on the SNR at the input of the decision device [Pro95]. For the case of a BPSK input symbol constellation, the probability of the error event, P_e, is proportional to

$$Q\left(\frac{d_{\min}}{2\sigma_v}\right), \tag{I.5.1}$$

where, $Q(x) = 1/\sqrt{2\pi}\int_x^{+\infty} e^{-\frac{x^2}{2}}dx$, is the so called Gaussian distribution tail function [Pap91] or the Q-function and is related to the complementary error function as $Q(x) = 0.5\,\mathrm{erfc}\{x/\sqrt{2}\}$, and σ_v^2 is the additive noise variance[8], and $d_{\min}$ is the minimum distance between the signal constellation points. In the literature [CGKS92], the square of the argument of the Q function is called the *Matched Filter Bound*.

$$\mathrm{MFB} \triangleq \frac{d_{\min}}{2\sigma_v}. \tag{I.5.2}$$

In the multichannel (multiuser) context with ISI and MAI, if we suppose that the contribution of all other symbols of all users, apart from symbol $a_1(n-d)$ has been removed (or does not exist) fig. I.9,

[8] $\frac{\mathcal{N}_0}{2}$ for real signals

then the error probability is given by

$$P_e = Q\left(\sqrt{\mathrm{MFB}}\right) = Q\left(\frac{\sigma_a \|\boldsymbol{G}_{1,N_1}\|}{\sigma_v}\right). \tag{I.5.3}$$

$\sigma^2\|\boldsymbol{G}_{1,N_1}\|_F^2$ defines all the energy transmitted by the ISI channel due to the isolated symbol, $a_1(n-d)$. A thorough treatment of the MFB is given in [Tri99].

Although the MFB represents a good performance measure, and corresponds to the performance of the joint optimal MLSE [For72, Ver86], we shall prefer to compare the performance of parameter estimators and the proposed interference cancelation schemes with their theoretical values. The reason for such treatment is that all algorithms presented in this document are based upon statistical information (second order statistics) of the received signal, and the major problem is to be able to estimate these statistics with finite amount of data.

Another notion is that of the signal-to-interference-plus-noise ratio (SINR) at the output of a receiver. The interference will be considered to include both ISI and MAI. We shall consider a single user receiver $\boldsymbol{f}$ applied to the received signal in (I.3.29). Considering the input symbols as *i.i.d.* zero-mean with variance σ_a^2, the output SINR of the receiver for the desired symbol is given as

$$\mathrm{SINR} = \frac{\sigma_a^2 \boldsymbol{f}\widetilde{\boldsymbol{g}}_1\widetilde{\boldsymbol{g}}_1^H\boldsymbol{f}^H}{\boldsymbol{f}\left(\boldsymbol{R}_{YY} - \sigma_a^2\widetilde{\boldsymbol{g}}_1\widetilde{\boldsymbol{g}}_1^H\right)\boldsymbol{f}^H}. \tag{I.5.4}$$

In this document, we basically concentrate on linear receivers for interference cancelation [Ver98]. Therefore, we shall look at the output SINR as the performance measure for these receivers, and the reference will be the optimal MMSE receiver of section § I.6.2.2(of a certain FIR length) [9].

An approximation to the BER is to evoke the steady-state Gaussian approximation which consists of modeling the residual interference plus noise at the output of the receiver as a Gaussian zero-mean random variable noise [Mil95, Cai99]. The non-Gaussianity of this residual term in the two user case is analyzed in [PV97]. Extension to more users is extremely difficult. Therefore in most cases, it is assumed that the Gaussian assumption holds leading to

$$P_e \approx Q\left(\sqrt{\mathrm{SINR}}\right). \tag{I.5.5}$$

I.6 Receiver Structures

DS-CDMA receivers can basically be classified into two types. We shall refer to these as *conventional* and *multiuser* receivers, thus adhering to the nomenclature in the existing literature [Ver98].

I.6.1 Conventional DS-CDMA Reception

For communications over an additive white Gaussian noise (AWGN) channel, and synchronous DS-CDMA users ($\tau_k = 0, \ \forall k$), transmission of mutually orthogonal spreading waveforms for the K users results in an orthogonal system like FDMA/TDMA.

$$\int_{-\infty}^{+\infty} \psi_j(t)\psi_k^*(t)dt = \begin{cases} 1, & \text{for} \quad j = k \\ 0, & \text{for} \quad j \neq k \end{cases}, \tag{I.6.1}$$

[9] optimal MMSE receiver is essentially IIR

The $\psi_k(t)$ are the unit energy (normalized) spreading waveforms given by (I.3.3). A conventional matched filter receiver, matched to the desired user's spreading waveform results in automatic interference rejection. This behavior of the matched filter persists irrespective of the powers of interferers due to the orthogonality of the modulation scheme. However, any diversion from this ideal system, e.g., choice of non-orthogonal spreading codes, deviation of the TX/RX filters from a Nyquist pulse, non-optimality of the RX timing, mutual asynchrony of users, multipath propagation, or a combination of these phenomena results in a non-zero interference term at the output of the matched filter.

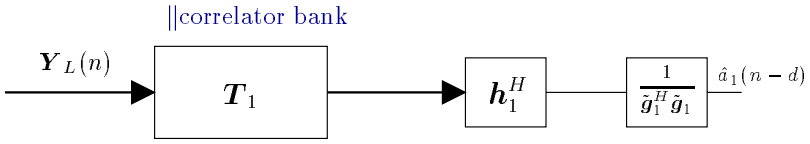

Figure I.13: Discrete time coherent RAKE receiver.

I.6.1.1 Frequency Diversity and the RAKE Receiver

The bandwidth $W \approx \frac{1}{T_c}$ of a CDMA signal is much greater than the coherence bandwidth f_0 of the channel. As discussed in section § I.2.1.1, such a signal will result in multipath components which are ideally considered to be independently fading. Considering that the time resolution of the receiver is T_c, for a multipath delay spread of T_m, we have $\frac{T_m}{T_c}$ resolvable signal components. Hence, the wideband spread signal results in frequency diversity of the order $\zeta \approx \frac{W}{f_0} \approx \frac{T_m}{T_c}$. Some of the multipath components may be zeros due to the sparse nature of the multipath channel [Rap96]. In this case the diversity order is not $\frac{T_m}{T_c}$ any longer but of the order of the number of non-zero components. The optimum receiver for processing the wideband signal (in the single user case) is the RAKE receiver invented by Price and Green in 1958 [PG58, Pro95], which is a matched filter, matched to the cascade of the spreading sequence and the propagation channel, thus combining the delayed multipath signals coherently.

In the multichannel discrete time context discussed in section § I.3.2, the RAKE receiver consists of a bank of correlators matched to the delayed multipath components given by $\boldsymbol{T}_1^H = \boldsymbol{C}_1 \otimes \boldsymbol{I}_{MJ}$, and the propagation channel, $\boldsymbol{h}_1$. Note that $\tilde{\boldsymbol{g}}_1 = \boldsymbol{T}_1^H \boldsymbol{h}_1$ (see fig. I.9).

I.6.1.2 The Near-Far Problem

In the multiuser context, the relative powers of interfering users have a significant impact on the interference term at the output of the matched filter, thus giving rise to the much dreaded *near-far* problem [Ver98]. When powers can be perfectly controlled [Vit95], then, under asynchronous conditions in an AWGN channel, the matched filter receiver is still an optimal decentralized receiver from the average signal to interference plus noise (SINR) maximization point of view, if aperiodic (noise-like) spreading sequences spread successive symbols of users. This behavior of the matched filter is explained by the nature of PN interference from other users (cyclostationary with chip period, hence stationary after chip rate sampling) which essentially acts much the same way as uncorrelated channel noise. Consequently, the performance might still be acceptable yielding a reasonable bit-error rate if the number of users is much lesser than the processing gain ($\mathrm{LF} < 1$, yielding far lower capacity than an orthogonal system). The noise-like nature of the interfering users persists at the RAKE output, but now, the phenomenon of dimensional crowding creeps in, since each interferer's delayed multipath component contributes as

an extra interference. Most studies like chapter IV and [DHZ95] (and references therein) show that the RAKE easily becomes interference limited for moderate loading fractions.

I.6.2 Multiuser Detection

The driving force, advocating the use of more sophisticated receivers for DS-CDMA systems, is the near-far problem associated with the RAKE receiver [Ver98]. The weaker signals from users lying on cell boundaries suffer the danger of being swamped out by nearer (stronger) users unless tight power control is exercised [Vit95]. Multiuser detectors propose to use some information on the MAI to improve performance. In this section, some of the most important multiuser detection schemes are briefly reviewed. We classify these multiuser receivers into the following two major classes depending upon their structure and the way MAI is treated, namely the *centralized* and *decentralized* receivers. A description of various multiuser detectors is given in [Slo99].

I.6.2.1 Centralized Multiuser Receivers

Also known as *joint* multiuser detectors, these receivers attempt to jointly decode all active users in the system. It is clear that the signal model (I.3.29) addresses a multiuser setup suitable for joint detection of all K users provided the timing information, $\tau_k, \quad k = 1, \ldots, K$ and spreading codes, $\boldsymbol{c}_k$ of all users are available.

First in line among near-far resistant multiuser detectors was the joint optimum MUD [Ver86] for asynchronous multiple-access Gaussian channels was presented. There is nothing magic about this detector. It is simply the multiuser version of the single user maximum likelihood sequence estimator [For72].

- ***The Optimum MUD***:

  Consider the flat channel (no multipath) version of the signal model depicted in (I.3.29). This refers to having $\boldsymbol{h}_k, \quad k = 1, \ldots, K$ scalars instead of vectors in (I.3.21). Furthermore, consider a grouping of symbols in the data vector, $\boldsymbol{A}_{N+K(L-1)}(n)$ in the order of increasing delay, e.g., $\tau_1 < \tau_2 \cdots < \tau_K$, instead of per user as shown in (I.3.29). We still consider a window (slot-length) of LT. With this reordering, $\mathcal{T}_L(\boldsymbol{G}_N)$ is *irregularly banded*. Then the maximum likelihood criterion, in white Gaussian noise, can be written as

$$\min_{A \in \Omega^{KL}} \|Y_L - \mathcal{T}_L(\boldsymbol{G}_N)\boldsymbol{A}\|^2 \leftrightarrow \min_{A \in \Omega^{KL}} \|\boldsymbol{U}^{-1}\mathcal{T}_L^H(\boldsymbol{G}_N)\boldsymbol{Y}_L - \boldsymbol{U}^H\boldsymbol{A}\|^2, \tag{I.6.2}$$

  where, $\mathcal{T}_L(\boldsymbol{G}_N)\mathcal{T}_L^H(\boldsymbol{G}_N)$ is the banded matrix with $K-1$ non-zero diagonals above and below the main diagonal, and $\mathcal{T}_L^H(\boldsymbol{G}_N)\mathcal{T}_L(\boldsymbol{G}_N) = \boldsymbol{U}\boldsymbol{U}^H$ is the Cholesky (triangular) factorization [GL89] with $\boldsymbol{U}$ upper triangular and banded with K non-zero diagonals.

  Note that $\mathcal{T}_L^H(\boldsymbol{G}_N)$ is simply the multichannel matched filter, $\boldsymbol{U}^{-1}$ the anti-causal noise-whitening filter, and thus, $\boldsymbol{U}^{-1}\mathcal{T}_L^H(\boldsymbol{G}_N)$ is a whitened matched filter.

$$\boldsymbol{U}^{-1}\mathcal{T}_L^H(\boldsymbol{G}_N)(\sigma_v^2\boldsymbol{I})\mathcal{T}_L(\boldsymbol{G}_N)\boldsymbol{U}^{-H} = \sigma_a^2\boldsymbol{U}^{-1}\mathcal{T}_L^H(\boldsymbol{G}_N)\mathcal{T}_L(\boldsymbol{G}_N)\boldsymbol{U}^{-H} = \sigma_a^2\boldsymbol{I}. \tag{I.6.3}$$

  $\boldsymbol{U}^H$ represents causal filtering with a filter of memory $K-1$. The MLSE can be implemented as a Viterbi algorithm [For73] with the number of states equaling $|\Omega|^{K-1}$. In the case of delay spread, more states will be required (larger memory).

- ***Suboptimal MUD***:

  Unfortunately, the Viterbi algorithm for multiuser MLSE in the optimum MUD has a complexity that is exponential in K, the number of users (even more if channels have memory). Various sub-optimal multiuser detectors have therefore been proposed that provide a trade-off between receiver performance and complexity, among them *linear* multiuser detectors [LV89, LV90, MH94, XRS90, CR94], and *non-linear* (DF or multistage) ones [DH93, VA90, VA91]. We shall briefly review some of these techniques in the following.

  – *Joint RAKE Outputs*:

  The centralized (joint) RAKE receiver $\mathbf{G}^\dagger(q)$ takes decisions on

  $$\boldsymbol{x}(n) = \mathbf{G}^\dagger(q)\boldsymbol{y}(n) = \mathbf{G}^\dagger(q)\mathbf{G}(q)\boldsymbol{A}(n) + \mathbf{G}^\dagger(q)\boldsymbol{v}(n). \tag{I.6.4}$$

  $\mathbf{G}^\dagger(q)\mathbf{G}(q)$ is a square matrix with diagonal elements corresponding to signal energies if $\sigma_a^2 = 1$. The off diagonal elements are non-zero and correspond to the MAI. If $\mathbf{S}_{\rm vv} = \sigma_v^2\boldsymbol{I}$, then the RAKE corresponds to optimal preprocessing for all MUD, since it projects the received signal on the signal subspace. As shown in the following, all linear MUD start with the RAKE.

  – *Zero-Forcing Linear Detector*:

  The ZF MUD is analogous to a ZF linear equalizer of the single user case [Slo94c]. In the multiuser case, it is a MIMO equalizer and obtains a linear estimate of the transmitted symbols as

  $$\widehat{A}(n) = \mathbf{F}^\dagger(q)\boldsymbol{y}(n), \tag{I.6.5}$$

  with, $\mathbf{F}(z)\mathbf{G}(z) = \boldsymbol{I}_K$.

  The ZF MUD is not unique. However, one of these receivers is the one that gives the minimal noise enhancement, and is known as the *decorrelating* detector derived in [LV89] and [LV90]. In these works, however, the authors derive the decorrelator directly without mentioning the non-uniqueness aspect. The decorrelating detector's output is given by

  $$\widehat{A}(n) = \left(\mathbf{G}^\dagger(q)\mathbf{G}(q)\right)^{-1}\boldsymbol{x}(n). \tag{I.6.6}$$

  Note that the ideal decorrelating detector is IIR in both causal and anti-causal directions. The decorrelator is analogous to the MMSE-ZF receiver in the equalization literature [CDEF95].

  – *MMSE Linear Detector*: The MMSE linear MUD obtains an estimate of $\boldsymbol{A}(n)$ as

  $$\begin{aligned}\widehat{A}(n) = \mathbf{S}_{ay}(q)\mathbf{S}_{\rm yy}^{-1}(q)\boldsymbol{y}(n) &= \mathbf{S}_{aa}\mathbf{G}^\dagger\left(\mathbf{G}\mathbf{S}_{aa}\mathbf{G}^\dagger + \mathbf{S}_{\rm vv}\right)^{-1}\boldsymbol{y}(n)\\ &= \left(\mathbf{G}^\dagger\mathbf{G} + \frac{\sigma_v^2}{\sigma_a^2}\boldsymbol{I}_K\right)^{-1}\boldsymbol{x}(n),\end{aligned} \tag{I.6.7}$$

  where, the last equality holds if $\mathbf{S}_{aa}(z) = \sigma_a^2\boldsymbol{I}_K$ and $\mathbf{S}_{\rm vv}(z) = \sigma_v^2\boldsymbol{I}_{PMJ}$.

- ***Nonlinear MUD***

  Let us introduce the notation

  $$\mathbf{Q}(z) = \sum_{m=-N_c+1}^{N_c-1}\boldsymbol{q}(m)z^{-m} = \left(\mathbf{G}^\dagger(z)\mathbf{G}(z)\right) + \begin{cases}\mathbf{0}, & \text{MMSE}-\text{ZF}\\ \frac{\sigma_v^2}{\sigma_a^2}\boldsymbol{I}_K, & \text{MMSE}\end{cases} \tag{I.6.8}$$

Then we need to solve

$$\begin{aligned}\mathbf{Q}(z)\widehat{A}(n) =& \boldsymbol{q}(N_c-1)\widehat{A}(n-N_c+1)+\\ &\cdots+\boldsymbol{q}(0)\widehat{A}(n)+\cdots+\boldsymbol{q}(-N_c+1)\widehat{A}(n+N_c-1)=\boldsymbol{x}(n),\end{aligned} \tag{I.6.9}$$

for $\widehat{A}(n)$. Then, subtractive interference algorithms can be applied, i.e., one can solve for one symbol at a time and use the decisions for values of other symbols. This can be done in the following three ways.

– *Successive Interference Cancelation*:

In (I.6.9), we assume that future decisions are all zero, i.e.,

$$\boldsymbol{q}(0)\widehat{A}(n)=\boldsymbol{x}(n)-\boldsymbol{q}(1)\widehat{A}(n-1)-\cdots-\boldsymbol{q}(N_c-1)\widehat{A}(n-N_c+1). \tag{I.6.10}$$

Then we order a_k along k in order of decreasing powers, and consider RAKE detection for the current user (strongest). We take a decision for this user and subtract its contribution from the received signal, by reconstructing its contribution to the latter. Users are therefore successively decoded. Naturally, a certain minimum performance level of the RAKE receiver for the strongest user is required in order to avoid unreliable decisions. Wrong decisions have a disastrous effect and the interferer's power is increased rather than its elimination. This scheme works best if there is significant disparity among users' received powers [KIHP90b, PH94]. Robust forward error correction codes [Vit90] can be devised for improved performance in the SIC framework, which makes it of interest from the information theoretical point of view, since, essentially, remaining users see less MAI [Car75].

SIC can further be improved in an iterative fashion when all users have been detected: *multistage* SIC. In that case, not only decisions of stronger users of the current iteration are subtracted, but also those of weaker users from the previous iteration.

– *Parallel Interference Cancelation*:

PIC [KIHP90a, VA90] corresponds to MLSE for a particular symbol, once all other symbols have been detected. This is done for all symbols in parallel. We take all past and future decisions from the previous $(i-1)$st iteration. Thus

$$\boldsymbol{q}(0)\widehat{A}^{(i)}(n)=\boldsymbol{x}(n)-\sum_{\substack{m=-N_c+1\\ m\neq 0}}^{N_c-1}\boldsymbol{q}(m)\widehat{A}^{(i-1)}(n-m). \tag{I.6.11}$$

The above needs to be solved for the ith iteration. PIC as opposed to SIC works particularly well in power-controlled situations. Initial decisions can be obtained by a linear detector.

Several variants of the above schemes are possible. For example, PIC can be improved by using already detected symbols in the present stage for the detection of remaining ones. Other ways consist of combining PIC with SIC or to implement multistage versions of these algorithms.

– *Decision Feedback MUD*:

Let us introduce the spectral factorization

$$\mathbf{Q}(z)=\mathbf{F}^{\dagger}(z)\boldsymbol{D}\mathbf{F}(z), \tag{I.6.12}$$

where, $\mathbf{F}(z) = \boldsymbol{f}(0) + \boldsymbol{f}(1)z^{-1} + \ldots + \boldsymbol{f}(N_c - 1)z^{-N_c+1}$ is a minimum phase spectral factor, $\boldsymbol{D}$ is diagonal, real, and positive, and $\boldsymbol{f}(0)$ is unit-diagonal lower triangular in structure. $\mathbf{F}^{-\dagger}(z)$ is the backward prediction filter for $\mathbf{Q}(z)$. Then the DF algorithm consists of solving for $\widehat{A}(n)$ from $\boldsymbol{x}(n)$ by removing anti-causal MAI and ISI linearly, and causal MAI and ISI non-linearly, i.e.,

$$\mathbf{F}(q)\widehat{A}(n) = \boldsymbol{D}^{-1}\mathbf{F}^{-\dagger}(q)\boldsymbol{x}(n) = \boldsymbol{z}(n) \Rightarrow \mathbf{F}^{\dagger}(q)\boldsymbol{D}\boldsymbol{z}(n) = \boldsymbol{x}(n). \tag{I.6.13}$$

Then going backwards in time

$$\boldsymbol{f}^H(0)\boldsymbol{D}\boldsymbol{z}(n) = \boldsymbol{x}(n) - \boldsymbol{f}^H(1)\boldsymbol{D}\boldsymbol{z}(n+1) \ldots - \boldsymbol{f}^H(N_c - 1)\boldsymbol{D}\boldsymbol{z}(n + N_c - 1), \tag{I.6.14}$$

and forwards in time

$$\boldsymbol{f}(0)\widehat{A}(n) = \boldsymbol{z}(n) - \boldsymbol{f}(1)\widehat{A}(n-1) \ldots - \boldsymbol{f}(N_c - 1)\widehat{A}(n - N_c + 1). \tag{I.6.15}$$

The performance of the ZF DF MUD is similar to the decorrelator for the strongest user and gradually approaches the single user bound as the user's power decreases relative to other interferers. So the DF mainly favors weaker users.

Added advantages can be gained by using the soft-decision strategy in MUD. One way is taking decisions when reliable decisions are available. Otherwise symbol estimates are left undecided.

I.6.2.2 Decentralized Receivers

It is seen in (I.3.29), that any of the above multiuser detection schemes can be implemented as long as timing information, $\tau_k,\ k = 1, \ldots, K$, and spreading sequences, $c_k,\ k = 1, \ldots, K$, of all users are available. These quantities need to be estimated from the received signal. Another relatively recent development in the field of multiuser detection is the advent of the *blind adaptive multiuser detector* [HMV95], where it was shown that the multiuser problem could be cast in a single user *decentralized* framework, thus enabling MAI based upon single user information (desired user delay and spreading sequence), the same as the RAKE receiver. In this framework, the linear receiver operates directly on the received signal to extract the desired user. This breakthrough step in multiuser detection was motivated by the developments in the field of *blind* channel identification and detection (see survey [Mad98]).

- *The Optimal Linear MMSE Receiver*:

  Let $\mathbf{G}_1(z)$ denote the channel transfer function for the desired user. The structure of the optimal MMSE linear receiver is given in fig. I.14. We find,

  $$\boldsymbol{f}_{\mathrm{MMSE}}(z) = \mathbf{S}_{ay}(z)\mathbf{S}_{\mathrm{yy}}^{-1}(z) = \sigma_a^2\mathbf{G}_1^{\dagger}(z)\mathbf{S}_{\mathrm{yy}}^{-1}(z), \tag{I.6.16}$$

  where, $\mathbf{G}_1(z)$ needs to be estimated in some manner and $\mathbf{G}_1^{\dagger}(z) = \mathbf{G}_1^H(1/z^H)$ is the multichannel matched filter.

  For a simplified implementation of the receiver, consider multichannel linear prediction with the predictor transfer function $\mathbf{P}(z)$ yielding prediction error $\widetilde{\boldsymbol{y}}(n) = \mathbf{P}(z)\boldsymbol{y}(n)$. We then have,

$\mathbf{P}(z)\mathbf{S}_{\mathrm{yy}}(z)\mathbf{P}^{\dagger}(z) = \mathbf{S}_{\widetilde{\mathrm{yy}}}(z)$. The prediction errors are white for infinite prediction order [Slo94b]. $\mathbf{S}_{\mathrm{yy}}(z)$ is the power spectral density matrix of the received signal. To determine its inverse, a finite number of correlation lags of $\boldsymbol{y}(k)$ are adequate to determine the prediction error filters $\mathbf{P}(z)$ leading to the FIR model $\mathbf{S}_{\mathrm{yy}}^{-1}(z) \approx \mathbf{P}^{\dagger}(z)\boldsymbol{R}_{\tilde{\boldsymbol{y}}\tilde{\boldsymbol{y}}}^{-1}\mathbf{P}(z)$ [Slo96]. It is seen that $\mathbf{S}_{\mathrm{yy}}^{-1}(z)$ is Infinite Impulse Response (IIR) in general. In the noiseless (singular) case, however, the FIR assumption on $\mathbf{S}_{\mathrm{yy}}^{-1}(z)$ turns out to be exact. In other words, a finite number of correlation lags of $\boldsymbol{y}(k)$ are adequate for its estimation. We shall compare the performance of other linear receiver derived in

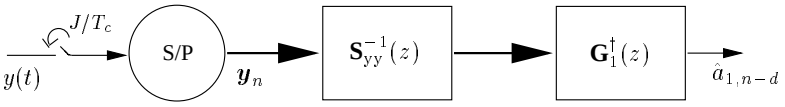

Figure I.14: Optimal MMSE receiver structure.

this thesis with the optimal MMSE receiver described above.

I.6.2.3 Discussion

The decentralized scheme is suitable for applications such as at mobile terminals or as a suboptimal processing or initialization stage at the base station. It carries the advantage that no distinction is made between intracell and intercell interference. Centralized schemes, on the other hand consider a fixed number of intracell users. Intercell interference is usually ignored, which might incur performance loss due to a residual interference term at the input to the decision device. Some work on residual interference cancelation in PIC receivers can be found in [LA98].

I.7 Thesis Outline and Contributions

We described the general DS-CDMA discrete-time multichannel model in section § I.3.1. This oversampling/multiple senor aspect of this model holds in general for the remainder of this thesis. The signal model described in section § I.3.2 depicts an asynchronous periodic sequences based DS-CDMA system. This is a typical uplink situation. Minor changes in the model for the case of the downlink scenario will be indicated when needed. The rest of this thesis is organized as follows.

Chapter II presents the blind projection receiver obtained in a decentralized fashion for multiuser asynchronous frequency-selective channels. A new receiver and channel identification algorithm are thus obtained. Identifiability conditions are discussed in detail and simulations in various scenarios are presented. Simplified channel identification algorithms are also investigated. Results of this chapter are partially presented in the following publications.

- Irfan Ghauri and Dirk T. M. Slock, *Blind Decentralized Projection Receiver for Asynchronous CDMA in Multipath Channels*, Annals of Telecommunications, July/August 1999
- Irfan Ghauri and Dirk T. M. Slock, *Blind MMSE-ZF Receiver and Channel Identification for Asynchronous CDMA in Multipath Channels*, Proceedings of the 3rd European Personal Mobile Communications Conference, Paris, France, March 1999
- Irfan Ghauri and Dirk T. M. Slock, *Blind Channel and Linear MMSE Receiver Determination in DS-CDMA Systems*, Proceedings of the International Conference on Acoustics, Speech, and Signal Processing, Phoenix, AZ, vol. 5, pp. 2699-2702, March 1999

Semi-blind implementations of the projection receiver of chapter II are investigated in chapter III. Adaptive interference suppression algorithms are also addressed. Methods of improving the channel estimate by means of semi-blind schemes are also presented. Performance of blind, semi-blind, and decision-directed algorithms is compared in this chapter. Related publications are

- Irfan Ghauri and Dirk T. M. Slock, *Blind and Semi-Blind Single User Receiver Techniques for Asynchronous CDMA in Multipath Channels*, IEEE Global Communications Conference, Sydney, Australia, November 1998
- Irfan Ghauri and Dirk T. M. Slock, *Adaptive Interference Suppression for DS-CDMA in Multipath Channels*, in 33rd Asilomar Conference on Signals, Systems, and Computers, Pacific Grove, CA, Oct. 1999.

Chapter IV addresses the downlink situation in CDMA systems [TIA93, ETS97a], and provides blind and training based algorithms for that problem. Performance of the RAKE receiver is compared with two alternatives, namely the zero-forcing and the maximum SINR receivers proposed in this chapter, and the parameters influencing the choice of a particular receiver are discussed. Partial results of this chapter have been presented in

- Irfan Ghauri and Dirk T. M. Slock, *Linear Receivers for the DS-CDMA Downlink Exploiting Orthogonality of Spreading Sequences*, in 32nd Asilomar Conference on Signals, Systems, and Computers, Pacific Grove, CA, Nov. 1998.
- Dirk T. M. Slock and Irfan Ghauri, *Blind Maximum SINR Receiver for the DS-CDMA Downlink*, submitted to International Conference on Acoustics, Speech, and Signal Processing, Istanbul, Turkey, March 2000.

The last three chapters are dedicated to spatio-temporal array processing at the base-station in order to pre-cancel the interference on the downlink. These can be considered to constitute part-II of this thesis. The problem addressed is that of exploiting channel state information at the base station (obtained from the uplink estimates) to design spatio-temporal filters for efficient downlink transmission. The publications related to these chapter are

- Giuseppe Montalbano, Irfan Ghauri and Dirk T. M. Slock, *Spatio-Temporal Array Processing for CDMA/SDMA Downlink Transmission*, in 32nd Asilomar Conference on Signals, Systems, and Computers, Pacific Grove, CA, Nov. 1998
- Giuseppe Montalbano, Irfan Ghauri and Dirk T. M. Slock, *Spatio-Temporal Array Processing for FDD/CDMA/SDMA Downlink Transmission*, in Proceedings of the IEEE Vehicular Technology Conference (Fall), Amsterdam, The Netherlands, September 1999
- Giuseppe Montalbano, Irfan Ghauri and Dirk T. M. Slock, *Spatio-Temporal Array Processing for Aperiodic CDMA Downlink Transmission*, in 33rd Asilomar Conference on Signals, Systems, and Computers, Pacific Grove, CA, Oct. 1999

General conclusions are drawn the final chapter and future research directions are indicated. Wherever relevant we also give an account of the application of the algorithms presented in this thesis for existing and future mobile and wireless communication systems.

Chapter II

Blind Channel Identification and Linear Receivers for Asynchronous CDMA

In this chapter, we consider an asynchronous DS-CDMA system employing periodic spreading sequences operating in a frequency selective channel. The desired user's multipath channel estimate is obtained by means of a blind technique which exploits the spreading sequence of the user and the second-order statistics of the received signal. The decentralized blind Minimum Mean Square Error-Zero Forcing (MMSE-ZF) receiver or projection receiver is subsequently obtained. This receiver represents the proper generalization of the anchored minimum output energy (MOE) receiver [HMV95] to the asynchronous case with delay spread. Classification of linear receivers obtained by various criteria is provided and the MMSE-ZF receiver is shown to be obtainable in a decentralized fashion by proper implementation of the unbiased MOE receiver, leading to the minimum variance distortionless response (MVDR) receiver for the signal of the desired user. This MVDR receiver is then adapted blindly by applying Capon's principle. A channel impulse response is obtained as a by-product. Lower bounds on the receiver filter length are derived, giving a measure of the ISI and MAI tolerable by the receiver and ensuring its identifiability.

II.1 Introduction

A breakthrough step in multiuser detection, following developments in the field of *blind* channel identification and detection (see survey [Mad98]), was the introduction of the *blind adaptive multiuser detector* [HMV95], where it was shown that the multiuser problem could be cast in a single user *decentralized* framework, thus enabling multiple access interference cancelation based on single user information (desired user delay and spreading sequence). In this framework, the linear receiver operates directly on the received signal. The receiver in [HMV95] is the so-called *anchored* minimum-output energy (MOE) receiver. The anchored receiver is split into two components - one fixed, and proportional to the desired user's signature waveform (matched filter receiver), while the other, its orthogonal complement. The algorithm constrains the inner product of the received signal with the desired user spreading sequence to be fixed, thus restricting the optimization problem to within the constrained space. No effort is made to exploit the structure of the MAI except for the assumption of it being uncorrelated with the desired signal. A decentralized scheme of this nature can evidently be

of considerable interest in some applications, like at the mobile terminal in a cellular network, where knowledge of interferer parameters is not readily available, or as a suboptimal/initialization approach at the base station. Blind adaptive multiuser detectors based on second-order statistics (non-decision directed/ data-aided) are developed for the case of short/periodic spreading sequences, leading to cyclostationarity at symbol period.

The problem addressed in [HMV95] was that of DS-CDMA communications over a flat channel (no delay spread) [Skl97]. A constrained optimization scheme was proposed in [Tsa97] for multipath channels by forcing to zero the receiver response to all but one of the multipath components. An immediate performance loss was noticeable resulting from the rejection of a major part of the desired signal energy contained in the other paths. This signal cancelation effect was alleviated in [TX97b], where the receiver's output energy was minimized subject to a fixed response constraint for the desired signal. Connections with the *Capon* philosophy were drawn in that paper. The above mentioned receivers can be shown to converge asymptotically (SNR$\rightarrow \infty$) to the zero-forcing (ZF) or the decorrelating solution. It was shown in [GS97] that in order to accommodate a number of users approaching the code space dimension (spreading factor), longer receivers are required for the ZF solution to be achievable. Moreover, we presented in [GS97] the optimal MMSE receiver for multipath channels and asynchronous conditions, obtained by applying multichannel linear prediction to the received cyclostationary signal. Direct estimation of the MMSE receiver from spreading sequence properties and the noise subspace was introduced in [GSP98] following the observation that the MMSE receiver vector dwells in the signal subspace. The ZF and the MMSE detectors in the case of high data-rate systems in dispersive channels inducing significant ISI, were investigated in [WP98a]. Adaptive implementations are shown in [WP98b]. The channel estimate in these two publications was obtained as a generalization to longer delay spreads of the subspace technique originally proposed in [TX97a]. Both these schemes, however, evoke a high computational complexity since a subspace decomposition is required. It is worth mentioning that in the context of blind methods based on second-order statistics and spatio-temporal processing techniques [PP97], direct sequence CDMA systems allow quite robust channel estimation (compared to TDMA systems) due to the bandwidth expansion and integrated *a priori* knowledge and structure in terms of distinct spreading sequences that enables separation of user signals.

The purpose of this chapter is to introduce a decentralized blind minimum mean-square error zero-forcing (MMSE-ZF) receiver for DS-CDMA systems in multipath channels. The receiver is MMSE-ZF in the sense that among all ZF receivers, it is the one that minimizes the mean-square error. The MMSE-ZF receiver is also called the projection receiver [SRAX96] or the decorrelating detector [LV89]. This blind receiver exploits spreading sequence properties in conjunction with the second-order statistics of the received signal to estimate the FIR channel for the desired user at a low cost. The delay spread for the kth user is assumed to be possibly more than a symbol period, i.e., $\Delta_k T_c > T$ in (I.3.5), and can be different for different users.

The rest of the chapter is organized as follows. In section § II.2, the non-blind MMSE-ZF receiver is derived and its interpretation in terms of existing methods is provided. Section § II.4 lays the groundwork for the blind MMSE-ZF receiver by providing analogies between the interference cancelation problem and some related results from the array processing literature. Section § II.5 is dedicated to the derivation of the blind MMSE-ZF receiver through an alternate and simple method, namely the unbiased minimum output energy (MOE) criterion. Blind channel estimation via the blind MMSE-ZF algorithm is also discussed. An alternate interpretation of the MMSE-ZF receiver as a Generalized Side-lobe Canceler (GSC) is also discussed. Receivers obtained from other projections are also discussed and a reduced complexity channel estimation method is presented in the last section of this chapter.

II.2 The MMSE-ZF/Projection Receiver

In the multiuser problem given in (I.3.29), there exists a multitude of possible zero-forcing constraints, ranging from zero MAI only, or zero ISI only, to zero forcing for both MAI and ISI, which we shall consider here. For the purpose of our problem, let us consider the ZF or the zero-distortion constraint, which can be written as,

$$\boldsymbol{f}^H \mathcal{T}(\boldsymbol{G}_N) = \boldsymbol{e}_d^T, \tag{II.2.1}$$

where, $\boldsymbol{e}_d^T = [0 \cdots 0 | \overbrace{0 \cdots 0}^{d} \; 1 \; 0 \cdots 0 | 0 \cdots 0]$, with d the "equalization" delay for the desired user.

Considering all user symbols $a_k(n)$ to be uncorrelated, the received signal covariance matrix can be written as $\boldsymbol{R}_{YY} = \sigma_a^2 \mathcal{T}\mathcal{T}^H + \sigma_v^2 \boldsymbol{I}$, where $\mathcal{T}$ replaces $\mathcal{T}(\boldsymbol{G}_N)$ to simplify the notation. The MMSE-ZF receiver is by definition the solution to the MMSE criterion under the ZF constraint, which can be written as

$$\min_{\boldsymbol{f}:\boldsymbol{f}^H\mathcal{T}=\boldsymbol{e}_d^T} \boldsymbol{f}^H \boldsymbol{R}_{YY} \boldsymbol{f} = \sigma_a^2 + \min_{\boldsymbol{f}:\boldsymbol{f}^H\mathcal{T}=\boldsymbol{e}_d^T} \boldsymbol{f}^H \boldsymbol{R}_{VV} \boldsymbol{f} \Rightarrow \min_{\boldsymbol{f}:\boldsymbol{f}^H\mathcal{T}=\boldsymbol{e}_d^T} \boldsymbol{f}^H \boldsymbol{f} \tag{II.2.2}$$

Let us further express the receiver vector $\boldsymbol{f}$ as

$$\boldsymbol{f} = \mathcal{T}\boldsymbol{f}_1 + \mathcal{T}^\perp \boldsymbol{f}_2, \tag{II.2.3}$$

where, $\mathcal{T}^\perp$ spans the orthogonal complement of $\mathcal{T}$ and satisfies $P_{\mathcal{T}^\perp} = P_{\mathcal{T}}^\perp$. From the ZF constraint, $\boldsymbol{f}^H\mathcal{T} = \boldsymbol{e}_d^T = \boldsymbol{f}_1^H \mathcal{T}^H \mathcal{T}$, and therefore,

$$\boldsymbol{f}_1 = (\mathcal{T}^H\mathcal{T})^{-1} \boldsymbol{e}_d. \tag{II.2.4}$$

Hence, $\boldsymbol{f} = \mathcal{T}(\mathcal{T}^H\mathcal{T})^{-1}\boldsymbol{e}_d + \mathcal{T}^\perp \boldsymbol{f}_2$, where $\boldsymbol{f}_2$ is the unconstrained part which becomes zero upon solving the minimization problem in (II.2.2). Thus the projection receiver is given by

$$\boldsymbol{f} = \mathcal{T}(\mathcal{T}^H\mathcal{T})^{-1}\boldsymbol{e}_d, \tag{II.2.5}$$

and we can write the MMSE-ZF criterion as:

$$\min_{\boldsymbol{f}:\boldsymbol{f}^H\mathcal{T}=\boldsymbol{e}_d^T} \boldsymbol{f}^H \boldsymbol{R}_{YY} \boldsymbol{f} = \sigma_a^2 + \sigma_v^2 \boldsymbol{e}_d^T \left(\mathcal{T}^H\mathcal{T}\right)^{-1} \boldsymbol{e}_d. \tag{II.2.6}$$

The ZF solution in the noiseless case gives the distortionless response for the desired user's signal.

We can provide one more interpretation of the MMSE-ZF receiver in terms of a projection receiver as indicated in the following proposition.

Proposition 1: The MMSE-ZF receiver is equivalent to a projection receiver [SRAX96] that first projects the received data onto the orthogonal complement of the subspace spanned by ISI and MAI, and then projects the resulting vector onto a one-dimensional subspace that is matched to the signal part that remains in the data.
Proof: See appendix IIA.

The MMSE-ZF receiver derived above needs the knowledge of the channel convolution matrix (arrival delays and impulse responses of all user channels) for its implementation. However, as we shall see in the sequel, it is possible to determine this receiver blindly in a decentralized fashion, as a solution to the minimum variance distortionless response (MVDR) criterion.

II.3 Asymptotic Equivalence of the MMSE and Projection Receivers

Considering the input symbol sequence to be *i.i.d.*, the MMSE receiver of section § I.6.2.2 can be written as

$$\boldsymbol{f}^H = \boldsymbol{R}_{a\boldsymbol{Y}}\boldsymbol{R}_{\boldsymbol{Y}\boldsymbol{Y}}^{-1} = \sigma_a^2 \boldsymbol{e}_d^T \mathcal{T}^H \left(\sigma_a^2 \mathcal{T}\mathcal{T}^H + \sigma_v^2 \boldsymbol{I}\right)^{-1}, \tag{II.3.1}$$

Upon applying the matrix inversion lemma, this can be written as

$$\boldsymbol{f}^H = \boldsymbol{e}_d^T \left(\sigma_a^2 \mathcal{T}^H\mathcal{T} + \frac{\sigma_v^2}{\sigma_a^2}\boldsymbol{I}\right)^{-1} \mathcal{T}^H. \tag{II.3.2}$$

As $\frac{\sigma_v^2}{\sigma_a^2} \to 0$, the MMSE receiver becomes the decorrelator.

II.4 LCMV Beamforming

It is insightful to compare the problem of blind ISI and MAI rejection to that of beamforming and direction of arrival (DOA) estimation in the antenna array processing literature [JD93]. Let us look at a generic DOA estimation problem of a single narrowband source located at an angle θ_0 with respect to an antenna array. The observation or snapshot vector $\boldsymbol{Y}(n)$ at the array output is

$$\boldsymbol{Y}(n) = \boldsymbol{S}(\theta_0)a(n) + \boldsymbol{V}(n), \tag{II.4.1}$$

with $\boldsymbol{S}(\theta_0)$ being the *array response* or *steering* vector associated with the look-direction θ_0, and $\boldsymbol{V}(n)$ the complex circularly-symmetric additive (spatially) white Gaussian noise (AWGN) vector. $a(n)$ is the sampled source signal, with variance σ_a^2. In this problem there are two unknowns, namely the direction of arrival θ_0 (and the corresponding steering vector) and the source signal $a(n)$. In the first instance, we shall consider θ_0 known. A beamformer with the weight vector $\boldsymbol{f}$ is employed to obtain the estimate $\hat{a}(n) = \boldsymbol{f}^H\boldsymbol{Y}(n)$, where the superscript ^{H} stands for Hermitian transpose. Intuitively, any desirable beamformer should emphasize signals arriving from the direction θ_0, while the noise must be suppressed. We therefore impose the zero-distortion constraint, $\boldsymbol{f}^H\boldsymbol{S}(\theta_0) = 1$, on the beamformer, and minimize its output variance $E|\boldsymbol{f}^H\boldsymbol{Y}(n)|^2$ subject to this constraint. The weight vector of the linearly constrained minimum variance (LCMV) beamformer is the solution to the problem

$$\min_{\boldsymbol{f}:\boldsymbol{f}^H S(\theta_0)=1} E|\hat{a}_k|^2 \leftrightarrow \min_{\boldsymbol{f}:\boldsymbol{f}^H S(\theta_0)=1} \boldsymbol{f}^H\boldsymbol{R}_{YY}\boldsymbol{f} \;=\; \mathrm{MV}, \tag{II.4.2}$$

which results in

$$\boldsymbol{f} = \frac{1}{\boldsymbol{S}^H(\theta_0)\boldsymbol{R}_{YY}^{-1}\boldsymbol{S}(\theta_0)}\boldsymbol{R}_{YY}^{-1}\boldsymbol{S}(\theta_0),\ \mathrm{MV} = \left(\boldsymbol{S}^H(\theta_0)\boldsymbol{R}_{YY}^{-1}\boldsymbol{S}(\theta_0)\right)^{-1}. \tag{II.4.3}$$

At this point we realize that we do not yet know θ_0. However, we can obtain θ_0 by *Capon's* method [SM97] as the argument of the maximum of the minimum variance over all possible look directions. Thus,

$$\begin{aligned}\widehat{\theta} &= \arg\max_{\theta} \left(\boldsymbol{S}^H(\theta)\boldsymbol{R}_{YY}^{-1}\boldsymbol{S}(\theta)\right)^{-1} = \arg\min_{\theta} \boldsymbol{S}^H(\theta)\boldsymbol{R}_{YY}^{-1}\boldsymbol{S}(\theta) \\ &= \boldsymbol{S}^{-1}\left(V_{\max}(\boldsymbol{R}_{YY})\right) = \boldsymbol{S}^{-1}\left(\boldsymbol{S}(\theta_0)\right) = \theta_0,\end{aligned} \tag{II.4.4}$$

since $\boldsymbol{R}_{YY} = \sigma_a^2 \boldsymbol{S}(\theta_0)\boldsymbol{S}^H(\theta_0) + \sigma_v^2 \boldsymbol{I}$, and assuming a proper normalization of $\boldsymbol{S}(\theta)$. We denote by $V_{\max}(\boldsymbol{R}_{YY})$, the eigenvector of $\boldsymbol{R}_{YY}$ associated with the maximum eigenvalue.

Note that Capon's approach could be extended to the multisource case if the sources are uncorrelated and if they are treated jointly. Here, we shall stick to the decentralized single source formulation of the Capon's method. The rest of the developments in this paper are based upon the striking similarity between the purely spatial (beamforming) problem discussed above, and the ISI and MAI cancelation issue depicted in fig. I.9. In particular, we show in the sequel that for the DS-CDMA problem, given certain conditions on the number of concurrent users and their channel orders, partial knowledge of the channel vectors, $\boldsymbol{g}_k(i)$'s in terms of distinct spreading code matrices, $\boldsymbol{C}_k(i)$'s, leads to an unambiguous estimate of the channel vector $\boldsymbol{h}_k$ for the kth user.

II.5 Connections between Linear Receivers

We can classify the unbiased linear MOE[1] receiver in relation with other optimization criteria as indicated in the following proposition.

Proposition 2: The minimum mean-squared error (MMSE), and the minimum output energy (MOE) are interchangeable criteria under the unbiased constraint, and are equivalent to the maximization of the output SINR.

$$\arg \min_{f:f^H\tilde{g}_1=1} \text{MSE}_{\text{unbiased}} = \arg \min_{f:f^H\tilde{g}_1=1} \text{OE} = \arg \max_f \text{ SINR}, \tag{II.5.1}$$

Proof: (i) Consider first, the MMSE criterion

$$\begin{aligned} \text{MSE} &= E|a_1(n-d) - \hat{a}_1|^2 = E|a_1(n-d) - \boldsymbol{f}^H\boldsymbol{Y}|^2 \\ &= \sigma_a^2 - \sigma_a^2 \boldsymbol{f}^H\tilde{\boldsymbol{g}}_1 - \sigma_a^2\tilde{\boldsymbol{g}}_1^H\boldsymbol{f} + \underbrace{\boldsymbol{f}^H\boldsymbol{R}_{YY}\boldsymbol{f}}_{\text{output energy}} \end{aligned},$$

$$\Rightarrow \min_{f:f^H\tilde{g}_1=1} \text{MSE} = \text{unbiased MOE} \tag{II.5.2}$$

proving the first equality in (II.5.1).

(ii) The signal part in $\boldsymbol{Y}_L(n)$ is $\boldsymbol{Y}_{\text{s}} = \tilde{\boldsymbol{g}}_1 a_1(n-d)$, whereas the interference (MAI & ISI) plus noise is $\boldsymbol{Y}_{\text{in}} = \overline{\mathcal{T}}_L\bar{\boldsymbol{A}} + \boldsymbol{V}_L$, where, $\overline{\mathcal{T}}_L$ is the same as $\mathcal{T}_L(G_N)$ with the column $\tilde{\boldsymbol{g}}_1$ removed. Similarly, $\bar{\boldsymbol{A}}$ is the same as $\boldsymbol{A}(n)$ in (I.3.29) without the symbol $a_1(n-d)$, i.e., the symbol that multiplies $\tilde{\boldsymbol{g}}_1$. Then, for an arbitrary $\boldsymbol{f}$, assuming uncorrelated symbols, we obtain,

$$\text{SINR} = \frac{\boldsymbol{f}^H\boldsymbol{R}_{\text{s}}\boldsymbol{f}}{\boldsymbol{f}^H\boldsymbol{R}_{\text{in}}\boldsymbol{f}} = \frac{\sigma_a^2\boldsymbol{f}^H\tilde{\boldsymbol{g}}_1\tilde{\boldsymbol{g}}_1^H\boldsymbol{f}}{\boldsymbol{f}^H\left(\boldsymbol{R}_{YY} - \sigma_a^2\tilde{\boldsymbol{g}}_1\tilde{\boldsymbol{g}}_1^H\right)\boldsymbol{f}}, \tag{II.5.3}$$

from where,

$$\begin{aligned} &\max_f \text{ SINR} \leftrightarrow \min_f \text{ SINR}^{-1} \leftrightarrow \min_f \frac{\boldsymbol{f}^H\boldsymbol{R}_{YY}\boldsymbol{f}}{\sigma_a^2|\boldsymbol{f}^H\tilde{\boldsymbol{g}}_1|^2} \\ &\Rightarrow \min_{f:f^H\tilde{g}_1=1} \boldsymbol{f}^H\boldsymbol{R}_{YY}\boldsymbol{f}, \end{aligned} \tag{II.5.4}$$

which is the unbiased MOE criterion of (II.5.5). ■

[1] a derivative of the minimum variance distortionless response (MVDR) method, and a particular instance of the linearly constrained minimum-variance (LCMV) criterion

II.5.1 Relationships between Various Constraints

At this juncture, we are able to identify the relationship between the unbiased linear MOE and the unbiased linear MMSE approaches which give the same receiver filter $\boldsymbol{f}$. Note that the unbiased MMSE criterion yields the MMSE-ZF receiver in the noiseless case and so does the unbiased MOE. A further observation is that the unbiasedness constraint ($f^H\widetilde{\boldsymbol{g}}_1 = 1$) is not the distortionless constraint (the ZF constraint) given by (II.2.1). It is only the ZF (distortionless) constraint which guarantees the minimum variance (σ_a^2) with a fixed response for the desired user signal, which is the desired goal in the original MVDR approach.

In [TX97b], the authors interpreted zero distortion of the Capon's method as unbiasedness, and maximized the MOE to obtain the channel impulse response for the desired user. It was also shown there, that the distinct spreading sequences allowed identifiability of users' channel responses. However, unbiasedness is a weaker constraint as compared to the zero distortion constraint. Intuitively, with only the unbiasedness constraint, the other symbols (ISI) remain present in the estimator output and do not allow the application of the single user form of Capon's principle, which corresponds to the maximization of the MOE (minimum variance) under the zero-distortion constraint. However, unbiased MOE on noiseless data corresponds to the MMSE-ZF, which in turn is equivalent to zero forcing MOE on noiseless data. Hence, in conclusion, we can determine the MMSE-ZF receiver by applying the unbiased MOE on denoised data, leading to a simple treatment of the problem.

II.5.2 Blind Unbiased Linear MOE Receiver

Suppose that $\boldsymbol{f}$ is a linear FIR receiver applied to the received data, $\boldsymbol{Y}_L(n)$. The goal is to obtain a linear estimate of the transmitted symbol, $a_1(n-d)$ for the desired user symbol (with a possible delay of d symbols). Then, $\hat{a}_1(n-d) = \boldsymbol{f}^H\boldsymbol{Y}_L(n)$ is the linear estimate of the desired symbol. Finite alphabet information can later be applied to the this estimate to determine the symbol value. $\boldsymbol{f}$ is said to be *unbiased* if $\boldsymbol{f}^H\widetilde{\boldsymbol{g}}_1 = 1$, where, $\widetilde{\boldsymbol{g}}_1 = \boldsymbol{T}_1^H\boldsymbol{h}_1$ (see fig. I.9), with $\boldsymbol{T}_1 = \left[\begin{array}{ccc}\boldsymbol{0} & \boldsymbol{C}_1^H & \boldsymbol{0}\end{array}\right] \otimes \boldsymbol{I}_{MJ}$ being the signature matrix for the desired user. $\widetilde{\boldsymbol{g}}_1 a_1(n-d)$ is the contribution of $a_1(n-d)$ to $\boldsymbol{Y}_L(n)$. The energy at the output of the receiver (noiseless case) can be written as $E|\boldsymbol{f}^H\boldsymbol{Y}_L(n)|^2 = \boldsymbol{f}^H\boldsymbol{R}_{YY}^d\boldsymbol{f}$, where the superscript ^{d} stands for noiseless or denoised data. The unbiased MOE criterion proposed in [TX97b], which is a generalization of the instantaneous channel case of [HMV95], is in principle a max/min problem solved in two steps with,

step:1 *unbiased MOE*

$$\min_{f:f^H\tilde{g}_1=1} \boldsymbol{f}^H\boldsymbol{R}_{YY}^d\boldsymbol{f} \Rightarrow \boldsymbol{f} = \frac{1}{\widetilde{\boldsymbol{g}}_1^H\boldsymbol{R}_{YY}^{-d}\widetilde{\boldsymbol{g}}_1}\boldsymbol{R}_{YY}^{-d}\widetilde{\boldsymbol{g}}_1, \tag{II.5.5}$$

with $\mathrm{MOE}(\hat{h}_1) = \frac{1}{\widetilde{\boldsymbol{g}}_1^H\boldsymbol{R}_{YY}^{-d}\widetilde{\boldsymbol{g}}_1}$, followed by,

step:2 *Capon's method*

$$\max_{\hat{h}_1:\|\hat{h}_1\|=1} \mathrm{MOE}(\hat{\boldsymbol{h}}_1) \Rightarrow \min_{\hat{h}_1:\|\hat{h}_1\|=1} \hat{\boldsymbol{h}}_1^H\left(\boldsymbol{T}_1\boldsymbol{R}_{YY}^{-d}\boldsymbol{T}_1^H\right)\hat{\boldsymbol{h}}_1, \tag{II.5.6}$$

from where, $\hat{\boldsymbol{h}}_1 = V_{\min}(\boldsymbol{T}_1\boldsymbol{R}_{YY}^{-d}\boldsymbol{T}_1^H)$, which is the estimate (up to a scalar phase factor) of the desired user's FIR channel response.

II.5.3 Discussion and Comparisons

The minimum output energy (MOE) receiver, first proposed in [HMV95] was developed for asynchronous users in the AWGN channel, where the channel is simply represented by a complex gain factor. The linear receiver $\boldsymbol{f}$ can be expressed as $\boldsymbol{f} = \boldsymbol{c}_1 + \boldsymbol{x}$, where, $\boldsymbol{c}_1$ is the fixed component, viz., the desired user's spreading sequence, and $\boldsymbol{x}$ is it orthogonal complement ($\boldsymbol{x}^H \boldsymbol{c}_1 = \boldsymbol{0}$), i.e., a blocking transformation for the desired signal. The fixed response, $\|c_1\| = 1$, (the *anchor*) constrains the desired signal's output variance to an arbitrary constant, which is determined by the channel gain, and the MOE criterion minimizes the output variance of the rest. The receiver is therefore determined blindly up to a scale factor. This receiver, upon scaling the output response to unity for the desired signal corresponds to the unbiased MMSE-ZF receiver of section II.2, leading to a distortionless (ZF) response in the noiseless case. The extension to the multipath channels of this scheme is elaborated upon in [TX97b]. However, in the later approach, the distortionless response (and thus the proper implementation of Capon's method) will only be guaranteed if denoised statistics were employed in the MOE cost function.

II.5.4 Unbiased MOE via the Generalized Side-lobe Canceler

The generalized side-lobe canceler (GSC) [JD93], is a particular implementation of the LCMV beamformer. Hence, the unbiased MOE criterion, which itself is a particular instance of the LCMV approach can be implemented in the GSC fashion as elucidated in the following. Let us denote by

$$\boldsymbol{T}_1 = \begin{bmatrix} \boldsymbol{0} & \boldsymbol{C}_1^H & \boldsymbol{0} \end{bmatrix} \otimes \boldsymbol{I}_{MJ}, \text{ and } \quad \boldsymbol{T}_2 = \begin{bmatrix} \boldsymbol{I} & \boldsymbol{0} & \boldsymbol{0} \\ \boldsymbol{0} & \boldsymbol{C}_1^{\perp} & \boldsymbol{0} \\ \boldsymbol{0} & \boldsymbol{0} & \boldsymbol{I} \end{bmatrix} \otimes \boldsymbol{I}_{MJ}, \tag{II.5.7}$$

the partial signature of the desired user and its orthogonal complement employed, respectively, in the upper and lower branches of the GSC, as shown in fig. II.1. $\boldsymbol{C}_1^{\perp H}$ is the orthogonal complement of $\boldsymbol{C}_1$, the tall code matrix given in section fig. I.8 ($\boldsymbol{C}_1^{\perp} \boldsymbol{C}_1 = \boldsymbol{0}$). Then, $\boldsymbol{C}_1^H \boldsymbol{Y}_{N_1} = \boldsymbol{T}_1 \boldsymbol{Y}_L$ and the matrix $\boldsymbol{T}_2$ acts as a blocking transformation for all components of the signal of interest. Note that $P_{T_1^H} + P_{T_2^H} = \boldsymbol{I}$, where, P_X is the projection operator (projection on the column space of $\boldsymbol{X}$). Then the LCMV problem can be written as

$$\min_{f : f^H T_1^H = (h_1^H h_1)^{-1} h_1^H} \boldsymbol{f}^H \boldsymbol{R}_{YY}^d \boldsymbol{f} = \min_{\substack{f \,:\, f^H T_1^H h_1 = 1 \\ f^H T_1^H h_1^{\perp} = 0}} \boldsymbol{f}^H \boldsymbol{R}_{YY}^d \boldsymbol{f}, \tag{II.5.8}$$

where, $\begin{bmatrix} \boldsymbol{h}_1 & \boldsymbol{h}_1^{\perp} \end{bmatrix}$ is a square non-singular matrix, and $\boldsymbol{h}_1^H \boldsymbol{h}_1^{\perp} = \boldsymbol{0}$. Note that in the LCMV problem (GSC formulation) there is a number of constraints to be satisfied. However, imposing the second set of constraints, namely $\boldsymbol{f}^H \boldsymbol{T}_1^H \boldsymbol{h}_1^{\perp} = 0$ has no consequence because the criterion automatically leads to their satisfaction once, $\text{span}\{\boldsymbol{R}_{YY}^d\} \cap \text{span}\{\boldsymbol{T}_1^H\} = \text{span}\{\boldsymbol{T}_1^H \boldsymbol{h}_1\}$, i.e., when the intersection of the signal subspace and the subspace spanned by the columns of $\boldsymbol{T}_1^H$ is one dimensional.

The matrix $\boldsymbol{T}_1$ is nothing but a bank of correlators matched to the Ψ_1 delayed multipath components of user 1's code sequence. Note that the main branch in fig. II.1 by itself gives an unbiased response for the desired symbol, $a_1(n-d)$, and corresponds to the (normalized) coherent RAKE receiver. For the rest, we have an estimation problem, which can be solved in the least squares sense, for some matrix $\boldsymbol{Q}$. This interpretation of the GSC corresponds to the pre-combining (or pathwise) interference (ISI and MAI) canceling approach [DHZ95, WMN93, ZB92].

The vector of estimation errors is given by

$$\boldsymbol{Z}(n) = [\boldsymbol{T}_1 - \boldsymbol{Q}\boldsymbol{T}_2]\, \boldsymbol{Y}_L(n). \tag{II.5.9}$$

Since the goal is to minimize the estimation error variances, or in other words, estimate the interference term in the upper branch as closely as possible from $\boldsymbol{T}_2\boldsymbol{Y}_L(n)$, the interference cancelation problem settles down to minimization of the trace of the estimation error covariance matrix $\boldsymbol{R}_{ZZ}$ for a matrix filter $\boldsymbol{Q}$, which results in

$$\boldsymbol{Q} = \left(\boldsymbol{T}_1\boldsymbol{R}^d\boldsymbol{T}_2^H\right)\left(\boldsymbol{T}_2\boldsymbol{R}^d\boldsymbol{T}_2^H\right)^{-1}, \tag{II.5.10}$$

and where, $\boldsymbol{R}^d$ is the noiseless (denoised) data covariance matrix, $\boldsymbol{R}_{YY}$, with the subscript removed for convenience. The output $\boldsymbol{Z}(n)$ can directly be processed by a multichannel matched filter to get the symbol estimate, $\hat{a}_1(n-d)$, the data for the user 1.

$$\hat{a}_1(n-d) = \frac{1}{\widetilde{\boldsymbol{g}}_1^H\widetilde{\boldsymbol{g}}_1}\boldsymbol{f}^H\boldsymbol{Y}_L(n) = \frac{1}{\widetilde{\boldsymbol{g}}_1^H\widetilde{\boldsymbol{g}}_1}\boldsymbol{h}_1^H\left(\boldsymbol{T}_1 - \boldsymbol{Q}\boldsymbol{T}_2\right)\boldsymbol{Y}_L(n) \tag{II.5.11}$$

The covariance matrix of the prediction errors is then given by

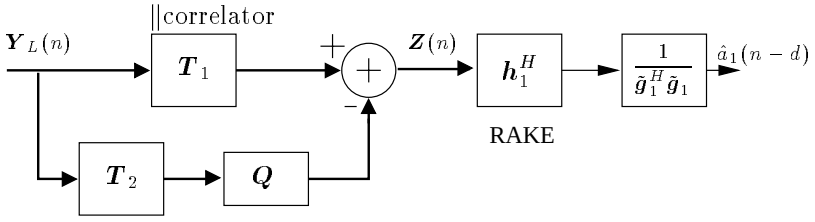

Figure II.1: GSC implementation of the MMSE-ZF receiver.

$$\boldsymbol{R}_{ZZ} = \boldsymbol{T}_1\boldsymbol{R}^d\boldsymbol{T}_1^H - \boldsymbol{T}_1\boldsymbol{R}^d\boldsymbol{T}_2^H\left(\boldsymbol{T}_2\boldsymbol{R}^d\boldsymbol{T}_2^H\right)^{-1}\boldsymbol{T}_2\boldsymbol{R}^d\boldsymbol{T}_1^H, \tag{II.5.12}$$

From the above structure of the interference canceler, we observe that when $\boldsymbol{T}_1\left(\boldsymbol{Y}_L - \widetilde{\boldsymbol{g}}_1 a_1(n)\right)$ can be perfectly estimated from $\boldsymbol{T}_2\boldsymbol{Y}_L$, the matrix $\boldsymbol{R}_{ZZ}$ is rank-1 in the noiseless case! Using this fact, the desired user channel can be obtained (up to a scale factor) as the maximum eigenvector of the matrix $\boldsymbol{R}_{ZZ}$, since $\boldsymbol{Z}(n) = (\boldsymbol{C}_1^H\boldsymbol{C}_1) \otimes \boldsymbol{I}_{MJ}\boldsymbol{h}_1\tilde{a}_1(n-d)$. It can further be shown easily that if $\boldsymbol{T}_2 = \boldsymbol{T}_1^{\perp}$, then

$$\boldsymbol{T}_1\boldsymbol{R}_{YY}^{-1}\boldsymbol{T}_1^H = \left(\boldsymbol{T}_1\boldsymbol{T}_1^H\right)\boldsymbol{R}_{ZZ}^{-1}\left(\boldsymbol{T}_1\boldsymbol{T}_1^H\right), \tag{II.5.13}$$

where, $\boldsymbol{R}_{ZZ}$ is given by (II.5.12), and $\boldsymbol{Q}$, given by (II.5.10), is optimized to minimize the estimation error variance. $\boldsymbol{R}^d$ replaces $\boldsymbol{R}_{YY}$ in the above developments. From this, we can obtain the propagation channel estimate for the desired user, $\hat{\boldsymbol{h}}_1$ as

$$\hat{\boldsymbol{h}}_1 = V_{\max}\left\{\left(\boldsymbol{T}_1\boldsymbol{T}_1^H\right)^{-1}\boldsymbol{R}_{ZZ}\left(\boldsymbol{T}_1\boldsymbol{T}_1^H\right)^{-1}\right\}.$$

The above structure results in perfect interference cancelation (both ISI and MAI) in the noiseless case, the evidence of which is the rank-1 estimation error covariance matrix, and a consequent distortionless response for the desired user. In the noiseless case ($v(t) \equiv 0$), we have the following two cases of interest.

II.5.4.1 Uncorrelated symbols

In the absence of noise, with *i.i.d.* symbols, the stochastic estimation of $\boldsymbol{T}_1\boldsymbol{Y}$ from $\boldsymbol{T}_2\boldsymbol{Y}$ is the stochastic estimation of $\boldsymbol{T}_1\mathcal{T}_L(\boldsymbol{G}_N)\boldsymbol{A}$ from $\boldsymbol{T}_2\mathcal{T}_L(\boldsymbol{G}_N)\boldsymbol{A}$ with $\boldsymbol{R}_A = \sigma_a^2\boldsymbol{I}$. Hence, it is equivalent to the deterministic estimation of $\mathcal{T}_L^H(\boldsymbol{G}_N)\boldsymbol{T}_1^H$ from $\mathcal{T}_L^H(\boldsymbol{G}_N)\boldsymbol{T}_2^H$, i.e.,

$$\min_{\boldsymbol{Q}} \|\mathcal{T}_L^H(\boldsymbol{G}_N)\boldsymbol{T}_1^H - \mathcal{T}_L^H(\boldsymbol{G}_N)\boldsymbol{T}_2^H\boldsymbol{Q}^H\|_2^2.$$

Then, given the condition

$$\begin{aligned}
&\operatorname{span}\{\boldsymbol{T}_1^H\} \cap \operatorname{span}\{\mathcal{T}_L(\boldsymbol{G}_N)\} = \operatorname{span}\{\mathcal{T}_L(\boldsymbol{G}_N)\boldsymbol{e}_d^{'}\} \\
&\Rightarrow \operatorname{span}\{\mathcal{T}_L(\boldsymbol{G}_N)\} \subset \operatorname{span}\{\boldsymbol{T}_2^H\} \oplus \operatorname{span}\{\widetilde{\boldsymbol{g}}_1\} \\
&\because \mathcal{T}_L(\boldsymbol{G}_N)\boldsymbol{e}_d^{'} = \mathcal{T}_L(\boldsymbol{G}_{1,N_1})\boldsymbol{e}_d = \widetilde{\boldsymbol{g}}_1 = \boldsymbol{T}_1\boldsymbol{h}_1,
\end{aligned} \tag{II.5.14}$$

and where, $\boldsymbol{e}_d^{'}$ and $\boldsymbol{e}_d$ are vectors of appropriate dimensions with all zeros and one 1 selecting the desired column in $\mathcal{T}_L(\boldsymbol{G}_N)$ and $\mathcal{T}_L(\boldsymbol{G}_{1,N_1})$ respectively. We can write the channel convolution matrix $\mathcal{T}_L(\boldsymbol{G}_N)$ as

$$\mathcal{T}_L(\boldsymbol{G}_N) = \widetilde{\boldsymbol{g}}_1\boldsymbol{e}_d^{'T} + \mathcal{T}_L(\boldsymbol{G}_N)P_{\boldsymbol{e}_d^{'}\perp} = [\widetilde{\boldsymbol{g}}_1 \quad \boldsymbol{T}_2^H]\boldsymbol{B}, \tag{II.5.15}$$

for some $\boldsymbol{B}$. Then we can write,

$$\begin{aligned}
\mathcal{T}_L^H(\boldsymbol{G}_N)\left(\boldsymbol{T}_1^H - \boldsymbol{T}_2^H\boldsymbol{Q}^H\right) =& \boldsymbol{e}_d^{'}\boldsymbol{h}_1^H\boldsymbol{T}_1\boldsymbol{T}_1^H + \boldsymbol{B}^H\begin{bmatrix}\widetilde{\boldsymbol{g}}_1\boldsymbol{T}_1^H \\ \boldsymbol{0}\end{bmatrix} - \boldsymbol{B}^H\begin{bmatrix}\boldsymbol{0} \\ \boldsymbol{T}_2\boldsymbol{T}_2^H\end{bmatrix}\boldsymbol{Q}^H \\
=& \boldsymbol{e}_d^{'}\boldsymbol{h}_1^H\boldsymbol{T}_1\boldsymbol{T}_1^H + \boldsymbol{B}_1^H\widetilde{\boldsymbol{g}}_1^H\boldsymbol{T}_1^H - \boldsymbol{B}_2^H\left(\boldsymbol{T}_2\boldsymbol{T}_2^H\right)\boldsymbol{Q}^H.
\end{aligned} \tag{II.5.16}$$

Note that $\boldsymbol{e}_d^{'H}\boldsymbol{B}_i^H = 0, i \in \{1,2\}$. This implies that the first term on the R.H.S. of (II.5.17) is not predictable from the third. Therefore, if the second term is perfectly predictable from the third, then the two terms cancel each other out and $\boldsymbol{R}_{ZZ}$ turns out to be rank-1, and $\hat{\boldsymbol{h}}_1 = \left(\boldsymbol{T}_1\boldsymbol{T}_1^H\right)^{-1}V_{\max}(\boldsymbol{R}_{ZZ})$.

II.5.4.2 Correlated symbols

In the case of correlated symbols, with a finite amount of data, given the conditions in (II.5.15), it still holds that $\operatorname{span}\{\mathcal{T}_L^H(\boldsymbol{G}_N)\boldsymbol{T}_2^H\} = \operatorname{span}\{P_{\boldsymbol{e}_d^{'}\perp}\mathcal{T}_L(\boldsymbol{G}_N)\}$. Now, we can write the received vector $\boldsymbol{Y}_L(n)$ as

$$\boldsymbol{Y}_L(n) = \mathcal{T}_L(\boldsymbol{G}_N)\boldsymbol{A} = \mathcal{T}_L(\boldsymbol{G}_N)\boldsymbol{e}_d^{'}a_1(n-d) + \overline{\mathcal{T}}_L\bar{\boldsymbol{A}}. \tag{II.5.17}$$

Now, the estimation of $\boldsymbol{T}_1\boldsymbol{Y}$ in terms of $\boldsymbol{T}_2\boldsymbol{Y} = \boldsymbol{T}_2\mathcal{T}_L(\boldsymbol{G}_N)\boldsymbol{A} = \boldsymbol{T}_2\overline{\mathcal{T}}_L\bar{\boldsymbol{A}}$ is equivalent to estimation of $\boldsymbol{T}_1\boldsymbol{Y}$ in terms of $\bar{\boldsymbol{A}}$.

$$\begin{aligned}
\widetilde{\boldsymbol{T}_1\boldsymbol{Y}}|_{\boldsymbol{T}_2\boldsymbol{Y}} &= \boldsymbol{T}_1\boldsymbol{Y} - \widehat{\boldsymbol{T}_1\boldsymbol{Y}} \\
&= \boldsymbol{T}_1\boldsymbol{Y} - \left(\boldsymbol{T}_1\boldsymbol{R}_{YY}^d\boldsymbol{T}_2^H\right)\left(\boldsymbol{T}_2\boldsymbol{R}_{YY}^d\boldsymbol{T}_2^H\right)^{-1}\boldsymbol{T}_2\boldsymbol{Y} \\
\widetilde{\boldsymbol{T}_1\boldsymbol{Y}}|_{\bar{\boldsymbol{A}}} &= \boldsymbol{T}_1\mathcal{T}_L(\boldsymbol{G}_N)\boldsymbol{e}_d^{'}\tilde{a}_1(n-d) \\
&= \boldsymbol{T}_1\boldsymbol{T}_1^H\boldsymbol{h}_1\tilde{a}_1(n-d)|_{\bar{\boldsymbol{A}}}.
\end{aligned} \tag{II.5.18}$$

This results in,

$$\left(\boldsymbol{T}_1 \boldsymbol{R}_{YY}^{-d} \boldsymbol{T}_1^H\right)^{-1} = \sigma^2_{\tilde{a}_1(n-d)|\bar{\boldsymbol{A}}} \boldsymbol{h}_1 \boldsymbol{h}_1^H, \tag{II.5.19}$$

The rank-1 results in a normalized estimate of the channel. It must however be noted that the estimation error variance of the desired symbol is now smaller ($\sigma^2_{\tilde{a}_1(n-d)} < \sigma^2_a$).

II.5.5 Identifiability Conditions for the Blind MMSE-ZF Receiver

Let us continue with the assumption of uncorrelated symbols. We also consider the noiseless case, or the denoised version of second-order statistics of the received signal, i.e., $\boldsymbol{R}_{YY}$ is replaced by $\boldsymbol{R}^d_{YY} = \sigma_a^2 \mathcal{T}_L(\boldsymbol{G}_N)\mathcal{T}_L^H(\boldsymbol{G}_N)$. Then, we see from the derviations in section § II.5.4.1, that

$$\min_{\boldsymbol{f}:\boldsymbol{f}^H\widetilde{\boldsymbol{g}}_1=1} \boldsymbol{f}^H \boldsymbol{R}^d_{YY} \boldsymbol{f} = \sigma_a^2, \quad \textit{iff} \quad \boldsymbol{f}^H \mathcal{T}_L(\boldsymbol{G}_N) = \boldsymbol{e}_d^{'T}, \tag{II.5.20}$$

i.e., the zero-forcing condition must be satisfied. Hence, the unbiased MOE criterion corresponds to ZF in the noiseless case. This implies that $\mathrm{MOE}(\hat{\widetilde{\boldsymbol{g}}}_1) < \sigma_a^2$ *if* $\hat{\widetilde{\boldsymbol{g}}}_1 \not\sim \widetilde{\boldsymbol{g}}_1$. We consider that:

(i). *FIR zero-forcing conditions are satisfied*, and
(ii). $\mathrm{span}\{\mathcal{T}_L(\boldsymbol{G}_N)\} \cap \mathrm{span}\{\boldsymbol{T}_1^H\} = \mathrm{span}\{\boldsymbol{T}_1^H \boldsymbol{h}_1\}$.

The two step max/min problem boils down to

$$\max_{\hat{\boldsymbol{h}}_1:\|\hat{\boldsymbol{h}}_1\|=1} \hat{\boldsymbol{h}}_1^H \left(\boldsymbol{T}_1 \boldsymbol{T}_1^H\right)^{-1} \boldsymbol{T}_1 \mathcal{T}_L P^{\perp}_{\mathcal{T}_L^H \boldsymbol{T}_2^H} \mathcal{T}_L^H \boldsymbol{T}_1^H \left(\boldsymbol{T}_1 \boldsymbol{T}_1^H\right)^{-1} \hat{\boldsymbol{h}}_1, \tag{II.5.21}$$

where, $P^{\perp}_{\boldsymbol{X}} = \boldsymbol{I} - \boldsymbol{X}(\boldsymbol{X}^H\boldsymbol{X})^{-1}\boldsymbol{X}^H$. Then identifiability implies that

$$\mathcal{T}_L P^{\perp}_{\mathcal{T}_L^H \boldsymbol{T}_2^H} \mathcal{T}_L^H = \boldsymbol{T}_1^H \boldsymbol{h}_1 \boldsymbol{h}_1^H \boldsymbol{T}_1 = \widetilde{\boldsymbol{g}}_1 \widetilde{\boldsymbol{g}}_1^H,$$

or

$$P^{\perp}_{\mathcal{T}_L^H \boldsymbol{T}_2^H} \mathcal{T}_L^H(\boldsymbol{G}_N) = P_{\boldsymbol{e}_d'} \mathcal{T}_L^H(\boldsymbol{G}_N), \tag{II.5.22}$$

Condition (i) above implies that $\boldsymbol{e}_d' \in \mathrm{span}\{\mathcal{T}_L^H(\boldsymbol{G}_N)\}$. From condition (ii), since $\boldsymbol{T}_1^H \boldsymbol{h}_1 = \mathcal{T}_L(\boldsymbol{G}_N)\boldsymbol{e}_d'$, we have

$$\begin{aligned} \mathrm{span}\{\mathcal{T}_L(\boldsymbol{G}_N)\boldsymbol{T}_2^H\} &= \mathrm{span}\{P^{\perp}_{\boldsymbol{e}_d'} \mathcal{T}_L^H(\boldsymbol{G}_N)\} \\ \mathrm{span}\{\mathcal{T}_L^H(\boldsymbol{G}_N)\} &= \mathrm{span}\{\mathcal{T}_L^H(\boldsymbol{G}_N)\boldsymbol{T}_2^H\} \oplus \mathrm{span}\{\boldsymbol{e}_d'\} \end{aligned} \tag{II.5.23}$$

from which, $\mathcal{T}_L^H(\boldsymbol{G}_N) = P_{\mathcal{T}_L^H \boldsymbol{T}_2^H} \mathcal{T}_L^H(\boldsymbol{G}_N) + P_{\boldsymbol{e}_d'} \mathcal{T}_L^H(\boldsymbol{G}_N)$, which is the same as (II.5.22).

II.5.5.1 A Note on Sufficiency of Conditions

We consider first the conditions **(i)**. Furthermore, in the following developments, we consider that $K < PMJ$, which is easily achievable with a small (e.g, 2) multiple sensor and/or oversampling factor. The effective number of channels is given by $(PMJ)_{\text{eff}} = \mathrm{rank}\{\boldsymbol{G}_N\}$, where $\boldsymbol{G}_N$ is given in (I.3.23). Let $\mathbf{G}_1(z) = \sum_{n=0}^{N_1-1} \boldsymbol{g}_1(n) z^{-n}$ be the channel transfer function for user 1, with $\mathbf{G}(z) = [\mathbf{G}_1(z) \cdots \mathbf{G}_K(z)]$. Then let us assume the following:

(**a**). $\mathbf{G}(z)$ *is irreducible*, i.e., $\quad \mathrm{rank}\{\mathbf{G}(z)\} = K, \forall z.$
(**b**). $\mathbf{G}(z)$ *is column reduced*: $\quad \mathrm{rank}\{[\boldsymbol{g}_1(N_1-1)\cdots\boldsymbol{g}_K(N_K-1)]\} = K.$

Given that the above two conditions hold, the channel convolution matrix $\mathcal{T}(\boldsymbol{G}_N)$ is full rank w.p. 1, and the FIR length L required is given by,

$$L \geq \overline{L} = \left\lceil \frac{N-K}{(PMJ)_{\text{eff}} - K} \right\rceil. \tag{II.5.24}$$

Note that condition (**a**) holds with probability 1 due to the quasi-orthogonality of spreading sequences. As for (**b**), it can be violated in certain limiting cases e.g., in the synchronous case where $\boldsymbol{g}_k(N_k-1)$'s contain very few non-zero elements. Under these circumstances, instantaneous (static) mixture of the sources can null out some of the $\boldsymbol{g}_k(N_k-1)$ (more specifically, at most $K-1$ of them). Then N gets reduced by at most $K-1$. However, even then, L given by (II.5.24) remains sufficient.

The condition (**ii**) can be restated as the following dimensional requirement:

$$\mathrm{rank}\{\mathcal{T}_L(\boldsymbol{G}_N)\} + \mathrm{rank}\{\boldsymbol{T}_1^H\} \leqslant \mathrm{row}\{\mathcal{T}_L(\boldsymbol{G}_N)\} + 1, \tag{II.5.25}$$

from where, under the irreducible channel and column reduced conditions,

$$L \geq \underline{L} = \left\lceil \frac{N - K + \Psi_1 MJ - 1}{(PMJ)_{\text{eff}} - K} \right\rceil, \tag{II.5.26}$$

where, Ψ_1 is the channel length for user 1 in chip periods. If (II.5.26) holds, then condition (**ii**) is fulfilled w.p. 1, regardless of the N_k's, i.e., the $\mathrm{span}\{\boldsymbol{T}_1^H\}$ does not intersect with all shifted versions of $\boldsymbol{g}_k$'s, $\forall k \neq 1$, i.e., the columns of $\mathcal{T}_L(\boldsymbol{G}_N)$, which further means that no confusion is possible between the channel of the user of interest and those of other users, whether the mixing is static (same orders) or dynamic (different channel lengths), with lengths measured in symbol periods.

*II.5.5.2 Violation of condition **(ii)***

If the length Ψ_1, of $\boldsymbol{h}_1$ is over-estimated by such a number that N_1 gets over-estimated, then condition (**ii**) is violated w.p. 1. In that case, more than one shifted versions of $\boldsymbol{g}_1$ will fit in the column space of $\boldsymbol{T}_1^H$. The estimated channel in that case can be expressed as $\widehat{\mathbf{G}}_1(z) = \mathbf{G}_1(z)b(z)$, where, $b(z)$ is a scalar polynomial of the order that equals the amount by which the channel has been over- estimated. An ad hoc but expensive solution to this would be to try all orders for N_1 and stop at the correct one. Once, the delay estimates have been obtained, however, overestimation of the channel order is highly unlikely in most DS-CDMA systems, where, the delay spread $\Psi < P$, and in which case, $N_k = 2$ for a synchronized user k.

II.5.6 Case of Sparse Channels

An immediate extension to the case of sparse channels can be made by considering the relations (I.3.23) including the pulse shaping filter $p(t)$ and the low-pass front end RX filter. In that case, we simply redefine $\boldsymbol{T}_1$ and $\boldsymbol{T}_2$ as

$$\boldsymbol{T}_1 = \begin{bmatrix} \mathbf{0} & \widetilde{\widetilde{\boldsymbol{C}}}_1^H & \mathbf{0} \end{bmatrix}, \text{and} \quad \boldsymbol{T}_2 = \begin{bmatrix} \boldsymbol{I} & \mathbf{0} & \mathbf{0} \\ \mathbf{0} & \widetilde{\widetilde{\boldsymbol{C}}}_1^{\perp} & \mathbf{0} \\ \mathbf{0} & \mathbf{0} & \boldsymbol{I} \end{bmatrix}, \tag{II.5.27}$$

so that ($\widetilde{\widetilde{\boldsymbol{C}}}_1^{\perp H}\widetilde{\widetilde{\boldsymbol{C}}}_1 = \mathbf{0}$). Note that the number of columns in $\widetilde{\widetilde{\boldsymbol{C}}}_1$ is much lesser than in $\boldsymbol{C}_1$. Thus the main GSC branch is tuned to a few fingers of the channel represented by $\widetilde{\boldsymbol{\phi}}_{1,m}$ at the mth receiver sensor. The identifiability conditions presented in section § II.5.5 will be accordingly modified and the stacking factor required, L, will be reduced. Then, $\Psi_1 MJ$ will be replaced by MQ in equation (II.5.26).

II.5.7 Two-Sided Linear Prediction

We can give one more interpretation of the MMSE-ZF receiver in terms of two-sided linear prediction (TSLP) of the received signal. Let us consider the noiseless case ($v(t) \equiv 0$), and replace the $\boldsymbol{T}_1$ and $\boldsymbol{T}_2$ in (II.5.7) by,

$$\overline{\boldsymbol{T}}_1 = \begin{bmatrix} \mathbf{0} & \boldsymbol{I}_{PN_1} & \mathbf{0} \end{bmatrix} \otimes \boldsymbol{I}_{MJ}, \text{ and } \quad \overline{\boldsymbol{T}}_2 = \begin{bmatrix} \boldsymbol{I} & \mathbf{0} & \mathbf{0} \\ \mathbf{0} & \mathbf{0} & \boldsymbol{I} \end{bmatrix} \otimes \boldsymbol{I}_{MJ}, \tag{II.5.28}$$

This corresponds to the *least squares smoothing* approach of [TZ98] in a single user case. We can proceed with a similar treatment as previously discussed in section II.5.4 for the GSC implementation of the unbiased MOE algorithm. However, now,

$$\text{rank}\{\boldsymbol{R}_{ZZ}\} \geq \overline{K}, \tag{II.5.29}$$

where $\overline{K}$ denotes the number of users with channel orders shorter than or equal to N_1 [GS99b] [ZT98]. A mixture (instantaneous when channel orders are the same) of different users' channels is now obtained. In the event of $\overline{K} = 1$ (the desired user), the composite channel vector $\widetilde{\boldsymbol{g}}_1$ can be obtained from the rank-1 $\boldsymbol{R}_{ZZ}$, although the stacking factor L required will be much longer than $\underline{L}$ given by (II.5.26).

From the above discussion it is obvious that the two-sided linear prediction approach has some capability of multiuser interference cancelation in very special situations ($N_1 < N_k,\ \forall k \neq 1$). However, for the DS-CDMA problem under discussion, the presence of $\boldsymbol{C}_1^{\perp}$ term in the blocking matrix $\boldsymbol{T}_2$ "cleans up" the contributions of interfering users without regard to their channel orders, and highlights the great degree of robustness of the system *vis-à-vis* the channel and thus receiver identification issue.

II.6 Numerical Examples

We consider $K = 5$ asynchronous users in the system with a spreading factor of $P = 16$. The channel $\boldsymbol{h}_k$ (including the pulse shaping filter) for the kth user is modeled as a FIR channel of order Ψ_k ranging from $8 - 21$ chip periods for different k's. The channel delay spread is therefore shorter than one symbol period for some users while longer for others. Mild near-far conditions prevail in that the interfering users are randomly (ranging from 8 to 15 dB.) stronger than the user of interest. Fig. II.2 shows the bit error-rate performance of the blind MMSE-ZF receiver and the MMSE receiver ($\sigma_a^2 \widehat{\boldsymbol{R}}_{YY}^{-1}\widetilde{\boldsymbol{g}}_1$). It can be seen that the performance depends on the quality of the correlation matrix estimate. Better results are therefore obtained if more data is available. This figure highlights the major drawback in the implementation of second-order statistics based linear receiver algorithms. Under power controlled conditions, with good choice of spreading sequences, and a small loading fraction, a simple RAKE receiver may outperform the linear receivers, unless a good estimate of $\widehat{\boldsymbol{R}}_{YY}$ is available. On the other hand, as seen in fig. II.3, the channel is estimated fairly accurately (normalized mean

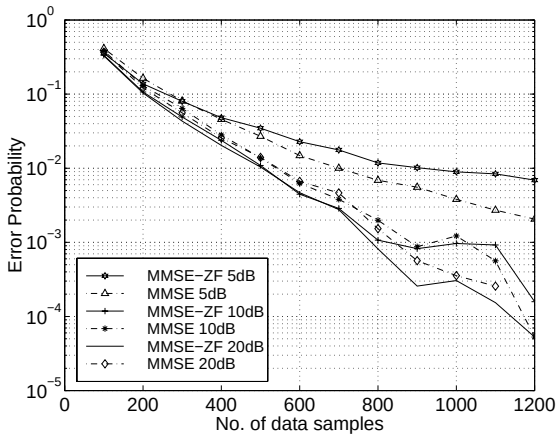

Figure II.2: Measured bit-error rate performance for $P = 16$, and $K = 5$ users for different size of data blocks used in the estimation algorithm.

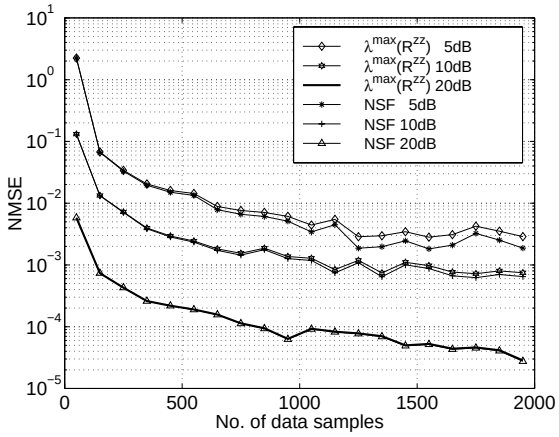

Figure II.3: Channel estimation performance for $P = 16$, and $K = 5$ users for different size of data blocks used in the estimation algorithm.

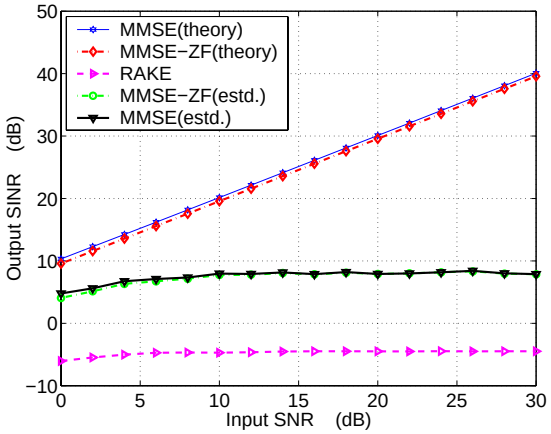

Figure II.4: Output SINR performance of different receivers in near-far conditions for spreading factor, P=16, and K=5 users.

squared error[2] (NMSE) of the order of -25 dB at 20 dB SNR) with a data block size of $70 - 100$ symbols from the rank-1 $\boldsymbol{R}_{ZZ}$ (see section II.5.4). Performance of the noise-subspace fitting based algorithm [TX97a] is also shown for several input SNR's.

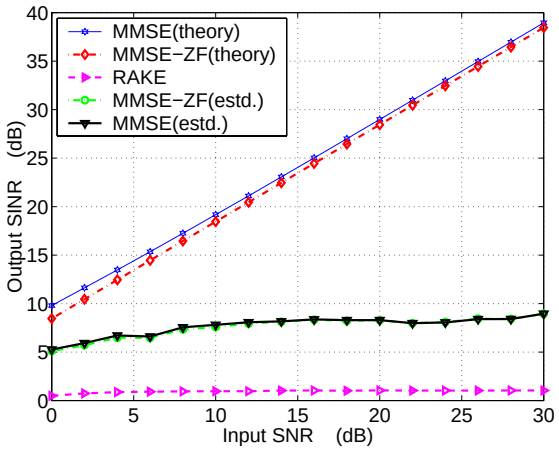

Figure II.5: Output SINR performance of different receivers in power-controlled conditions for spreading factor, P=16, and K=5 users.

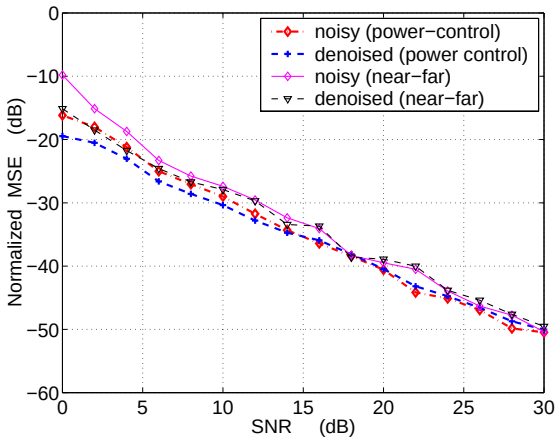

Figure II.6: Normalized channel estimation MSE for the denoised and non-denoised $\boldsymbol{R}_{YY}$, for spreading factor, P=16, and K=5 users

In fig. II.4 and II.5, we show the performance of blind MMSE-ZF receiver in near-far and power-controlled conditions, respectively, and compare it with that of the theoretical curve for the MMSE ($\boldsymbol{R}_{YY} = \sigma_a^2 \mathcal{T}_L(\boldsymbol{G}_N)\mathcal{T}_L(\boldsymbol{G}_N) + \sigma_v^2 \boldsymbol{I}$), and the theoretical MMSE-ZF (II.2.5) receivers. A data record of 200 data samples is employed to estimate the receivers. It comes as no surprise that the optimal unbiased MMSE is not approached by any of the other receivers due to finite data effect. A theoretical curve for the MMSE-ZF is also provided. Fig. II.6 shows the quality of the channel estimates for the case when denoised statistics are employed in the unbiased MOE algorithm. It can be observed that the blind channel estimate is relatively near-far resistant.

[2] NMSE$= E\frac{\|\boldsymbol{h}_1 - \hat{\boldsymbol{h}}_1\|^2}{\|\boldsymbol{h}_1\|^2} = \frac{1}{N}\sum_{i=1}^{N} \frac{\|\boldsymbol{h}_1 - \hat{\boldsymbol{h}}_1^{(i)}\|^2}{\|\boldsymbol{h}_1\|^2}$

II.7 Receivers from Other Projections and Reduced Complexity Blind Channel Estimation

Let $\boldsymbol{f}$ be any linear receiver applied to the received data $\boldsymbol{Y}_L(n)$. A linear estimate of the desired symbol $a_1(n-d)$ is obtained as $\hat{a}_1(n-d) = \boldsymbol{f}^H \boldsymbol{Y}_L(n)$. If the channel convolution matrix $\mathcal{T}(\boldsymbol{G}_N)$ were known, a minimal noise-enhancing projection (decorrelating) receiver [GS99c] could be obtained simply as $\boldsymbol{f} = P_{\overline{\mathcal{T}}}^{\perp} \widetilde{\boldsymbol{g}}_1$, where $P_{\overline{\mathcal{T}}}^{\perp} = \boldsymbol{I} - P_{\overline{\mathcal{T}}}$, $P_X = X(X^H X)^{-1} X^H$ is the projection operator, and $\overline{\mathcal{T}}$ is the channel convolution matrix $\mathcal{T}(\boldsymbol{G}_N)$ without the column $\widetilde{\boldsymbol{g}}_1$. However, as shown in II.5.2, the projection receiver or the MMSE-ZF can be obtained blindly from the received signal second-order statistics and only the desired user's timing and spreading sequence knowledge.

We maintain the notation introduced in (II.5.7) where, $\boldsymbol{T}_1$ and $\boldsymbol{T}_2$ represent the *partial signature* or the transmit filter (including the pulse shape and the signature) of the desired user and its orthogonal complement respectively, so that the desired user's overall channel is written as $\widetilde{\boldsymbol{g}}_1 = \boldsymbol{T}_1^H \boldsymbol{h}_1$, and $\boldsymbol{T}_2 \boldsymbol{T}_1^H = \boldsymbol{0}$ ($\boldsymbol{C}_1^{\perp} \boldsymbol{C}_1 = \boldsymbol{0}$). Then the projection receiver can be obtained in a simple manner as indicated by the following proposition.

Proposition 1: Any receiver vector $\boldsymbol{f}$ obtained as the eigenvector lying the noise subspace of the of the matrix $\boldsymbol{R}_{YY}^d \boldsymbol{T}_2^H \boldsymbol{T}_2 \boldsymbol{R}_{YY}^d$ is a projection receiver.

Proof: See appendix B.

$\boldsymbol{R}_{YY}^d$ denotes the noiseless or the denoised version of the received signal covariance matrix $\boldsymbol{R}_{YY}$.

II.7.1 Existence of the Projection Receiver

Let us consider the noiseless case ($v(t) \equiv 0$). The above result can be interpreted in terms of the signal and noise subspaces $\mathcal{B}_s$ and $\mathcal{B}_n$, of $\boldsymbol{R}_{YY}^d$ and $\mathcal{U}_s$ and $\mathcal{U}_n$ of $\boldsymbol{R}_{YY}^d \boldsymbol{T}_2^H \boldsymbol{T}_2 \boldsymbol{R}_{YY}^d$. The receiver vector $\boldsymbol{f}$ lies in the signal subspace, $\mathcal{B}_s$ but it also lies in $\mathcal{U}_n$. If the intersection of the two subspaces is one-dimensional, then $\boldsymbol{f}$ exists. This condition is simply the condition (**ii**) of section §II.5.5, leading to the same stacking factor as given by (II.5.26). Note that $\mathrm{rank}\{\overline{\mathcal{T}}\} = \mathrm{rank}\{P_{\boldsymbol{T}_2^H} \overline{\mathcal{T}}\}$, since,

$$\mathrm{span}\{\mathcal{T}_L(\boldsymbol{G}_N)\} \subset \mathrm{span}\{\boldsymbol{T}_2^H\} \oplus \mathrm{span}\{\widetilde{\boldsymbol{g}}_1\}. \tag{II.7.1}$$

Furthermore,

$$\mathrm{span}\{\mathcal{T}_L(\boldsymbol{G}_N)\} \cap \mathrm{span}\{\boldsymbol{T}_2^H\} = \mathrm{span}\{\overline{\mathcal{T}}\}. \tag{II.7.2}$$

Hence, the projection of $\overline{\mathcal{T}}$ on the range space of $\boldsymbol{T}_2^H$ is a projection on a larger dimensional subspace. The noise subspace of $\overline{\mathcal{T}}\,\overline{\mathcal{T}}^H P_{\boldsymbol{T}_2^H} \overline{\mathcal{T}}\,\overline{\mathcal{T}}^H$ is therefore a subset of the noise subspace of $\overline{\mathcal{T}}\,\overline{\mathcal{T}}^H$. We know that any vector lying in the noise subspace of the latter qualifies as a projection receiver. Hence, any vector in the subset of this noise subspace does so as well.

Alternatively, we can see that the dimension of $\mathcal{B}_n$ is $PMJL - (N + K(L-1))$ while $\mathcal{U}_n$ contains exactly one more vector, if the above conditions are satisfied. Needless to say, that the span and rank conditions are satisfied w.p. 1 for the case of randomly chosen spreading sequences. It is also observable that given that the condition (II.5.25) is satisfied, the criterion by construction leads to zero only if $\boldsymbol{R}_{YY}^d \boldsymbol{f} = \widetilde{\boldsymbol{g}}_1$.

Unfortunately, the performance of $\boldsymbol{f}$ thus obtained is extremely poor due to the estimation errors in the signal covariance matrix, especially for short data records, and in the low SNR region. The former

is an estimation problem. Temporal averaging for $\widehat{\boldsymbol{R}}_{YY}$ requires a large number of data samples to give a consistent estimate. The latter is due to the large noise enhancement, since the projection is on a subspace orthogonal to a large dimensional subspace ($\widetilde{\mathcal{T}}_i$ instead of $\overline{\mathcal{T}}$) for the decorrelator). However, interference is still rejected if the subspace structure exists and the receiver vector somewhat compensates for the estimation errors in $\boldsymbol{R}_{YY}$ in the estiamtion of the channel vector.

Proposition 2: A channel estimate can be obtained from the projection receiver exploiting the fact that the latter lies in the signal subspace.

Proof: See appendix C.

II.7.2 Uniqueness of the Projection Receiver

The matrix $\mathcal{Q}_i$ in appendix B is not unique which means that the orthogonal decompositions are as many as the dimension of the noise subspace of $\sigma_a^2\overline{\mathcal{T}}\,\overline{\mathcal{T}}^H$. In other words, all noise subspace vectors in $\mathcal{U}_n$ qualify as projection receivers. Note, however, that the objective in the above approach is to obtain an estimate of the channel impulse response, $\widetilde{\boldsymbol{g}}_1$, and not to estimate the receiver vector (which results in very poor performance). Any of the $\mathcal{Q}_i$'s therefore suffices for our purpose.

II.8 Numerical Examples

We consider the same simulations scenario as for the blind MMSE-ZF receiver discussed above. As mentioned, the receiver performance is very poor since a projection on a very low rank of the interference free subspace is obtained. The interest is to observe the channel estimate obtained from these projections. Fig. II.7 shows the normalized mean-square error (NMSE) [3] of channel estimates for the proposed method. Channel estimated from Capon's method (the MVDR approach) is also shown. It can be seen that the performance of the blind projection receiver based method falls short of the MVDR method by several dB's, but as this example exhibits, this quality of channel estimates is largely sufficient for most purposes.

II.9 Conclusions

The blind MMSE-ZF or the projection receiver for DS-CDMA was presented in this chapter. This receiver is the ZF solution that leads to the minimum noise enhancement among all possible ZF receivers, and is also called the decorrelating receiver in the literature.

The receiver was shown to be the proper extension of the anchored MOE receiver [HMV95] to the general asynchronous case in multipath channels, leading to the distortionless response for the desired symbol of the desired user. It was also demonstrated, that the receiver is obtainable from the blind unbiased linear MOE criterion in a decentralized manner. A simpler implementation in the form of a Generalized Side-lobe Canceler (GSC) or the MVDR was also shown. In terms of its implementation, the blind algorithm, like the MMSE linear receiver, requires a large amount of data for the estimation of the channel covariance matrix thus making it rather impractical for rapidly changing environments (fast fading) and large numbers of users ($K \rightarrow P$). Such algorithms can find their utility in indoor

[3] NMSE$= E\frac{\|\boldsymbol{h}_1-\hat{\boldsymbol{h}}_1\|^2}{\|\boldsymbol{h}_1\|^2} = \frac{1}{L}\sum_{i=1}^{L}\frac{\|\boldsymbol{h}_1-\hat{\boldsymbol{h}}_1^{(i)}\|^2}{\|\boldsymbol{h}_1\|^2}$

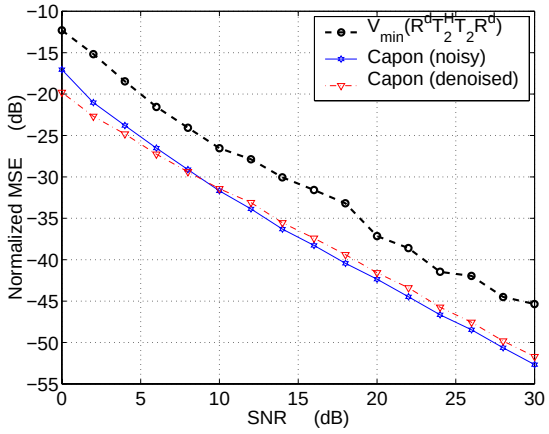

Figure II.7: Channel estimates from the Capon's method and the projection algorithm, $P = 16$**,** $K = 5$**.**

wireless LANs where channels change at relatively slow rates and a fair amount of data is available for the estimation of the covariance matrix. A possible implementation can be at the uplink, where, knowledge of spreading codes and timing of all users in the cell can be exploited to obtain a better $\hat{\boldsymbol{R}}_{YY}$.

Identifiability conditions of the blind MMSE-ZF receiver, for channels of arbitrary length (even longer than a symbol period) were given and it was shown that the channel is blindly identifiable w.p.1 (up to a scalar phase factor), unless it is overestimated. The likelihood of overstimation in DS-CDMA systems with large spreading gains is low, but cannot be ruled out if delay spread is of the order of or is larger than the spreading gain.

Alternative projections were also discussed and it was shown that even though a projection receiver itself may perform poorly, being obtained from a projection on a very low rank subspace of the desired decorrelation subspace, it is still sufficient to give a channel estimate of reasonable quality. This rather surprising phenomenon can be explained as the attempt of the projection receiver to compensate for finite-data estimation errors of the correlation matrix of the received signal,

Appendix IIA

The MMSE-ZF receiver was derived in section II.2 as $\boldsymbol{f}^H = \boldsymbol{e}_d^T(\mathcal{T}^H\mathcal{T})^{-1}\mathcal{T}^H$, where, we $\mathcal{T}$ denotes here, a column-permuted version of the channel convolution matrix $\mathcal{T}(\boldsymbol{G}_N)$, i.e.,

$$\mathcal{T} = [\widetilde{\boldsymbol{g}}_1 \quad \overline{\mathcal{T}}]\,, \text{ with } \quad \widetilde{\boldsymbol{g}}_1 = \mathcal{T}\boldsymbol{e}_d\,, \text{ and } \quad \boldsymbol{e}_d = [1\ 0\ \cdots\ 0]\,.$$

Let us further define a square transformation matrix, $\mathcal{Q}$, given by

$$\mathcal{Q} = \begin{bmatrix} 1 & \boldsymbol{0} \\ \boldsymbol{X} & \boldsymbol{I} \end{bmatrix}, \tag{II.9.1}$$

so that

$$\mathcal{T}\mathcal{Q} = [\widetilde{\boldsymbol{g}}_1 \quad \overline{\mathcal{T}}] \begin{bmatrix} 1 & \boldsymbol{0} \\ \boldsymbol{X} & \boldsymbol{I} \end{bmatrix} = \left[P^{\perp}_{\overline{\mathcal{T}}}\widetilde{\boldsymbol{g}}_1 \quad \overline{\mathcal{T}}\right] \triangleq \overline{\overline{\mathcal{T}}}, \tag{II.9.2}$$

and,

$$\overline{\overline{\mathcal{T}}}\mathcal{Q}^{-1} = \left[P_{\overline{\overline{\mathcal{T}}}}^{\perp}\widetilde{\boldsymbol{g}}_1 \quad \overline{\mathcal{T}} \right] \begin{bmatrix} 1 & \mathbf{0} \\ -\boldsymbol{X} & \boldsymbol{I} \end{bmatrix} = [\widetilde{\boldsymbol{g}}_1 \quad \overline{\mathcal{T}}] = \mathcal{T}, \tag{II.9.3}$$

and where, $\boldsymbol{X} = -(\overline{\mathcal{T}}^H\overline{\mathcal{T}})^{-1}\overline{\mathcal{T}}^H\widetilde{\boldsymbol{g}}_1$. Then, the MMSE-ZF receiver can be written as

$$\begin{aligned} \boldsymbol{f}^H &= \boldsymbol{e}_d^T \left[(\overline{\overline{\mathcal{T}}}\mathcal{Q}^{-1})^H (\overline{\overline{\mathcal{T}}}\mathcal{Q}^{-1}) \right]^{-1} (\overline{\overline{\mathcal{T}}}\mathcal{Q}^{-1})^H \\ &= \boldsymbol{e}_d^T \mathcal{Q} \left(\overline{\overline{\mathcal{T}}}^H \overline{\overline{\mathcal{T}}} \right)^{-1} \overline{\overline{\mathcal{T}}}^H \\ &= \boldsymbol{e}_d^T \begin{bmatrix} 1 & \mathbf{0} \\ \boldsymbol{X} & \boldsymbol{I} \end{bmatrix} \begin{bmatrix} \widetilde{\boldsymbol{g}}_1^H P_{\overline{\mathcal{T}}}^{\perp} \widetilde{\boldsymbol{g}}_1 & \mathbf{0} \\ \mathbf{0} & \overline{\mathcal{T}}^H\overline{\mathcal{T}} \end{bmatrix}^{-1} \begin{bmatrix} (P_{\overline{\mathcal{T}}}^{\perp}\widetilde{\boldsymbol{g}}_1)^H \\ \overline{\mathcal{T}}^H \end{bmatrix} \\ &= \frac{1}{\widetilde{\boldsymbol{g}}_1^H P_{\overline{\mathcal{T}}}^{\perp}\widetilde{\boldsymbol{g}}_1} \widetilde{\boldsymbol{g}}_1^H P_{\overline{\mathcal{T}}}^{\perp}, \end{aligned} \tag{II.9.4}$$

where $P_{\overline{\mathcal{T}}}^{\perp}$ is the projection operator that projects the received data vector $\boldsymbol{Y}_L(n)$ onto the low rank subspace defined by the orthogonal complement of the subspace spanned by the columns of $\overline{\mathcal{T}}$, and matched filtering with $\widetilde{\boldsymbol{g}}_1$ is the projection on the one-dimensional subspace matched to the desired signal. ■

Appendix IIB

For the purpose of this discussion let us consider the input symbols to be *i.i.d.*, with $\sigma_a^2 = 1$. In order to show that $\boldsymbol{f}$ is a projection receiver, we write the cost function as

$$\min_{\boldsymbol{f}:\|\boldsymbol{f}\|=1} \boldsymbol{f}^H \boldsymbol{R}_{YY} \boldsymbol{T}_2^H \boldsymbol{T}_2 \boldsymbol{R}_{YY} \boldsymbol{f}, \tag{II.9.5}$$

Let us express a column permuted version of the channel convolution matrix $\mathcal{T}(\boldsymbol{G}_N)$ as $\mathcal{T} = [\widetilde{\boldsymbol{g}}_1 \quad \overline{\mathcal{T}}]$. Then, $\widetilde{\boldsymbol{g}}_1 = \mathcal{T}\boldsymbol{e}_d$, and $\boldsymbol{e}_d = [1\ 0\ \cdots\ 0]^T$. Let us define the eigen decomposition of $\overline{\mathcal{T}}\,\overline{\mathcal{T}}^H$ by

$$\begin{bmatrix} \mathcal{V}_s & \mathcal{V}_n \end{bmatrix} \begin{bmatrix} \Lambda_s & \mathbf{0} \\ \mathbf{0} & \mathbf{0} \end{bmatrix} \begin{bmatrix} \mathcal{V}_s \\ \mathcal{V}_n \end{bmatrix}. \tag{II.9.6}$$

Then we can write as

$$\boldsymbol{R}_{YY}^d = \begin{bmatrix} \widetilde{\boldsymbol{g}}_1 & \overline{\mathcal{T}} & \mathcal{V}_n \end{bmatrix} \begin{bmatrix} 1 & \mathbf{0} & \mathbf{0} \\ \mathbf{0} & \boldsymbol{I} & \mathbf{0} \\ \mathbf{0} & \mathbf{0} & \mathbf{0} \end{bmatrix} \begin{bmatrix} \widetilde{\boldsymbol{g}}_1^H \\ \overline{\mathcal{T}}^H \\ \mathcal{V}_n^H \end{bmatrix}. \tag{II.9.7}$$

Let us further define a square invertible transformation matrix, $\mathcal{Q}_1$, given by

$$\mathcal{Q}_1 = \begin{bmatrix} 1 & \mathbf{0} \\ \boldsymbol{X} & \boldsymbol{I} \end{bmatrix}, \tag{II.9.8}$$

so that

$$\left[\begin{array}{cc} \mathcal{T} & \mathcal{V}_{n,1} \end{array}\right] \mathcal{Q}_1 = \left[\begin{array}{cc} \widetilde{\boldsymbol{g}}_1 & \widetilde{\mathcal{T}}_1 \end{array}\right] \mathcal{Q}_1 = \left[P^{\perp}_{\widetilde{\mathcal{T}}_1}\widetilde{\boldsymbol{g}}_1 \quad \widetilde{\mathcal{T}}_1\right], \tag{II.9.9}$$

where, $\widetilde{\mathcal{T}}_1 = [\overline{\mathcal{T}} \quad \mathcal{V}_{n,1}]$, $\mathcal{V}_{n,1}$ denotes $n-1$ out of n orthonormal eigenvectors (thus all except the first) of the noise subspace of $\sigma_a^2\overline{\mathcal{T}}\,\overline{\mathcal{T}}^H$. $\boldsymbol{X} = -(\widetilde{\mathcal{T}}_1^H\widetilde{\mathcal{T}}_1)^{-1}\widetilde{\mathcal{T}}_1^H\widetilde{\boldsymbol{g}}_1$, and $P^{\perp}_{\widetilde{\mathcal{T}}_1}$ is the projection operator on the complementary subspace of $\widetilde{\mathcal{T}}_1$. In a similar fashion, we can write $\widetilde{\mathcal{T}}_2 = [\overline{\mathcal{T}} \quad \mathcal{V}_{n,2}]$, and so on up to $\widetilde{\mathcal{T}}_n$, where n is the dimension of $\mathcal{V}_n$. Each time we take $n-1$ vectors out of n to compose $\widetilde{\mathcal{T}}_i$, $i = 1, \ldots, n$. $\mathcal{Q}_i$, $i = 1, \ldots, n$ are the corresponding transformation matrices. Next, we define but do not specify an invertible transformation $\mathcal{Q}$ such that,

$$\left[\mathcal{T} \quad \mathcal{V}_n\right] \mathcal{Q} = \left[P^{\perp}_{\widetilde{\mathcal{T}}_1}\widetilde{\boldsymbol{g}}_1 \quad P^{\perp}_{\widetilde{\mathcal{T}}_2}\widetilde{\boldsymbol{g}}_1 \quad \cdots \quad P^{\perp}_{\widetilde{\mathcal{T}}_n}\widetilde{\boldsymbol{g}}_1 \quad \overline{\mathcal{T}}\right]. \tag{II.9.10}$$

Note that in the above formulation,

$$P^{\perp}_{\widetilde{\mathcal{T}}_i}\widetilde{\boldsymbol{g}}_1 = P_{\mathcal{V}_i}\widetilde{\boldsymbol{g}}_1, \tag{II.9.11}$$

and therefore,

$$\widetilde{\boldsymbol{g}}_1^H P^{\perp}_{\widetilde{\mathcal{T}}_1} P^{\perp}_{\widetilde{\mathcal{T}}_2}\widetilde{\boldsymbol{g}}_1 = 0,$$

and $[P^{\perp}_{\widetilde{\mathcal{T}}_1}\widetilde{\boldsymbol{g}}_1 \quad P^{\perp}_{\widetilde{\mathcal{T}}_2}\widetilde{\boldsymbol{g}}_1 \quad \cdots \quad P^{\perp}_{\widetilde{\mathcal{T}}_n}\widetilde{\boldsymbol{g}}_1]$ qualifies as the noise subspace of $\sigma_a^2\overline{\mathcal{T}}\,\overline{\mathcal{T}}^H$. Furthermore, from (II.7.2), the noise subspace of $\boldsymbol{R}^d_{YY}P_{T_2^H}\boldsymbol{R}^d_{YY}$ also qualifies as the noise subspace of $\sigma_a^2\overline{\mathcal{T}}\,\overline{\mathcal{T}}^H$. Moreover, both contain the contribution of $\widetilde{\boldsymbol{g}}_1$. This results in

$$\boldsymbol{f} = \zeta P^{\perp}_{\widetilde{\mathcal{T}}_i}\widetilde{\boldsymbol{g}}_1, \tag{II.9.12}$$

where ζ is a complex scalar scale factor, and $i = 1, \ldots, n$. ■

Appendix IIC

Let us continue with the noiseless case ($v(t) \equiv 0$). The overall channel for the desired user is determined from the projection receiver as

$$\boldsymbol{R}_{YY}\boldsymbol{f} = \zeta\widetilde{\boldsymbol{g}}_1. \tag{II.9.13}$$

We can write the left side of the above equation as

$$\begin{aligned}\zeta\widetilde{\boldsymbol{g}}_1 &= \sigma_a^2\left[\widetilde{\boldsymbol{g}}_1 \quad \widetilde{\mathcal{T}}_i\right]\left[\begin{array}{ccc} 1 & \mathbf{0} & \mathbf{0} \\ \mathbf{0} & \boldsymbol{I} & \mathbf{0} \\ \mathbf{0} & \mathbf{0} & \mathbf{0} \end{array}\right]\left[\begin{array}{c} \widetilde{\boldsymbol{g}}_1^H \\ \widetilde{\mathcal{T}}_i^H \end{array}\right] P^{\perp}_{\widetilde{\mathcal{T}}_i}\widetilde{\boldsymbol{g}}_1 \\ &= \sigma_a^2\left[\widetilde{\boldsymbol{g}}_1 \quad \widetilde{\mathcal{T}}_i\right]\mathcal{Q}_i^H\left[\begin{array}{c} \widetilde{\boldsymbol{g}}_1^H P^{\perp}_{\widetilde{\mathcal{T}}_i} \\ \widetilde{\mathcal{T}}_i^H \end{array}\right] P^{\perp}_{\widetilde{\mathcal{T}}_i}\widetilde{\boldsymbol{g}}_1 \end{aligned} \tag{II.9.14}$$

Upon some algebraic manipulations, the right side of the above equation shrinks to

$$\sigma_a^2\left[\widetilde{\boldsymbol{g}}_1 \quad \widetilde{\mathcal{T}}_i\right]\left[\begin{array}{c} \widetilde{\boldsymbol{g}}_1^H P^{\perp}_{\widetilde{\mathcal{T}}_i}\widetilde{\boldsymbol{g}}_1 \\ \mathbf{0}_{(PMJ-1)\times 1} \end{array}\right] = \left(\widetilde{\boldsymbol{g}}_1^H P^{\perp}_{\widetilde{\mathcal{T}}_i}\widetilde{\boldsymbol{g}}_1\right)\widetilde{\boldsymbol{g}}_1, \tag{II.9.15}$$

with $i = 1, \ldots, n$. The above gives a scaled estimate of the channel. ■

Chapter III

Semi-Blind and Decision-Directed Algorithms: Implementation Issues

The blind MMSE-ZF receiver proposed in chapter II is a batch mode receiver, and relies on a consistent estimate of the signal covariance matrix $\boldsymbol{R}_{YY}$, which requires a large number of data samples, especially if a large number of users are concurrently active. In this chapter, we propose a semi-blind *alternative for the estimation of the interference canceling filter, $\boldsymbol{Q}$. We also investigate the channel estimation by training and semi-blind methods. Iterative improvements of the IC filter based upon exploitation of the finite-alphabet are also discussed. Performances of different interference cancelation schemes are compared in terms of the output signal-to-interference-plus-noise ratio (SINR). Adaptive implementations are also addressed. A low-complexity version of the IC scheme, namely, the Interference Canceling RAKE Receiver (ICRR) is presented, which can reduce the number of IC filter coefficients to be estimated once the channel impulse response is available.*

III.1 Introduction

Semi-blind approaches [dCS97] have recently kicked off with the intuitively attractive idea of employing, in the estimation problem, as much *a priori* knowledge as can be made available. Forthcoming third generation mobile cellular systems like the European UMTS Wideband CDMA and TDMA/CDMA [ETS97a] [ETS97b] standards both anticipate the use of a training sequence integrated within the signal frame. It is worth mentioning that in the context of blind estimation, CDMA systems possess the most desirable characteristics of all existing multiple access systems with the necessary (extra) bandwidth and integrated *a priori* knowledge in terms of spreading sequences. Any further information, like known training data, should provide further gains resulting in more efficient interference suppression and reduced computational complexity.

Although scant, the CDMA literature on *semi-blind* has had the term employed with varying signification. Semi-blindness to some comes from known spreading codes of intracell users, with the inter-cell co-channel users contributing to the blind part [HM98]. In our problem, we shall consider knowledge of only the spreading sequence of the user of interest, with known training symbols for this user (thus a semi-blind problem).

Batch processing complexity is usually considered prohibitive for most real-time applications. A de-

composition of the Wiener filter based upon orthogonal projections and leading to a multistage implementation using a nested chain of scalar Wiener filters was presented in [GRS98]. This decomposition leads to a reduced rank Wiener filter which evolves a basis using successive projections of the desired signal onto orthogonal, lower dimensional subspaces. Applications to the DS-CDMA problem of this reduced rank filter have been explored in [HG98, HX99]. However, no results presented until now have shown that the Wiener filter estimation becomes data efficient if reduced rank approximations of it are considered. Other work in the area of reduced complexity MVDR approaches [KBP98] suggests using an arbitrary number of auxiliary vectors for the blocking transformation (see II.1) instead of a transformation spanning the whole noise subspace. Again, results have not been very promising in terms of data efficiency/performance trade-off.

Of particular interest for stochastic gradient based adaptive implementation are the MOE receiver of [XT98], where two algorithms for the adaptation of the receiver coefficients and the channel impulse response are introduced. The drawback of both is the interdependence of the two entities to be adapted, which makes it difficult to choose adaptation step sizes, μ, for the two. Furthermore as pointed out there, the presence of local minima cannot *a priori* be dismissed. One particular implementation of the MMSE-ZF receiver, given in chapter II which also corresponds to the pre-combining interference canceler followed by coherent combining lends itself to a particular disjoint adaptation of the interference canceling filter and the channel. We shall investigate, in this chapter, an LMS based adaptation of this receiver. It is shown that the quadratic cost-function viz. the estimation error covariance at the output of the bank of correlators is quadratic in coefficients of the interference canceling filter leading to guaranteed global convergence. The channel coefficients, on the other hand, are separately optimized based upon the knowledge of the interference canceler, assuming that interference has already been done away with. We explore the particularly attractive case of sparse channels and present a decision directed strategy to improve the quality of the IC filter. It is shown that significant performance gains can be achieved if decisions are reused in a soft fashion to influence the adaptation procedure.

III.2 Semi-Blind Algorithms for DS-CDMA Systems

Fig. I.12 in section § I.4.4 depicts the semi-blind philosophy. In multipath (ISI) channels, it is advantageous to keep the training symbols grouped together in the transmitted burst, as is the case in GSM. The reason for this grouping is that the channel impulse response has a certain length (N symbols) and the number of equations of the least-squares criterion should be sufficient to solve this linear equation problem. At the two edges of the training burst, some symbols (precisely $N-1$) are unusable for building the afore mentioned equations, since they contain contributions from unknown symbols. However, if $N = 1$ (no ISI), the channel convolution matrix is a block diagonal, and each symbol irrespective of its position contributes one equation to the least squares problem. Nevertheless, the above arguments are valid only for the single user situation. A variety of algorithms have been presented for this problem in [dC99]. We shall investigate the semi-blind problem in the DS-CDMA multiuser problem from various angles in this chapter, while maintaining as receiver and channel estimation algorithm, the MMSE-ZF and Capon's method respectively of the previous chapter.

In third generation wireless cellular systems like the UMTS WCDMA [ETS97a], training symbols are allocated for all users in the uplink. It is however, well-known that channel estimation by single-user LS leads to a biased estimate in the multiuser problem. Joint channel estimation is then, one alternative which requires timing information and some kind of alignment of user signal arriving at the base-station. Although the TDD situation [ETS97b] is well-suited for joint LS channel estimation, satisfying

the afore mentioned conditions of alignment and quasi-synchronism due to block transmission, the UMTS FDD uplink is not, and channel estimation is a rather critical issue in these systems. The channel identification issue is further aggravated if power control is not efficient. This brings one to the conclusion that interference not only affects the receiver performance if not handled properly but is also a nuisance for the parameter estimation problem, which also needs to be near-far resistant in the interest of the receiver which is based upon its quality.

III.2.1 MMSE-ZF Receiver and Semi-Blind Channel Estimation

Consider the GSC-like implementation of the MMSE-ZF (projection) receiver depicted in fig. II.1. The fact that the two-sided linear prediction (supplemented by the $\boldsymbol{C}^{\perp}$ in the desired signal portion) leads to an estimation error covariance matrix, $\boldsymbol{R_{ZZ}}$, that is rank-1, has the following very interesting implication.

Proposition: The two-sided linear prediction problem converts the MAI and ISI problem to a $N = 1$ (non-ISI) problem.
Proof: Let us stack together successive prediction error vectors $\boldsymbol{Z}$ in a super-vector $\widetilde{\boldsymbol{Z}}$ as

$$\begin{aligned}\widetilde{\boldsymbol{Z}} = \begin{bmatrix} \boldsymbol{Z}_1 \\ \vdots \\ \boldsymbol{Z}_M \end{bmatrix} &= \mathcal{T}(\boldsymbol{T}_1)\boldsymbol{Y}_{L+M-1} - \mathcal{T}(\boldsymbol{Q})\mathcal{T}(\boldsymbol{T}_2)\boldsymbol{Y}_{L+M-1} \\ &= \mathcal{D}(\boldsymbol{h}_1)\boldsymbol{A}_1 + \boldsymbol{E} = \mathcal{A}_1\boldsymbol{h}_1 + \boldsymbol{E}, \end{aligned} \tag{III.2.1}$$

where, $\mathcal{T}(\boldsymbol{T}_1)$ represents the block Toeplitz convolution matrix composed of appropriately shifted blocks $\boldsymbol{T}_1$. Same holds for $\mathcal{T}(\boldsymbol{T}_2)$ and $\mathcal{T}(\boldsymbol{Q})$. $\boldsymbol{A}_1$ denotes the length M data vector for user 1. $\mathcal{D}(\boldsymbol{h}_1) = \boldsymbol{h}_1 \otimes \boldsymbol{I}_M$ denotes the block diagonal matrix of the propagation channel vector for the user 1 signifying a channel length of $N = 1$ symbol. $\boldsymbol{E} = [\boldsymbol{E}_1^T \ \ldots \ \boldsymbol{E}_M^T]^T$ stands for the noise (plus residual interference) term in the estimation error $\widetilde{\boldsymbol{Z}}$.

III.2.1.1 Training Based Channel Estimation

We observe that the pre-combining interference cancelation structure of fig. II.1 cleans up the contribution of the ISI and the MAI from the signal of interest. If $M = M_k + M_u$, where M_k and M_u denote the number of known and unknown symbols respectively, the least-squares cost function [Kay93] can be written as

$$\widehat{\boldsymbol{h}}_1 = \arg \min_{\boldsymbol{h}_1} |\widetilde{\boldsymbol{Z}}_{M_k} - \mathcal{D}_{M_k}(\boldsymbol{h}_1)\boldsymbol{A}_{1,M_k}|^2 = \arg \min_{\boldsymbol{h}_1} |\widetilde{\boldsymbol{Z}}_{M_k} - \mathcal{A}\boldsymbol{h}_1|^2, \tag{III.2.2}$$

where, the second equality is due to the commutativity of convolution.

III.2.1.2 Semi-Blind Channel Estimation

In semi-blind channel estimation methods, the goal is to combine the TS cost-function with some blind criterion in some optimal manner. Let us write the estimation error vector as

$$\widetilde{\boldsymbol{Z}} = \mathcal{D}(\boldsymbol{h}_1)\boldsymbol{A}_1 + \boldsymbol{E} = \mathcal{D}_k(\boldsymbol{h}_1)\boldsymbol{A}_k + \mathcal{D}_u(\boldsymbol{h}_1)\boldsymbol{A}_u + \boldsymbol{E} = \mathcal{A}_k\boldsymbol{h}_1 + \mathcal{A}_u\boldsymbol{h}_1 + \boldsymbol{E}. \tag{III.2.3}$$

Let us consider a Gaussian model for the input symbols, i.e., the input symbols are considered to be *i.i.d.* Gaussian random variables with mean 0 and variance σ_a^2. Then, $\boldsymbol{R_{AA}} = \sigma_a^2 \boldsymbol{I}$, which implies that

$$\boldsymbol{R}_{\mathcal{D}_u(\boldsymbol{h}_1)\boldsymbol{A}_u} = \sigma_a^2 \mathcal{D}_u(\boldsymbol{h}_1)\mathcal{D}_u^H(\boldsymbol{h}_1) = \left(\sigma_a^2 \boldsymbol{h}_1 \boldsymbol{h}_1^H\right) \otimes \mathcal{I}_u, \tag{III.2.4}$$

where $\mathcal{I}_u$ is a $M \times M$ matrix with zero off-diagonal elements and 1's in positions of unknown symbols on the diagonal. An intuitively reasonable semi-blind criterion can therefore be devised as

$$\sum_{n \in \Omega_k} \|\boldsymbol{Z}_n - \boldsymbol{h}_1 a_{1,n}\|^2 + \boldsymbol{h}_1^H \left(\boldsymbol{R}_{\boldsymbol{ZZ}}^{-1} - \lambda_{\min}(\boldsymbol{R}_{\boldsymbol{ZZ}}^{-1})\boldsymbol{I}\right) \boldsymbol{h}_1, \tag{III.2.5}$$

simply combining, without any optimality consideration, the blind (rank-1 $\boldsymbol{R}_{\boldsymbol{ZZ}}$) and TS based criteria. In the above, $\boldsymbol{R}_{\boldsymbol{ZZ}} = \sum_{n \in \Omega_u} \boldsymbol{Z}_n \boldsymbol{Z}_n^H$, and Ω_k and Ω_u denote the set of known and unknown symbols respectively.

III.2.1.3 Semi-Blind Gaussian Maximum–Likelihood

In section § I.4.3, the Gaussian model for the received signal is described. Note that in the K-user problem, the parameter vector θ depends upon channels $\boldsymbol{g}_k$ of all K users along with the noise variance, σ_v^2. However, if we consider the TSLP approach to have cleaned up the contribution of the MAI and the ISI, then, assuming $\boldsymbol{Y}$ to be Gaussian, the estimation error vector, $\widetilde{\boldsymbol{Z}}$ can also be considered to be Gaussian distributed: $\widetilde{\boldsymbol{Z}} \sim \mathcal{N}\left(\mathcal{A}_k \boldsymbol{h}_1, \boldsymbol{R}_{\boldsymbol{EE}} + (\sigma_a^2 \boldsymbol{h}_1 \boldsymbol{h}_1^H) \otimes \mathcal{I}_u\right)$. The semi-blind GML criterion for $\widetilde{\boldsymbol{Z}}$ minimizes the log-likelihood cost function

$$\mathcal{L}(\theta) = \ln \det\left(\boldsymbol{R}_{\mathcal{D}_u(\boldsymbol{h}_1)\boldsymbol{A}_u}\right) + \left(\widetilde{\boldsymbol{Z}} - \mathcal{A}_k \boldsymbol{h}_1\right)^H \left(\boldsymbol{R}_{\boldsymbol{EE}} + \boldsymbol{R}_{\mathcal{D}_u(\boldsymbol{h}_1)\boldsymbol{A}_u}\right)^{-1} \left(\widetilde{\boldsymbol{Z}} - \mathcal{A}_k \boldsymbol{h}_1\right). \tag{III.2.6}$$

Note that the cost function in (III.2.6) is quadratic in $\boldsymbol{Q}$. Furthermore, for a fixed $\boldsymbol{Q}$, and σ_v^2, it can be solved for $\boldsymbol{h}_1$, resulting in an iterative solution in the three parameters.

The difficult part is the estimation of $\boldsymbol{R}_{\boldsymbol{EE}}$. In the signal user case addressed in [dC99], one can obtain a theoretical expression for $\boldsymbol{R}_{\boldsymbol{EE}}$ by plugging in the previous iteration's results for $\widehat{\boldsymbol{h}}_1$ and $\widehat{\sigma_v^2}$. In the K-user CDMA problem (III.2.1) addressed in the decentralized TLSP or GSC fashion as in the present development, this approach is not feasible since channel estimates for all users will be needed. One possible approach consists of estimating $\boldsymbol{R}_{\boldsymbol{EE}}$ from averaging over a number of realizations, naturally requiring a large number of data samples. A possible low-complexity approach consists of exploiting the block Toeplitz structure of $\boldsymbol{R}_{\boldsymbol{EE}}$ and limit it to $\boldsymbol{R}_{\boldsymbol{EE}} = \boldsymbol{R}_{\boldsymbol{E}_1\boldsymbol{E}_1} \otimes \boldsymbol{I}_M$, in which case (III.2.6) reduces to

$$\begin{aligned}\mathcal{L}(\theta) =& M_k \ln \det\left(\boldsymbol{R}_{\boldsymbol{E}_1\boldsymbol{E}_1}\right) + M_u \ln \det\left(\boldsymbol{R}_{\boldsymbol{E}_1\boldsymbol{E}_1} + \sigma_a^2 \boldsymbol{h}_1 \boldsymbol{h}_1^H\right) \\ &+ \sum_{n \in \Omega_k} \left(\boldsymbol{Z}_n - \boldsymbol{h}_1 a_n\right)^H \boldsymbol{R}_{\boldsymbol{E}_1\boldsymbol{E}_1}^{-1} \left(\boldsymbol{Z}_n - \boldsymbol{h}_1 a_n\right) + \sum_{n \in \Omega_u} \boldsymbol{Z}_n^H \left(\boldsymbol{R}_{\boldsymbol{E}_1\boldsymbol{E}_1} + \sigma_a^2 \boldsymbol{h}_1 \boldsymbol{h}_1^H\right)^{-1} \boldsymbol{Z}_n.\end{aligned} \tag{III.2.7}$$

Note that the above approximation for $\boldsymbol{R}_{\boldsymbol{EE}}$ reduces optimality but still leads to a useful semi-blind criterion.

Let us assume that $\boldsymbol{R}_{\boldsymbol{E}_1\boldsymbol{E}_1} = \sigma_e^2 \boldsymbol{I}$, i.e., the contributions of the residual interference in the prediction error $\boldsymbol{Z}_n$ is white. We furthermore assume that the coefficients of $\boldsymbol{h}_1$ are real, although an extension to

the case of complex parameters can be easily made. The gradient of the cost function, apart from the third term that takes into account the training (LS) portion, can now be written as

$$\frac{\partial \mathcal{L}(\theta)}{\partial h_i} = M_u \mathrm{tr}\left\{ \left(\sigma_e^2 \boldsymbol{I} + \sigma_a^2 \boldsymbol{h}_1 \boldsymbol{h}_1^H\right)^{-1} \frac{\partial}{\partial h_i}\left(\sigma_e^2 \boldsymbol{I} + \sigma_a^2 \boldsymbol{h}_1 \boldsymbol{h}_1^H\right) \right\} \tag{III.2.8}$$
$$- \mathrm{tr}\left\{ \left(\sigma_e^2 \boldsymbol{I} + \sigma_a^2 \boldsymbol{h}_1 \boldsymbol{h}_1^H\right)^{-1} \frac{\partial}{\partial h_i}\left(\sigma_e^2 \boldsymbol{I} + \sigma_a^2 \boldsymbol{h}_1 \boldsymbol{h}_1^H\right) \left(\sigma_e^2 \boldsymbol{I} + \sigma_a^2 \boldsymbol{h}_1 \boldsymbol{h}_1^H\right)^{-1} \sum_{n \in \Omega_k} Z_n Z_n^H \right\}.$$

Furthermore,

$$\frac{\partial}{\partial h_i}\left(\sigma_e^2 \boldsymbol{I} + \sigma_a^2 \boldsymbol{h}_1 \boldsymbol{h}_1^H\right) = \boldsymbol{H}_i = \begin{bmatrix} & & h_1 & & & \\ & \mathbf{0} & \vdots & & \mathbf{0} & \\ & & h_{i-1} & & & \\ h_1 & \cdots & 2h_i & \cdots & & h_{MJ\Psi} \\ & & h_{i+1} & & & \\ & \mathbf{0} & \vdots & & \mathbf{0} & \\ & & h_{MJ\Psi} & & & \end{bmatrix}, \tag{III.2.9}$$

and applying the matrix inversion lemma [Kay93],

$$\left(\sigma_e^2 \boldsymbol{I} + \sigma_a^2 \boldsymbol{h}_1 \boldsymbol{h}_1^H\right)^{-1} = \frac{1}{\sigma_e^2}\left[\boldsymbol{I} - \boldsymbol{h}_1 \left(\frac{\sigma_e^2}{\sigma_a^2} + \boldsymbol{h}_1^H \boldsymbol{h}_1\right)^{-1} \boldsymbol{h}_1^H\right], \tag{III.2.10}$$

which in the limit as $\frac{\sigma_e^2}{\sigma_a^2} \to 0$, leads to

$$\left(\sigma_e^2 \boldsymbol{I} + \sigma_a^2 \boldsymbol{h}_1 \boldsymbol{h}_1^H\right)^{-1} = \frac{1}{\sigma_e^2} P_{h_1}^{\perp}. \tag{III.2.11}$$

It can be seen that as $\frac{\sigma_v^2}{\sigma_a^2} \to 0$, $\boldsymbol{R}_{ZZ}$ becomes rank-1, and $\boldsymbol{R}_{\boldsymbol{ZZ}}^{-1} - \lambda_{\min}(\boldsymbol{R}_{\boldsymbol{ZZ}}^{-1})\boldsymbol{I} \to \frac{1}{\sigma_e^2} P_{h_1}^{\perp}$, the value of the gradient becomes zero, and the sub-optimal semi-blind GML becomes equivalent to the semi-blind criterion in (III.2.5).

Other semi-blind channel estimation criteria are also possible but are beyond the scope of this thesis and will be discussed no further. We shall refer to the [dC99] for details and performance analysis of these methods, while emphasizing that channel estimation (rapidly changing parameters that constitute $\boldsymbol{h}_1$ must be estimated by first nulling out the interference which in the current framework is based upon slowly varying parameters (path delays).

III.2.2 Semi-blind Adaptation of the IC Filter

Fig. II.2 shows the bit-error rate performance of the MMSE (employing $\widehat{\boldsymbol{R}}_{YY}^{-1}$) and the MMSE-ZF receiver derived in chapter II. It can be seen that the receivers are plagued by the finite-data effect. Here, we show that when training data side-information is available, this problem can be partially alleviated. To this end, we proceed with the linear prediction problem formulated in the GSC fashion described in section § II.5.4. First, the channel vector, $\widehat{\widehat{\boldsymbol{g}}}_1$ is determined as an initial estimate from the TS, blind, or the semi-blind problem. It is actually the presence of a strong desired signal contribution in the main

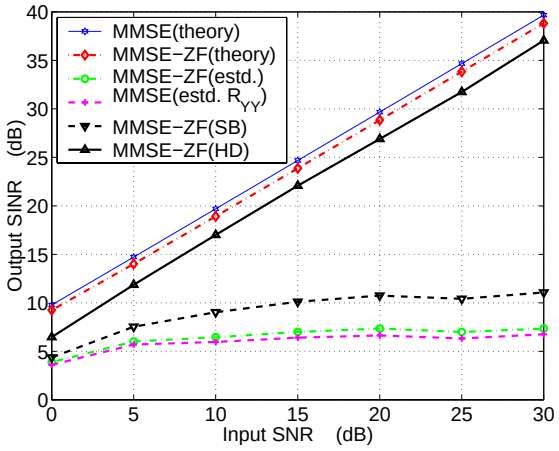

Figure III.1: Output SINR performance of blind vs. semi-blind receiver, along with the performance improvement obtained by iterative HD reuse

branch of the GSC that perturbs the estimation of the interference term in that branch. This effect is more obvious in the case when the input SNR is low. To alleviate the excess-mean-square error effect and to improve the estimate of the IC filter $\boldsymbol{Q}$, semi-blind information can be used. This will be done over the training period by removing the contribution of the desired signal from the main branch of the GSC. To incorporate the training information, we formulate the following *weighted least-squares* (WLS) cost function:

$$\min_{\boldsymbol{Q}} \left\{ \frac{1}{\sigma_u^2} \sum_{n \in \Omega_u} \| \boldsymbol{Z}_n \|_2^2 + \frac{1}{\sigma_k^2} \sum_{n \in \Omega_k} \| \boldsymbol{Z}_n - \boldsymbol{T}_1^H \widehat{\boldsymbol{h}}_1 a_{1,n-d} \|_2^2 \right\}, \tag{III.2.12}$$

where, $a_{1,n-d}$ is constrained to lie within the training sequence. The weighting factors σ_u^2 and σ_k^2 can be determined respectively as the ensemble averages of $\| \boldsymbol{Z}_n \|_2^2$ and $\| \boldsymbol{Z}_n - \boldsymbol{T}_1^H \widehat{\boldsymbol{h}}_1 a_{1,n-d} \|_2^2$ for the blind and training sequence parts of the given data sequence. The denoised signal covariance matrix $\widehat{\boldsymbol{R}}^d = \widehat{\boldsymbol{R}}_{YY} - \lambda_{\min}(\widehat{\boldsymbol{R}}_{YY}) \boldsymbol{I}$, where, $\lambda_{\min}$ is the minimum eigenvalue of the estimated covariance matrix, and

$$\widehat{\boldsymbol{R}}_{YY} = \frac{1}{\sigma_b^2} \sum_{n \in \Omega_u} \boldsymbol{Y}_n \boldsymbol{Y}_n^H + \frac{1}{\sigma_k^2} \sum_{n \in \Omega_k} \boldsymbol{Y}_n \boldsymbol{Y}_n^H. \tag{III.2.13}$$

The algorithm is semi-blind for the estimation of the interference canceler $\boldsymbol{Q}$ and can involve a blind estimate of the channel. An update of the channel vector, in iterative implementations, is also possible based upon the knowledge that in the noiseless case $\boldsymbol{R}_{ZZ}$ is rank one. The performance of the semi-blind adapted version of the MMSE-ZF receiver is illustrated in fig. III.1.

III.2.3 Exploitation of Finite Alphabet

An iterative implementation of the MMSE-ZF algorithm is possible when decisions are re-used at each iteration to re-estimate the filter $\boldsymbol{Q}$. We propose to start from the semi-blind cost function (III.2.12) and make hard-decisions at the output of the receiver, thus exploiting the finite signal constellation

(BPSK in this case). The decisions taken are fed-back to re-estimate the IC filter. Upon each iteration, more correct decisions are available resulting in improved performance. We compare results with the limiting case where all symbols are known (ASK) at the receiver and their effect is removed from the estimation of $\boldsymbol{Q}$. The hard-decision (HD) algorithm converges to this state in a small number of iterations, as seen in fig. III.1. In this numerical example, we consider a spreading factor of 16, with a burst length of 200 data samples of which 25 are the training symbols.

III.3 Interference Canceling Rake Receiver

The generalized side-lobe canceler (GSC), is a particular implementation of the linearly-constrained minimum variance (LCMV) beamformer. It was shown in chapter II (where it was referred to as the decentralized receiver) that the projection receiver could be implemented in a GSC manner. However, in II, the emphasis was on channel identification. Here, we proceed with the case where the channel has been estimated beforehand to obtain an improved, low-complexity receiver, termed as the interference canceling RAKE receiver (ICRR).

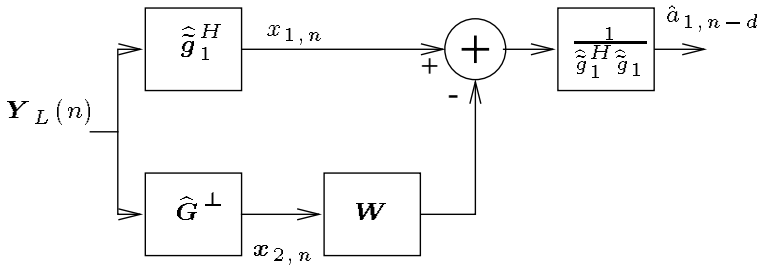

Figure III.2: Interference canceling rake receiver.

The GSC implementation of the receiver is shown in fig. III.2. Note that the main branch in fig. III.2 is the multichannel matched filter, $\widehat{\widetilde{\boldsymbol{g}}}_1^H$. When $\widehat{\widetilde{\boldsymbol{g}}}_1 \sim \widetilde{\boldsymbol{g}}_1$, we have an unbiased response for the desired symbol, $a_{1,n-d}$, (after scaling) and corresponds to the (normalized) coherent RAKE receiver. This second branch contains first, $\boldsymbol{G}^{\perp}$, which is any blocking transformation (of appropriate dimensions) for the signal of interest. In our problem for example, $\boldsymbol{T}_2$ qualifies as a blocking transformation and so does a blocker parameterized by the channel coefficients [Slo96], given in the z-transform domain by

$$\mathbf{G}^{\perp}(z) = \begin{bmatrix} -G_2(z) & G_1(z) & 0 & \dots & 0 \\ 0 & -G_3(z) & G_2(z) & \dots & \vdots \\ \vdots & & \ddots & \ddots & \\ G_{PMJ}(z) & 0 & \dots & & -G_1(z) \end{bmatrix}, \tag{III.3.1}$$

with $\boldsymbol{G}^{\perp}$ its time-domain counterpart. In all cases, $\boldsymbol{G}^{\perp}\widetilde{\boldsymbol{g}}_1 = 0$. Note that $P_{\widetilde{\boldsymbol{g}}_1} + P_{\boldsymbol{G}^{\perp H}} = \boldsymbol{I}$. In the above,

$$x_{1,n} = \widehat{\widetilde{\boldsymbol{g}}}_1^H \boldsymbol{Y}_L(n), \quad \text{and} \quad \boldsymbol{x}_{2,n} = \widehat{\boldsymbol{G}}^{\perp}\boldsymbol{Y}_L(n). \tag{III.3.2}$$

It is clear that $\boldsymbol{x}_{2,n}$ contains no signal of interest but some of its components are correlated with $x_{1,n}$ and can be used to lower the interference level in the latter. We thus have an estimation problem, which

can be solved in the least squares sense, for some vector filter, $\boldsymbol{W}$. This interpretation of the GSC corresponds to the post-combining interference (ISI and MAI) canceling approach [DHZ95, LA98].

The estimation error is given by

$$z(n) = \left[\widehat{\widetilde{\boldsymbol{g}}}_1^H - \boldsymbol{W}\widehat{\boldsymbol{G}}^{\perp}\right] \boldsymbol{Y}_L(n). \tag{III.3.3}$$

Since the goal is to minimize the estimation error variance, the interference cancelation problem settles down to the estimation of the Wiener filter $\boldsymbol{W}$, minimizing the estimation error variance and resulting in

$$\boldsymbol{W} = R_{x_1\boldsymbol{x}_2} R^{-1}_{\boldsymbol{x}_2\boldsymbol{x}_2} = \widehat{\widetilde{\boldsymbol{g}}}_1^H \boldsymbol{R}^d_{YY} \widehat{\boldsymbol{G}}^{\perp H} \left(\widehat{\boldsymbol{G}}^{\perp} \boldsymbol{R}^d_{YY} \widehat{\boldsymbol{G}}^{\perp H}\right)^{-1}, \tag{III.3.4}$$

The output, $\hat{a}_{1,n-d}$, the data for the user 1 is given by

$$\hat{a}_{1,n-d} = \frac{1}{\widehat{\widetilde{\boldsymbol{g}}}_1^H \widehat{\widetilde{\boldsymbol{g}}}_1} \boldsymbol{f}^H \boldsymbol{Y}_L(n) = \frac{1}{\widehat{\widetilde{\boldsymbol{g}}}_1^H \widehat{\widetilde{\boldsymbol{g}}}_1} \left(\widehat{\widetilde{\boldsymbol{g}}}_1^H - \boldsymbol{W}\widehat{\boldsymbol{G}}^{\perp}\right) \boldsymbol{Y}_L(n) \tag{III.3.5}$$

III.3.1 Semi-Blind Receiver

The mean square estimation error σ_z^2 is given by

$$\text{MSE} = |z_n|^2 = \left(\widehat{\widetilde{\boldsymbol{g}}}_1^H - \boldsymbol{W}\widehat{\boldsymbol{G}}^{\perp}\right) \boldsymbol{R}^d_{YY} \left(\widehat{\widetilde{\boldsymbol{g}}}_1 - \widehat{\boldsymbol{G}}^{\perp H} \boldsymbol{W}^H\right). \tag{III.3.6}$$

There is an excess mean square estimation error term in $z(n)$ due to the presence of the desired user's signal, $\sigma_a^2 \widetilde{\boldsymbol{g}}_1^H \widetilde{\boldsymbol{g}}_1$ in the main branch. Since there is no signal component in the bottom branch, this term is uncorrelated with all components of the lower branch. Therefore, to estimate the interference term in the RAKE output, ideally, there should be no signal term in the main branch. Since the channel is known (estimated), we can subtract the contribution of the desired user during the training period to reduce the excess MSE resulting in improved performance. Then the main branch output is given by $x_{1,n} = \widehat{\widetilde{\boldsymbol{g}}}_1^H \left[\boldsymbol{Y}_L(n) - \widehat{\widetilde{\boldsymbol{g}}}_1 a_1(n)\right]$ and the Wiener filter is determined in the same way as before.

III.4 Numerical Examples

We consider $K = 6$ asynchronous users in the system with a spreading factor of $P = 16$. The overall channel (including the transmit and receive filters) for the kth user is modeled as an FIR channel of length Ψ_k ranging from $6 - 14$ chip periods for different k. Mild near-far conditions prevail in that the interfering users are randomly (ranging from 8 to 10 dB) stronger than the user of interest.

In fig. III.3, we show the performance of blind and semi-blind (ICRR) receivers and compare it with that of the theoretical MMSE receiver ($\boldsymbol{R}_{YY} = \sigma_a^2 \mathcal{T}_L(\boldsymbol{G}_N)\mathcal{T}_L(\boldsymbol{G}_N) + \sigma_v^2 \boldsymbol{I}$). It comes as no surprise that the optimal MMSE is not approached by any of the other receivers due to finite data effect. A theoretical curve for the MMSE-ZF or the decorrelating receiver is also provided. It can be seen that the semi-blind ICRR does relatively well. In all simulations of the ICRR, channel estimates obtained from the proposed blind method are employed. In these simulations we consider 20 training symbols in a packet of 200 symbols. More training symbols result in improved performance.

There is a flooring effect in the high SNR region for the semi-blind receiver which is due to the fact that if the blocking transformation $\widehat{\boldsymbol{G}}^{\perp}$ is parameterized by the channel coefficients, then a bit of the desired user's signal creeps into the interference cancelation branch due to estimation errors in $\widehat{\widehat{\boldsymbol{g}}}_1$. The blocking transformation $\boldsymbol{T}_2$ therefore qualifies as a better blocker, since it is based upon spreading code and delay spread information, and both these quantities are known *a priori*. Simulations further show that the quality of the blocking transformation affects the performance of the training based ICRR more than that of the estimated multichannel matched filter, $\widehat{\widehat{\boldsymbol{g}}}_1$.

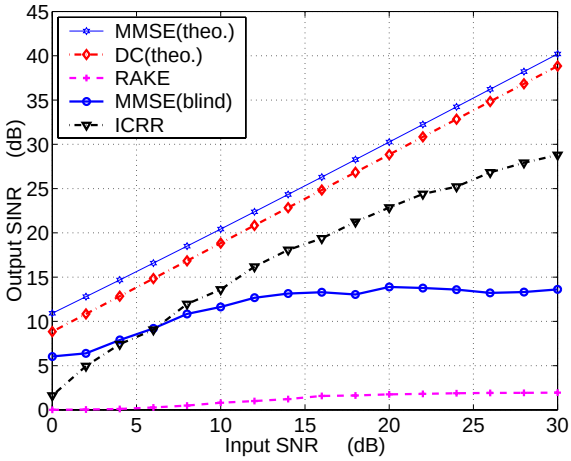

Figure III.3: Output SINR vs. SNR for different receivers, $M_k = 20$, $K = 6$, $P = 16$, near-far conditions.

III.5 Adaptive Implementations

The GSC formulation of the MMSE-ZF as given in section II.5.4, converts the constrained optimization problem (unbiasedness constraint) into an unconstrained one [JD93]. In [XT98], the authors propose to adapt the MOE problem in a GSC fashion by splitting it into two optimization problems, one for the interference canceling filter, and the other for the channel impulse response, $\boldsymbol{h}_1$. The problem with such an approach is that the problem becomes that of joint optimization thus rendering it susceptible of falling into local minima. The alternative formulation is that of a *pre-combining* interference canceler, as shown in fig. II.1. The interference canceler operates independently of the channel response. The optimization problem however becomes that of optimizing for a matrix filter, $\boldsymbol{Q}$. The entity that needs to be minimized is the trace of $\boldsymbol{R}_{ZZ}$.

One situation of interest is that of sparse channels (section § II.5.6) where $\boldsymbol{T}_1$, defined by (II.5.27) contains a small number of non-zero rows, highlighting the fact that only these directions of the correlator bank carry the signal plus interference energy. Note that as $\boldsymbol{T}_1$ no longer contains only the code, but also the contribution of the pulse shaping filter, the channel parameter vector $\widetilde{\boldsymbol{\phi}}_1$ is a short $(MQ \times 1)$ vector with the Q non-zero elements of the sparse channel per RX sensor. If the corresponding rows of the IC filter $\boldsymbol{Q}$ can be assumed to operate independently so as to cancel interference in these directions, they can be adapted independently. Let us denote by $\boldsymbol{q}_i$ and $\boldsymbol{t}_i$, the ith row of the matrix $\boldsymbol{Q}$ and $\boldsymbol{T}_1$ respectively, then the cost function to be optimized becomes

$$\mathcal{Z}_i = \boldsymbol{R}_{ZZ}^{ii} = (\boldsymbol{t}_i - \boldsymbol{q}_i \boldsymbol{T}_2)\, \boldsymbol{R}^d\, (\boldsymbol{t}_i - \boldsymbol{q}_i \boldsymbol{T}_2)^H . \tag{III.5.1}$$

where, $i \in \{1, \ldots, l_1\}$, and l_1 is the number of non-zero taps of the sparse channel. $\mathcal{Z}_i$ is quadratic in $\boldsymbol{q}_i$, and can be optimized in the LMS or the NLMS fashion. It can be noticed that while minimizing $\mathcal{Z}_i$, its contribution to the trace of $\boldsymbol{R}_{ZZ}$ also gets minimized. Same applies for other $\boldsymbol{q}_i$'s. Then, the update equation will be of the from

$$\boldsymbol{q}_{i,n+1} = \boldsymbol{q}_{i,n} - \mu_q \nabla_{q^*} \mathcal{Z}_i, \tag{III.5.2}$$

where, μ_q is the step size for the LMS algorithm [WS85]. The derivative (the gradient) can be computed as

$$\nabla_{q^*} \mathcal{Z}_i = -\boldsymbol{T}_2 \boldsymbol{R}^d \boldsymbol{t}_i^H + \boldsymbol{T}_2 \boldsymbol{R}^d \boldsymbol{q}_i^H, \tag{III.5.3}$$

leading to the recursive update equation

$$\boldsymbol{q}_{i,n+1} = \boldsymbol{q}_{i,n} - \mu_q \left[\boldsymbol{T}_2 \boldsymbol{R}^d \boldsymbol{q}_{i,n}^H - \boldsymbol{T}_2 \boldsymbol{R}^d \boldsymbol{t}_i^H \right]. \tag{III.5.4}$$

As $\boldsymbol{R}_{ZZ}$ is rank-1 in the batch processing mode, the adaptive search for path coefficients $\widetilde{\boldsymbol{\phi}}_1$ can then be based upon the maximization of the signal variance, $\sigma_a^2 (\widetilde{\boldsymbol{\phi}}_1^H \boldsymbol{T}_1 \boldsymbol{T}_1^H \widetilde{\boldsymbol{\phi}}_1) / \|\widetilde{\boldsymbol{g}}_1\|$ at the output of the maximum ratio combiner, resulting in a recursive update as

$$\widetilde{\boldsymbol{\phi}}_{1,n+1} = \widetilde{\boldsymbol{\phi}}_{1,n} + \mu_{\widetilde{\phi}_1} \left[\boldsymbol{T}_1 - \boldsymbol{Q}_n \boldsymbol{T}_2 \right] \boldsymbol{R}^d \left[\boldsymbol{T}_1 - \boldsymbol{Q}_n \boldsymbol{T}_2 \right]^H \widetilde{\boldsymbol{\phi}}_{1,n}. \tag{III.5.5}$$

In the above adaptive algorithm, $\boldsymbol{R}^d$ is approximated by $\boldsymbol{Y}_n \boldsymbol{Y}_n^H - \widehat{\sigma_v^2} \boldsymbol{I}$, where $\widehat{\sigma_v^2}$ accounts for the denoising operation.

III.5.1 Hard/Soft Decision Directed Mode

The adaptive interference cancelation scheme can be adapted in a decision directed mode to improve the quality of the filter $\boldsymbol{Q}_n$. The presence of the signal term in the output of correlators, $\boldsymbol{T}_1$, perturbs the estimation of the IC filters. The hard/soft decision-directed mechanism works by examining at the scaled soft outputs $\hat{a}_{1,n-d}$ of the receiver (see fig II.1). If $\hat{a}_{1,n-d} \geq \zeta$, then an update is made by subtracting the contribution of the desired term as $\boldsymbol{T}_1 (\boldsymbol{Y} - \widehat{\widetilde{\boldsymbol{g}}}_1 \hat{a}_{1,n-d})$ from the correlator outputs. Otherwise no update is made. Several more sophisticated schemes are also possible. For example, the update can always be made while subtracting the soft output rather than the hard decision.

III.5.2 Delay Tracking

In the above framework, $\boldsymbol{T}_1$ is assumed to be fixed. However, the discrete path components of the sparse channel tend to drift from their nominal positions. $\boldsymbol{T}_2$ is no longer a strict signal blocker if it is obtained from $\boldsymbol{T}_1$ as the orthogonal complement. $P^{\perp}_{T_1^H}$ qualifies as a blocking transformation. An update of the $\boldsymbol{T}_1$ can be when oversampling the received signal w.r.t. the chip rate is employed. Considering an oversampled version of the pulse-shaping filter, $p(t)$, we can write as

$$p(k\frac{T_c}{J}) \approx p(\frac{kT_c}{J}) + \tau \dot{p}(\frac{kT_c}{J}), \tag{III.5.6}$$

where $\dot{p}(t)$ is the first derivative of the pulse shaping filter, and τ is a continuous time delay. Hence the positions in $\boldsymbol{T}_1$ can be updated as discrete shifts every time a decision is made based upon the values of matched filter outputs of $p(kT_c/J)$ and $\dot{p}(kT_c/J)$ for a given k. This adds a little in terms of complexity since two matched filtering operations are required. However, this complexity is justified by a better choice of delay on which the entire interference canceling structure is based.

III.6 Numerical Examples

We consider $K = 6$ asynchronous users in the system with a spreading factor of $P = 16$. The propagation channel (excluding the transmit and receive filters, which is a raised-cosine pulse, and the effect of which are absorbed in the code convolution matrix $\widetilde{\widetilde{\boldsymbol{C}}}_1$) as shown in equation (II.5.27)), for the kth user is modeled as a sparse channel with $Q = 4$ discrete paths spanning a delay spread of $8 - 21$ chip periods for different k's. The interfering users are randomly (ranging from 8 to 10 dB) stronger than the user of interest.

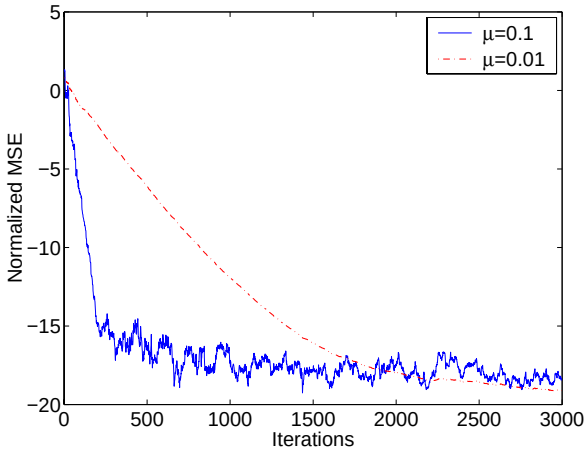

Figure III.4: Channel estimation error for the adaptive algorithm $K = 5$, $P = 16$, SNR=15 dB.

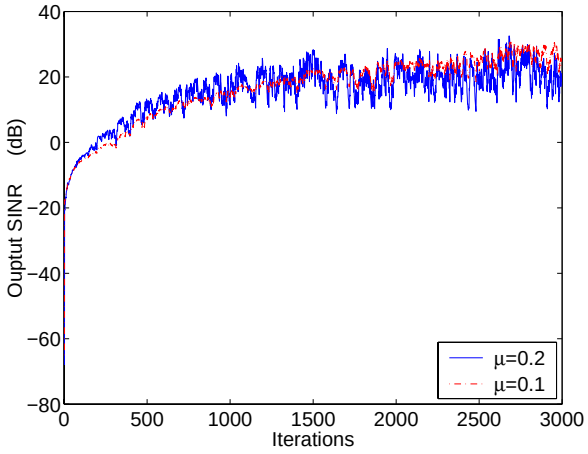

Figure III.5: Output SINR for two step sizes $K = 6$, $P = 16$, SNR=25 dB, near-far conditions.

In general, the normalized LMS (NLMS) results in better convergence due to the gradient noise amplification problem in the original LMS algorithm [WS85]. We shall therefore consider the normalized version of the LMS algorithm in these simulations. Fig. III.4 shows the normalized mean-square error (NMSE) [1] of adaptive channel estimation algorithm. We start with random initialization for the channel

[1] NMSE$= E\frac{\|\boldsymbol{h}_1 - \hat{\boldsymbol{h}}_1\|^2}{\|\boldsymbol{h}_1\|^2} = \frac{1}{L}\sum_{i=1}^{L}\frac{\|\boldsymbol{h}_1 - \hat{\boldsymbol{h}}_1^{(i)}\|^2}{\|\boldsymbol{h}_1\|^2}$

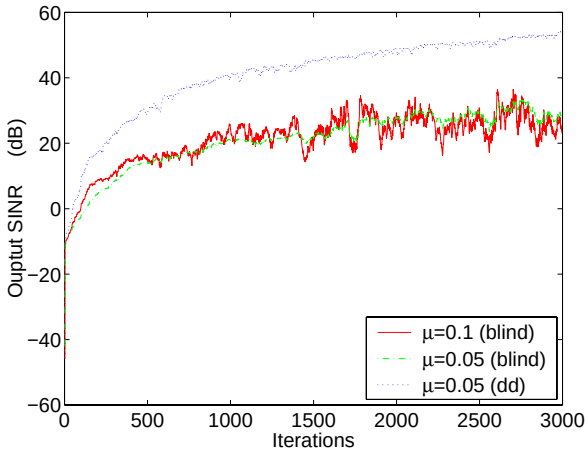

Figure III.6: Output SINR for blind and decision-directed algorithms $K = 6$, $P = 16$, SNR=25 dB.

taps since the interference canceling filter does not need path amplitudes and phases. Path delays are assumed to be known and fixed in these examples.

In fig. III.5, we show the convergence of the NLMS adaptive algorithm [WS85] for two different values of the step size. Convergence is guaranteed in all cases due to the quadratic nature of the cost function, once the step size, μ lies in the region of interest. In fig. III.6, we show the performance of the decision-directed algorithm. It is seen that the blind algorithm suffers from a saturation effect due to the presence of the desired signal component in the estimation of the interference canceling filter, while removing this contributions over reliable decisions gives significant performance gains. No simulation examples are presented for the case of joint channel and MOE receiver optimization as presented in [TX98]. It appears that the choice of step sizes (there are two) in the joint optimization problem is a complicated issue. We tried to compare the performance of our approach numerically with the joint optimization one of [TX98], however, no definite range of step sizes could be obtained for convergence for the latter case.

III.7 Conclusions

Semi-blind adaptation of the MMSE-ZF receiver leads to improved performance as compared to the purely blind approach; this occurs due to the excess MSE term in the estimation of the IC filter in the latter. Semi-blind algorithms for channel estimation are also possible. However, practical implementation of such algorithms in the MMSE-ZF algorithm may be unnecessary since a blind estimate of the channel is obtainable from Capon's method, i.e., as the principal eigenvector of the rank-1 error covariance matrix $\boldsymbol{R}_{ZZ}$.

The adaptive receiver presented above distinguishes clearly between two issues, namely channel identification and receiver adaptation, i.e., the interference canceling part of the receiver operate in a fashion that it attempts to cancel the interference independently of the channel parameters apart from the delay. In this respect, it qualifies as a pre-combining interference canceler. The disjointness of the two estimation algorithms leads to global convergence of the two once the system is identifiable in the batch mode. It was also seen that the decision-directed mode of operation results in much

improved performance over the blind method. It must however be mentioned that the quality of the blocking transformation is crucial in all cases. If the desired signal component leaks through this branch, performance of the algorithm greatly suffers due to the desired signal cancelation. Delay tracking is therefore necessary for operation in fading.

Chapter IV

Downlink Solutions

This chapter deals with the problem of downlink interference rejection in a DS-CDMA system. Periodic orthogonal Walsh-Hadamard sequences spread different users' symbols followed by scrambling by a symbol-aperiodic, base-station specific overlay sequence. This corresponds to the downlink of the second generation North American IS-95 standard, and the European UMTS Wideband CDMA proposal for third generation wireless cellular systems. The point-to-point propagation channel from the cell-site to a certain mobile station is the same for all downlink signals (desired user as well as the interference). The composite channel can be shorter than a symbol period under certain circumstances while it can be longer for some cases, like for high-rate users in a multirate configuration. In the latter case there is significant ISI when the channel is frequency selective. In any case, orthogonality of the underlying Walsh-Hadamard sequences is destroyed by multipath propagation, resulting in a multiuser interference contribution at the output of the coherent combiner (the RAKE receiver). Alternatives to the RAKE receiver are proposed; these include the linear zero-forcing (ZF) and the maximum SINR receivers which equalize for the estimated channel, thus attempting to render user signals orthogonal at the output of the equalizer. A simple desired user code correlator subsequently suffices to cancel the multiple access interference (MAI) from intracell users.

IV.1 Introduction

While sophisticated joint multiuser detection techniques are being pursued for the uplink of the third generation wireless systems mostly due to the inability of the RAKE receiver in combating the *near-far* effect, downlink situations are considered to be much too deficient in terms of information and processing power to implement multiuser techniques. However, the net capacity of a communication network can only be increased if both links can support similar transmission rates. Other recent studies argue that the real bottle-neck occurs in the downlink for high rate applications, like internet surfing, where asymmetric traffic is likely to take place. The existing trend in downlink capacity enhancing techniques, nevertheless, remains to be improved transmission schemes like transmit antenna diversity [Win98], and advanced receiver algorithms at mobile stations are virtually non-existent in the DS-CDMA literature.

In situations where a relatively small number of users are active ($\approx 20\%$ of the processing gain),

the RAKE receiver [Pro95] might perform in an adequate manner and more complex signal processing may be deemed unnecessary. Under power controlled conditions, this loading fraction approximately corresponds to a SIR of approximately 7 dB and advocates support of about 50 users in a system with a processing gain of 256, as is the case of UMTS WCDMA proposal [ETS97a]. Increasing the number of users to approach the spreading factor, however, has a catastrophic effect on the performance since small contributions of multipath signals of each interferer captured by the matched-filter bank add up to large values, even in the power controlled case. This effect is simply due to the suboptimal treatment of the MAI as uncorrelated noise by the RAKE receiver.

As an alternative to the RAKE, linear receiver techniques based upon single user *a priori* information have lately been an active topic of research [GS98a] (and the references therein). These receiver algorithms are based upon symbol rate wide sense cyclostationarity (see also chapter II) and have been shown to converge asymptotically to the MMSE solution. The application of these techniques in existing systems, however, is not straightforward, since symbol rate time-invariant processing can no longer be performed when aperiodic overlay sequences spread/randomize the orthogonal user sequences.

It is to be noted that in the structure of the downlink problem, the only entity fixed over the processing interval is the propagation channel. Burst processing techniques can thus be applied once the channel has been estimated, and single user information (symbol spreading code of the user of interest) and cell specific randomizing codes of active base stations are available.

In the IS-95 CDMA standard, a perpetually active known wideband downlink pilot signal is used to estimate the downlink channel. This pilot is much stronger (typically 10 dB) than other user signals and a correlation based searcher constantly searches the best fingers for building the coherent RAKE receiver [PG58, Pro95]. Channel estimation on the downlink using the known pilot symbols was presented in [WF97], where it was assumed that all downlink codes were known. Such an assumption is reasonable in the case of the UMTS WCDMA norm [ETS97a], where a fixed number of downlink codes can be used at one time, and all common cell information is constantly broadcast over the entire cell. Some blind algorithms exploiting the *i.i.d.* nature of the spreading sequences and symbols have been presented [LZ97, MS98a, WLLZ98]. However, these algorithms rely on averaging out of multiuser interference, and happen to be data inefficient.

In this chapter, we start by introducing a linear zero-forcing (ZF) receiver for the DS-CDMA downlink which equalizes for the propagation channel, once the latter has been estimated; this equalizer in the noiseless case renders the user signals orthogonal again, doing away with the frequency selective distortion introduced by the propagation channel. To counter the noise enhancement problem of the ZF algorithm, a maximum SINR receiver is subsequently introduced. These schemes are shown to be attractive alternatives to the RAKE receiver under certain circumstances pertaining to delay spread and transmission rates, which will be discussed in detail. Oversampling/multiple sensors are used at the mobile station to facilitate equalization. Multichannels can also be created by treating real and imaginary parts of a signal when the input constellation is one dimensional, e.g. BPSK.

IV.2 Downlink Signal Model

Fig. IV.1 illustrates the downlink channel model. The K intracell users are assumed to transmit linearly modulated signals over a linear multipath channel with additive Gaussian noise. It is assumed that the signal is received at the mobile station through multiple (diversity) discrete-time channels, obtained from oversampling the received signal multiple times per chip or through multiple sensors

(or a combination of the two schemes). We shall consider the signal to be received through precisely M channels where, M = no. of sensors $\times$ oversampling factor. The signal received through the mth channel can be written in baseband notation as

$$y_m(t) = \sum_{k=1}^{K} \sum_{n} b_{k,n} h_{km}(t - nT_c) + v_m(t), \tag{IV.2.1}$$

where the subscript k denotes the user index; T_c is the chip period; the chip sequences $\{b_{k,n}\}_{k=1}^{K}$ are assumed to be independent of the additive noise $\{v_m(t)\}$; and $h_{km}(t)$ characterizes the channel impulse response between the kth user signal and the mth sensor or the oversampled phase of the received signal. Let us denote by $\boldsymbol{w}_k^l = [w_{k,P_k-1}^l, w_{k,P_k-2}^l, \ \ldots, \ w_{k,0}^l]^T$, the structured aperiodic

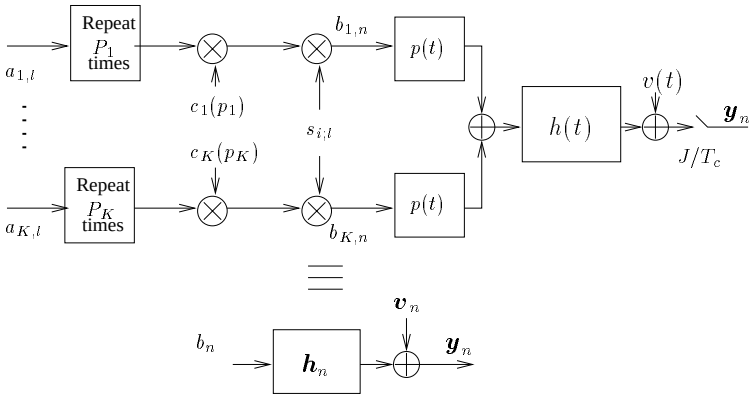

Figure IV.1: The downlink signal model.

spreading sequence vector for the lth symbol of the kth user. The aperiodic spreading sequences consist of a periodic Walsh-Hadamard spreading sequence $\boldsymbol{c}_k = [c_{k,P_k-1}, \ldots, c_{k,0}]$, overlaid by a base-station specific scrambling sequence $s_{i,l}$. Then, $w_{k,i}^l = c_{k,i} s_{i,l}$, $i \in \{0, \cdots, P_k - 1\}$. We can write the chip sequence $\{b_{k,n}\}$ corresponding to the data symbol, $a_{k,l}$, for the kth user as

$$b_{k,n} = a_{k,l} w_{k,n \bmod P_k}^l. \tag{IV.2.2}$$

The chip period, T_c, is a constant, while the symbol period, $T_k, \forall k$, is a function of the transmission rate of the kth user. The symbol and chip periods are related through the processing gain, P_k: $T_k = P_k T_c$. We shall also consider the chip sequence to have normalized energy: $|\boldsymbol{c}_k|^2 = 1$. While orthogonal Walsh-Hadamard sequences [Vit95] can be chosen as underlying spreading codes for users in a system with a common spreading factor, future systems [ETS97a] envision multirate applications where spreading codes are selected from a tree structure to ensure orthogonality between users with all rates.

For the purpose of the following discussion, let us assume a common spreading factor, P, and a common symbol period, T. As the downlink propagation channel is the same for all k in a single cell/sector, we shall suppress the subscript k from $h_{km}(t)$ in the sequel. We consider that there are no intercell interferers (or are considerably weaker) and their effect is momentarily ignored. We assume that the timing information has already been acquired from the initial synchronization procedure. Due to the synchronous nature of the channel, user signals will be considered to arrive perfectly aligned at the receiver.

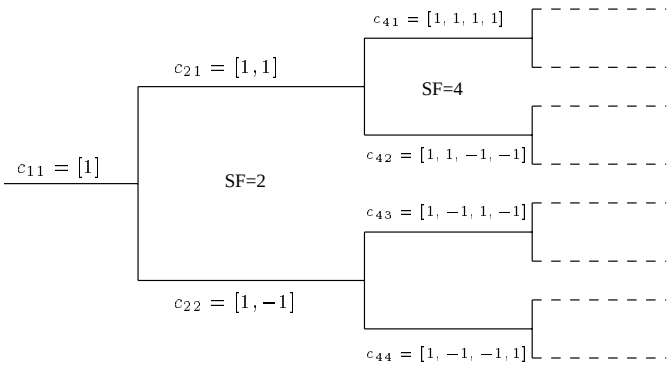

Figure IV.2: The tree structure for spreading codes selection for multirate systems.

The oversampled cyclostationary received signal at M times the chip rate can be stacked together to obtain the $M \times 1$ stationary vector signal $\boldsymbol{y}_n$ at the chip rate, which can be expressed as

$$\boldsymbol{y}_n = \sum_{k=1}^{K} \sum_{i=0}^{N-1} \boldsymbol{h}_i b_{k,n-i} + \boldsymbol{v}_n = \sum_{i=0}^{N-1} \boldsymbol{h}_i \left(\sum_{k=1}^{K} b_k \right)_{n-i} + \boldsymbol{v}_n = \boldsymbol{H}_N \boldsymbol{B}_n + \boldsymbol{v}_n, \tag{IV.2.3}$$

where,

$$\boldsymbol{y}_n = \begin{bmatrix} y_{1,n} \\ \vdots \\ y_{M,n} \end{bmatrix}, \boldsymbol{h}_n = \begin{bmatrix} h_{1,n} \\ \vdots \\ h_{M,n} \end{bmatrix}, \boldsymbol{v}_n = \begin{bmatrix} v_{1,n} \\ \vdots \\ v_{M,n} \end{bmatrix},$$

$\boldsymbol{H}_N = [\boldsymbol{h}_0 \ \boldsymbol{h}_1 \ \ldots \ \boldsymbol{h}_{N-1}]$ is the $M \times N$ channel matrix, once again including the TX/RX filters, and $\boldsymbol{B}_n = \sum_{k=1}^{K} \boldsymbol{B}_{k,n}$, with $\boldsymbol{B}_{k,n} = [b_{k,n} \ \ldots \ b_{k,n-N+1}]^T$, the nth instant input chip sequence for the kth user. Let us consider a block of $l_1 P + l_2 + l_6$ data vectors $\boldsymbol{y}_n$, and denote it by $\boldsymbol{Y}_n$ to write as,

$$\boldsymbol{Y}_n = \mathcal{T}(\boldsymbol{h}) \widetilde{\boldsymbol{S}}_n \sum_{k=1}^{K} \widetilde{\boldsymbol{C}}_k \boldsymbol{A}_{k,n} + \boldsymbol{V}_n, \tag{IV.2.4}$$

where,

$$\boldsymbol{Y}_n = \begin{bmatrix} \boldsymbol{y}_{n,l_6-1} \\ \vdots \\ \boldsymbol{y}_{n,0} \\ \boldsymbol{y}_{n-1,P-1} \\ \vdots \\ \boldsymbol{y}_{n-l_1,0} \\ \boldsymbol{y}_{n-l_1-1,P-1} \\ \vdots \\ \boldsymbol{y}_{n-l_1-1,P-l_2} \end{bmatrix}, \qquad \boldsymbol{h} = \begin{bmatrix} \boldsymbol{h}_{N-1}^H, \cdots, \boldsymbol{h}_0^H \end{bmatrix}^H$$

$$\widetilde{\boldsymbol{C}}_k = \begin{bmatrix} \underline{\boldsymbol{c}}_k & \boldsymbol{0} & \cdots & & \boldsymbol{0} \\ \boldsymbol{0} & \boldsymbol{c}_k & \boldsymbol{0} & \cdots & \\ \vdots & & \ddots & & \vdots \\ & & & \boldsymbol{c}_k & \\ \boldsymbol{0} & \cdots & & & \overline{\boldsymbol{c}}_k \end{bmatrix}$$

$$\boldsymbol{c}_k = \begin{bmatrix} c_{k,P-1} \\ \vdots \\ c_{k,1} \\ c_{k,0} \end{bmatrix}, \overline{\boldsymbol{c}}_k = \begin{bmatrix} c_{k,P-1} \\ \vdots \\ c_{k,P-l_4} \end{bmatrix}, \underline{\boldsymbol{c}}_k = \begin{bmatrix} c_{k,l_6-1} \\ \vdots \\ c_{k,0} \end{bmatrix}.$$

$\mathcal{T}(\boldsymbol{h})$ is the $M(L+P-1) \times \overline{N}$ block Toeplitz channel convolution matrix filled up with the channel coefficients grouped together in $\boldsymbol{h}$, and has full column rank. $\overline{N} = L+P+N-2$, and the periodic code matrix $\widetilde{\boldsymbol{C}}_k$ is the $(l_3 P + l_4 + l_6) \times (l_3 + 2)$ matrix accounting for the contribution of $l_3 + 2$ symbols in the received signal $\boldsymbol{Y}_n$. $\underline{\boldsymbol{c}}_k$ and $\overline{\boldsymbol{c}}_k$ denote the partial contribution of the end symbols of the data block. We

shall denote the l_3+2 columns of $\widetilde{\boldsymbol{C}}_k$ as $\boldsymbol{C}_{k,l}$, for $l \in \{0,\ldots,l_3+1\}$. $\boldsymbol{A}_{k,n} = [a_{k,n}, \ldots, a_{k,n-l_3-1}]^T$ is the symbol sequence vector, and $\widetilde{\boldsymbol{S}}_n$ denotes the $L+P+N-2 = l_3P+l_4+l_6$ diagonal scrambling code matrix with the diagonal element given by

$$\left[s_{n,l_6-1},\ldots,s_{n,0},s_{n-1,P-1},\cdots,s_{n-l_3,0},s_{n-l_3-1,P-1},\ldots,s_{n-l_3-1,P-l_4}\right].$$

IV.3 Training based Channel Estimation

Consider a downlink synchronous slot corresponding of $L+P-1$ received data vectors as depicted in (IV.2.4). As mentioned before, the MIMO problem can simply be cast into a SIMO framework due to the point-to-point nature of the downlink channel permitting one to write (IV.2.4) as $\boldsymbol{Y}_n = \mathcal{T}(\boldsymbol{h})\boldsymbol{B}_n + \boldsymbol{V}_n$.

We suppose here that the training symbols for all active users are known over the common training period of the frame/slot. In the UMTS WCDMA downlink, the control/data slot contains a fixed number of training symbols for all users which are time-aligned due to the synchronous nature of the downlink. As in the current GSM standard, the training symbols $\boldsymbol{A}_{k,n}$ can be pre-selected quantities. In the case of intracell users, the number of active users and their rate information is broadcast on a common downlink channel, thus making the spreading code information available to all mobile stations managed by the cell site. Then, the estimation of the channel is the one obtained by the least-squares criterion. By exploiting the commutativity of the convolution, we get: $\mathcal{T}(\boldsymbol{h})\boldsymbol{B}_n = \mathcal{B}\boldsymbol{h}$, where,

$$\begin{aligned}\mathcal{B} &= B_{\overline{N},N} \otimes \boldsymbol{I}_M \\ B_{\overline{N},N} &= \begin{bmatrix} b_{-N+1} & b_{-N+2} & \cdots & b_0 \\ b_{-N+2} & \iddots & \iddots & \vdots \\ \vdots & \iddots & \iddots & \vdots \\ b_{\overline{N}-N} & \cdots & \cdots & b_{\overline{N}-1} \end{bmatrix}.\end{aligned}$$

Then, solving the maximum likelihood criterion

$$\min_h \|\boldsymbol{Y} - \mathcal{T}\boldsymbol{B}_n\|^2 \Leftrightarrow \min_h \|\boldsymbol{Y} - \mathcal{B}\boldsymbol{h}\|^2, \tag{IV.3.1}$$

for the channel, admits as solution: $\widehat{\boldsymbol{h}} = (\mathcal{B}^H\mathcal{B})^{-1}\mathcal{B}^H\boldsymbol{Y}$. The inputs $\boldsymbol{B}_n$ are from a modified discrete constellation alphabet which comes about from the linear combinations of the individual user chip alphabets summed together before entering the discrete time channel $\boldsymbol{h}$.

IV.4 Downlink Zero-Forcing Receiver

In the CDMA downlink problem, there are several kinds of zero-forcing criteria that can be pursued. We shall consider the following two special cases:

IV.4.0.1 Zero-Forcing for ISI and MAI

Extension of (IV.2.4) to a symbol rate channel model of (I.3.29) is immediate. However, the channel convolution matrix $\mathcal{T}(\boldsymbol{G}_N)$ now is time varying due to the aperiodic nature of spreading sequences. If

the scrambling were inactive, then the downlink channel model collapses into the uplink channel model presented in section § I.3, with channel lengths, N_k, same for all users issuing from the same cell-site. The development of chapter II therefore holds and we can derive an MVDR receiver just like for the uplink case. It is straightforward to see that the receiver results in perfect ISI and MAI rejection, in the noiseless case - the decorrelating solution.

IV.4.0.2 Zero-forcing for ISI only

Alternatively, one may concentrate on the inter-chip interference (and thus ISI) introduced by the multipath channel. Exploiting the fact that the downlink channel is the same for all signals, we can treat the problem as a single-input multiple-output (SIMO) vector channel transfer function, obtained from the single input $b_n = \sum_{k=1}^{K} b_{k,n}$ to the multiple outputs through the $\boldsymbol{M} \times 1$ z-domain FIR transfer function of the channel, $\mathbf{h}(z) = \sum_{i=0}^{N-1} \boldsymbol{h}_i z^{-i}$. The received signal can now be written as: $\boldsymbol{y}_n = \mathbf{h}(q)b_n + \boldsymbol{v}_n$, where, $q^{-1}b_n = b_{n-1}$. As shown in fig. IV.3, the downlink receiver has a constrained structure composed of a channel equalizer followed by a descrambler and a desired user code correlator. It is well known, that a $1 \times M$ FIR equalizer $\mathbf{f}(z) = \sum_{i=0}^{L-1} \boldsymbol{f}_i z^{-i}$ qualifies as a zero-forcing equalizer with a delay d if $\mathbf{f}(z)\mathbf{h}(z) = z^{-d}$. Let us further note that $d = l_5 P + l_6$. This gives us a reduced set of constraints

$$\boldsymbol{f}\mathcal{T}_L(\boldsymbol{h}) = [0 \cdots 0\ 1\ 0 \cdots 0], \tag{IV.4.1}$$

with 1 in the dth position. To be able to satisfy all the constraints (IV.4.1), we need to choose the filter length such that the system of equations is exactly or underdetermined. Hence,

$$L \geq \overline{L} = \left\lceil \frac{N-1}{M_{\text{eff}} - 1} \right\rceil, \tag{IV.4.2}$$

where, $M_{\text{eff}} = \text{rank}\{\boldsymbol{H}_N\}$ is the effective number of channels, and L is measured in chip periods.

IV.4.1 Discussion

In DS-CDMA systems, it is of course meaningful to suppress both the ISI and the MAI. Interference cancelation after despreading is one way to proceed resulting in a treatment of the problem as discussed in chapter II. The approach presented above corresponds to zero-forcing equalization before despreading, i.e., a chip-rate ZF receiver. The chip-rate equalizer/correlator structure is well suited to the single cell downlink problem. However, the disadvantage can be a significant noise enhancement, since the *chip* SNR is usually low in high spreading factor systems and constraining all the energy in one tap could be highly sub-optimal. Such is not the case for the RAKE receiver which collects the energy from all paths to maximize the SNR at the output (being a matched filter). However, when interferers are present, constraining all the energy in one tap is still sub-optimal for the user of interest *vis-á-vis* the

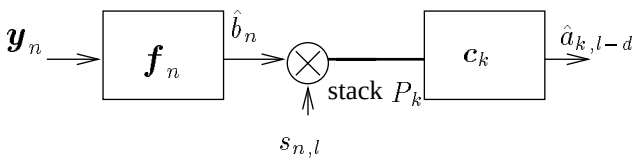

Figure IV.3: Downlink receiver structure.

noise enhancement, but a better SINR is achieved since the interference is cancelled. We shall discuss these trade-off issues in a subsequent section, when comparing the performance of different receivers.

IV.4.2 Multicellular Environment

If strong signals from U base stations are received (usually, $U = 3$ is a maximum number given hexagonal cell geometries), the L received vectors, $\boldsymbol{y}_n = \sum_{u=1}^{U} \boldsymbol{H}_{N_u} \boldsymbol{B}_{u,n} + \boldsymbol{v}_n$, can be stacked together to give $\boldsymbol{Y}_n = \sum_{u=1}^{U} \mathcal{T}(\boldsymbol{h}_u) \boldsymbol{B}_{u+L-1,n} + \boldsymbol{V}_n$. We further assume that given fairly long *i.i.d.* sequences, their linear combination is also an *i.i.d.* sequence.

Note that soft hand-off can be handled in a natural way by the ZF solution by forcing to zero the ISI from all cells but keeping one channel tap for each cell-site. Once again, the channel can be estimated jointly from the least squares criterion, and a zero-forcing equalizer satisfying (IV.4.1) can be determined, given a certain smoothing factor, $\overline{L}$.

IV.4.2.1 Dimensional Requirement

Consider the noiseless case ($v(t) \equiv 0$). Then we can write the received signal vector as $\boldsymbol{Y}_n = \mathcal{T}(\boldsymbol{h}) \boldsymbol{B}_{N+L-1} = [\mathcal{T}(h_1) \cdots \mathcal{T}(h_U)][\boldsymbol{b}_{1,N_1+L-1}^T \cdots \boldsymbol{b}_{U,N_U+L-1}^T]^T$. Now, $\mathcal{T}(\boldsymbol{h})$ is of dimension $ML \times N + U(L-1)$, with $N = \sum_{u=1}^{U} N_u$. Then in order to be zero-forcing in the noiseless case, L has to be such that $\mathcal{T}(\boldsymbol{h})$ is a tall matrix of full column rank in general. Then, $L \geq \underline{L} = \left\lceil \frac{N-U}{M_{\text{eff}}-U} \right\rceil$, where, U is the number of active base stations for the mobile user. Note that $M_{\text{eff}} > U$ is a condition that is easily satisfied for worst-case scenarios, i.e., $U = 3$, in the hexagonal cell geometry.

IV.4.3 Cyclostationary nature of intercell interferers

It is interesting to observe the behavior of intercell interference in terms of its statistical properties. Due to the aperiodic overlay sequences, the out-of-cell interferers add up as cyclostationary noise at the chip rate, $\sigma_b^2 \sum_{u=2}^{U} \mathcal{T}(\boldsymbol{h}_u)\mathcal{T}^H(\boldsymbol{h}_u) \rightarrow \sigma_b^2 \boldsymbol{R}_{\boldsymbol{hh}}$. Now $\boldsymbol{R}_{\boldsymbol{hh}}$ is a banded Toeplitz matrix with a strong diagonal element (considering chip-rate sampling is performed), and $\boldsymbol{R}_{\boldsymbol{hh}} \rightarrow \boldsymbol{I}$, as the delay spread of the channel reduces. If these interferers are weak, then their effect can be ignored due to the relatively small terms on the bands of $\boldsymbol{R}_{\boldsymbol{hh}}$.

IV.5 Blind Maximum SINR Receiver

Let us assume an arbitrary $\boldsymbol{f}$ which gives $\mathbf{f}(z)\mathbf{h}(z) = \sum_{i=0}^{L+N-2} \alpha_i z^{-i}$. We can write this set of equations as

$$\mathcal{T}(\boldsymbol{f})\mathcal{T}(\boldsymbol{h}) = \mathcal{T}(\underline{\boldsymbol{\alpha}}) = \mathcal{T}(\underline{\boldsymbol{\alpha}}_d) + \mathcal{T}(\overline{\underline{\boldsymbol{\alpha}}}_d), \tag{IV.5.1}$$

where, $\mathcal{T}(\boldsymbol{f})$ is a $P \times M(L+P-1)$ block Toeplitz convolution matrix filled up with the equalizer coefficients. $\mathcal{T}(\underline{\boldsymbol{\alpha}})$ denotes a Toeplitz matrix with the first row $[\underline{\boldsymbol{\alpha}} \;\; \mathbf{0}_{P-1}]$. Same holds for $\mathcal{T}(\underline{\boldsymbol{\alpha}}_d)$ and $\mathcal{T}(\overline{\underline{\boldsymbol{\alpha}}}_d)$, where,

$$\begin{aligned} \underline{\boldsymbol{\alpha}} &= [\alpha_0 \; \alpha_1 \; \ldots \; \alpha_{L+N-2}], \;\; \underline{\boldsymbol{\alpha}}_d = [0 \ldots 0 \; \alpha_d \; 0 \ldots 0] \\ \overline{\underline{\boldsymbol{\alpha}}}_d &= [\alpha_0 \; \ldots \; \alpha_{d-1} \; 0 \; \alpha_{d+1} \; \ldots \; \alpha_{L+N-2}]. \end{aligned} \tag{IV.5.2}$$

The $P \times 1$ vector of successive equalizer outputs can now be written as

$$\boldsymbol{Z}_n = \mathcal{T}(\boldsymbol{f})\boldsymbol{Y}_n = \mathcal{Y}_n \boldsymbol{f}^T, \tag{IV.5.3}$$

where, the last equality follows from the commutativity property of convolution. $\mathcal{Y}_n$ is a block Hankel matrix with $1 \times M$ blocks (received signal components, $\boldsymbol{y}_n^T$). The equalized signal, $\boldsymbol{Z}_n$ needs to be descrambled as $\boldsymbol{X}_n = \boldsymbol{S}_{n-l_5-1}^H \boldsymbol{Z}_n$, where

$$\boldsymbol{S}_n = \mathrm{diag}\left\{s_{n,P-1}, \ldots, s_{n,1}, s_{n,0}\right\}.$$

Note that if the equalizer is ZF ($\underline{\overline{\boldsymbol{\alpha}}}_d = \boldsymbol{0}$), then in the noiseless case ($v(t) \equiv 0$), the correlator by itself suffices to suppress the interference contributions in $\boldsymbol{X}_n$ [GS98b].

Let us denote by

$$\underline{\underline{C}} = [\boldsymbol{c}_1 \ \ldots \boldsymbol{c}_K], \text{ and } \underline{\underline{C}}^{\perp} = [\boldsymbol{c}_{K+1} \ \ldots \boldsymbol{c}_P],$$

the matrices whose columns are constituted by the used and unused Walsh-Hadamard sequences respectively for the system ($\underline{\underline{C}}^{\perp H}\underline{\underline{C}} = \boldsymbol{0}$). Then an equalizer $\boldsymbol{f}$ can be obtained by imposing that the descrambled output of the equalizer be orthogonal to the codes $\underline{\underline{C}}^{\perp}$ in the absence of noise [LL99]. In other words, the equalizer can be obtained as the argument of the following cost function:

$$\arg \min_{\boldsymbol{f}} \ E\|\underline{\underline{C}}^{\perp H}\boldsymbol{X}_n\|^2. \tag{IV.5.4}$$

A fixed response constraint must be applied to the descrambled output of the equalizer for the desired signal (user 1) to avoid signal cancelation, i.e.,

$$E|\boldsymbol{c}_1^H \boldsymbol{X}_n|^2 = \mathrm{cnst}.. \tag{IV.5.5}$$

The solution to this constrained optimization problem can be written as the following generalized eigenvalue problem

$$\boldsymbol{f}^T = \arg \min_{\boldsymbol{f}} \ \frac{\boldsymbol{f}^* \widehat{\boldsymbol{R}}_0 \boldsymbol{f}^T}{\boldsymbol{f}^* \widehat{\boldsymbol{R}}_1 \boldsymbol{f}^T}, \tag{IV.5.6}$$

where, $\widehat{\boldsymbol{R}}_0 = \mathrm{avg}\{\mathcal{Y}_n \boldsymbol{S}_n \underline{\underline{C}}^{\perp}\underline{\underline{C}}^{\perp H}\boldsymbol{S}_n^H \mathcal{Y}_n^H\}$, and $\widehat{\boldsymbol{R}}_1 = \mathrm{avg}\{\mathcal{Y}_n \boldsymbol{S}_n \boldsymbol{c}_1 \boldsymbol{c}_1^H \boldsymbol{S}_n^H \mathcal{Y}_n^H\}$, and avg denotes the temporal averaging operation, and can be replaced by an expectation operator if the scrambler is inactive, i.e., $\boldsymbol{S}_n \equiv \boldsymbol{I}_P$ and $\widetilde{\boldsymbol{S}}_n \equiv \boldsymbol{I}$.

Upon first sight, it is difficult to tell what optimization problem is the equalizer a solution of. The criterion can be interpreted as the output energy of the receiver contained in the orthogonal space of $\underline{\underline{C}}$, i.e., $\underline{\underline{C}}^{\perp}$. Intuitively, this should be minimized. The constraint on the other hand imposes a constant response for the desired user. As we show in the sequel, the overall receiver (equalizer followed by descrambler and correlator) turns out to be the receiver that maximizes the SINR at its output.

IV.5.1 Asymptotic Analysis

Note that, $\boldsymbol{S}_n^H \mathcal{T}(\underline{\boldsymbol{\alpha}}_d)\widetilde{\boldsymbol{S}}_n \equiv \mathcal{T}(\underline{\boldsymbol{\alpha}}_d)$. The scrambler is modeled as *i.i.d.*, and hence asymptotic results need to be averaged over it. We shall assume symbol period cyclostationarity and that the input sequence is zero mean *i.i.d.* with variance σ_a^2. User powers β_k are included in the input sequence variance, $\sigma_k^2 = \beta_k \sigma_a^2$. We shall replace $\boldsymbol{S}_{n-l_5-1}$ by $\boldsymbol{S}_n$ in the definition of $\boldsymbol{X}_n$ to simplify notation. Let us now examine the constraint and the criterion separately in terms of their asymptotic behaviors.

IV.5.1.1 RX Output Energy - The Constraint

The output energy (variance) of the receiver which also is the constraint term, can be written as

$$E|\boldsymbol{c}_1^H\boldsymbol{X}_n|^2=E\{\boldsymbol{c}_1^H\boldsymbol{S}_n^H\mathcal{T}(\boldsymbol{f})\boldsymbol{R}_{VV}\mathcal{T}^H(\boldsymbol{f})\boldsymbol{S}_n\boldsymbol{c}_1\}+\sum_{k=1}^{K}\sigma_k^2E\left\{\boldsymbol{c}_1^H\boldsymbol{S}_n^H\mathcal{T}(\underline{\boldsymbol{\alpha}})\widetilde{\boldsymbol{S}}_n\widetilde{\boldsymbol{C}}_k\widetilde{\boldsymbol{C}}_k^H\widetilde{\boldsymbol{S}}_n^H\mathcal{T}^H(\underline{\boldsymbol{\alpha}})\boldsymbol{S}_n\boldsymbol{c}_1\right\}, \tag{IV.5.7}$$

where, $\boldsymbol{R_{VV}}=E\{\boldsymbol{V}_n\boldsymbol{V}_n^H\}$ is the noise covariance matrix of appropriate dimensions. In order to treat the problem in its generality, we consider $\boldsymbol{V}_n$ to be composed of not only the additive (white) channel noise but also the intercell interference contributed by a few base stations. $\boldsymbol{R_{VV}}$ is then banded instead of diagonal, representing the noise color. We shall maintain the notation $\boldsymbol{R_{VV}}$ wherever necessary, irrespective of its dimensions. We shall consider the following two cases of interest:

a. ***no scrambler***

In the absence of the scrambler, $\boldsymbol{S}_n\equiv\boldsymbol{I}_P$ and $\widetilde{\boldsymbol{S}}_n\equiv\boldsymbol{I}$, and the receiver output energy is given by

$$\begin{aligned}E|\boldsymbol{c}_1^H\boldsymbol{X}_n|^2=\boldsymbol{f}\boldsymbol{R}_1\boldsymbol{f}^H\ &+\textstyle\sum_{k=1}^{K}\sigma_k^2\Big\{\boldsymbol{c}_1^H\mathcal{T}(\underline{\boldsymbol{\alpha}}_d^{'})\widetilde{\boldsymbol{C}}_k\widetilde{\boldsymbol{C}}_k^H\mathcal{T}^H(\underline{\boldsymbol{\alpha}}_d^{'})\boldsymbol{c}_1+\boldsymbol{c}_1^H\mathcal{T}(\underline{\boldsymbol{\alpha}}_d^{'})\widetilde{\boldsymbol{C}}_k\widetilde{\boldsymbol{C}}_k^H\mathcal{T}^H(\overline{\underline{\boldsymbol{\alpha}}}_d^{'})\boldsymbol{c}_1\\&+\boldsymbol{c}_1^H\mathcal{T}(\overline{\underline{\boldsymbol{\alpha}}}_d^{'})\widetilde{\boldsymbol{C}}_k\widetilde{\boldsymbol{C}}_k^H\mathcal{T}^H(\underline{\boldsymbol{\alpha}}_d^{'})\boldsymbol{c}_1+\boldsymbol{c}_1^H\mathcal{T}(\overline{\underline{\boldsymbol{\alpha}}}_d^{'})\widetilde{\boldsymbol{C}}_k\widetilde{\boldsymbol{C}}_k^H\mathcal{T}^H(\overline{\underline{\boldsymbol{\alpha}}}_d^{'})\boldsymbol{c}_1\Big\},\end{aligned} \tag{IV.5.8}$$

which, upon some algebraic manipulations reduces to

$$E|\boldsymbol{c}_1^H\boldsymbol{X}_n|^2=\boldsymbol{f}\boldsymbol{R}_1\boldsymbol{f}^H+\sigma_1^2\|\underline{\boldsymbol{\alpha}}_d^{'}\|^2+2\sigma_1^2\mathrm{Re}\left\{\underline{\boldsymbol{\alpha}}_d^{''}\widetilde{\boldsymbol{C}}_1^H\mathcal{T}^H(\overline{\underline{\boldsymbol{\alpha}}}_d^{'})\boldsymbol{c}_1\right\}+\sum_{k=1}^{K}\sigma_k^2\|\widetilde{\boldsymbol{C}}_k^H\mathcal{T}^H(\overline{\underline{\boldsymbol{\alpha}}}_d^{'})\boldsymbol{c}_1\|^2, \tag{IV.5.9}$$

where, $\boldsymbol{R}_1=\mathcal{T}(\boldsymbol{c}_1^H)\boldsymbol{R}_{VV}\mathcal{T}^H(\boldsymbol{c}_1^H)$, $\underline{\boldsymbol{\alpha}}_d^{'}=[\ldots\ 0\ \alpha_{d-P}\ 0\ \ldots\ 0\ \alpha_d\ 0\ \ldots\ 0\ \alpha_{d+P}\ 0\ \ldots]$, $\overline{\underline{\boldsymbol{\alpha}}}_d^{'}=\underline{\boldsymbol{\alpha}}-\underline{\boldsymbol{\alpha}}_d^{'}$, and $\underline{\boldsymbol{\alpha}}_d^{''}=[\ldots\ \alpha_{d-P}\ \alpha_d\ \alpha_{d+P}\ \ldots]$ is a $1\times l_3$ vector consisting of non-zero elements of $\underline{\boldsymbol{\alpha}}_d^{'}$. Not that if $\boldsymbol{f}$ is a ZF equalizer, then in the noiseless case ($v(t)\equiv 0$), $\overline{\underline{\boldsymbol{\alpha}}}_d^{'}=0$, and the only remaining contribution is the second term in (IV.5.9), from which it becomes clear that upon ZF, contributions from l_3 symbols appear in the output amounting to residual ISI in the receiver output.

b. ***with scrambler***

In this case,

$$\begin{aligned}E|\boldsymbol{c}_1^H\boldsymbol{X}_n|^2=&\boldsymbol{c}_1^H\mathrm{diag}\left\{\mathcal{T}(\boldsymbol{f})\boldsymbol{R}_{VV}\mathcal{T}^H(\boldsymbol{f})\right\}\boldsymbol{c}_1+\sum_{k=1}^{K}\sigma_k^2\Big[\boldsymbol{c}_1^H\mathcal{T}(\underline{\boldsymbol{\alpha}}_d)\widetilde{\boldsymbol{C}}_k\widetilde{\boldsymbol{C}}_k^H\mathcal{T}^H(\underline{\boldsymbol{\alpha}}_d)\boldsymbol{c}_1\\&+E\Big\{\boldsymbol{c}_1^H\mathcal{T}(\underline{\boldsymbol{\alpha}}_d)\widetilde{\boldsymbol{C}}_k\widetilde{\boldsymbol{C}}_k^H\widetilde{\boldsymbol{S}}_n^H\mathcal{T}^H(\overline{\underline{\boldsymbol{\alpha}}}_d)\boldsymbol{S}_n\boldsymbol{c}_1\Big\}+E\Big\{\boldsymbol{c}_1^H\boldsymbol{S}_n^H\mathcal{T}(\overline{\underline{\boldsymbol{\alpha}}}_d)\widetilde{\boldsymbol{S}}_n\widetilde{\boldsymbol{C}}_k\widetilde{\boldsymbol{C}}_k^H\mathcal{T}^H(\underline{\boldsymbol{\alpha}}_d)\boldsymbol{c}_1\Big\}\\&+E\left\{\boldsymbol{c}_1^H\boldsymbol{S}_n^H\mathcal{T}(\overline{\underline{\boldsymbol{\alpha}}}_d)\widetilde{\boldsymbol{S}}_n\widetilde{\boldsymbol{C}}_k\widetilde{\boldsymbol{C}}_k^H\widetilde{\boldsymbol{S}}_n^H\mathcal{T}^H(\overline{\underline{\boldsymbol{\alpha}}}_d)\boldsymbol{S}_n\boldsymbol{c}_1\right\}\Big].\end{aligned} \tag{IV.5.10}$$

It can be easily verified that the first term inside the summation over K in (IV.5.10) gives $\sigma_a^2|\alpha_d|^2$ i.e., the desired signal energy, instead of l_3 terms as in the case without scrambling (IV.5.9). The fourth term in (IV.5.10) can be written as $\sum_{l=0}^{l_3+1}E\{\boldsymbol{c}_1^H\boldsymbol{S}_n^H\mathcal{T}^H(\overline{\underline{\boldsymbol{\alpha}}}_d)\widetilde{\boldsymbol{S}}_n\boldsymbol{C}_{k,l}\}\boldsymbol{C}_{k,l}^H\mathcal{T}^H(\underline{\boldsymbol{\alpha}}_d)\boldsymbol{c}_1$, of which the term outside the expectation is non-zero only for $k=1$ and $l=l_5+1$ (corresponding to the correct positioning for the scrambler). The expectation term can be written as $\mathrm{tr}\{\mathcal{T}(\overline{\underline{\boldsymbol{\alpha}}}_l)E(\widetilde{\boldsymbol{S}}_n\boldsymbol{C}_{1,l}\boldsymbol{c}_1^H\boldsymbol{S}_n^H)\}$, $l\in$

$\{0,\ldots,l_3+1\}$, and is always zero due to expectation over the scrambler. Similar treatment applies for the third term. As for the last contribution of (IV.5.10), which can be written as

$$\sum_{l=0}^{l_3+1} E\{\boldsymbol{c}_1^H \boldsymbol{S}_n^H \mathcal{T}(\underline{\overline{\boldsymbol{\alpha}}}_d)\widetilde{\boldsymbol{S}}_n \boldsymbol{C}_{k,l}\boldsymbol{C}_{k,l}^H \widetilde{\boldsymbol{S}}_n^H \mathcal{T}^H(\underline{\overline{\boldsymbol{\alpha}}}_d)\boldsymbol{S}_n \boldsymbol{c}_1\},$$

it is a fourth-order expectation in matrices $\boldsymbol{S}_n$ and $\widetilde{\boldsymbol{S}}_n$ and using the relations

- $E\{\boldsymbol{S}_n^H \mathcal{T}(\underline{\overline{\boldsymbol{\alpha}}}_d)\widetilde{\boldsymbol{S}}_n\} = 0$
- $E\{\widetilde{\boldsymbol{S}}_n \boldsymbol{C}_{k,l}\boldsymbol{C}_{k,l}^H \widetilde{\boldsymbol{S}}_n^H\} = \frac{1}{P}\boldsymbol{I}_{\overline{N}}$
- $E\{\boldsymbol{S}_n \boldsymbol{c}_1 \boldsymbol{c}_1^H \boldsymbol{S}_n^H\} = \frac{1}{P}\boldsymbol{I}_P$
- $E\{\boldsymbol{x}\boldsymbol{x}^T\} = 0$, if $\boldsymbol{x}$ is a circular random variable [JS88],

can be written as a sum of three (two) second order terms in the case of real (complex) scrambling. It can be shown that the overall contribution can be written as $\|\underline{\overline{\boldsymbol{\alpha}}}_d\|^2/P$ per user in the complex scrambling case, to which a term $\sum_{k=1}^K \sigma_k^2 \,\mathrm{tr}\{\boldsymbol{B}\boldsymbol{D}_k\boldsymbol{D}_1\boldsymbol{B}^*\boldsymbol{D}_k\boldsymbol{D}_1\}$ is added in the real scrambling case. $\boldsymbol{D}_k = \mathrm{diag}\{\boldsymbol{c}_k\}$ and

$$\boldsymbol{B} = \begin{bmatrix} 0 & \alpha_{d+1} & \cdots & \alpha_{d+P-1} \\ \alpha_{d-1} & 0 & \ddots & \vdots \\ \vdots & \ddots & \ddots & \alpha_{d+1} \\ \alpha_{d-P+1} & \cdots & \alpha_{d-1} & 0 \end{bmatrix}.$$

is a $P \times P$ Toeplitz matrix. We can now write the RX output variance as

$$E|\boldsymbol{c}_1^H \boldsymbol{X}_n|^2 = \boldsymbol{f}\boldsymbol{R}_{VV}\boldsymbol{f}^H + \sigma_1^2|\alpha_d|^2 + \frac{1}{P}\left(\sum_{k=1}^K \sigma_k^2\right)\|\underline{\overline{\boldsymbol{\alpha}}}_d\|^2 + \sum_{k=1}^K \sigma_k^2 \,\mathrm{tr}\left\{\boldsymbol{B}\boldsymbol{D}_k\boldsymbol{D}_1\boldsymbol{B}^*\boldsymbol{D}_k\boldsymbol{D}_1\right\}, \tag{IV.5.11}$$

where tr stands for the *trace* operator, and * is the complex conjugation operation. The output SINR of the receiver can finally be written as

$$\Gamma_r = \frac{\sigma_1^2|\alpha_d|^2}{\boldsymbol{f}\boldsymbol{R}_{VV}\boldsymbol{f}^H + \frac{1}{P}\left(\sum_{k=1}^K \sigma_k^2\right)\|\underline{\overline{\boldsymbol{\alpha}}}_d\|^2 + \sum_{k=1}^K \sigma_k^2 \,\mathrm{tr}\left\{\boldsymbol{B}\boldsymbol{D}_k\boldsymbol{D}_1\boldsymbol{B}^*\boldsymbol{D}_k\boldsymbol{D}_1\right\}} \tag{IV.5.12}$$

in the case of real scrambling, which reduces to

$$\Gamma_c = \frac{\sigma_1^2|\alpha_d|^2}{\boldsymbol{f}\boldsymbol{R}_{VV}\boldsymbol{f}^H + \frac{1}{P}\left(\sum_{k=1}^K \sigma_k^2\right)\|\underline{\overline{\boldsymbol{\alpha}}}_d\|^2}, \tag{IV.5.13}$$

in the case of complex scrambling, due to the circularity property of the scrambling sequence matrix.

IV.5.1.2 The Criterion

Let us now examine the criterion (IV.5.4) more closely. Similar treatment as for the constraint and the fact that the columns of $\underline{\underline{\boldsymbol{C}}}^{\perp}$ consist of mutually orthogonal codes allows us to expand the criterion as

$$E\|\underline{\underline{\boldsymbol{C}}}^{\perp H}\boldsymbol{X}_n\|^2 = \mathrm{tr}\left[E\left\{\underline{\underline{\boldsymbol{C}}}^{\perp H}\boldsymbol{S}_n^H\mathcal{T}(\boldsymbol{f})\boldsymbol{R}_{VV}\mathcal{T}^H(\boldsymbol{f})\boldsymbol{S}_n\underline{\underline{\boldsymbol{C}}}^{\perp}\right\}\right] + \sum_{k=1}^{K}\sigma_k^2\,\mathrm{tr}\left[E\left\{\underline{\underline{\boldsymbol{C}}}^{\perp H}\boldsymbol{S}_n^H\mathcal{T}(\underline{\boldsymbol{\alpha}})\widetilde{\boldsymbol{S}}_n\widetilde{\boldsymbol{C}}_k\widetilde{\boldsymbol{C}}_k^H\widetilde{\boldsymbol{S}}_n^H\mathcal{T}^H(\underline{\boldsymbol{\alpha}})\boldsymbol{S}_n\underline{\underline{\boldsymbol{C}}}^{\perp}\right\}\right]. \tag{IV.5.14}$$

Again let us analyze the following two cases:

a. ***no scrambler***

Again substituting for $\boldsymbol{S}_n \equiv \boldsymbol{I}_P$ and for $\widetilde{\boldsymbol{S}}_n \equiv \boldsymbol{I}$, and observing that $\underline{\underline{\boldsymbol{C}}}^{\perp H}\mathcal{T}(\underline{\boldsymbol{\alpha}}_d^{'})\widetilde{\boldsymbol{C}}_k = 0$, for $k = 1,\ldots,K$, equation (IV.5.14) reduces to

$$E\|\underline{\underline{\boldsymbol{C}}}^{\perp H}\boldsymbol{X}_n\|^2 = \boldsymbol{f}\boldsymbol{R}\boldsymbol{f}^H + \sum_{i=k+1}^{P}\sum_{l=0}^{l_3+1}\sum_{k=1}^{K}\sigma_k^2|\boldsymbol{c}_i^H\mathcal{T}(\overline{\boldsymbol{\alpha}}_d^{'})\boldsymbol{C}_{k,l}|^2, \tag{IV.5.15}$$

where, $\boldsymbol{R} = \sum_{i=K+1}^{P}\mathcal{T}(\boldsymbol{c}_i^H)\boldsymbol{R}_{VV}\mathcal{T}^H(\boldsymbol{c}_i^H)$. In the above, we note that $\underline{\underline{\boldsymbol{C}}}^{\perp H}\mathcal{T}(\underline{\boldsymbol{\alpha}}_d^{'})\boldsymbol{c}_k = 0,\ \forall k = 1\ \ldots\ K$. This criterion becomes zero and the fixed output energy constraint in (IV.5.7) can be satisfied in the high SNR region ($v(t) \to 0$ and $\boldsymbol{f}\boldsymbol{R}_1\boldsymbol{f}^H$ and $\boldsymbol{f}\boldsymbol{R}\boldsymbol{f}^H$ both small) at zero-forcing. This follows from $\overline{\boldsymbol{\alpha}}_d^{'} = \boldsymbol{0}$. However, $\underline{\boldsymbol{\alpha}}_d^{'} \neq \boldsymbol{0}$. This shows why several terms contribute in the solution to the criterion. The ZF criterion gets satisfied without removing the ISI contributions. In other words, if there is no scrambler, nothing distinguishes one symbol period from another neither in the criterion, nor in the constraint. The resulting ISI can possibly be removed by applying a symbol rate equalizer at the correlator output. However, a serious handicap in the realm of blind symbol-rate equalization will be the monochannel aspect of the correlator output.

b. ***with scrambler***

The criterion can be shown to result in the following relation in the instance of a scrambling whose alphabet is chosen from a real constellation

$$E\|\underline{\underline{\boldsymbol{C}}}^{\perp H}\boldsymbol{X}_n\|^2 = (P-K)\,\boldsymbol{f}\boldsymbol{R}_{VV}\boldsymbol{f}^H + \frac{P-K}{P}\sum_{k=1}^{K}\sigma_k^2\|\overline{\boldsymbol{\alpha}}_d\|^2 + \sum_{i=K+1}^{P}\sum_{k=1}^{K}\sigma_k^2\,\mathrm{tr}\left\{\boldsymbol{B}\boldsymbol{D}_k\boldsymbol{D}_i\boldsymbol{B}^*\boldsymbol{D}_k\boldsymbol{D}_i\right\}, \tag{IV.5.16}$$

It is the final contribution in (IV.5.16) that arises only in the case of real scrambling. The overall problem for the complex scrambling case then be expressed as

$$\min_{\boldsymbol{f}}\ \boldsymbol{f}\boldsymbol{R}_{VV}\boldsymbol{f}^H + \frac{1}{P}(\sum_{k=1}^{K}\sigma_k^2)|\overline{\boldsymbol{\alpha}}_d\|^2 \quad \text{s.t.} \quad \boldsymbol{f}\boldsymbol{R}_{VV}\boldsymbol{f}^H + \frac{1}{P}(\sum_{k=1}^{K}\sigma_k^2)|\overline{\boldsymbol{\alpha}}_d\|^2 + \sigma_1^2|\alpha_d|^2 = \mathrm{cnst}.$$

Apart from a scale factor, this is equivalent to $\max\ \mathrm{SINR}$.

IV.5.2 Alternative Criteria and Constraints

A number of alternatives exist for criteria and constraint sets. For example, the constraint can also involve all used codes. The modified constraint can now be expressed as

$$E\|\underline{\underline{\boldsymbol{C}}}^H \boldsymbol{X}_n\|^2 = \sum_{i=1}^{K} |\boldsymbol{c}_i^H \boldsymbol{X}_n|^2 = K \boldsymbol{f} \boldsymbol{R}_{VV} \boldsymbol{f}^H + \left(\sum_{k=1}^{K} \sigma_k^2 \right) |\alpha_d|^2 + \left(\sum_{k=1}^{K} \sigma_k^2 \right) \frac{K}{P} \|\overline{\underline{\boldsymbol{\alpha}}}_d\|^2 + \sum_{i=1}^{K} \sum_{k=1}^{K} \sigma_k^2 \, \mathrm{tr}\left\{ \boldsymbol{B} \boldsymbol{D}_k \boldsymbol{D}_i \boldsymbol{B}^* \boldsymbol{D}_k \boldsymbol{D}_i \right\}, \tag{IV.5.17}$$

The criterion in (IV.5.16) subject to the above constraint still gives the max SINR receiver. The sum of (IV.5.16) and (IV.5.17), i.e.,

$$E\|\boldsymbol{X}_n\|^2 = \left(\sum_{k=1}^{K} \sigma_k^2 \right) |\alpha_d|^2 + P \left\{ \boldsymbol{f} \boldsymbol{R}_{VV} \boldsymbol{f}^H + \left(\sum_{k=1}^{K} \sigma_k^2 \right) \frac{1}{P} \|\overline{\underline{\boldsymbol{\alpha}}}_d\|^2 \right\}. \tag{IV.5.18}$$

which holds for both real and complex scrambling owing to the disappearance of the last term in the sum ($\sum_{i=1}^{P} \boldsymbol{D}_i \boldsymbol{B} \boldsymbol{D}_i = \boldsymbol{0}$), can also be maximized subject to the $E\|\underline{\underline{\boldsymbol{C}}}^{\perp H} \boldsymbol{X}_n\|^2 = \mathrm{cnst.}$, or

$$\max_{\boldsymbol{f}} \frac{E\|\boldsymbol{X}_n\|^2}{E\|\underline{\underline{\boldsymbol{C}}}^{\perp H} \boldsymbol{X}_n\|^2} \tag{IV.5.19}$$

Let us consider

$$E\|\boldsymbol{X}_n\|^2 = \mathrm{cnst.} \Rightarrow \boldsymbol{f} \boldsymbol{R}_{VV} \boldsymbol{f}^H + \left(\sum_{k=1}^{K} \sigma_k^2 \right) \frac{1}{P} \|\overline{\underline{\boldsymbol{\alpha}}}_d\|^2 = \mathrm{cnst.} - \frac{1}{P} \left(\sum_{k=1}^{K} \sigma_k^2 \right) |\alpha_d|^2. \tag{IV.5.20}$$

We can also write the output energy as

$$E|\boldsymbol{c}_1^H \boldsymbol{X}_n|^2 = \mathrm{cnst.} + \left\{ \sigma_1^2 - \frac{1}{P} \left(\sum_{k=1}^{K} \sigma_k^2 \right) \right\} |\alpha_d|^2. \tag{IV.5.21}$$

Then, another alternative is

$$\max_{\boldsymbol{f}} \; E|\boldsymbol{c}_1^H \boldsymbol{X}_n|^2 \;\; \text{s.t.} \quad E\|\boldsymbol{X}_n\|^2 = \mathrm{cnst.}, \tag{IV.5.22}$$

if $\sigma_1^2 - (\sum_{k=1}^{K} \sigma_k^2)/P > 0$. Also, since

$$E\|\underline{\underline{\boldsymbol{C}}}^H \boldsymbol{X}_n\|^2 = \mathrm{cnst.} + \left\{ \left(\sum_{k=1}^{K} \sigma_k^2 \right) - \frac{K}{P} \left(\sum_{k=1}^{K} \sigma_k^2 \right) \right\} |\alpha_d|^2 > 0, \tag{IV.5.23}$$

we can also do

$$\max_{\boldsymbol{f}} \; E\|\underline{\underline{\boldsymbol{C}}}^H \boldsymbol{X}_n\|^2 \;\; \text{s.t.} \quad E\|\boldsymbol{X}_n\|^2 = \mathrm{cnst.}. \tag{IV.5.24}$$

It is easy to see that all these criterion and constraint sets lead to the $\max_{\boldsymbol{f}}$ SINR solution. Furthermore, in terms of asymptotic performance, all criteria are equivalent. Computationally, however, one implementation may have numerical advantages over another.

IV.6 The RAKE Receiver

If a RAKE receiver is employed for the desired user's signal at the mobile station, then, $\mathbf{f}(z) = \mathbf{h}^{\dagger}(z)$, and $\underline{\boldsymbol{\alpha}}$ in (IV.5.2) represents the autocorrelation sequence of the channel. Let us introduce the superscript ^{h} to account for this fact.

$$\begin{aligned}
\underline{\boldsymbol{\alpha}}^{h} &= [\alpha_{-N+1}\ \alpha_{-N+2}\ \ldots\alpha_0\ \ldots\alpha_{N-2}\ \alpha_{N-1}], \\
\underline{\boldsymbol{\alpha}}_d^{h} &= [0\ \ldots\ 0\ \alpha_0\ 0\ \ldots\ 0], \text{ and} \\
\overline{\underline{\boldsymbol{\alpha}}}_d^{h} &= [\alpha_{-N+1}\ \alpha_{-N+2}\ \ldots\alpha_{-1}\ 0\ \alpha_1\ldots\alpha_{N-2}\ \alpha_{N-1}],
\end{aligned} \tag{IV.6.1}$$

where, $\alpha_0 = \|\boldsymbol{h}\|^2$ represents the middle tap, or the autocorrelation at lag zero of the channel. Then, using the same set of derivations as before, the RX output energy can be expressed by the following relation.

$$E|\boldsymbol{c}_1^H \boldsymbol{X}_n|^2 = \boldsymbol{h}^H \boldsymbol{R}_{VV} \boldsymbol{h} + \sigma_1^2 \|\boldsymbol{h}\|^4 + \frac{1}{P}\left(\sum_{k=1}^{K} \sigma_k^2\right) \|\overline{\underline{\boldsymbol{\alpha}}}_d^{h}\|^2 + \sum_{k=1}^{K} \sigma_k^2 \,\mathrm{tr}\left\{\boldsymbol{B}_h \boldsymbol{D}_k \boldsymbol{D}_1 \boldsymbol{B}_h^* \boldsymbol{D}_k \boldsymbol{D}_1\right\}, \tag{IV.6.2}$$

where,

$$\boldsymbol{B}_h = \begin{bmatrix} 0 & \alpha_1 & \cdots & \alpha_{P-1} \\ \alpha_{-1} & 0 & \ddots & \vdots \\ \vdots & \ddots & \ddots & \alpha_1 \\ \alpha_{-P+1} & \cdots & \alpha_{-1} & 0 \end{bmatrix}.$$

is the $P \times P$ Toeplitz matrix comprised of the channel correlation sequence elements. The output SINR of the RAKE receiver can finally be written as

$$\Gamma_{\mathrm{RAKE},r} = \frac{\sigma_1^2 \|\boldsymbol{h}\|^4}{\boldsymbol{h}^H \boldsymbol{R}_{VV} \boldsymbol{h} + \frac{1}{P}\left(\sum_{k=1}^{K} \sigma_k^2\right) \|\overline{\underline{\boldsymbol{\alpha}}}_d^{h}\|^2 + \sum_{k=1}^{K} \sigma_k^2 \,\mathrm{tr}\left\{\boldsymbol{B}_h \boldsymbol{D}_k \boldsymbol{D}_1 \boldsymbol{B}_h^* \boldsymbol{D}_k \boldsymbol{D}_1\right\}}, \tag{IV.6.3}$$

for the case of real scrambling, shrinking for complex scrambling to

$$\Gamma_{\mathrm{RAKE},c} = \frac{\sigma_1^2 \|\boldsymbol{h}\|^4}{\boldsymbol{h}^H \boldsymbol{R}_{VV} \boldsymbol{h} + \frac{1}{P}\left(\sum_{k=1}^{K} \sigma_k^2\right) \|\overline{\underline{\boldsymbol{\alpha}}}_d^{h}\|^2} \tag{IV.6.4}$$

Note that the matrix $\boldsymbol{B}_h$ will be a banded matrix (with a zero diagonal) in the case where $N < P$, i.e., when the delay spread of the propagation channel is smaller than the processing gain, as usually is the case in spread-spectrum systems [TIA93].

IV.6.1 Comments

Equations (IV.5.12) (IV.5.13) and (IV.6.3) (IV.6.4) are highly illustrative in comparing the performances of different receivers for the DS-CDMA downlink in the case of a single cell. The first observation is that complex scrambling yields improved performance irrespective of the type of receiver. Computationally however, the averaging operation might require longer time (more samples) if complex scrambling is applied. Another observation is that the use of orthogonal signature sequences is justified, as opposed to randomly chosen sequences. In the latter case, as seen from (IV.5.10), the interference term in the denominator will be augmented by $\gamma_k |\alpha_d|^2$ for the kth user, where γ_k represents the

cross-correlation between the spreading sequences of the desired user[1] and the kth user. Same holds for the RAKE receiver.

Another consideration is the spreading factor, P, in relation with the delay spread, N, of the channel. For the case of high rate users in a multirate situation [ETS97a], P is small and so is K. The chip energy to noise ratio ($\frac{E_c}{N_0}$) is fairly good in such an instance. However, N can be fairly large (significant delay spread), and the denominator term in the SINR equations will be dominated by the ISI. Consequently, an equalizer/correlator approach appears to be more attractive in these situations. The ISI terms at the RAKE output will act as several equal power interferers resulting in a flooring effect in the output SINR, which is typical of the RAKE receiver in interference. Another argument in favor of the equalizer/correlator receiver structure is that the RAKE does not benefit from inherent interference rejection property of a spread spectrum system when the processing gain is so small (e.g., $P = 4$), and is highly suboptimal if the input signal-to-noise ratio is reasonably high. As P decreases, the system effectively starts looking more and more like a TDMA based system. For $P = 4$, for example, only one user is likely to be active at a certain instant [ETS97a] in a network.

On the other hand, in multicode communications, the RAKE appears to be the more judicious choice owing to a worse E_c/N_0 ratio which will render the operation of a ZF receiver impossible due to significant noise-enhancement. Furthermore, ISI can essentially be ignored if $P >> N$, and under power controlled conditions, sophisticated receivers may be too complex to be of utility.

Another consideration is that $\boldsymbol{R}_{VV}$ can account for the intercell interference. Nevertheless, since the scramblers are base-station dependent it is banded and approaches a multiple of identity if the channel from interfering base-stations are short, and can be ignored if powers of these interferers are very weak.

IV.7 Numerical Examples

The simulation framework models the downlink of a UMTS Wideband CDMA type system with orthogonal channelization codes overlaid by a cell-site specific scrambler randomizing the periodic user code sequences. Several values for the spreading gain, P are assumed for these examples. We consider a fixed value of delay spread (approximately 9 chip periods) in these examples. The extent of ISI will naturally depend on the value of P for different cases. Note that there is no change in the model if users with different rates are present, since the basic signature waveforms are orthogonal.

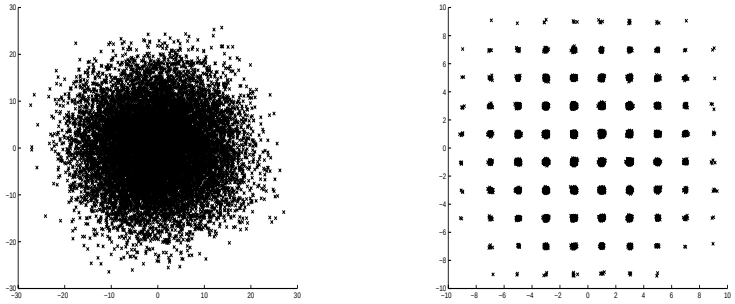

Figure IV.4: Eye of the received and equalized signals for the ZF receiver with as SNR$= 30$ dB, and $K = 9$ intracell users, $P = 16$, with an input symbol constellation of QPSK.

[1] user 1 is considered as the desired user

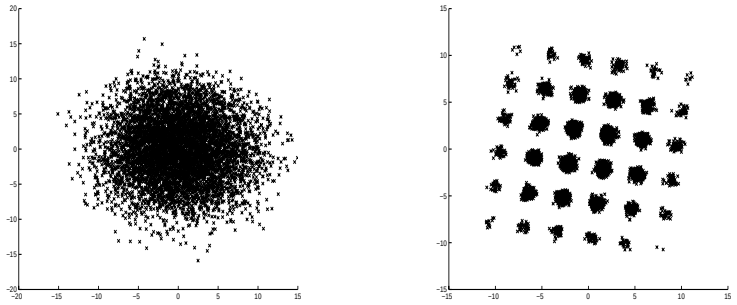

Figure IV.5: Eye of the received and equalized signals for the maximum SINR receiver with as SNR$= 20$ dB, and and $K = 5$ intracell users, $P = 16$, with an input symbol constellation of QPSK.

The input signal constellation is QPSK with the primary spreading sequences from the binary Walsh-Hadamard set, followed by the randomly selected scrambler with an alphabet $s_n \in \{+1, -1\}$ for the real case, and $s_n \in \{\pm(1+j), \pm(1-j)\}$. The eye of the received and equalized signals are shown in fig. IV.4 for the ZF equalizer at a SNR of 30 dB. As expected the equalized signal vectors are combinations of the input alphabets. A root-raised cosine pulse with a roll-off factor of 0.22 is used in these simulations conform with the UMTS WCDMA norm [ETS97a]. Fig. IV.5 shows the eye diagram for the blind maximum SINR receiver with 5 intracell users and an input SNR of 20 dB. It comes as no surprise that the constellation is slightly rotated showing the phase ambiguity classical of second-order statistics based methods (see [dC99] for details). We choose a relatively long (3 symbol periods) equalizer in these simulations in order to satisfy $\overline{L}$ for zero-forcing in all cases. Furthermore, it is a well-known result that longer equalizers give improved performances. Another issue that can be verified by using equalizers spanning several symbols is the max. SINR output where scrambling is inactive. Indeed, contributions from several symbols are seen when the blind maximum SINR receiver is adapted without scrambling. Fig. IV.6 compares the output signal-to-interference-and-noise ratio

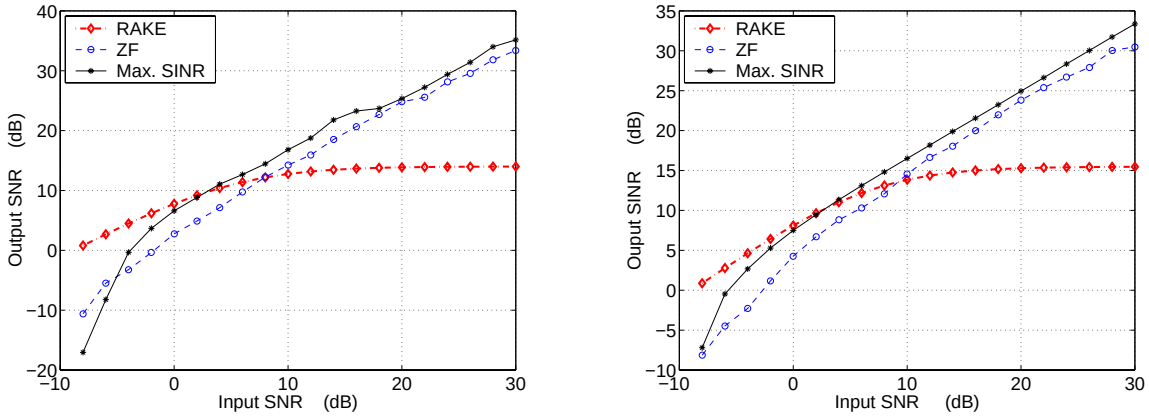

Figure IV.6: SINR comparison of RAKE, ZF and the max SINR receiver for $P = 16$, $K = 1$ intracell users, real scrambling (left), and complex scrambling (right), an input symbol constellation of QPSK, and a delay spread of approximately 9 chip periods.

(SINR) performance of the ZF and the maximum SINR receivers with that of the coherent RAKE receiver for the case of a single user system with a processing gain, $P = 16$. On the SNR axis, the

performance cross-over point is SNR$=8$ dB for the ZF receiver while SNR$=2$ dB for the max. SINR receiver. The RAKE performance is the theoretical performance in all case since the actual channel is supposed to be known for all RAKE curves. The other two receivers are estimated entities, and thus suffer from estimation errors in the low SNR region. Similar effects are observable for the case of complex scrambler. The term contributed by real scrambler in equations (IV.5.12) and (IV.6.3) fluctuates around zero and is ignored in these simulations. A flooring effect is noticeable for the RAKE receiver. As for the ZF and MMSE receivers, once the channel is equalized, the effect of other users can be perfectly removed owing to the underlying orthogonality. It is observable in these plots that at low SNRs, a significant performance loss for the ZF receiver is incurred due to the noise enhancement.

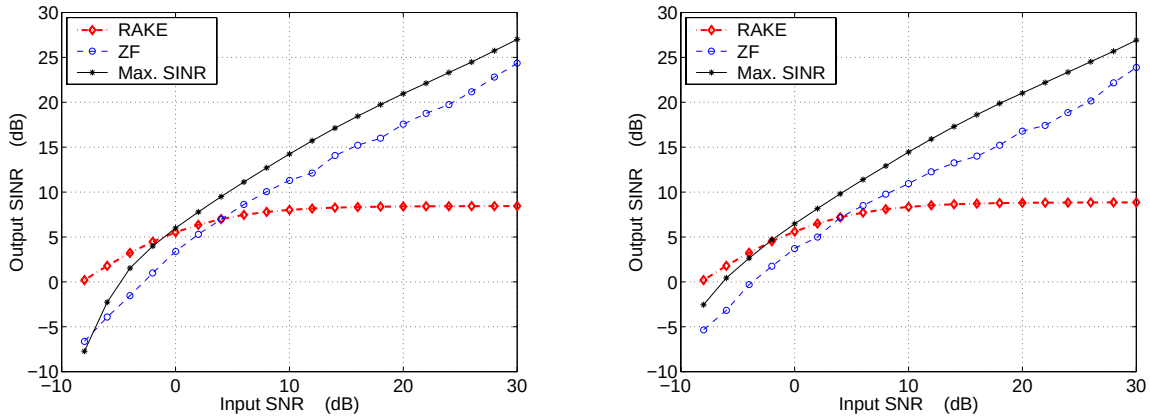

Figure IV.7: SINR comparison of RAKE, ZF and the max SINR receiver for $P = 4$, $K = 1$ intra-cell users, real scrambling (left), and complex scrambling (right), an input symbol constellation of QPSK, and a delay spread of approximately 9 chip periods.

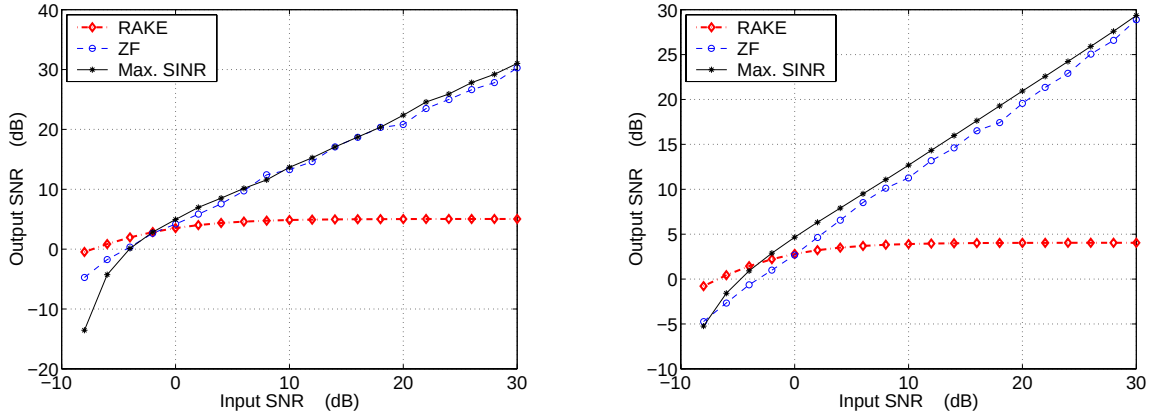

Figure IV.8: SINR comparison of RAKE, ZF and the max SINR receiver for $P = 16$, $K = 10$ intracell users, real scrambling (left), and complex scrambling (right), an input symbol constellation of QPSK, and a delay spread of approximately 9 chip periods.

Fig. IV.7 shows the performance of the three receivers in a single cell case with $K = 1$ user and a spreading gain of $P = 4$. The performance of the RAKE receiver is affected by increased ISI, while the

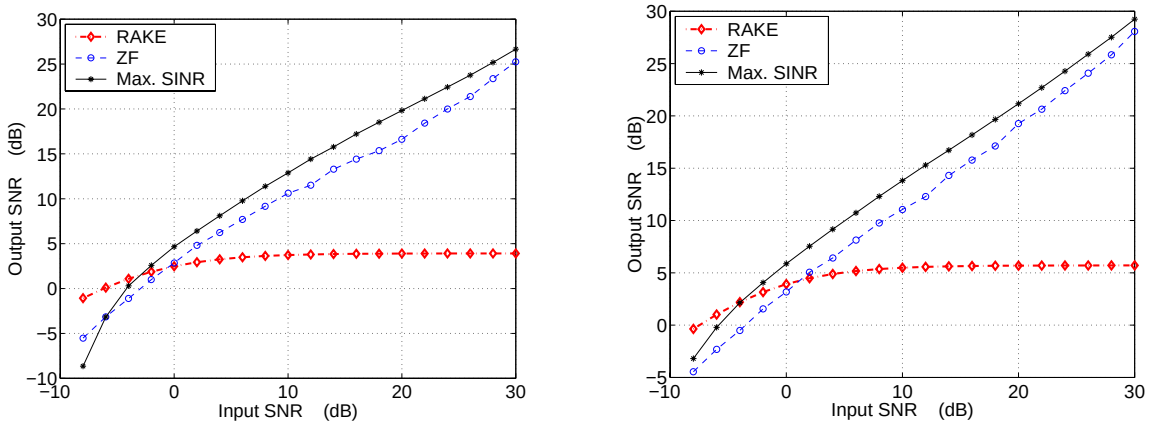

Figure IV.9: SINR comparison of RAKE, ZF and the max SINR receiver for $P = 4$, $K = 2$ intracell users, real scrambling (left), and complex scrambling (right), an input symbol constellation of QPSK, and a delay spread of approximately 9 chip periods.

cross-over now occurs at a much reduced SNR value. Fig. IV.8 shows results for $K = 10$ with $P = 16$. This time the RAKE suffers due to a large contribution of MAI. This again results in a cross-over at low SNR. Similar trends are observed in fig. IV.9 for $P = 4$, and $K = 2$, and in fig. IV.10 for $P = 4$, and $K = 3$, which represents LF$= 75\%$. Comparing the two figures, we see that such heavy loading has its effect on the max SINR receivers, since the number of unused codes is reduced to 1, and numerical errors may be enhanced due to a projection on a one-dimensional subspace. However, the receiver still is fairly robust in terms of the output SINR over a reasonable input SNR range.

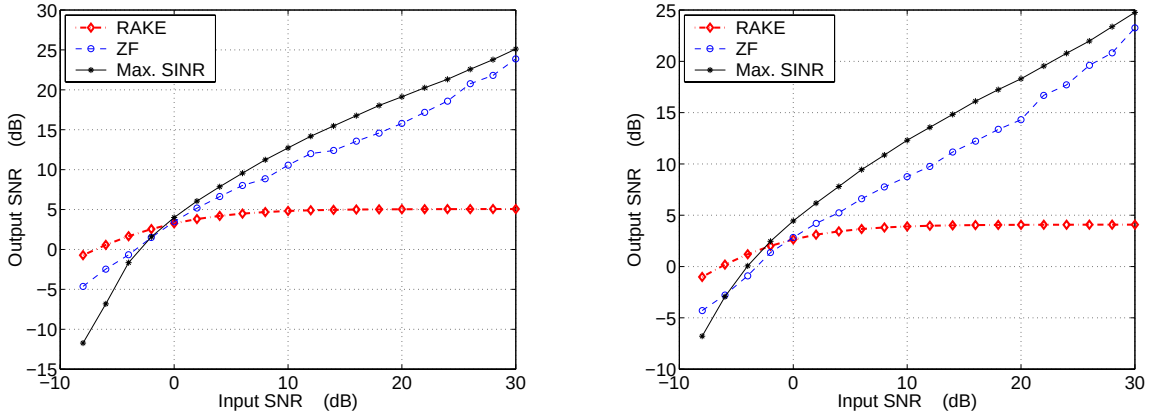

Figure IV.10: SINR comparison of RAKE, ZF and the max SINR receiver for $P = 4$, $K = 3$ intracell users, real scrambling (left), and complex scrambling (right), an input symbol constellation of QPSK, and a delay spread of approximately 9 chip periods.

The left curve in fig. IV.11 shows on one part the degradation of the training sequence based channel estimate as $K_2 = 7$ intercell interfereres (10 dB weaker) from a different cell sites interfere with $K_1 = 8$ incell users, and on the other the improvement when powers of extracell users is reduced gradually. The right curve in this figure also illustrates the same phenomenon for a fixed SNR$= 5$ dB, and reducing interferer powers. Finally, fig. IV.12 shows the performance degradation of the receivers

as intercell interference starts to creep in. We have $K = 15$ users in a code space of $P = 16$, of which $K_1 = 10$ are orthogonal users sharing the same downlink channel. The other $K_2 = 5$ issue from the neighboring cell site and are getting weaker and weaker with w.r.t. the user of interest. The figure depicts performance loss incurred by ignoring such interference.

IV.8 Conclusions

We presented a linear training based ZF receiver and a blind maximum SINR receiver as alternatives to the coherent RAKE for the downlink of a DS-CDMA system. This work has generated a lot of interest in the CDMA community was taken up in [KZ99] among others. It is seen that given an estimate of the common downlink channel, perfect zero-forcing equalization is possible in the noiseless case, irrespective of the number of users, as long as their inner spreading sequences are orthogonal (which is the case in various existing and future CDMA standards), and if sufficient spatio-temporal diversity is made available. Performance comparison with the RAKE receiver shows that in the absence of intercell

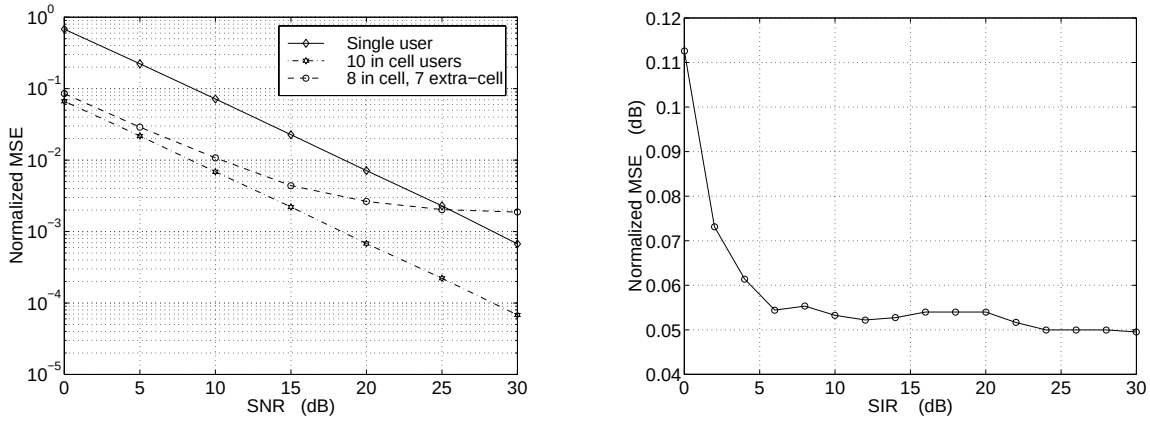

Figure IV.11: Channel estimation normalized MSE for TS method, with $P = 16$. for varying number of users and extracell users 10 dB weaker as a function of input SNR (left), and as a function of extracell interference (right), with SNR=5 dB with $K = 15$ users of which 5 are extracell users.

interference, these receivers are near far resistant and provide promising gains. Extension to multicellular environments is also possible if all downlink channels can be estimated. However, more diversity channels will be needed to zero-force in this case. Burst processing based ZF downlink receivers have also been proposed in [Kle97, FV98] for the monochannel case. However, the processing involves complex matrix operations over blocks of data and the *being tall* condition of the channel matrix is satisfied by considering zeros transmitted before and after the burst instead of multiple channels in our formulation. Furthermore, in the approach presented in this chapter, performance of the receivers is expected to be much better due to the multichannel aspect.

We also presented the blind maximum SINR receiver for the DS-CDMA downlink. It is an attractive alternative to the ZF receiver since it does not suffer from the noise enhancement problem of the latter. The max. SINR receiver can be adapted blindly only if the scrambler is active. In the absence of scrambling, the receiver can still be adapted blindly if the cascade of the channel and equalizer does not span more than one full symbol period. Otherwise, all desired user symbols contribute in the output

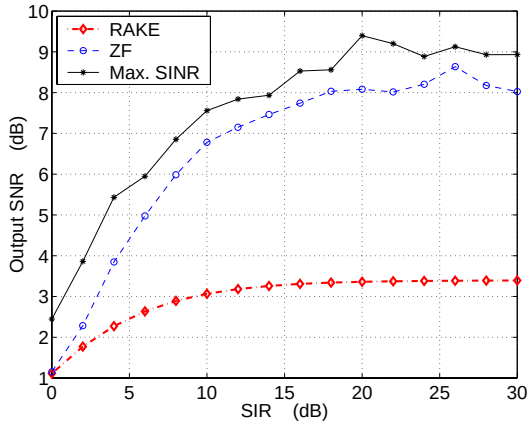

Figure IV.12: Output SINR vs. SIR in a two-cell case with $K = 15$ users, $P = 16$, with an input SNR of 5 dB, and real scrambling.

leading to ISI, and a symbol rate equalizer will be needed at the correlator output. Once must mention, however, that in order to reduce the effects of intercell interference, scrambling is always integrated on the downlink of cellular wireless systems.

Chapter V

Spatio-Temporal Array Processing for TDD/CDMA Downlink Transmission

In this chapter we address the problem of performing optimum spatio-temporal processing when using adaptive antenna arrays at base stations for multiuser downlink transmission in CDMA systems, using periodic spreading sequences and assuming the knowledge of the channel of all the users. This assumption typically holds in TDD based mobile communication systems. We consider the SDMA strategy for using antenna arrays to gain system capacity. In that case the number of interfering users located in the same cell, namely K, can be higher than the spreading factor. The goal is to design FIR transmission filters at the base station in order to maximize the minimum matched filter bound among the K users. Several approaches, namely the zero-forcing, linear minimum mean square error, minimum output energy and the pre-rake are considered to solve the problem.

V.1 Introduction

The use of adaptive antenna arrays at the base station can increase the capacity of a mobile radio network allowing an increase in the number of users. In the downlink however, the possibility of spatial diversity reception by Multiple Antennas (MA) is limited due to complexity and space limitations. Furthermore, some third generation systems like the UMTS TDMA/CDMA [ETS97b] envision operation in the time-division duplex (TDD) mode. Note that in TDD based systems the uplink and the downlink channels can be considered to be practically the same over two successive slots, assuming the mobile velocity low enough and the receiver and transmitter appropriately calibrated. Under these circumstances, since the channel is known (or estimated) from the uplink, efficient spatio-temporal processing can be performed at the base station during transmission as well as during reception. Recently, in [MS98b], the problem of performing optimum spatio-temporal processing at base stations for multiuser downlink transmission was addressed in the context of TDD/TDMA based mobile communication systems. Here, we consider the same problem but in the CDMA case. In CDMA systems for low transmission-rate users, the length of the channel is fairly short compared to the symbol duration resulting in very little Inter-Symbol Interference (ISI). In typical downlink transmission (e.g., IS-95), the multiuser channel is synchronous and the users are assigned orthogonal Walsh-Hadamard spreading sequences. It must be noted, however, that the orthogonality is destroyed by the multipath

propagation phenomenon and the actual capacity is much lower than the theoretical one. In the present work, we propose to restore the orthogonality of the spreading codes through proper pre-filtering at the base station, exploiting the knowledge of the downlink channels, which corresponds to Zero-Forcing (ZF) the Inter-User Interference (IUI). More appropriate Minimum Mean Square Error (MMSE) cost functions can be formulated when ZF cannot be obtained. In the existing literature, array processing techniques have been employed at the base station with uplink capacity improvements as objective [SNXP93, NP94]. However, emphasis is almost exclusively on purely spatial techniques. More recent work [RZ97] addresses the spatio-temporal aspect in terms of a two dimensional rake receiver with the cancelation of strong inter-user-interference (IUI) on the uplink. In our treatment the cost function results from the formulation of the Matched Filter Bound (MFB) optimization problem. We assume a TDD/CDMA mobile communication system employing Periodic Spreading Sequences (PSS), operating with Spatial Division Multiple Access (SDMA) frequency reuse technique to gain system capacity. Then more interfering users may be located in the same cell than the spreading factor (interference coming from other cells is neglected, except for the users in soft-handover mode). We point out that the framework can be easily extended to also include interferers from other cells. The maximization of the MFB leads to the minimum probability of error for an optimal receiver. We also assume that the reciprocity between up-link and downlink channels holds, i.e, the channel remains the same within successive uplink and downlink time slots. The base station performs transmission through m channels resulting from the inherent Over-Sampling (OS) due to the spreading factor, from the use of MA and/or from additional OS w.r.t. the chip rate, towards K users. Each of the K mobile receivers is assumed to have one antenna, to sample at the chip rate (i.e., no additional OS is provided at the receivers) and to employ a correlator receiver. The goal is to design the $m \times K$ FIR transmission filters in order to maximize the minimum MFB among the K users.

V.2 MFB optimization problem formulation

We assume a CDMA based system employing periodic spreading sequences, with a period equal to one symbol. Assuming the channels time-invariant for the observation time, because of such periodicity, the cascade of the code filter, the transmit filter, the channel and the receive filter results in a time-invariant system. Since the overall system is time-invariant we attempt to maximize the minimum MFB among all the K users. Actually, the ith user discrete-time received signal, for $i = 1 \ldots, K$, is

$$y_i(n) = \mathbf{c}_i^H(q)\mathbf{H}_i^T(q)\sum_{j=1}^{K}\mathbf{F}_j(q)a_j(n) + v_i(n) \tag{V.2.1}$$

where the $a_j(n)$ are the transmitted symbols intended for the jth user, q^{-1} is the unit sample delay operator (i.e., $q^{-1}y_i(n) = y_i(n-1)$), $\mathbf{H}_i^T(z)$ is the channel transfer function between the base station and the ith user, $\mathbf{c}_i^H(z)$ is the combiner matched to the code for the ith user, $\mathbf{c}_i$, $\mathbf{F}_j(z) = \mathbf{F}'_j(z)\mathbf{c}_j$ is the spatio-temporal filter for the transmitted symbols, accounting for both the actual transmit filter $\mathbf{F}'_j(z)$ to be optimized and the spreading code for the jth user, and $v_i(n)$ is the additive noise at the ith receiver. The superscripts ^{T} and ^{H} denote transpose and Hermitian transpose respectively. Assuming we have m_c chips per symbol period, each transmission filter $\mathbf{F}_i(z)$ will perform sampling at least at the chip rate, i.e., it will be at least a $m_c \times 1$ column vector. If no additional OS or MA are provided, the optimization problem for all the $\mathbf{F}_i(z)$'s reduces to one of spreading codes optimization at the transmitter in the presence of multiuser multipath channels. Moreover, in general $\mathbf{F}_j(z)$ will be a $m \times 1$ column vector, with $m = m_c m_{\mathrm{ma}} m_{\mathrm{os}}$, where m_{ma} is the number of MA and m_{os} is the additional OS rate.

We denote $\mathbf{G}_i^T(q) = \mathbf{c}_i^H \mathbf{H}_i^T(q)$ the overall channel associated to the ith user as seen from the base station. Note that since the receiver is assumed to sample at the chip rate, $\mathbf{H}_i^T(z)$ is a $m_c \times m$ matrix, $\mathbf{c}_i^H$ is a $1 \times m_c$ row vector, so that $\mathbf{G}_i^T(z)$ is a $1 \times m$ row vector, and $\mathbf{F}_j(z)$ is a $m \times 1$ column vector. Note that $\mathbf{G}_i(z)$ is the $m \times 1$ channel in the uplink from the ith user to the m base station channels.

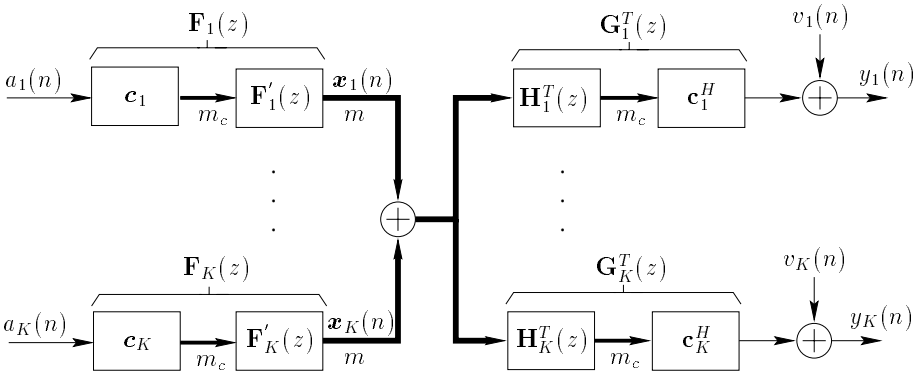

Figure V.1: Transmission filters and channels for K users

V.2.1 Frequency Domain Problem Formulation

The frequency domain MFB definition for the ith user, considering interferers as Gaussian noise, is

$$\text{MFB}_i = \frac{1}{2\pi \mathrm{j}} \oint \frac{\sigma_a^2 \mathbf{T}_{ii}^\dagger(z)\mathbf{T}_{ii}(z)}{\sigma_a^2 \sum_{j\neq i} \mathbf{T}_{ji}(z)\mathbf{T}_{ji}^\dagger(z) + \sigma_{v_i}^2} \frac{\mathrm{d}z}{z} \tag{V.2.2}$$

where $\mathbf{T}_{ji}(z) = \mathbf{G}_i^T(z)\mathbf{F}_j(z)$, $\sigma_a^2 = \mathrm{E}\{|a_i(n)|^2\}$, $\sigma_{v_i}^2$ is the variance of the additive noise $v_i(n)$, assumed temporally and spatially white hereafter, for $i, j = 1, \ldots, K$, and, in general $\mathbf{T}^\dagger(z) = \mathbf{T}^H(1/z^*)$, where the superscript * denotes conjugate. The symbols are assumed to be i.i.d. and the symbol constellation is assumed to be circular (for a real constellation, the complex signals should be split into in phase and in quadrature components). The cost function is given by

$$\max_{\{\mathbf{F}_j(z)\}} \min_i \{\text{MFB}_i\} \tag{V.2.3}$$

V.2.2 Burst Processing Time Domain Problem Formulation

Consider the ith user I/O transmission chain (see fig. V.1) regardless of the contributions intended for the other users. The channel $\boldsymbol{g}_i^T(t) = \boldsymbol{c}_i^H \boldsymbol{H}_i^T(t)$ and the transmission filter $\boldsymbol{f}_i(t) = \boldsymbol{F}_i'(t)\boldsymbol{c}_i$ are assumed to be FIR filters with duration N_iT and LT respectively (approximately), where $T = m_cT_c$ is the symbol period and T_c is the chip period. In discrete-time representation we have

$$\begin{aligned}
&\boldsymbol{x}_i(n) = \textstyle\sum_{l=0}^{L-1} \boldsymbol{f}_i(l) a_i(n-l) = \boldsymbol{F}_i A_{i,L}(n) \\
&y_i(n) = \textstyle\sum_{k=0}^{N_i-1} \boldsymbol{g}_i^T(k)\boldsymbol{x}_i(n-k) + v_i(n) = \boldsymbol{G}_i^t \boldsymbol{X}_{i,N_i}(n) + v_i(n) \\
&\boldsymbol{G}_i^t = [\boldsymbol{g}_i^T(N_i-1) \ \ldots \ \boldsymbol{g}_i^T(0)], \ \boldsymbol{F}_i = [\boldsymbol{f}_i(L-1) \ \ldots \ \boldsymbol{f}_i(0)] \\
&\boldsymbol{X}_{i,N_i}(n) = [\boldsymbol{x}_i^H(n-N_i+1) \ \ldots \ \boldsymbol{x}_i^H(n)]^H \\
&A_{i,L}(n) = [a_i(n-L+1) \ \ldots \ a_i(n)]^T
\end{aligned} \tag{V.2.4}$$

where superscript ^{t} denotes transposition of the blocks in a block matrix. If we accumulate M consecutive symbol periods

$$Y_{i,M}(n) = \mathcal{T}_M(\boldsymbol{G}_i^t)\mathcal{T}_{M+N_i-1}(\boldsymbol{F}_i)A_{i,M+N_i+L-2}(n) + V_{i,M}(n)$$

where $Y_{i,M}(n) = [y_i^H(n-M+1)\ \dots\ y_i^H(n)]^H$ and similarly for $V_{i,M}(n)$. $\mathcal{T}_M(\boldsymbol{A})$ is in general a block Toeplitz matrix with M block rows and $[\boldsymbol{A}\ \mathbf{0}_{p\times q(M-1)}]$ as first block row, where $\boldsymbol{A}$ is a matrix with $p \times q$ block entries.

Then, introducing also the contributions of all the other users, for the ith user we have

$$Y_{i,M}(n) = \sum_{j=1}^{K}\mathcal{T}_M(\boldsymbol{G}_i^t)\mathcal{T}_{M+N_i-1}(\boldsymbol{F}_j)A_{j,M+N_i+L-2}(n) + V_{i,M}(n) \tag{V.2.5}$$

and in the corresponding burst covariance matrix

$$\boldsymbol{R}_i^{(M)} = \sum_{j=1}^{K}\boldsymbol{R}_{ji}^{(M)} + \sigma_{v_i}^2\mathbf{I}_M$$

we can distinguish the following contributions

$$\begin{aligned}\boldsymbol{R}_{ii}^{(M)} &= \sigma_a^2\mathcal{T}_M(\boldsymbol{G}_i^t)\mathcal{T}_{M+N_i-1}(\boldsymbol{F}_i)\mathcal{T}_{M+N_i-1}^H(\boldsymbol{F}_i)\mathcal{T}_M^H(\boldsymbol{G}_i^t)\\ \boldsymbol{R}_{ji}^{(M)} &= \sigma_a^2\mathcal{T}_M(\boldsymbol{G}_i^t)\mathcal{T}_{M+N_i-1}(\boldsymbol{F}_j)\mathcal{T}_{M+N_i-1}^H(\boldsymbol{F}_j)\mathcal{T}_M^H(\boldsymbol{G}_i^t)\end{aligned} \tag{V.2.6}$$

where $\boldsymbol{R}_{ii}^{(M)}$ and $\boldsymbol{R}_{ji}^{(M)}$ are the contributions of the ith and jth transmitted signals respectively at the ith receiver, for $j \neq i$. Note that $\sum_{j\neq i}\boldsymbol{R}_{ji}^{(M)}$ represents the burst covariance matrix of the whole IUI at the ith receiver. Then the burst processing MFB is defined as

$$\mathrm{MFB}_i^{(M)} = \frac{1}{M}\,\mathrm{tr}\{\boldsymbol{R}_{ii}^{(M)}[\sum_{j\neq i}\boldsymbol{R}_{ji}^{(M)} + \sigma_{v_i}^2\mathbf{I}_M]^{-1}\} \tag{V.2.7}$$

where $\mathrm{tr}\{\cdot\}$ denotes the trace operator. Remark that as $M \to \infty$, $\mathrm{MFB}_i^{(M)} \to \mathrm{MFB}_i$ in (V.2.2).

In a similar fashion to the frequency domain formulation (V.2.3) the optimization criterion results in

$$\max_{\{F_j\}}\ \min_i\ \{\mathrm{MFB}_i^{(M)}\} \tag{V.2.8}$$

Both problem formulations (V.2.3), (V.2.8) are too complicated to allow any analytical approach to find the optimum solution. Nevertheless analytical solutions can be found under the following assumption that the optimal solution corresponds to a low Interference-to-Noise Ratio (INR) for all the users, i.e.,

$$\mathrm{INR}_i = \frac{\sigma_a^2}{2\pi\mathrm{j}\sigma_{v_i}^2}\sum_{j\neq i}\oint \mathbf{T}_{ji}^\dagger(z)\mathbf{T}_{ji}(z)\frac{\mathrm{d}z}{z} \ll 1, \qquad \forall i. \tag{V.2.9}$$

In that case, it is easy to see that maximizing the MFB is approximately equivalent to maximizing the Signal-to-Interference-plus-Noise Ratio (SINR) and vice versa.

Hence, referring to the burst processing problem formulation, the SINR definition for the ith user is

$$\mathrm{SINR}_i = \frac{\mathrm{tr}\{\boldsymbol{R}_{ii}^{(M)}\}}{\mathrm{tr}\{\sum_{j\neq i}\boldsymbol{R}_{ji}^{(M)} + \sigma_{v_i}^2\mathbf{I}_M\}} \tag{V.2.10}$$

By introducing $\boldsymbol{F}_i^t = [\boldsymbol{f}_i^T(L-1)\ \ldots\ \boldsymbol{f}_i^T(0)]$, it can be written as

$$\mathrm{SINR}_i = \frac{\sigma_a^2\boldsymbol{F}_i^t\boldsymbol{R}_i\boldsymbol{F}_i^{tH}}{\sigma_a^2\sum_{j\neq i}\boldsymbol{F}_j^t\boldsymbol{R}_i\boldsymbol{F}_j^{tH} + \sigma_{v_i}^2} \tag{V.2.11}$$

where $\boldsymbol{R}_i$ is a properly defined covariance matrix related to the channel $\boldsymbol{G}_i^t$, whose derivation is straightforward. In the continuous-processing case, we have $\boldsymbol{R}_i = \mathcal{T}_L(\boldsymbol{G}_i)\mathcal{T}_L^H(\boldsymbol{G}_i)$, where $\boldsymbol{G}_i = [\boldsymbol{g}(N_i-1)\ \ldots\ \boldsymbol{g}(0)]$. According to the definition (V.2.11) we denote $\mathrm{SINR}_i = \gamma_i$ in the sequel. Then let $\boldsymbol{F}_i^t = \sqrt{p_i}\boldsymbol{U}_i^t$, where $\boldsymbol{U}_i^t$ is a vector with unit norm (e.g., $\|\boldsymbol{U}_i^t\|_2 = 1$ or $\boldsymbol{U}_i^t\boldsymbol{R}_i\boldsymbol{U}_i^{tH} = 1$), the vector of the inverse SINR's $\boldsymbol{\gamma}^{-1} = [\gamma_1^{-1}\ \ldots\ \gamma_K^{-1}]^T$ and the vector of the transmit powers $\boldsymbol{p} = [p_1,\ldots,p_K]^T$. In addition we need to constrain the overall power transmitted by the base station to be less than or equal to $p_{\max}$. Hence the optimization criterion is

$$\min_{\boldsymbol{p},\{\boldsymbol{U}_i\}} \|\boldsymbol{\gamma}^{-1}\|_\infty \quad \text{s.t.} \quad \boldsymbol{\zeta}^T\boldsymbol{p} \leq p_{\max} \tag{V.2.12}$$

where[1] $\boldsymbol{\zeta} = [\|\boldsymbol{U}_1^t\|_2^2\ \ldots\ \|\boldsymbol{U}_K^t\|_2^2]^T$. In the rest of this development we shall consider the SINR optimization criterion (V.2.12), regardless of its relationship to the MFB criterion in (V.2.3). In that case $\sigma_{v_i}^2$ can account for the variance of the inter-cell interference also. Then we define the normalized power delivered by the jth transmission filter $\boldsymbol{F}_j$ to the ith user as $c_{ji} = \boldsymbol{U}_j^t\boldsymbol{R}_i\boldsymbol{U}_j^{tH}$. For any i we have

$$\gamma_i^{-1}p_ic_{ii} = \sum_{j\neq i}p_jc_{ji} + \nu_i \tag{V.2.13}$$

where we introduced $\nu_i = \sigma_{v_i}^2/\sigma_a^2$ for all the i's. In order to account for all the users we introduce the matrix $\boldsymbol{C}^T$ defined as

$$[\boldsymbol{C}^T]_{ij} = \begin{cases} c_{ji} & \text{for} j\neq i \\ 0 & \text{for} j = i \end{cases} \tag{V.2.14}$$

the matrix $\boldsymbol{D}_c = \mathrm{diag}\{[c_{11}\ \ldots\ c_{KK}]\}$, the vector $\boldsymbol{\nu} = [\nu_1\ \ldots\ \nu_K]^T$ and the matrix $\boldsymbol{P} = \mathrm{diag}(\boldsymbol{p})$. Then we have the following equation

$$\boldsymbol{\gamma}^{-1} = \boldsymbol{D}_c^{-1}\boldsymbol{P}^{-1}(\boldsymbol{C}^T\boldsymbol{p} + \boldsymbol{\nu}) \quad . \tag{V.2.15}$$

So the criterion (V.2.12) generally leads to a set of coupled problems which cannot be solved analytically. It can be shown however that the optimum (V.2.12) leads to the same γ for all the users. Indeed if some γ_i's are not the same, then we can scale the $\{p_i\}$ to improve $\gamma_{\min}$ (refer to [YX98] for a detailed proof).

V.3 MFB optimization problem solutions

Generally the optimization problem cannot be solved analytically for both $\boldsymbol{p}$ and $\{\boldsymbol{U}_i^t\}$ at the same time. Nevertheless under certain assumptions the optimization can be carried out in a decoupled way for $\boldsymbol{p}$ and $\{\boldsymbol{U}_i^t\}$ allowing analytical approaches to find the optimum.

[1] Actually, the proper norm for the $\boldsymbol{U}_i^t$'s in ζ is $\boldsymbol{U}_i^t\boldsymbol{W}\boldsymbol{U}_i^{tH}$, where $\boldsymbol{W}$ depends on the transmit pulse shape filter, but we shall ignore this issue in this development.

V.3.1 Zero-Forcing (ZF) Solution

In the noiseless case or assuming the assumption (V.2.9) holds, the MFB optimization becomes

$$\max_{\|\boldsymbol{U}_i^t\|_2=1} \{\boldsymbol{U}_i^t \boldsymbol{R}_i \boldsymbol{U}_i^{tH}\} \qquad \text{s.t.} \qquad \sum_{j\neq i} p_j \boldsymbol{U}_j^t \boldsymbol{R}_i \boldsymbol{U}_j^{tH} = 0 \tag{V.3.1}$$

Note that the condition $\sum_{j\neq i} p_j \boldsymbol{U}_j^{tH} \boldsymbol{R}_i \boldsymbol{U}_j^t = 0$ is equivalent to a set of ZF conditions in the form $\boldsymbol{U}_i^t \boldsymbol{R}_j \boldsymbol{U}_i^{tH} = 0$, for $j \neq i$. Then the optimization problem reduces to

$$\max_{\|\boldsymbol{U}_i^t\|_2=1} \|\boldsymbol{U}_i^t \mathcal{T}_L(\boldsymbol{G}_i)\|_2^2 \quad \text{s.t. } \boldsymbol{U}_i^t \mathcal{T}_L(\boldsymbol{G}_j) = \boldsymbol{0} \text{ for } j \neq i \tag{V.3.2}$$

Defining $\boldsymbol{B}_i = [\mathcal{T}_L(\boldsymbol{G}_j)]_{j\neq i}$, which is a block Toeplitz matrix accounting for all the channels but the channel $\boldsymbol{G}_i$, the solution of the problem (V.3.2) is $\boldsymbol{U}_i^{tH} = V_{\max}(\mathbf{P}_{\mathbf{B}_i}^{\perp} \boldsymbol{R}_i \mathbf{P}_{\mathbf{B}_i}^{\perp})$. In order for a non trivial solution to this problem to exist, we need $m > K - 1$, which is easily achievable when MA and/or additional OS are employed, and the constraints should not fix all the available degrees of freedom and we require

$$L > \frac{\sum_{j\neq i} N_j - (K-1)}{m_{\text{eff}} - (K-1)} \tag{V.3.3}$$

where m_{eff} denotes the effective number of channels and is given by the row rank of $\boldsymbol{G}_N = [\boldsymbol{G}_1 \ \ldots \ \boldsymbol{G}_d]$. Note that $m_{\text{eff}} = \min\{N - K + \Delta_s,\, N,\, m\}$, where $\Delta_s = \text{rank}\{[\boldsymbol{g}_1(N_1 - 1) \ \ldots \ \boldsymbol{g}_K(N_K - 1)]\}$. We also assumed $\boldsymbol{B}_i$ to be full column rank $\forall i$. The constraints present in the optimization problem (V.3.2) lead to perfect IUI cancelation. This is obtained at the expense of increased ISI at the receiver. In order to consider the ISI as well as the IUI rejection in the optimization problem we rely on the ZF pre-equalization conditions.

V.3.1.1 ZF Conditions for IUI and ISI Rejection

In order to ensure ZF conditions for IUI and ISI for the ith user the set of constraints to be considered is

$$\boldsymbol{U}_i^t \mathcal{T}_L(\boldsymbol{G}_N) = [0 \ \ldots 0 \ \ldots \overbrace{|0 \ \ldots 0 \, \alpha \, 0 \ \ldots 0|}^{i\text{th user}} \ \ldots 0 \ \ldots 0] \tag{V.3.4}$$

where $\mathcal{T}_L(\boldsymbol{G}_N) = [\mathcal{T}_L(\boldsymbol{G}_1) \ldots \mathcal{T}_L(\boldsymbol{G}_K)]$, $N = \sum_{j=1}^K N_j$ and $\alpha \neq 0$ is an arbitrary constant to be fixed in order to satisfy the constraint on the norm of $\boldsymbol{U}_i^t$. When IUI and ISI are zero-forced we have $\text{SINR}_i = \text{SNR}_i = \text{MFB}_i$ for any i. Assuming $m > K$ and $\mathcal{T}_L(\boldsymbol{G}_N)$ to be full column rank, to be able to satisfy all the constraints (V.3.4) we need to choose the length of each filter $\boldsymbol{U}_i^t$, L, such that the previous system is exactly or under-determined. Hence

$$L \geq \underline{L} = \left\lceil \frac{N - d - 1}{m_{\text{eff}} - d} \right\rceil \tag{V.3.5}$$

Then assuming $L \geq \underline{L}$ we can consider two limiting set of constraints:

- IUI rejection, no ISI rejection, as in section V.3.1.

- both IUI and ISI rejection: in this latter case the set of constraints is (V.3.4), i.e., we have $N_i + L - 1$ more constraints.

The goal is to maximize the MFB which, in the absence of IUI (equal to zero due to ZF), is proportional to the energy in the pre-filter-channel cascade. Then, the MFB decreases if all the energy is constrained in one tap. Hence if no ISI rejection is provided the best performance will be achieved, for a specified L, due to the larger number of degrees of freedom. However, in that case the ith receiver needs to equalize a delay spread of up to $N_i + L - 1$ symbol periods, corresponding to the whole delay spread due to the convolution between the channel and the transmission filter. We may prefer that the introduction of the pre-filter does not increase the delay spread, or we may want to limit the delay spread seen by the mobile to limit the complexity for the equalization task in the mobile. In those cases additional constraints in order to obtain at least partial ISI rejection, i.e., limited delay spread, can be added, leading to intermediate solutions between the previous two limiting cases. In general to have complete IUI and partial ISI rejection we add $(N_i+L-1)-L_{\mathrm{ISI}}$ constraints (coefficients of the pre-filter-channel cascade being zero), with $1 \leq L_{\mathrm{ISI}} \leq (N_i + L - 1)$, where L_{ISI} corresponds to the residual delay spread, i.e., residual ISI. This optimization problem has to be carried out for all possible positions of the nonzero part of length L_{ISI} of the pre-filter-channel cascade, and the best position should be chosen. Finally, note that as L increases the MFB increases as well. So, we shall choose the actual length of the transmission filters L according to a trade-off between performance and transmitter complexity.

Finally one may note that ZF here corresponds to the design of a bi-orthogonal perfect-reconstruction transmultiplexer in which the $\boldsymbol{F}_i$'s and $\boldsymbol{G}_i$'s are synthesis and analysis filter banks respectively.

V.3.2 Downlink Synchronous and Asynchronous Transmission

The downlink transmission can be performed in a synchronous or asynchronous fashion. In the asynchronous transmission mode the base station transmits maintaining the same asynchronous channel model for PSS-CDMA from the uplink, according to the TDD assumption of perfect channel reciprocity. On the contrary, the synchronous transmission mode corresponds to lining up all the user channels $\boldsymbol{g}_j(i)$'s in a synchronous fashion. In this case we have a *wide sense* TDD channel reciprocity, and the matrices $\boldsymbol{R}_{ji}^{(M)}$ in (V.2.6) have to be built *by hand* from the uplink channel estimates. In the previous developments we considered ZF-FIR conditions on both IUI and ISI, yielding an expression for the minimum transmission filter length $\underline{L}$. The condition for the ZF-FIR filter for IUI and ISI cancelation to exist is that the channel matrix $\mathcal{T}_L(\boldsymbol{G}_N)$ must have full column rank for a certain filter length $L \geq \underline{L}$. This assumption holds with probability close to one in the asynchronous mode for smaller $\underline{L}$ than in the synchronous mode. Indeed in the asynchronous mode $\Delta_s = K$ with probability close to one. On the contrary, in the synchronous mode Δ_s can almost surely decrease when the channel delay spreads for all users are smaller than the number of users. That results in a smaller m_{eff} which in turn results in a larger $\underline{L}$. Finally, note that $\mathcal{T}_L(\boldsymbol{G}_N)$ is full column rank with probability one for $L \geq N - K$.

V.3.3 Minimum Mean Square Error (MMSE) Solution

The MMSE criterion is given by

$$\min_{\{F_j\}} \max_i E\left\{\|y_i(n) - a_i(n-k)\|_2^2\right\}, \tag{V.3.6}$$

where n is a properly chosen delay to minimize the MMSE and

$$y_i(n) = \sum_{j=1}^{K} \boldsymbol{F}_j^t \mathcal{T}_L(\boldsymbol{G}_i) A_{j,\,N_i+L-1}(n) + v_i(n)$$

Then the criterion (V.3.6) can be written as

$$\min_{p,\,\|U_j^t\|_2=1} \max_i \{E\|p_i \boldsymbol{U}_i^t \mathcal{T}_L(\boldsymbol{G}_i) A_{i,\,N_i+L-1}(n) - a_i(n-k)\|_2^2 + \sigma_a^2 \sum_{j\neq i} p_j \boldsymbol{U}_j^t \mathcal{T}_L(\boldsymbol{G}_i) \mathcal{T}_L^H(\boldsymbol{G}_i) \boldsymbol{U}_j^{tH} + \sigma_{v_i}^2\} \tag{V.3.7}$$

where the first term corresponds to the ISI and the second one to the IUI. Hence it is straightforward to see that the MMSE corresponds to ZF on ISI and IUI when ZF conditions (V.3.4) can be applied.

V.3.4 Minimum Output Energy (MOE) Solution

Applying the MOE criterion leads to

$$\min_{\boldsymbol{p},\,\{\boldsymbol{U}_j^t\}} \max_i \{\sum_j p_j \boldsymbol{U}_j^t \boldsymbol{R}_i \boldsymbol{U}_j^{tH} + \sigma_{v_i}^2\} \quad \text{s.t. } p_i \boldsymbol{U}_i^t \mathcal{T}_L(\boldsymbol{G}_i) = \boldsymbol{q}_i \tag{V.3.8}$$

for any i, where $\boldsymbol{q}_i$ denotes a vector of constraints on the ith user pre-filter-channel cascade. It is straightforward to see that for $m_{\text{eff}} > K$ the MOE criterion leads to ZF conditions on IUI while the residual ISI depends on the constraint vector $\boldsymbol{q}_i$.

V.3.5 The Pre-Rake Scheme

The pre-rake solution consists of an independent pre-distortion of the downlink signal of each user by setting $\boldsymbol{U}_i^{tH} = \boldsymbol{G}_i^t / \|\boldsymbol{G}_i^t\|_2^2$. The mobile receiver then needs to tune to the largest peak of the pre-distorted signal. Although the pre-rake solution involves a low complexity, it is inherently sub-optimal in the presence of multiuser transmission, since it does not account for the IUI and the ISI. The aim is to avoid coherent combination of interfering signals while reducing the mobile receiver complexity.

V.3.6 Power Assignment Optimization

Assuming a given set $\{\boldsymbol{U}_i\}$, since the optimum involves all the γ_i's to be the same, expression (V.2.15) can be arranged in order to include the constraint on the transmitted power $\boldsymbol{\zeta}^T \boldsymbol{p} = p_{\max}$. By defining $\tilde{\boldsymbol{p}} = [\boldsymbol{p}^T\ 1]^T$, $\boldsymbol{\mu} = \boldsymbol{D}_c^{-1}\boldsymbol{\nu}$, $\boldsymbol{A}^T = \boldsymbol{D}_c^{-1}\boldsymbol{C}^T$, and $\boldsymbol{\zeta}^T\boldsymbol{p} = p_{\max}$, (V.2.15) reduces to the following problem (see [YX98] for details)

$$\boldsymbol{E}\tilde{\boldsymbol{p}} = \gamma^{-1}\tilde{\boldsymbol{p}}, \qquad \boldsymbol{E} = \begin{bmatrix} \boldsymbol{A}^T & \boldsymbol{\mu} \\ \frac{\boldsymbol{\zeta}^T \boldsymbol{A}^T}{p_{\max}} & \frac{\boldsymbol{\zeta}^T \boldsymbol{\mu}}{p_{\max}} \end{bmatrix} \tag{V.3.9}$$

Since $\boldsymbol{E}$ is a non-negative matrix its maximum eigenvalue is non-negative and the corresponding eigenvector is non-negative as well [HJ85]. Hence the solution to the problem (V.3.9) is unique and it is given by $\gamma^{-1} = \lambda_{\max}(\boldsymbol{E})$ and $\tilde{\boldsymbol{p}} = V_{\max}(\boldsymbol{E})$. Note that we can always re-scale $\tilde{\boldsymbol{p}}$ in order to make its last element equal to one.

V.3.7 Implementation Issues

The presence of the noise makes the optimization of the filters $\{\boldsymbol{U}_i^t\}$ involve a set of coupled problems that does not allow any analytical approach to find a solution. Therefore, we suggest to compute the vectors $\{\boldsymbol{U}_i^t\}$ applying ZF conditions (V.3.2), (V.3.4), MMSE criterion (V.3.6) or MOE criterion (V.3.8) assuming $m_{\text{eff}} > K$, which is always the case in practice. Then, given $\{\boldsymbol{U}_i^t\}$, we optimize the power assignment according to the criterion (V.3.9).

When the noise is present, since the base station cannot estimate the noise variance $\sigma_{v_i}^2$ at each receiver, unless such an estimate is provided by the mobile, the vector $\boldsymbol{\nu}$ cannot be estimated. To remedy this drawback we shall properly define the SNR at the receiver. A possible definition is given by

$$\text{SNR}_i = \frac{p_i}{\nu_i}\lambda_{\max}(\boldsymbol{R}_i), \quad \forall i$$

In practice we need

$$\min_i\{\text{SNR}_i\} \geq \text{SNR}_{\min} \tag{V.3.10}$$

where $\text{SNR}_{\min}$ is a value necessary for the mobile receiver to work with an outage probability below a specified maximum. Assuming all the users using the same receiver the worst case for the ith user occurs when $p_i = p_{\max}$ while $\nu_i = \nu_{\max} = \|\boldsymbol{\nu}\|_\infty$. Therefore a sufficient condition to satisfy the requirement (V.3.10) is given by setting

$$\text{SNR}_{\min} = \frac{p_{\max}}{\nu_{\max}}\min_i\{\lambda_{\max}(\boldsymbol{R}_i)\} \tag{V.3.11}$$

Given $\text{SNR}_{\min}$ and $p_{\max}$, $\nu_{\max}$ can be derived. Then setting $\nu_i = \nu_{\max}$ for all the i's the condition (V.3.10) is satisfied. Finally, note that for $p_{\max} \to \infty$ the optimum solution is the one in the absence of noise, for any $\nu_{\max} > 0$.

V.4 Simulations

The following simulations are provided to illustrate a practical implementation of the proposed solutions. Here we consider an CDMA/SDMA scenario in the presence of $K = 3$ users which receive signals transmitted from a base station. The channels $\boldsymbol{G}_i$'s are known (or estimated from the uplink). In the first simulation we assumed $m_c = 16$ chips per symbol, $m_{\text{ma}} = 2$ antennas and $m_{\text{os}} = 2$ OS factor w.r.t. the chip rate, so that $m = 64$. The channel delay spreads were $N_1 = N_2 = N_3 = 2$ symbol periods while $m_{\text{eff}} = 6$. Since $m_{\text{eff}} > K$ ZF conditions (V.3.4) can be applied. By setting the length of all the transmit filters equal to $L = 2$ symbol periods we obtain the performances plotted in figure V.2, in terms of SINR at each receiver versus the minimum SNR. Note that due to the large processing gain, m_c, w.r.t. the number of users and to the small delay spreads introduced by the channels the performances are insensitive to the residual delay spread L_{ISI} introduced by the pre-filter-channel cascade. Furthermore, extensive simulations have shown that larger values of L do not yield significant improvement of performances in that case. The second plot (fig. V.3), the effective number of subchannels is $m_{\text{eff}} = m = 8$. The channel delay spreads were $N_1 = N_2 = 3$ and $N_3 = 4$ symbol periods respectively. We can now apply ZF conditions. The transmit filters all are of length, $L = 4$ symbol periods. This situation corresponds to a loading fraction of 75%. Due to the high loading fraction, the residual delay spread, L_{ISI}, introduced by the pre-filter-channel cascade affects performances more

than for the previous case (fig. V.2). We may however observe that the ZF solution still provides good performance with an output SINR of 15 dB for an $\mathrm{SNR}_{\min} = 20$ dB for perfect ISI cancelation, i.e., $L_{\mathrm{ISI}} = 1$. The pre-rake falls much short of these performances for such a heavily loaded system.

In the third simulation we considered a *saturated* system configuration assuming $d = 3$, $m_c = 4$ and $m_{\mathrm{ma}} = m_{\mathrm{os}} = 1$. The channel delay spreads were $N_1 = N_2 = 3$ and $N_3 = 4$ symbol periods respectively. Also in this case $m_{\text{eff}} > K$ ($m_{\text{eff}} = 4$) and ZF conditions (V.3.4) can still be applied, but a larger filter length L will be needed. We fixed $L = 8$ symbol periods to achieve (V.3.4), whereas $L = 4$ suffices for the pre-rake. The resulting performances are plotted in fig. V.4 where significant differences arise for different values of L_{ISI}. Note that the pre-rake, even power controlled and assuming an ideal receiver, like in this case, performs always worse than the proposed solution, since it does not provide IUI cancelation. The effect of IUI can become catastrophic when working close to the system saturation, namely when the number of users approaches m.

V.5 Conclusions

We addressed the problem of the optimization of the MFB with respect to the transmit filters at a base station performing spatio-temporal processing. A general problem formulation yielded the proper cost function to be minimized. We showed that the ZF solution allows analytical approach to the optimization problem and, under certain assumptions, it is optimal for the MFB maximization. We showed that both MMSE and MOE criteria lead to the same solution as ZF conditions in cases where ZF conditions (V.3.4) apply. The pre-rake scheme was also considered and it was shown that it performs always much worse than our ZF solution. We also discussed the effects of different values of the transmit filter length and different delay spreads introduced by the pre-filter-channel cascade. Finally, we observe that the PSS-CDMA without any further array processing represents a particular case of the presented framework.

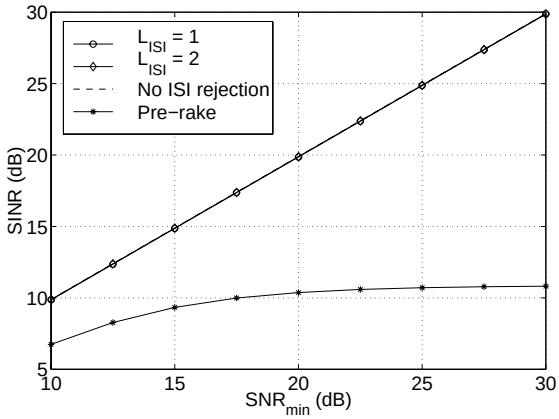

Figure V.2: Optimum SINR vs. $\mathrm{SNR}_{\min}$, pre-rake and ZF solution for different values of L_{ISI}, with $m = 64$, $m_{\mathrm{eff}} = 6$ and $K = 3$

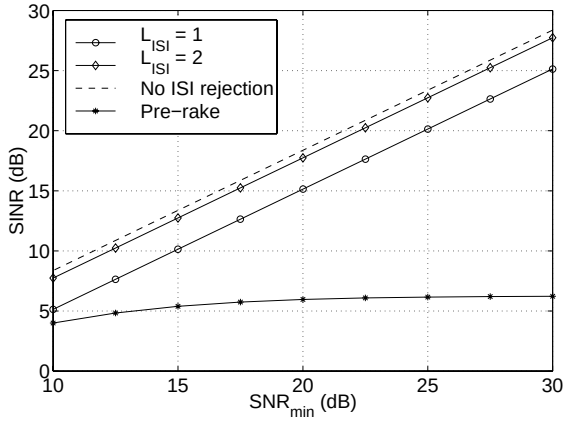

Figure V.3: Optimum SINR vs. $\mathrm{SNR}_{\min}$, pre-rake and ZF solution for different values of L_{ISI}, with $m = m_{\mathrm{c}} = m_{\mathrm{eff}} = 4$ and $K = 3$

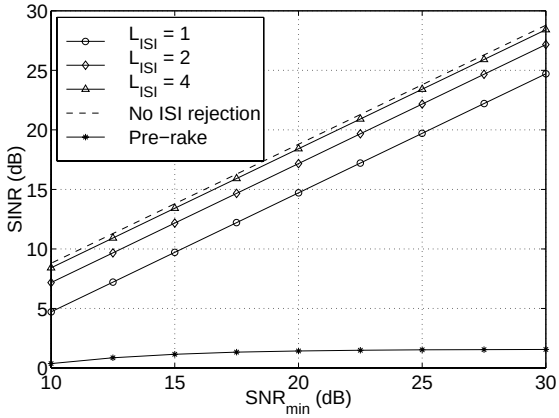

Figure V.4: Optimum SINR vs. $\mathrm{SNR}_{\min}$, pre-rake and ZF solution for different values of L_{ISI}, with $m = m_{\mathrm{c}} = m_{\mathrm{eff}} = 4$ and $K = 3$

Chapter VI

Spatio-Temporal Array Processing for FDD/CDMA Downlink Transmission

This chapter delas with the problem of performing optimum spatio-temporal processing when using adaptive antenna arrays at base stations for multiuser downlink transmission in DS-CDMA systems, using periodic spreading sequences and assuming partial knowledge of the channel parameters of all users. This assumption typically holds in frequency-division duplex (FDD) based mobile communication systems. We consider the SDMA strategy for using antenna arrays to gain system capacity. The channel is assumed to comprise specular multipath, and a per-path argument is pursued to design FIR transmission filters at the base station in order to maximize the signal-to-interference-plus-noise ratio (SINR) at the mobile receivers. Joint optimization of the transmitter and receiver is considered. The per path decorrelating pre-filter is introduced, and it is shown that due to the large number of degrees of freedom available because of the large processing gain (inherent oversampling with respect to the symbol rate in CDMA) and possible multiple antennas/oversampling, the downlink performance can be greatly improved in the FDD problem.

VI.1 Introduction

Transmit antenna diversity is known not to give the same gains as the receive antenna diversity if the no knowledge of the channel is available [Bel99]. Furthermore, it is seen at the receiver as time diversity and is of use to create multipath diversity in flat-fading channels. On the contrary, if some parameters of the downlink channel are known, pre-processing of some sort at the transmitter can result in improved performance and simplified, low complexity receivers for the mobile stations. The amount and nature of this *a priori* knowledge of the channels depends on the system architecture. In time-division duplex (TDD) based systems (see chapter V), the uplink and the downlink channels can be considered to be practically the same (reciprocity), assuming the mobile velocity low enough and the receiver and transmitter appropriately calibrated. Under these circumstances, since the channel is known (or estimated) from the uplink, efficient spatio-temporal processing can be performed at the base station during transmission as well as during reception. The TDD case has been treated in chapter V.

Contrary to TDD, in the FDD mode, the base station has no direct knowledge of the downlink channel, since it cannot be directly observed and therefore estimated. A solution to this problem consists

of providing the base station with feedback from the mobile station about the downlink channel at the cost of reduced spectral efficiency. On the other hand, if such feedback is not provided, the downlink channel characterization can only be based on the estimates of parameters related to the uplink channel, which are relatively frequency independent and whose rate of change is slow with respect to the frame duration. Actually in FDD based mobile communication systems, in the absence of feedback, the best one can obtain is an estimate of the downlink channel covariance matrix. In reality even a robust and reliable estimation of the channel covariance matrix represents a non-trivial issue.

The channel parameters of interest are typically the angle of arrival/departure, the delay, the magnitude and the phase for each path in the multipath propagation. We assume the knowledge of the covariance matrix of the channel impulse response averaged over the path phases and amplitudes (the quantities unknown at the base-station). For the purpose of transmit filter optimization, the specular nature of the paths, and the randomness of the path phases leads to the modeling of the multipath components of a certain mobile user as equivalent to several correlated users, each propagating through a single path. Assuming the individual paths to be spatio-temporally resolvable, the averaged covariance matrix can still be built. Delays for paths which are resolvable in space only can be adjusted prior to transmission to make them temporally distinguishable at the receiver.

In the light of the above arguments, we consider here the problem of performing optimal spatio-temporal processing when a FDD/DS-CDMA system is adopted. Due to the lack of knowledge of the path phases, the effective number of users is actually given by the sum of all the paths of all the users. If only the spreading (temporal) dimension is exploited, then, in order to restore the orthogonality we need the total number of paths to be less than the spreading factor. This in turn results in a low loading fraction[1]. The loading fraction can be increased by using spatial and other multichannel information in conjunction with the temporal (spreading factor/OS) dimension.

Theoretically, even a number of interfering users larger than the spreading factor may be located in the same cell (interference coming from other cells is neglected, except for the users in soft-handover mode). So zero IUI can be achieved as long as the total number of paths does not exceed the total number of sub-channels. The latter can be quite large is MA and OS is employed. In our treatment, the emphasis is on simple mobile receiver structures (e.g., a correlator or a RAKE receiver) while the optimization criterion consists of maximizing the minimum signal-to-interference and noise ratio (SINR) among the users considered, subject to a total transmit power constraint. Each of the K mobile receivers is assumed to have one antenna. We introduce the pre-combining like decorrelator filter to decouple the multipath signals [DHZ95]. The problem then settles down to the power assignment to signals through these pre-filters, in order to maximize the SINR at the mobile station. We show that the optimal power assignment turns out to correspond to *selection diversity*, an approach that has also been followed in [BJU+99] based on heuristic reasoning.

VI.2 The FDD Framework and Reciprocity

We consider a specular path channel model that consists of Q_i multipath components for the ith user. The ith's user qth multipath channel component as seen form the base station can be modeled in the continous-time domain as follows

$$\boldsymbol{h}_{iq}^T(\tau, t) = \alpha_{iq}(t)\mathbf{a}^T(\theta_{iq})\delta(\tau - \tau_{iq}) \tag{VI.2.1}$$

[1] defined as number of users per spreading factor

where τ_{iq}, θ_{iq}, and $\alpha_{iq}(t)$ denote the delay, the angle and the fading attenuation associated to the qth path of the ith user, respectively, and $\mathbf{a}(\theta)$ represents the array response vector. Assuming a similar multipath channel model for the uplink, the parameters which can be assumed approximately constant between the uplink and the downlink channels are the angles, the delays and the variances of the amplitudes. Since the difference in phase between up- and downlink is random it can be assumed uniformly distributed, whereas the magnitudes for both links are also random but can be assumed to have the same variance. The variances of the path amplitudes can be estimated by non-coherent averaging over a certain time interval. The angles can be estimated if the array manifold at the downlink carrier frequency is known. For particular array geometries and relatively small uplink–downlink frequency shifts, the array response can be transposed from the uplink to the corresponding response in the downlink via a linear transformation [AFFM98] without requiring explicit angle estimation. Another approach consists of performing a *beamspace* transformation (namely a spatial DFT) to estimate the beams in which the signal energy is located [CTK94]. The downlink transmission then occurs through the same beams as the uplink reception.

VI.2.1 The Pathwise Channel-Receiver Cascade

In order to reason in a pathwise manner, we assume that each receiver processes symbol rate data coming from the outputs of a bank of receive (RX) correlators. The number of correlators equals the number of paths for the intended user. For the pulse shaping matched filter at receiver we denote $w_i(\tau) = \sum_{l=0}^{m_c-1} c_{i,l}^* \psi(\tau - lT_c)$ as the cascade of the chip-pulse shape matched filter, $\psi(\tau)$, and the ith user correlator $c_i^*(-\tau) = \sum_{l=0}^{m_c-1} c_{i,l}^* \delta(\tau - lT_c)$, where T_c is the chip period and m_c the spreading factor. The superscripts *, ^{T} and ^{H} denote complex conjugate, transpose and Hermitian transpose respectively. We assume that $w(\tau)$ is a FIR filter with time duration approximately equal to $L_w T$. T is the symbol period. Then the following discrete-time channel model at the symbol rate $1/T$, where $T = m_c T_c$, can be described

$$\begin{aligned} \boldsymbol{g}_{iq}^T(k,\, n) &= \alpha_{iq}(n)[\mathbf{a}(\theta_{iq}) \otimes \mathbf{w}_{iq}(n)]^T \\ \boldsymbol{G}_{iq}^t(n) &= \alpha_{iq}(n)[\mathbf{a}(\theta_{iq}) \otimes \mathbf{W}_i(\tau_{iq})]^t \end{aligned}, \tag{VI.2.2}$$

where $\otimes$ denotes the Kronecker product and the superscript ^{t} denotes transposition of the blocks in a block matrix, $\mathbf{w}_{iq}(n) = \mathbf{w}_i(t_0 + kT - \tau_{iq})$,

$$\mathbf{w}_{iq}(n) = [w(t_0 + nT - \tau_q) \; \ldots \; w(t_0 + T(n + \frac{m_c - 1}{m_c}) - \tau_q)]^T$$

and $\mathbf{W}_i(\tau_{iq}) = [\mathbf{w}_{iq}(L_w - 1) \; \ldots \; \mathbf{w}_{iq}(0)]$ [2]. We could also account for OS w.r.t. the chip rate by replacing m_c with $m_c m_o$ in the expression above. We use the notation $\boldsymbol{V}_{iq} = \mathbf{a}(\theta_{iq}) \otimes \boldsymbol{W}_i(\tau_{iq})$ in the sequel. One may notice that the $\boldsymbol{V}_{iq}$'s can be built based upon the estimates of the path angles and delays, and the knowledge of the receiver correlator.

We also introduce the spatio-temporal channel covariance matrix associated with $\boldsymbol{G}_{iq}(n)$ averaged over the ith user's qth path phase, given by

$$\boldsymbol{R}_{iq}^{(L)} = \mathrm{E}[\mathcal{T}_L(\boldsymbol{G}_{iq}(n))\mathcal{T}_L^H(\boldsymbol{G}_{iq}(n))] = \sigma_{iq}^2 \mathcal{T}_L(\boldsymbol{V}_{iq})\mathcal{T}_L^H(\boldsymbol{V}_{iq}) \tag{VI.2.3}$$

[2] The length of L_w may be different for different users, although we shall neglect this issue in these developments

where $\sigma_{iq}^2 = \mathrm{E}[|\alpha_{iq}(n)|^2]$, , $\mathrm{E}[\cdot]$ denotes the expectation operator, and $\mathcal{T}_M(\boldsymbol{A})$ is in general a block Toeplitz matrix with M block rows and $[\boldsymbol{A}\ \mathbf{0}_{p\times s(M-1)}]$ as first block row, and $\boldsymbol{A}$ is a matrix with $p \times s$ block entries.

We shall observe that due to the assumption on the receiver structure the delays τ_{iq}'s denote the overall delay between the transmitter antenna(s) and the qth correlator output of the ith receiver. In general, a cost function for the transmit filter optimization should be formulated so as to optimize also each correlator synchronization time, i.e, to optimize the τ_{iq} by properly advancing or retarding the receiver correlator with respect to the base station transmitter clock. For the purpose of the overall channel description and the filter optimization algorithm, we shall assume the delays τ_{iq}'s to be fixed and known at the transmitter.

VI.3 Signal Model

Assuming the channels $\boldsymbol{h}_{iq}$ time-invariant for the observation time, the ith user discrete-time received signal, for $i = 1 \ldots, d$, is

$$y_{iq}(n) = \boldsymbol{c}_i^H \mathbf{H}_{iq}^T(\zeta) \sum_{j=1}^{K} \sum_{l=1}^{Q_j} \mathbf{F}_{jl}(\zeta) a_j(n) + v_{iq}(n) \tag{VI.3.1}$$

where the $a_j(n)$ are the transmitted symbols intended for the jth user, ζ^{-1} is the unit sample delay operator (i.e., $\zeta^{-1} y_i(n) = y_i(k-1)$), $\mathbf{H}_{iq}^T(z)$ is the channel transfer function between the base station and the qth path of the ith user channel, $\boldsymbol{c}_i^H$ is the ith user correlator, $\mathbf{F}_{jl}(z) = \mathbf{F}'_{jl}(z)\boldsymbol{c}_j$ is the spatio-temporal filter for the transmitted symbols, accounting for both the actual transmit filter $\mathbf{F}'_{jl}(z)$ to be optimized and the spreading code, $\boldsymbol{c}_j$, for the jth user, and $v_{iq}(n)$ is the additive noise associated to the qth path of the ith user.

Since we have m_c chips per symbol period, each transmission filter $\mathbf{F}_{iq}(z)$ will perform sampling at least at the chip rate, i.e., it will be at least a $m_c \times 1$ column vector. If no additional OS or MA are provided, the optimization problem for all the $\mathbf{F}_{iq}(z)$'s reduces to one of spreading code optimization at the transmitter in the presence of multiuser multipath channels. Moreover, in general $\mathbf{F}_{jl}(z)$ will be a $m \times 1$ column vector, with $m = m_c m_a m_o$, where m_a is the number of MA.

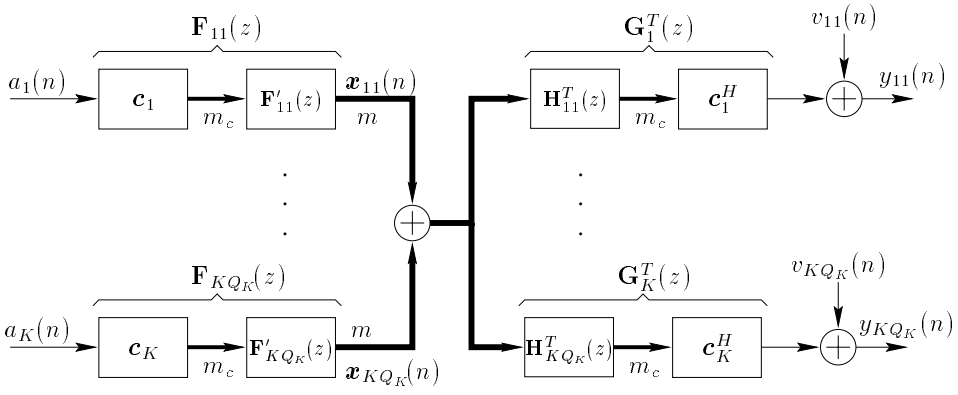

Figure VI.1: Transmission filters and single-path channels for K users

We denote $\mathbf{G}_{iq}^T(\zeta) = \boldsymbol{c}_i^H \mathbf{H}_{iq}^T(\zeta)$ the overall channel associated with the ith user's qth path as seen from the base station. Note that since the receiver is assumed to sample at the chip rate, $\mathbf{H}_{iq}^T(z)$ is a $m_c \times m$ matrix, $\boldsymbol{c}_i^H$ is a $1 \times m_c$ row vector, so that $\mathbf{G}_{iq}^T(z)$ is a $1 \times m$ row vector, and $\mathbf{F}_{jl}(z)$ is a $m \times 1$ column vector. $\mathbf{G}_{iq}(z)$ is the $m \times 1$ qth single path channel in the uplink from the ith user to the m base station channels.

VI.3.1 Burst Processing Time Domain Signal Model

Consider the I/O transmission chain (see fig. VI.1) associated to the qth path component of the ith user regardless of the contributions intended for the other paths and other users. The channel $\boldsymbol{g}_{iq}^T(t) = \boldsymbol{c}_i^H \boldsymbol{H}_{iq}^T(t)$ and the transmission filter $\boldsymbol{f}_{iq}(t) = \boldsymbol{F}'_{iq}(t)\boldsymbol{c}_i$ are assumed to be FIR filters with duration $N_{iq}T$ and LT respectively (approximately). In discrete-time representation we have

$$\begin{array}{l} \boldsymbol{x}_{iq}(n) = \sum_{l=0}^{L-1} \boldsymbol{f}_{iq}(l) a_i(n-l) = \boldsymbol{F}_{iq} A_{i,L}(n) \\ y_{iq}(n) = \sum_{k=0}^{L_w-1} \boldsymbol{g}_{iq}^T(k) \boldsymbol{x}_{iq}(n-k) + v_{iq}(n) = \boldsymbol{G}_{iq}^t \boldsymbol{X}_{iq,L_w}(n) + v_{iq}(n) \\ \boldsymbol{G}_{iq}^t = [\boldsymbol{g}_{iq}^T(L_w-1) \ \ldots \ \boldsymbol{g}_{iq}^T(0)], \quad \boldsymbol{F}_{iq} = [\boldsymbol{f}_{iq}(L-1) \ \ldots \ \boldsymbol{f}_{iq}(0)] \\ \boldsymbol{X}_{iq,L_w}(n) = [\boldsymbol{x}_{iq}^H(n-L_w+1) \ \ldots \ \boldsymbol{x}_{iq}^H(n)]^H \\ A_{i,L}(n) = [a_i(n-L+1) \ \ldots \ a_i(n)]^T \end{array} \tag{VI.3.2}$$

If we accumulate M consecutive symbol periods

$$Y_{iq,M}(n) = \mathcal{T}_M(\boldsymbol{G}_{iq}^t)\mathcal{T}_{M+L_w-1}(\boldsymbol{F}_{iq}) A_{i,M+L_w+L-2}(n) + V_{iq,M}(n)$$

where, $Y_{iq,M}(n) = [y_{iq}^H(n-M+1) \ \ldots \ y_{iq}^H(n)]^H$ and likewise for $V_{iq,M}(n)$.

Then, introducing also the contributions of all the other paths and all the other users, for the ith user's qth path component we have

$$Y_{iq,M}(n) = \sum_{j=1}^{K} \sum_{l=1}^{Q_l} \mathcal{T}_M(\boldsymbol{G}_{iq}^t)\mathcal{T}_{M+L_w-1}(\boldsymbol{F}_{jl}) A_{j,M+L_w+L-2}(n) + V_{iq,M}(n) \tag{VI.3.3}$$

We observe that $\boldsymbol{G}_{iq} = \alpha_{iq} \boldsymbol{V}_{iq}$.

VI.4 Transmit Filter Optimization

A major issue in the transmit filter design problem consists of the power assignment optimization among different paths and different users' pre-filters. In order to find an analytical solution we decouple the power assignment optimization problem by considering first the optimization of a set of unit norm transmit filters $\boldsymbol{U}_{iq}$ such that $\boldsymbol{F}_{iq} = \sqrt{p_{iq}}\boldsymbol{U}_{iq}$. Then, once the $\boldsymbol{U}_{iq}$ have been determined the powers p_{iq} will be properly assigned subject to a maximum total transmit power constraint.

For the sake of simplicity in the following developments, we introduce $\boldsymbol{F}_{iq}^t = [\boldsymbol{f}_{iq}^T(L-1) \ \ldots \ \boldsymbol{f}_{iq}^T(0)]$ and the respective unit norm filter $\boldsymbol{U}_{iq}^t$. We also remark that for the convolution of any $\boldsymbol{F}$ and $\boldsymbol{G}^t$, the relation

$$\boldsymbol{F}^t \mathcal{T}_L(\boldsymbol{G}) = \boldsymbol{G}^t \mathcal{T}_N(\boldsymbol{F})$$

holds, where L and N are the durations in symbol periods of $\boldsymbol{F}$ and $\boldsymbol{G}$ respectively.

VI.4.1 The Per-Path Pre-Decorrelator

A solution for the design of the filters $\boldsymbol{U}_{iq}$'s consists of pre-decorrelating the paths of the user of interst while canceling out the IUI, namely the contributions due to other user's paths. In order to achieve perfect IUI cancellation and IP pre-decorrelation, we shall consider the following set of ZF constraints

$$\max_{\|U_{iq}^t\|_2=1} \|\boldsymbol{U}_{iq}^t \mathcal{T}_L(\boldsymbol{V}_{iq})\|_2^2 \qquad \text{s.t.} \qquad \boldsymbol{U}_{iq}^t \mathcal{T}_L(\boldsymbol{V}_{jl}) = \boldsymbol{0} \tag{VI.4.1}$$

for any $i, j = 1, \ldots, K$, $l = 1, \ldots, Q_j$, $q = 1, \ldots, Q_i$ s.t. $q \neq l$ when $i = j$. Define $\boldsymbol{B}_{iq}$ as $[\mathcal{T}_L(\boldsymbol{V}_{jl})]$ as the matrix accounting for all the paths of all the users but the qth path of the ith user, and $\boldsymbol{A}_{iq} = \mathcal{T}_L(\boldsymbol{V}_{iq})\mathcal{T}_L(\boldsymbol{V}_{iq})$. Then, the solution to problem (VI.4.1) is $\boldsymbol{U}_{iq}^{tH} = V_{\max}(\mathbf{P}_{\boldsymbol{B}_{iq}}^{\perp} \boldsymbol{A}_{iq} \mathbf{P}_{\boldsymbol{B}_{iq}}^{\perp})$, where $\mathbf{P}_{\boldsymbol{B}_{iq}}^{\perp}$ is the projection matrix onto the null space of the column space of $\boldsymbol{B}_{iq}$. In order for a non-trivial solution to problem (VI.4.1) to exist we need the length L of the transmit filters $\boldsymbol{U}_{iq}^{t}$ to be

$$L \geq \frac{(L_w - 1)(Q - 1)}{m_{\text{eff}} - (Q - 1)} \tag{VI.4.2}$$

where $Q = \sum_i Q_i$ and m_{eff} is defined as the rank of $\boldsymbol{V}_Q = [\boldsymbol{V}_{i1} \ldots \boldsymbol{V}_{KQ_K}]$. Note that $m_{\text{eff}} = \min\{m, L_w Q, (L_w - 1)Q + \Delta\}$ where $\Delta = \text{rank}([\boldsymbol{v}_{11}(L_w - 1) \ldots \boldsymbol{v}_{KQ_K}(L_w - 1)])$. The constraints present in the optimization problem (VI.4.1) lead to perfect IUI cancellation along with an interpath pre-decorrelation for the user of interest. This is obtained at the expense of increased ISI at the receiver. In order to consider the ISI as well as the IUI rejection in the optimization problem, we rely on the ZF pre-equalization conditions.

VI.4.2 IP Pre-Decorrelation, ZF Conditions for IUI and ISI Cancellation

In order to ensure ZF conditions for IUI and ISI for the ith user's qth path the set of constraints to be considered is

$$\boldsymbol{U}_{iq}^t \mathcal{T}_L(\boldsymbol{V}_Q) = [0 \ \ldots \ 0 \ \ldots \overbrace{|\, 0 \ \ldots 0 \, \alpha \, 0 \ldots 0 \,|}^{i\text{th user's } q\text{th path}} \ \ldots \ 0 \ \ldots \ 0] \tag{VI.4.3}$$

where $\mathcal{T}_L(\boldsymbol{V}_Q) = [\mathcal{T}_L(\boldsymbol{V}_{11}) \ldots \mathcal{T}_L(\boldsymbol{V}_{KQ_K})]$, and $\alpha \neq 0$ is an arbitrary constant to be fixed in order to satisfy the constraint on the norm of $\boldsymbol{U}_{iq}^t$. Assuming $m > Q$ and $\mathcal{T}_L(\boldsymbol{V}_Q)$ to be full column rank, to be able to satisfy all the constraints (VI.4.3) we need to choose the length of each filter $\boldsymbol{U}_{iq}^t$, L, such that the system of equations VI.4.3 is exactly or underdetermined. Hence

$$L \geq \underline{L} = \left\lceil \frac{(L_w - 1)Q - 1}{m_{\text{eff}} - Q} \right\rceil \tag{VI.4.4}$$

Then assuming $L \geq \underline{L}$ we can consider two limiting set of constraints:

- IUI rejection, no ISI rejection, as in section VI.4.VI.4.1.
- both IUI and ISI rejection: in this case, the set of constraints is (VI.4.3), i.e., we have $L_w + L - 1$ more constraints.

In the absence of IUI (equal to zero due to ZF), the SNR at the output of each correlator is proportional to the energy in the prefilter-single path channel cascade. Then, the SNR decreases if all the energy is constrained in one tap. Hence if no ISI rejection is provided the highest SNR will be achieved, for a specified L, due to the larger number of degrees of freedom. However, in that case, once the strongest path has been selected, the ith receiver needs to equalize a delay spread of up to $L_w + L - 1$ symbol periods, corresponding to the whole delay spread due to the convolution between the single path channel and the selected transmission filter. We may prefer that the introduction of the prefilter does not increase the delay spread, or we may want to limit the delay spread seen by the mobile to limit the complexity for the equalization task in the mobile. In those cases additional constraints in order to obtain at least partial ISI rejection, i.e., limited delay spread, can be added, leading to intermediate solutions between the previous two limiting cases. In general to have complete IUI and partial ISI rejection we add $(L_w + L - 1) - L_{\mathrm{ISI}}$ constraints (coefficients of the prefilter-channel cascade being zero), with $1 \leq L_{\mathrm{ISI}} \leq (L_w + L - 1)$, where L_{ISI} corresponds to the residual delay spread, i.e., residual ISI. This optimization problem has to be carried out for all possible positions of the nonzero part of length L_{ISI} of the prefilter-channel cascade, and the best position should be chosen. Finally, note that as L increases the SNR increases as well. So, we shall choose the actual length of the transmission filters L according to a trade-off between performance and transmitter complexity.

One might think that by transmitting only through the strongest path per each user the amount of ISI at the receiver is negligible. However, although L_w is in practice very small (2, 3 symbol periods), for high loading fractions, i.e., for a large number of paths, the required L can become relatively large, in order to achieve the above ZF IUI conditions, which in turn results in significant ISI.

Finally, one may note that ZF-pre-decorrelating here corresponds to the design of a bi-orthogonal perfect-reconstruction transmultiplexer in which the $\boldsymbol{F}_{iq}$'s and $\boldsymbol{G}_{iq}$'s are synthesis and analysis filter banks respectively.

VI.4.3 RX Correlator Positioning / Delay Optimization

The ZF problem in (VI.4.3) supposes that the delays τ_{iq}, $\forall i = \{1, \ldots, K\}$, $q = \{1 \cdots Q_i\}$, for all users are known at the transmitter. This implies that the correlator at the receiver is also supposed to be located at a known fixed position in time. It is for this overall delay, τ_{iq}, and all others, τ_{jr}, $\forall j = \{1, \ldots, K\}$, $r = \{1 \cdots Q_j\}$, and $r \neq q$ when $j = i$, that the pre-decorrelating conditions are satisfied. In the optimization scheme, due to the presence of the RX correlators in the overall channel, it is taken for granted that the assumed delay would lead to the maximization of the SNR at the output. It would suffice then, that the correlator, in an independent operation mode, searches for the delay by sweeping over the field of interest of the assumed delays. However, since the ZF conditions are being satisfied for a set of discrete delays, the IUI and IPI will have its contributions at all intermediate positions. Furthermore, this may not necessarily be the global SNR maximization delay for the RX correlator.

In order to maximize the SNR, let us introduce $\boldsymbol{U}_{iqn}$, as the ZF prefilter for the qth path of the ith user with the correlator placed at a delay of n positions (e.g., chips periods) w.r.t. an arbitrary initial position. This can be seen as an n-shift of the elements in the columns of $\mathcal{T}_L(\boldsymbol{V}_{iq})$, (i.e., the first vector co-efficient now contains n more zeros). The optimization for $\boldsymbol{U}_{iqn}$ is still done at the symbol rate for the new $\mathcal{T}_L(\boldsymbol{V}_{iq})$. The optimization problem still stays the same as (VI.4.3) and the optimal n is selected to maximize the output SNR: $\max_n \mathrm{SNR}_n$. The RX correlator can still search for the delay. It can be seen, however, that the optimal delay selection is a coupled problem. Its choice, therefore,

influences and is influenced by the design of other users' prefilters.

An alternative approach for SNR maximization w.r.t. the correlator delay consists of searching over several transmit filters, $\boldsymbol{U}_{iqn}$ for the one that maximizes the SNR, considering that the RX correlator is fixed. Then, for the optimization problem of section VI.4.VI.4.1., assuming $m_a = m_o = 1$,

$$\boldsymbol{U}_{iqn}^{'t} = \left[\mathbf{0}_{1\times n} \quad \boldsymbol{U}_{iqn}^{t} \quad \mathbf{0}_{1\times(m_c-n)}\right],$$

and the $n \in \{0 \cdots m_c - 1\}$, in the case where chip-level resolution is sought in the delay optimization. The number of zeros is fixed, and the solution to (VI.4.1) is still

$$\boldsymbol{U}_{iqn}^{tH} = V_{\max}(\mathbf{P}_{\overline{\boldsymbol{B}}_{iq}}^{\perp} \overline{\boldsymbol{A}}_{iq} \mathbf{P}_{\overline{\boldsymbol{B}}_{iq}}^{\perp}).$$

The matrix $\overline{\boldsymbol{B}}_{iq}$ is built from $\boldsymbol{B}_{iq} = [\mathcal{T}_L(\boldsymbol{V}_{jl})]$ (section VI.4.1) by appending n zero rows at the top and $(m_c - n)$ zero rows at the bottom. Besides we have $\overline{\boldsymbol{A}}_{iq} = \overline{\mathcal{T}}(\boldsymbol{V}_{iq})\overline{\mathcal{T}}^H(\boldsymbol{V}_{iq})$, where $\overline{\mathcal{T}}(\boldsymbol{V}_{iq})$ is built from $\mathcal{T}_L(\boldsymbol{V}_{iq})$ in a similar fashion as $\overline{\boldsymbol{B}}_{iq}$. We have assumed in the above that the TX filter $\boldsymbol{U}_{iqn}^{t}$ is an integer number of symbols long, since it settles nicely in our framework (see sec. VI.4.1). This, however, is not necessary, and the filter length can, for example, be defined in number of chips. The two approaches discussed above lead to similar kinds of delay optimization. Both problems are coupled leading to joint oprimization for all users. Upon solving the joint optimization problem, the optimum delay is determined leading to the maximization of the SNR at the RX correlator output. A simpler, decoupled approach then consists of preselecting (see the following section) the dominant path *a priori*, i.e., before the design of $\boldsymbol{U}_{iq}^{t}$'s, and assuming that the RX correlators for all users are aligned to the delay of the dominant paths. The delay assignment thus assumes that *a priori* and *a posteriori* (after ZF-prefilter design) dominant paths will be the same, a very likely event. The prefilters for all users can now be designed as discussed previously in a decoupled fashion. Fine tuning of TX filter delays as discussed in the previous paragraph can still be applied, subject to the fixed delay constraint for the correlators. We concede that the pre-assigned delays may not, in all cases, be the optimal ones, but this simplifies the optimization problem making it much simpler to implement.

VI.5 TX Diversity and Power Assignment

We have assumed that each receiver consists of a correlator per multipath component. Assume that the correlator outputs are combined according to the maximum ratio combining (MRC) criterion. The multipath signal components are assumed to be spaced such that the correlator outputs are uncorrelated. The effect if IUI and ISI may be ignored at this point (we have seen that pre-filtering will cancel them). Fig. VI.2 shows the the TX-channel-RX cascade for the ith user. We assume a constraint on the total transmit power such that $\sum_{q=1}^{Q_i} p_{iq} = p_i$ (with $p_{iq} \geq 0$). The output signal-to-noise ratio (SNR) for the ith user is

$$\mathrm{SNR}_i = \frac{\mathrm{E}[|\sum_{q=1}^{Q_i} |\alpha_{iq}|^2 p_{iq} a_i(n)|^2]}{\sigma_{v_i}^2 \sum_{q=1}^{Q_i} \mathrm{E}|\alpha_{iq}|^2 p_{iq}} = \frac{\sigma_a^2}{\sigma_{v_i}^2} \sum_{q=1}^{Q_i} \mathrm{E}[|\alpha_{iq}|^2] p_{iq} \qquad \text{(VI.5.1)}$$

where $\sigma_a^2 = \mathrm{E}[|a_i(n)|^2]$ for all the i's and $\sigma_{v_i}^2$ is the variance of the noise at each correlator output (for the variance of the noise at the correlator output it is assumed that the spreading sequences are sufficiently white). The optimal power assignment among the different paths that maximize the SNR is

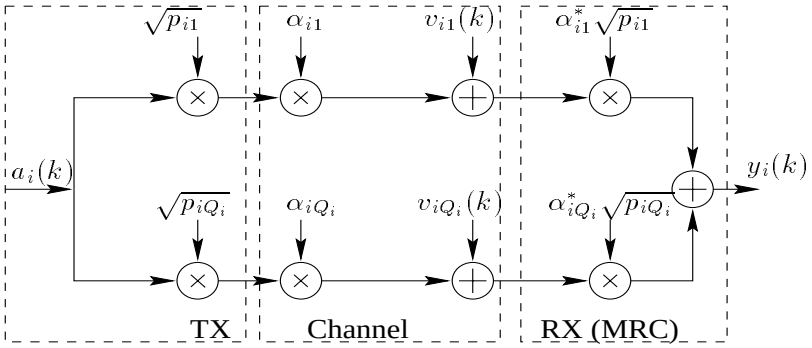

Figure VI.2: Transmit diversity for the ith user through Q_i diversity branches/paths after pre-decorrelating pre-filtering and ZF IUI

determined by solving the following problem

$$\max_{p_{iq}}\{\sum_{q=1}^{Q_i}(\mathrm{E}|\alpha_{iq}|^2)p_{iq}\} \qquad \text{s.t. } \textstyle\sum_{q=1}^{Q_i} p_{iq} = p_i, \tag{VI.5.2}$$

the solution to which is the well known *selection diversity* which corresponds to assigning the whole tranmsit power to the path carrying the most power (on the average). Hence, under the conditions above the previous receiver structure collapses into a single pulse shape matched filter and a correlator.

We remark that the strongest multipath component is the one with the maximum energy in the corresponding prefilter-channel. Then in general, when a pathwise pre-filtering is performed at the base station then, strictly speaking, the strongest path selection for a certain user can take place after the pre-filter design for each path. Hence, all paths need to be considered for the pre-filter design.

VI.5.1 Power Assignment Optimization

Since the transmission strategy consists of exciting one path per user, we refer to $\boldsymbol{U}_i^t$, $\boldsymbol{V}_i$ and σ_i^2 as the filter, the channel (up to the fading coefficient) and the variance of the fading associated with the selected path for the ith user. Once we have designed the normalized transmit filters $\boldsymbol{U}_i^t$ we need to optimize the transmit power assignment among the K users. In the absence of IUI due to ZF, we shall optimize the transmit power assignment in order to make the SNR at the output of each selected path correlator, the same for all the users, subject to a total transmit power constraint. The SNR for the ith user is given by

$$\gamma_i = \frac{\sigma_a^2}{\sigma_{v_i}^2} p_i \sigma_i^2 \|\boldsymbol{U}_i^t \mathcal{T}_L(\boldsymbol{V}_i)\|_2^2 \tag{VI.5.3}$$

where $\sum_i p_i = p_{\max}$. Since the optimal leads $\gamma_i = \gamma$ for all the users then it is straightforward to derive the following expressions for γ and the optimal p_i's

$$\begin{aligned} \frac{1}{\gamma} &= \frac{1}{p_{\max}\sigma_a^2} \sum_i \frac{\sigma_{v_i}^2}{\sigma_i^2 \|\boldsymbol{U}_i^t \mathcal{T}_L(\boldsymbol{V}_i)\|_2^2} \\ p_i &= \gamma \frac{\sigma_{v_i}^2}{\sigma_a^2} \frac{1}{\sigma_i^2 \|\boldsymbol{U}_i^t \mathcal{T}_L(\boldsymbol{V}_i)\|_2^2} \end{aligned} \tag{VI.5.4}$$

VI.6 Discussion

The pre-decorrelating transmit filters designed according to (VI.4.1) are optimal in the noiseless case. Indeed the limited power constraint does not affect in this case the SINR, which reduces to the Signal to Interference ratio (SIR) at each receiver, and which is infinity for any power assignment when ZF IUI is achieved. However, in the presence of noise at receivers as the number of ZF constraints will increase, a *noise enhancement* phenomenon will arise which might reduce the SINR gain obtained from the IUI cancellation. If the CDMA system under consideration allows a large number of degrees of freedom, namely a large m, compared to the number of paths of all the users, then the noise enhancement phenomenon will be practically negligible compared to the SINR gain yielded by ZF the IUI.

An alternative solution is represented by a pre-RAKE like pre-filtering. Due to the lack of knowledge of the path phases (and amplitudes) of the downlink channel, only non-coherent pre-RAKE processing is possible at the base station. However, the result of section VI.5, disagrees with pre-RAKE kind of prefiltering.

VI.7 Simulations

We consider an CDMA/SDMA scenario in the presence of $K = 3$ users having $Q_i = 2$ paths each, which receive signals transmitted from a base station. The total power $p_{\max}$ and σ_a^2 are constant, and the noise variances $\sigma_{v_i}^2 = \sigma_v^2$ is assumed and to be the same at all receivers and to be known at the transmitter. The single path delays τ_{iq}'s, the array response vectors $\mathbf{a}(\theta_{iq})$ to build the channels $\boldsymbol{V}_{iq}$'s, and the variances σ_{iq}^2 are estimated from the uplink.

In the first simulation we considered a *saturated* system configuration assuming the $m_c = 8$ and $m_a = m_o = 1$. In this case $m_{\text{eff}} > Q$ ($m_{\text{eff}} = m = 8$) and ZF conditions (VI.4.3) can be applied, if filter length is $L \geq 4$. We fixed $L = 4$ symbol periods to achieve (VI.4.3). The resulting performances are plotted in left plot of fig. VI.3 in terms of SNR at each receiver versus the residual ISI (L_{ISI} introduced by the pre-filter channel cascade. Due to the high system loading significant differences arise for different values of L_{ISI}. In the second simulation we considered the same user scenario as above, $m_c = 8$, but employing $m_a = 2$ antennas at the transmitter. Since $m_{\text{eff}} = 13$ and $Q = 6$ IP pre-decorrelation ZF IUI and ISI conditions (VI.4.3) can be applied. By setting the length of all the transmit filters equal to $L = 4$ symbol periods (even though $L = 1$ suffices to achieve ZF conditions) we obtain the performances plotted in the right plot in figure VI.3. Note that in this case due to the large m_{eff}, w.r.t. the number of user paths Q and to the small delay spreads introduced by the path channels the performances are quite insensitive to the residual delay spread L_{ISI}. It can be demonstrated that larger values of L yield improvement of performances, more significant when m_{eff} is not very large compared to Q.

Fig. VI.4 shows the performance improvement as the processing window length (TX filter length), L, is increased. The left plot is for the case of a single antenna, while $m_a = 2$ for the plot on the right.

VI.8 Conclusions

The FDD/CDMA downlink problem was addressed. It was shown that due to the partial knowledge of the downlink channel, each path of a particular user could be treated as a seperate user. Pre-decorrelation was applied on the downlink to cancel the IUI and IPI. For the desired user, the path

selection diversity scheme was shown to be the best power assignment choice in terms of the SNR optimization. Performance of the receiver *vis-à-vis* the residual ISI was also shown. It was observed that as long as the system has sufficient degrees of freedom (OS/MA factor), IUI can be cancelled by TX pre-filters, leading to low complexity, improved mobile receivers. RX delay optimization was shown to be a coupled problem and a simplified strategy was presented to obtain an individualized framework. We point out that the above framework can easily be extended to include more complex situations, like extracell interference etc.

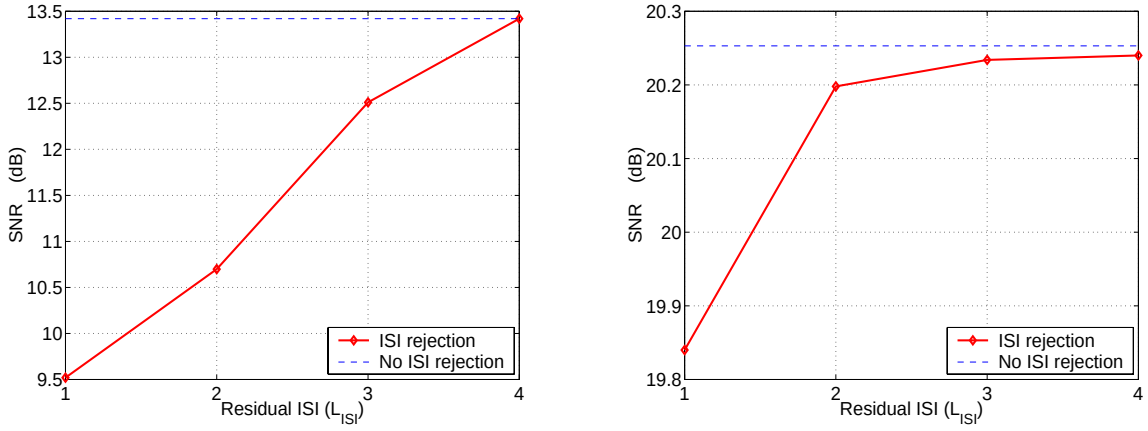

Figure VI.3: Optimum SNR vs. L_{ISI}, for $L = 4$, $Q = 6$, $m = m_c = 8$, and $m_{\mathrm{eff}} = 8$ (left), and, $L = 4$, $Q = 6$, $m_a = 2$, $m_c = 8$, and $m_{\mathrm{eff}} = 13$ (right), IP Pre-decorrelating ZF solution.

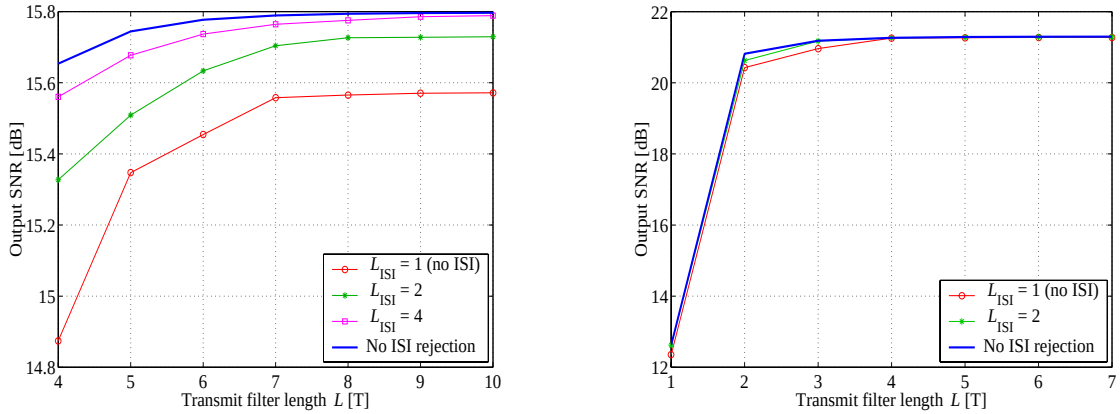

Figure VI.4: Optimum SNR vs. L, for $m_a = 1$, $m_c = 8$ (left), and $m_a = 2$, and $m_c = 8$ (right), IP Pre-decorrelating ZF solution.

Chapter VII

Spatio-Temporal Array Processing for Aperiodic CDMA Downlink Transmission

Consider a DS-CDMA system employing aperiodic spreading sequences (APS) as signature sequences for different users. Multiple transmission antennas (MA) are employed for increasing the network capacity. It is assumed that partial or total knowledge of the downlink channel is available at the base-station due to either a time-division duplex (TDD) or some feedback structure in the network. Spatial and temporal dimensions can no longer be jointly exploited due to the aperiodic spreading. Hence, spatio-temporal pre-cancellation of downlink interference (zero-forcing) is no longer possible. However, beamforming can be applied to maximize the signal-to- noise plus interference (SINR) ratio on a user-to-user basis. We proceed with such an approach and provide closed-form relations for the signal and interference terms at the output of a mobile station RAKE receiver. We also show that using the spatial dimension at the base station enhances the system performance. The mobile receiver can later employ an equalizer to do away with the residual intersymbol interference, thus maximizing the matched filter bound (MFB) at its output.

VII.1 Introduction

Third generation wireless communication systems envision the use of DS-CDMA employing aperiodic spreading sequences for the downlink, typically consisting of periodic Walsh-Hadamard sequences followed by masking by a symbol aperiodic base-station specific overlay sequence. Alternatively, even the scrambling sequence can be user dependent.

When periodic spreading sequences are adopted, effective spatial-temporal processing can be carried out at the base station transmitter relying on symbol rate wide sense stationarity. Under these circumstances in chapter V and VI it was demonstrated that orthogonality between the spread signals can be restored at each receiver by properly filtering/spreading the symbols intended for different users, based upon the information of the channel state associated with each user. Then a number of interfering users more than the processing gain may be located in the same cell, in particular accounting for the users in soft hand-off mode.

The application of these techniques is not straightforward when the symbol rate cyclostationarity no longer exists due to the use of aperiodic overlay spreading sequences which spread/randomize the

orthogonal user sequences. It has to be noted that, assuming the fading processes slow enough, in the structure of this downlink problem, the only entity fixed over the processing interval is the propagation channel. The actual channel as seen from the base station to a certain user will consists of the cascade of spreading, transmit filters, propagation channel, receive filters and RAKE receiver. Due to the aperiodicity of spreading sequences the previous cascade results in a time-variant filter from symbol to symbol. This precludes the possibility of performing feasible adaptive temporal pre-filtering at the base station, as in chapters V and VI, because the pre-filters need to be up-dated every symbol period. Some related work is also found in [RFT98].

It has been observed that in outdoor propagation the most scattering phenomena occur in the proximity of the mobile user and not of the base station. This translates in a relatively small angle spread at the base station antenna. Also due to cost reasons, the base station array consists of just a few antennas. This yields a small antenna aperture, namely a poor spatial resolution, so that in practice very few main nominal multipath directions can be resolved. As showed in the literature on channel modeling (e.g. [Zet97]), for outdoor channels there exist one or two main distinct directions of multipath components called *clusters*. On the other hand, due to the spreading operation in CDMA systems, a very high multipath temporal-delay resolution can be achieved, and temporally sparse channels exist in outdoor propagation with distinct multipath delays. The spatio-temporal channel can therefore be modeled as a clusterized channel where, to each nominal direction of propagation, correspond several multipath components which are temporally resolvable. Such a channel model can be factorized in spatial and temporal channel components for each spatio-temporal channel path cluster. The above arguments lead to an approach considering only the transmit spatial processing (namely beamforming) at the base station, and to maintain the temporal processing as the one traditionally done when RAKE receivers are employed at the mobile.

In the sequel we consider a scenario where K intra-cell users, each with a RAKE receiver, captures signals transmitted from a base station with m antennas. We shall consider both full and partial channel state information for each user, corresponding to TDD and FDD mode respectively. The goal consists of designing a proper set of beamforming weight vectors in order to maximize the minimum signal to interference plus noise ratio (SINR) at the K mobile receivers, under the constraint of a limited transmit power at the base station.

VII.2 Channel Model

Due to the high temporal resolution of CDMA systems we consider a specular path propagation channel model that consists of Q multipath components. The multipath channel as seen form the base station can be modeled in the continuous-time domain as follows

$$\boldsymbol{h}^T(\tau,\, t) = \sum_{q=1}^{Q} \alpha_q(t)\mathbf{a}^T(\theta_q)p(\tau - \tau_q) \tag{VII.2.1}$$

where τ_q, θ_q, and $\alpha_q(t)$ denote the delay, the angle and the fading attenuation associated to the qth path, respectively, $p(t)$ denotes the chip pulse shaping filter, and $\mathbf{a}(\theta)$ represents the array response vector. If the angle delay-spread is small compared to the base station antenna array resolution, paths can be collected in clusters yielding the following model for the lth channel cluster

$$\boldsymbol{h}_l^T(\tau,\, t) = \mathbf{a}^T(\theta_l) \sum_{q_l=1}^{Q_l} \alpha_{q_l}(t)p(\tau - \tau_{q_l}) \tag{VII.2.2}$$

where Q_l, $\alpha_{q_l}(t)$ and τ_{q_l} are the number of multipath components, the fading coefficients and the delays associated to the paths in the lth cluster, and θ_l is the corresponding direction of propagation. The whole channel can be modeled as the superposition of the single cluster channels, i.e.,

$$\boldsymbol{h}^T(\tau, t) = \sum_{q=l}^{L} \boldsymbol{h}_l^T(\tau, t) \tag{VII.2.3}$$

In a TDD framework assuming a similar multipath channel model for the uplink, the mobile velocity sufficiently slow compared to the round-trip time and the transmitter and receiver properly calibrated, the uplink and downlink channels for a certain user can be assumed to be approximately the same. So, the uplink channel estimate can be assumed as downlink channel for the transmit filters design. On the contrary operating in the FDD mode the uplink and downlink channels are not the same. The parameters in the channel model which can be assumed approximately constant between the uplink and the downlink channels are the angles, the delays and the variances of the amplitudes. Since the difference in phase between up- and downlink is random it can be assumed uniformly distributed, whereas the magnitudes for both links are also random but can be assumed to have the same variance. The variances of the path amplitudes can be estimated by non-coherent averaging over a certain time interval. The angles can be estimated if the array manifold at the downlink carrier frequency is known. For particular array geometries and relatively small uplink–downlink frequency shifts, the array response can be transposed from the uplink to the corresponding response in the downlink via a linear transformation [AFFM98] without requiring explicit angle estimation. Another approach consists of performing a *beamspace* transformation (namely a spatial DFT) to estimate the beams in which the signal energy is located [CTK94]. The downlink transmission then occurs through the same beams as the uplink reception.

VII.3 Signal Model

We assume a CDMA based system employing aperiodic spreading sequences, $c_i(t;\, nT)$, for $i = 1, \ldots, K$, where T is the symbol period and n is an integer. The spreading factor is m_c and $T_c = T/m_c$ denotes the chip period. Due to the time-variant nature of the spreading sequences the cascade of the spreading code filter, the transmit filter, the channel and the receive filter (a RAKE) results in a time-variant system. In the sequel the problem of the maximization of the minimum SINR of the K users is addressed, accounting for the presence of an equalizer following the RAKE receiver. In this case the ISI for the signal of interest will be considered as contributing to the signal and not to the interference energy. Notice that the actual temporal channel as seen from the base station is given by the autocorrelation sequence of the channel itself. This is straightforward if we commute the de-spreading and channel matched filtering operations in the RAKE receiver.

Assuming the channels, $\boldsymbol{h}_i$, time-invariant for the observation time, the ith user discrete-time received signal at the RAKE output, for $i = 1 \ldots, K$, is

$$y_i(n) = \boldsymbol{c}_i^H(n)\mathbf{G}_i^T(\zeta) \sum_{j=1}^{K} \boldsymbol{w}_j \otimes \boldsymbol{c}_j(n) a_j(n) + v_i(n) \tag{VII.3.1}$$

where the $a_j(n)$ are the transmitted symbols intended for the jth user, ζ^{-1} is the unit sample delay operator (i.e., $\zeta^{-1} y_i(n) = y_i(n-1)$), $\mathbf{G}_i^T(z)$ is the channel autocorrelation transfer function between

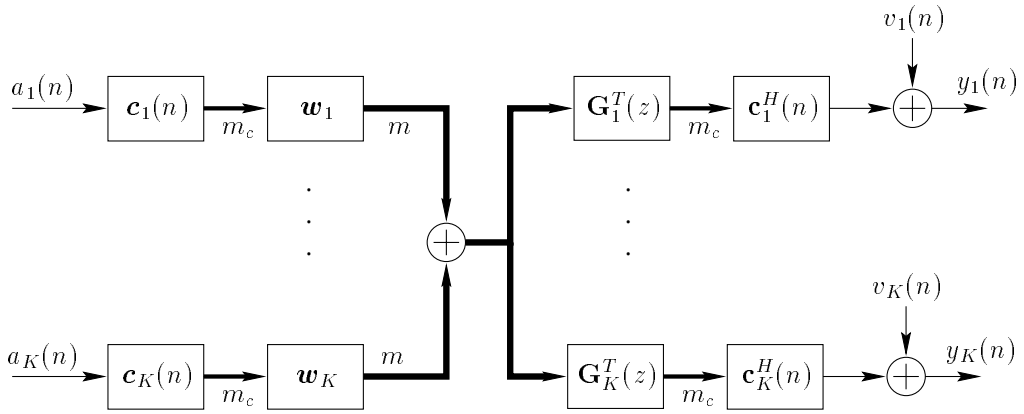

Figure VII.1: Transmission filters channels and RAKE receivers for K users

the base station and the ith user channel, $\boldsymbol{c}_i^H(n)$ is the ith user correlator, $\boldsymbol{w}_j$ is the beamforming weight vector for the transmitted chips $\boldsymbol{c}_j(n)a_j(n)$, that has to be optimized, $\otimes$ denotes Kronecker product, $\boldsymbol{c}_j(n)$ is the spreading code for the nth symbol of the jth user, and $v_i(n)$ is the additive noise at the output of the ith RAKE receiver. We remark that $v_i(n)$ will be a colored noise in general due to matched filtering to the channel.

The channel autocorrelation $\mathbf{G}_i^T(z)$ is a $m_c \times m$ matrix, and $\boldsymbol{c}_i^H$ is a $1 \times m_c$ row vector. The product of $\boldsymbol{w}_j \otimes \boldsymbol{c}_j(n) = \boldsymbol{f}_j(n)$ generates a $m \times 1$ column vector, with $m = m_c m_a$ where m_a is the number of multiple antennas.

VII.4 Temporal Channel Structure

Assume that the channel is of the form (VII.2.3). For simplicity we consider that there is only one path cluster. Several clusters can be analyzed separately and their effect can be combined afterwards. In the single cluster case the channel can easily be factorized in spatial and temporal components. Hence we analyze the temporal channel component, and we evaluate the signal and interference energies transmitted through it averaged over the spreading codes statistics.

The temporal channel for the ith, $h_i(t)$ is assumed to be an FIR filter of duration approximately equal to N_i chip periods. Let $\boldsymbol{h}_i = [h_i^H(0) \ \ldots \ h_i^H(n_i - 1)]^H$ denote the discrete-time representation of the ith channel. Let N_i be the length of the channel in symbol periods.

The autocorrelation sequence of the actual channel, written as $\boldsymbol{g}_i = [g_i^H(-n_i + 1) \ldots g_i^H(n_i - 1)]^H$ has duration $2n_i - 1$ chip periods, or $2N_i - 1$ symbol periods. The whole cascade spreading-channel autocorrelation-despreading will last at most $2N_i+1$ symbol periods, namely $m_c(2N_i+1)$ chip periods. Without loss of generality we may zero pad $\boldsymbol{g}_i$, in order to have $2N_i m_c + 1$ coefficients in the channel autocorrelation sequence.

Hence the overall energy in the spreader-channel-channel matched filter and correlator cascade for the ith user can be written as follows

$$S_i = \boldsymbol{g}_i^H \mathrm{E}\{\mathcal{C}_i(n)^H \boldsymbol{B}_i^H(n) \boldsymbol{B}_i(n) \mathcal{C}_i(n)\} \boldsymbol{g}_i \qquad \text{(VII.4.1)}$$

where $\mathrm{E}\{\cdot\}$ denotes the expectation operator, $\mathcal{C}_i(n)$ is a $(2N_i+1)m_c \times (2N_i m_c+1)$ Toeplitz matrix with $[\boldsymbol{c}_i(n)\mathbf{0}_{2N_i m_c \ \times 1}]^T$ as first column and $[c_i(1,\, n) \ \ \mathbf{0}_{1\times 2N_i m_c}]$ as first row, $\boldsymbol{B}_i(n) = \mathrm{blockdiag}\{\boldsymbol{c}_i^H(k -$

$N_i), \cdots, \boldsymbol{c}_i^H(k-N_i)\}$ is a $(2N_i+1)\times(2N_i+1)m_c$ block diagonal matrix, and, hereinafter $\boldsymbol{g}_i$ denotes the zero padded version of the channel autocorrelation sequence.

For the interference from jth user signal to the ith user receiver a similar expression as (VII.4.1) holds, i.e.,

$$I_{ji} = \boldsymbol{g}_i^H \mathrm{E}\{\mathcal{C}_j(n)^H \boldsymbol{B}_i^H(n)\boldsymbol{B}_i(n)\mathcal{C}_j(n)\}\boldsymbol{g}_i \tag{VII.4.2}$$

In the following we shall distinguish between the case of complex and real spreading sequences when taking the expectation in (VII.4.1) and (VII.4.2).

VII.4.1 Complex Spreading Sequences

We consider complex circularly symmetric spreading sequences $\boldsymbol{c}_i(n)$ where, without loss of generality, we normalize the chip energy to one. Taking the expectation in (VII.4.1) and (VII.4.2) we obtain

$$\boldsymbol{S}_i = \mathrm{E}\{\mathcal{C}_i(n)^H\boldsymbol{B}_i^H(n)\boldsymbol{B}_i(n)\mathcal{C}_i(n)\} = m_c\mathrm{diag}\{[\mathbf{1}_{N_i m_c} \;\; m_c \;\; \mathbf{1}_{N_i m_c}]\}$$

and

$$\boldsymbol{I}_{ji} = \mathrm{E}\{\mathcal{C}_j(n)^H\boldsymbol{B}_i^H(n)\boldsymbol{B}_i(n)\mathcal{C}_j(n)\} = m_c\mathbf{I}$$

respectively. Then (VII.4.1) and (VII.4.2) reduces to

$$\begin{array}{l} S_i^c = m_c^2\|\boldsymbol{h}_i\|^4 + m_c(\|\boldsymbol{g}_i\|^2 - \|\boldsymbol{h}_i\|^4) \\ I_{ji}^c = m_c\|\boldsymbol{g}_i\|^2 \end{array} \tag{VII.4.3}$$

where the superscript $(\cdot)^c$ denotes the use of complex spreading sequences. We remark that having normalized to one the energy per chip the energy per symbol is $\sigma_a^2 = m_c$.

VII.4.2 Real Spreading Sequences

If we consider real spreading sequences $\boldsymbol{c}_i(n)$, taking the expectation in (VII.4.1) yields an extra contribution with respect to the complex case, namely

$$\begin{array}{l} \boldsymbol{S}_i = m_c\mathrm{diag}([\mathbf{1}_{N_i m_c} \;\; m_c \;\; \mathbf{1}_{N_i m_c}])+ \\ \mathrm{antidiag}([\mathbf{0}_{(N_i-1)m_c}, 1, 2, \ldots, (m_c-1), 0, (m_c-1), \ldots, 1, \mathbf{0}_{(N_i-1)m_c}]) \end{array} \tag{VII.4.4}$$

On the contrary the interference term $I_{ji}^c = I_{ji}^r = I_{ji}$ does not change. The signal energy consists of two contributions, namely

$$S_i^r = S_i^c + 2m_c\left(\sum_{n=-m_c+1}^{m_c-1} n(\mathbf{Re}\{g(n)\})^2\right) \tag{VII.4.5}$$

where S_i^c is given in (VII.4.3). The additional contribution arising when using real spreading sequences can be considered negligible for the case of large channel delay spreads.

VII.4.3 Channel Covariance Matrices and Extension to Multi-Cluster Channels

Once the signal and the interference energy terms have been computed, the signal and interference spatial channel covariance matrices for the ith user are given by

$$\boldsymbol{R}_{ii} = \mathbf{a}(\theta_i)\mathbf{a}^H(\theta_i)S_i \qquad \boldsymbol{R}_{ji} = \mathbf{a}(\theta_i)\mathbf{a}^H(\theta_i)I_{ji} \quad \text{for } j \neq i, \tag{VII.4.6}$$

The approach above can be extended to treat multi-cluster channels, by simply computing each cluster contribution separately as shown previously, and summing up the corresponding covariance matrices.

VII.5 Transmit Beamforming Optimization

With the previous definitions for $\boldsymbol{R}_{ji}$ and $\boldsymbol{w}_j$ the SINR for the ith user is given by

$$\mathrm{SINR}_i = \frac{\boldsymbol{w}_i^H \boldsymbol{R}_{ii} \boldsymbol{w}_i}{\sum_{j=1,\, j\neq i}^{K} \boldsymbol{w}_j^H \boldsymbol{R}_{ji} \boldsymbol{w}_j + \nu_i} \tag{VII.5.1}$$

where $\nu_i = \sigma_{v_i}^2/\sigma_a^2$ where $\sigma_a^2 = \mathrm{E}\{|a_i(k)|^2\}$ for any i and $\sigma_{v_i}^2$ is the variance of the filtered noise $v_i(k)$. We denote $\mathrm{SINR}_i = \gamma_i$ for any i. Hence the general optimization problem is

$$\max_{\{\boldsymbol{w}_i\}} \min_i \{\gamma_i\} \tag{VII.5.2}$$

or

$$\min_{\{\boldsymbol{w}_i\}} \max_i \{\gamma_i^{-1}\} \tag{VII.5.3}$$

Then let $\boldsymbol{w}_i = \sqrt{p_i}\boldsymbol{u}_i$, with $\|\boldsymbol{u}_i\|_2 = 1$, the vector of the inverse MFB's $\boldsymbol{\gamma}^{-1} = [\gamma_1^{-1} \ldots \gamma_K^{-1}]^T$ and the vector of the transmit powers $\boldsymbol{p} = [p_1, \ldots, p_K]^T$. We also need to limit the maximum transmit power at the base station, i.e., $\|\boldsymbol{p}\|_1 \leq p_{\max}$.

The criterion (VII.5.3) can be reformulated as

$$\min_{\boldsymbol{p},\{\boldsymbol{u}_i\}} \|\boldsymbol{\gamma}^{-1}\|_\infty \quad \text{s.t. } \|\boldsymbol{p}\|_\infty \leq p_{\max}, \|\boldsymbol{u}_i\|_2 = 1 \,\forall i \tag{VII.5.4}$$

Then we define the normalized power delivered by the jth base station to the ith user as

$$c_{ji} = \boldsymbol{u}_j^H \boldsymbol{R}_{ji} \boldsymbol{u}_j \quad .$$

For any i we have

$$\gamma_i^{-1} p_i c_{ii} = \sum_{j\neq i} p_j c_{ji} + \nu_i \quad . \tag{VII.5.5}$$

In order to account for all the users we introduce the matrix $\boldsymbol{D}_c = \mathrm{diag}(c_{11}, \ldots, c_{KK})$, the matrix $\boldsymbol{C}^T$ defined as

$$[\boldsymbol{C}^T]_{ij} = \begin{cases} c_{ji} & \text{for} j \neq i \\ 0 & \text{for} j = i \end{cases} \tag{VII.5.6}$$

the vector $\boldsymbol{\nu} = [\nu_1 \ \ldots \ \nu_K]^T$ and the matrix $\boldsymbol{P} = \mathrm{diag}(\boldsymbol{p})$. Then we have the following equation

$$\boldsymbol{\gamma}^{-1} = \boldsymbol{D}_c^{-1}\boldsymbol{P}^{-1}[\boldsymbol{C}^T\boldsymbol{p} + \boldsymbol{\nu}] \ . \tag{VII.5.7}$$

So the criterion (VII.5.4) generally leads to a set of coupled problems which cannot be solved analytically. Furthermore it can be shown that once the vectors $\boldsymbol{u}_i$ are fixed the optimum power assignment vector $\boldsymbol{p}$ is unique.

We consider in the following an analytical approach for the optimization of the minimum signal to interference ratio (SIR) for the normalized weight vectors design. Once the we have obtained the vectors $\boldsymbol{u}_i$'s we can plug them in the problem (VII.5.4) and solve for $\boldsymbol{p}$.

VII.5.1 SIR Optimization

The SIR for the ith user is defined as

$$\mathrm{SIR}_i = \frac{\boldsymbol{w}_i^H \boldsymbol{R}_{ii} \boldsymbol{w}_i}{\sum_{j=1,\, j\neq i}^{K} \boldsymbol{w}_j^H \boldsymbol{R}_{ji} \boldsymbol{w}_j} \tag{VII.5.8}$$

The equation (VII.5.7) in the absence of noise reduces to

$$\boldsymbol{\gamma}^{-1} = \boldsymbol{D}_c^{-1}\boldsymbol{P}^{-1}\boldsymbol{C}^T\boldsymbol{p} \tag{VII.5.9}$$

where now $\gamma_i = \mathrm{SIR}_i$ for any i. Considering the criterion (VII.5.4) and the definition (VII.5.8) it is straightforward to see that the optimum is achieved when all the MAI is zero so that $\gamma_i^{-1} = 0$ for all i's. Then, if m_a is greater than the number of all the nominal propagation directions of all the users channels, the optimum approach in the absence of noise would lead to a zero-forcing (ZF) MAI solution. In practice this condition never arises so non-ZF approaches need to be considered.

Note that since the optimum still involves $\gamma_i = \gamma$ for any i, the equation (VII.5.9) reduces to

$$\gamma^{-1}\boldsymbol{p} = \boldsymbol{A}^T\boldsymbol{p} \tag{VII.5.10}$$

where $\boldsymbol{A}^T = \boldsymbol{D}_c^{-1}\boldsymbol{C}^T$ is a non-negative matrix. Moreover $\boldsymbol{p}$ has to be a non-negative vector and γ^{-1} has to be non-negative as well. On the basis of the following theorems ([HJ85, YX98])

Theorem 3
For a non-negative matrix, the eigenvalue of the largest norm is positive, and its corresponding eigenvector can be chosen to be non-negative.

Theorem 4
For a non-negative matrix $\boldsymbol{A}^T$, the non-negative eigenvector corresponding to the eigenvalue of the largest norm is positive.

Theorem 5
Given the matrix $\boldsymbol{A}^T$ there exists only one solution to equation (VII.5.10).

we can say that for a given set of unit norm vectors $\{\boldsymbol{u}_i\}$ then the optimum yields $\gamma^{-1} = \lambda_{\max}(\boldsymbol{A}^T)$ and $\boldsymbol{p} = V_{\max}(\boldsymbol{A}^T)$.

Having an estimate of $\boldsymbol{p}$, we can optimize $\{\boldsymbol{u}_i\}$. Indeed the optimization criterion is given by

$$\min_{\{\boldsymbol{u}_i\}} \lambda_{\max}(\boldsymbol{A}^T) \tag{VII.5.11}$$

In order to simplify the problem formulation without loss of generality, we consider $\boldsymbol{u}_i^t$'s normalized such that $\boldsymbol{u}_i^H \boldsymbol{R}_{ii} \boldsymbol{u}_i = 1$, so that $\boldsymbol{D}_c = \mathbf{I}$ and $\boldsymbol{A}^T = \boldsymbol{C}^T$. Then the criterion (VII.5.11) becomes

$$\min_{\{\boldsymbol{u}_i\}} \boldsymbol{q}^T \boldsymbol{A}^T \boldsymbol{p} \quad \text{s.t.} \quad \boldsymbol{u}_i^H \boldsymbol{R}_{ii} \boldsymbol{u}_i = 1 \tag{VII.5.12}$$

where $\boldsymbol{q} = V_{\max}(\boldsymbol{A})$. The criterion (VII.5.12) leads to a set of K decoupled problems whose solution is given by $\boldsymbol{u}_i = \frac{\boldsymbol{e}_i}{\sqrt{\boldsymbol{e}_i^H \boldsymbol{R}_{ii} \boldsymbol{e}_i}}$, where $\boldsymbol{e}_i = V_{\max}(\boldsymbol{R}_{ii}, \sum_{j \neq i}^K q_j \boldsymbol{R}_{ij})$ for any i. The new set of vectors $\{\boldsymbol{U}_i^t\}$ can be used to re-optimize the powers $\boldsymbol{p}$ according to (VII.5.10).

VII.5.1.1 $\|\boldsymbol{A}^T\|_1$ minimization based solution

As sub-optimal approach or initialization we might use the following criterion

$$\min_{\{\boldsymbol{u}\}} \|\boldsymbol{A}^T\|_1 \quad \text{s.t.} \quad \boldsymbol{u}_i^H \boldsymbol{R}_{ii} \boldsymbol{u}_i = 1 \tag{VII.5.13}$$

This approach has the advantage of optimizing the direction vectors $\{\boldsymbol{u}_i\}$ independently from the powers $\boldsymbol{p}$. In that sense it is suitable to initialize an iterative procedure to find the global optimum. Indeed it leads to a set of K decoupled minimization problems whose solution is given by $\boldsymbol{u}_i = \frac{\boldsymbol{e}_i}{\sqrt{\boldsymbol{e}_i^H \boldsymbol{R}_{ii} \boldsymbol{e}_i}}$, where, in this case, $\boldsymbol{e}_i = V_{\max}(\boldsymbol{R}_i, \sum_{j=1}^K \boldsymbol{R}_{ij})$ for any i.

Note that the criterion (VII.5.13) corresponds to minimizing the power delivered to the undesired users while maximizing the power delivered to the desired user, by each spatial filter $\boldsymbol{u}_i$.

A similar criterion was already proposed in [Zet97, GF97] to optimize the weight vectors for transmit beamforming.

VII.5.1.2 $\lambda_{\max}(\boldsymbol{A}^T)$ minimization based algorithm

According to the previous arguments, we propose the iterative procedure summarized in Table VII.1 to find the global optimum in the absence of noise.

Table VII.1: $\lambda_{\max}(\boldsymbol{A}^T)$ minimization based algorithm

(i)	Initialize $\boldsymbol{u}_i$ using (VII.5.13) for $i = 1, \ldots, K$;
(ii)	Compute $\boldsymbol{q} = V_{\max}(\boldsymbol{A})$;
(iii)	Compute $\boldsymbol{e}_i = V_{\max}(\boldsymbol{R}_{ii}, \sum_{j \neq i} q_j \boldsymbol{R}_{ij})$;
(iv)	Compute $\boldsymbol{u}_i = \frac{\boldsymbol{e}_i}{\sqrt{\boldsymbol{e}_i^H \boldsymbol{R}_{ii} \boldsymbol{e}_i}}$;
(v)	Go back to (ii) until convergence;
(vi)	Compute $\boldsymbol{p} = V_{\max}(\boldsymbol{A}^T)$;
(vii)	Compute $\boldsymbol{w}_i = \sqrt{p_i} \boldsymbol{u}_i$.

VII.5.2 Power assignment optimization

Assuming a given set $\{\boldsymbol{u}_i\}$, since the optimum involves all the γ_i's to be the same, the expression (VII.5.7) can be arranged in order to include the constraint on the transmitted power as follows

$$\boldsymbol{Q}\tilde{\boldsymbol{p}} = \gamma^{-1}\boldsymbol{S}\tilde{\boldsymbol{p}} \tag{VII.5.14}$$

where $\tilde{\boldsymbol{p}} = [\boldsymbol{p}^T\ 1]^T$,

$$\boldsymbol{Q} = \begin{bmatrix} \boldsymbol{A}^T & \boldsymbol{\mu} \\ \mathbf{0}_{1\times K} & 0 \end{bmatrix} \qquad \boldsymbol{S} = \begin{bmatrix} \mathbf{I}_K & \mathbf{0}_{K\times 1} \\ \boldsymbol{s}^T & -p_{\max} \end{bmatrix}$$

where $\boldsymbol{\mu} = \boldsymbol{D}_c^{-1}\boldsymbol{\nu}$, $\boldsymbol{s} = [\|\boldsymbol{u}_1\|^2\ \dots\ \|\boldsymbol{u}_K\|^2]^T$ and $\boldsymbol{s}^T\boldsymbol{p} = p_{\max}$. Then similarly to [YX98] since $\boldsymbol{S}$ is invertible we have

$$\boldsymbol{E}\tilde{\boldsymbol{p}} = \gamma^{-1}\tilde{\boldsymbol{p}}, \qquad \boldsymbol{E} = \boldsymbol{S}^{-1}\boldsymbol{Q} = \begin{bmatrix} \boldsymbol{A}^T & \boldsymbol{\mu} \\ \dfrac{\boldsymbol{s}^T\boldsymbol{A}^T}{p_{\max}} & \dfrac{\boldsymbol{s}^T\boldsymbol{\mu}}{p_{\max}} \end{bmatrix} \tag{VII.5.15}$$

which is a non-negative matrix. Relying on theorems 1–3 we can say that $\gamma^{-1} = \lambda_{\max}(\boldsymbol{E}^T)$ and $\tilde{\boldsymbol{p}} = V_{\max}(\boldsymbol{E})$. Further, note that we can always re-scale $\tilde{\boldsymbol{p}}$ in order to make its last element equal to one.

VII.6 Simulations

In this section we consider a scenario with $K = 4$ users operating in CDMA system with a spreading factor $m_c = 6$, corresponding to a loading fraction of 66%. Each user has a single cluster channel characterized by a nominal angle and a several delays. The users are in near-far conditions, namely the useful signal powers are proportional to 20 dB, -60 dB, 20 dB, and -20 dB. The angles are $\theta_1 = -45$, $\theta_2 = -25$, $\theta_3 = 5$, $\theta_4 = 30$ degrees respectively for the first the second, the third and the fourth user. An array of $m_a = 3$ antennas is used at the base station to transmit at the 4 users. In fig. VII.2 it is shown the convergence of the proposed algorithm. The output SIR is 11.6 dB, 2.8 dB with 3 and 1 antenna respectively (i.e., only RAKE temporal processing).

Fig. VII.3 shows the beam radiation pattern after the optimization. The arrows in the graph represent the angles associated with the different users while their amplitude is approximately proportional to the strength of the corresponding user. In general the beamformer of strong users attempts at putting nulls in correspondence of weak users while weak users aim at maximizing the energy in their own direction.

Finally fig. VII.4 shows the output SINR after the optimization versus the input SNR. The SINR improvement with respect to pure RAKE processing is larger as the SNR increases. This is due to the zero-forcing nature of the optimization algorithm.

VII.7 Conclusions

We addressed the problem of SINR maximization at the mobile stations by performing spatial filtering at the base-station and emplying a RAKE receiver at the mobile stations. It is shown that in cases where spatio-temporal processing cannot be employed to precancel the interference, significant performance gains can still be achieved by spatial filtering only. The case of complex spreading was treated

along with that of real spreading sequences. The behavior of these two cases is slightly different, leading to an extra term for the signal part in the real codes' case. An algorithm for power allocation and spatial filter optimization was also presented.

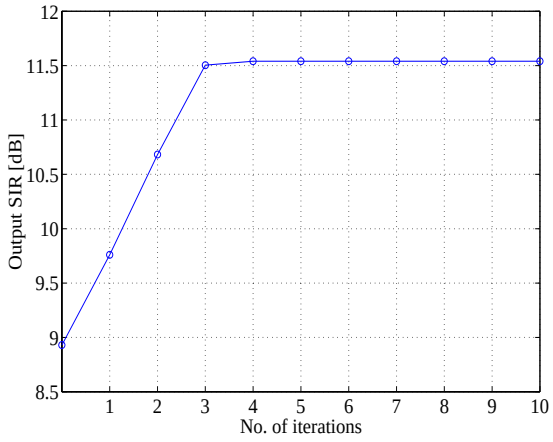

Figure VII.2: Optimum SIR (dB) convergence vs. no. of iterations

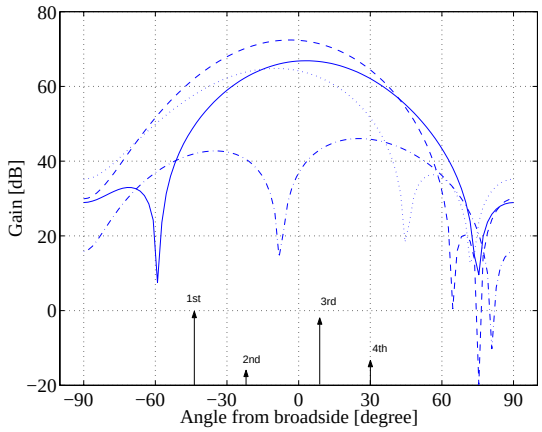

Figure VII.3: Radiation patterns after optimization

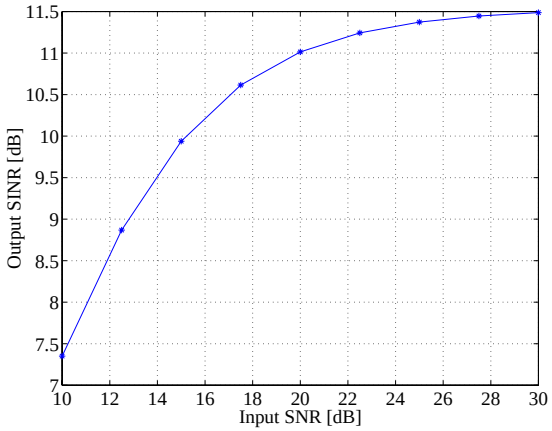

Figure VII.4: Optimum output SINR vs. input SNR

Chapter VIII

Concluding Remarks

We addressed the problem of linear interference rejection for DS-CDMA systems. Since the received DS-CDMA signal comprises contribution of all active users, single user information cannot be used in the classical way, e.g., by least-squares, in order to estimate parameters of interest of the desired user. Single user reception techniques like the matched filter (or RAKE in multipath channels) also suffer from performance degradation due to the presence of interfering user signals. The problem therefore becomes that of user separation, and alternative receivers and parameter estimation algorithms need to be devised.

It was shown that these systems have inherent properties of interference mitigation owing to the multichannel aspect that comes about due to the large (extra) bandwidth occupied by the signal. Further gains can be obtained by temporal oversampling in excess of the chip-rate or exploiting the space dimension in terms of multiple antennas. In this thesis, several blind channel estimation and interference cancelation approaches were considered for different situations in DS-CDMA systems.

In chapter II we presented a blind uplink (asynchronous channel) projection receiver structure obtained by solving the MOE criterion subject to the unbiasedness constraint. The received signal is cyclostationary at the symbol rate owing to the periodicity of spreading sequences. The receiver is a representative of decentralized linear multiuser detection schemes where the knowledge of parameters like spreading sequence and timing information of only the user of interest is considered to be available. The origin, powers, and relative asynchrony of interferers is not a concern in this problem. Only their number has to stay below a certain loading fraction in order to satisfy identification requirements for the channel and for the receiver to exist. Bounds on receiver length as a function of the number of users was given in this work. The important issues pertaining to this approach can be summarized as follows

- The MOE criterion solved subject to unbiasedness constraint (or ZF MOE) gives the MMSE-ZF or the projection receiver.
- The interference canceling scheme is similar to the pre-combining interference canceler. The IC stage converts the MAI/ISI problem into a single user no ISI problem (thus cleaning up the interference), and a channel matched filter subsequently suffices to coherently combine the multipath signals.
- Applying Capon's method in conjunction with the MOE criterion leads to an unambiguous blind estimate of the channel impulse response of the desired user, as a by-product of the IC scheme.

The receiver therefore falls in the category of directly estimated receivers, i.e., the channel estimate falls out of the interference canceling scheme.

- Training and semi-blind channel estimation is also possible due to the single user aspect of the residual problem after interference cancelation.
- The approach is of particular interest for channel estimation of the user of interest in the asynchronous uplink of a DS-CDMA system employing periodic spreading sequences, since all users can be treated in a similar fashion once spreading sequences and timing information is available for each of them.
- The blind channel identification algorithm was shown to be robust and identifiability exists w.p. 1 unless the channel is overestimated beyond a certain limit.
- The receiver can be seen as an extension of the RAKE receiver. This extension comes about from the interference canceling aspect. The lower branch of the GSC version accounts for the added complexity incurred by the interference canceling algorithm. This branch can be switched off if the performance of a RAKE is deemed sufficient for a particular application.
- The interference cancelation algorithm can be adapted independently of the channel impulse response estimation and is based only upon the knowledge of delays of the multipath components.
- Sparse channels can be easily handled in the structure leading to reduced complexity adaptation of the receiver.
- The receiver structure lends itself readily to reduced complexity LMS adaptive implementation.
- Semi-blind and decision-directed implementation also lead to improved performance.

Future research in the area of receiver algorithms for asynchronous DS-CDMA systems will need to address the issue of fast-convergence and tracking algorithms, particular ways of soft-decision re-use in decision-directed implementations and extensions to the case of aperiodic spreading sequences.

Chapter IV deals with the downlink interference rejection problem exploiting the very particular structure of the downlink problem - the fact that all downlink user signals arrive at the mobile receiver through the same channel. The following series of conclusions can be drawn from the results of this chapter.

- Alternatives to the RAKE receiver are desirable for low spreading factors and significant ISI.
- A ZF receiver is obtainable if the channel impulse response is available.
- The ZF receiver suffers from significant noise enhancement and its performance is poor within the SNR region of interest.
- The maximum SINR receiver is an attractive alternative and can be obtained blindly from the knowledge of unused spreading sequences and the desired spreading sequence.
- The presence of scrambling renders the blind algorithm a maximum SINR receiver. In the absence of scrambling, the MAI is still canceled by the blind receiver structure but the criterion and constraint set lead to residual ISI if the receiver is long, i.e., the delay spread of the propagation channel is sufficiently large.

- The RAKE receiver's output SINR depends on the ratio of delay spread and the processing gain, and also on the loading fraction. These three parameters decide whether the RAKE suffices for a certain application or if more advanced receivers are inevitable.
- The use of orthogonal spreading sequences as underlying signature spreading is the best choice for intracell interference in downlink transmission.

An interesting problem to investigate for the case of downlink equalizer/correlator approach is the training based or semi-blind adaptation of the SINR maximizing receiver. This may lead to speedy convergence.

We have also considered the problem of performing optimum spatio-temporal processing for multiuser downlink transmission in wireless communication systems. This particular method of exploiting the plurality of antennas at the base-station assumes total or partial knowledge of downlink channel parameters. This channel-state information is considered to be available up to varying degrees in TDD or FDD based communication systems respectively. Exploiting some knowledge of downlink channels allows one to strategically pre-filter the transmitted signal to account, prior to transmission, for not only the MAI bound to be added in the forward channel but also the signal distortion (ISI) introduced due to multipath. This results in significant gains compared to the case where the forward channel is not known, and where transmit antennas couple energy into the spatial channel without regard to interference created towards concurrent users.

The assumption of channel reciprocity is considered to hold for TDD. On the other hand the frequency shift between uplink and downlink carrier frequencies is enough to destroy the reciprocity. However, this shift is usually small enough to render invariant certain parameters like angles of arrival, the delays, and the average powers associated with the uplink and downlink channels. Nevertheless, this information is not enough to build an estimate of the downlink channel. We consider a base-station transmitting through multiple channels coming about due to multiple antennas and/or oversampling of the transmitted signal. For both TDD and FDD cases, we proposed ZF approaches to cancel the interference prior to transmission on the downlink. It was shown that spatio-temporal processing is an attractive means of enhancing the network capacity by controlling the interference upon transmission, and building low-complexity mobile receivers. The major conclusions drawn from this work are as follows.

- ZF pre-cancelation can be achieved in the FDD problem by considering each path as a distinct user as opposed to the TDD case where the downlink channel is considered known. A small number of paths per user can therefore be handled for the FDD case
- Selection diversity is the best possible power assignment approach when path phases are unknown, and corresponds to exciting the best path or cluster of paths for downlink transmission.
- When aperiodic spreading sequences are employed, spatio-temporal processing can no longer be performed to pre-cancel the interference. However, spatial processing (beamforming) can still performed to enhance the SINR at the mobile station
- Once the transmission filters have been designed, powers can be allocated in all cases to maximize the minimum SINR among all mobile stations

Appendix A

Sommaire détaillé en Français

A.1 Introduction

Les systèmes de communications mobiles de troisième génération sont fondés sur la technique d'accès multiple par répartition en codes (AMRC) utilisant la méthode de séquence directe. L'AMRC à été choisi comme technique d'accès multiples dans les normes car elle présente un certain nombres d'avantages liés à la capacité en terme de nombre d'utilisateurs coexistants dans une cellule, et à la facilité liée à la gestion de ressources dans ces systèmes.

Dans cette méthode d'accès multiple séquences d'étalement différentes et *a priori* orthogonales sont attribuées aux utilisateurs. Cependant, le canal à trajets multiples détruit l'orthogonalité entre les signaux de ces utilisateurs et crée le phénomène d'interférence entre utilisateurs. Il faut donc trouver des méthodes pour annuler ces interférences. Plusieurs aspects de ce problème ont été étudiés dans le cadre de cette thèse et plusieurs méthodes ont été proposées pour diverses situations rencontrés dans les systèmes. L'accent à été mis sur l'utilisation des connaissances *a priori* existantes dans les différents problèmes comme celles de filtres de transmission et de réception, les conditions de synchronisation des utilisateurs pour la liaison descendante, et l'orthogonalité de codes d'étalement.

A.2 Modèle du signal AMRC

Le modèle du signal en bande de base a été décrit dans la section § I.3, qui tient compte du phénomène de trajets multiples. Dans ce modèle, T signifie la durée du symbole, T_c la durée du chip et le rapport $P = \frac{T}{T_c}$ est connu sous le nom de facteur d'étalement ou facteur d'expansion de bande de fréquence. On considère que le k-ième utilisateur transmet une séquence de symboles $a_k(n)$ appartenant à un alphabet fini Ω. La séquence de symboles est d'abord étalée par la séquence d'étalement périodique de l'utilisateur k, $c_k(p), \quad p \in \{1, \ldots, P-1\}$. Ensuite, cette séquence de chips, est embrouillée par une séquence longue pseudo-aléatoire (PN), $s_k(l)$. Les chips de la séquence d'étalement et du brouilleur appartiennent à un alphabet fini Θ. On considère exclusivement le cas de modulations linéaires. Le signal en temps continu en bande de base (enveloppe complexe) à la sortie du modulateur linéaire peut s'écrire comme

$$x_k(t) = \sum_{l=-\infty}^{+\infty} p(t - lT_c) b_k(l). \tag{A.2.1}$$

où $p(t)$ est le filtre de mise en forme de largeur de bande unilatérale $W/2$ [Pro95], qui est le plus souvent un cosinus surélevé (raised cosine) ou un racine carré de cosinus soulevé (root-raised cosine). W est aussi la largeur de bande du signal étalé. Dans les systèmes à spectre étalé, $W \approx \frac{1}{T_c}$. Le séquence des chips, $b_k(l)$ est une *i.i.d*. Dans le modèle ci-dessus, le signal étalé peut être considéré comme apériodique puisque le brouilleur enlève la périodicité introduite par la séquence $c_k(p)$. On peut ainsi écrire (A.2.1) sous la forme

$$x_k(t) = \sum_{n=-\infty}^{+\infty} \psi_k(t - nT) a_k(n) \tag{A.2.2}$$

avec,

$$\psi_k(t) = \sum_{i=0}^{P-1} p(t - iT_c) c_k(i) \tag{A.2.3}$$

où $\psi_k(t)$ est la signature de l'utilisateur k en absence de brouillage. Si le brouilleur est actif et opérant, on peut ajouter l'indice n dans les équations (A.2.2) et (A.2.3) pour exprimer la dépendance sur l'indice du symbole.

A.2.1 Canal à trajets multiples

Le canal de propagation est caractérisé par une matrice $K \times M$ avec des éléments $\phi_{k,m}$, $(1 \leq k \geq K;\ 1 \leq m \geq M)$, ayant K entrées (nombre d'utilisateurs) et M sorties (nombre d'antennes). Il s'agit d'un modèle linéaire dans lequel le principe de superposition (des différents signaux) est applicable. Pour les signaux à bande limité, on peut approximer l'environnement de propagation par un ensemble de trajets multiples atténués et déphasés. Ainsi, la fonction de transfert entre l'utilisateur k et l'antenne m peut s'écrire comme

$$\phi_{k,m}(t) = \sum_{q=0}^{Q-1} \delta(t - \tilde{\tau}_{q,km}) \widetilde{\phi}_{k,m}(q) \tag{A.2.4}$$

ou Q et le nombre de trajets, et $\widetilde{\phi}_{k,m}(q)$ et $\tilde{\tau}_{q,km}$ sont respectivement l'amplitude complexe et le retard du trajet q pour l'utilisateur k et l'antenne m. Le retard $\tilde{\tau}_{q,km}$ dépend de l'angle d'arrivée de l'onde et de la géométrie de l'antenne. La distribution des amplitudes et les valeurs (déterministes) des retards dépendent de l'environnement de la propagation (urbain, rural etc). Dans un contexte multi-utilisateurs, un retard τ_k lié a l'utilisateur k qui est uniformément réparti sur une période symbole vient s'ajouter à l'ensemble des retards.

A.2.2 Filtre de réception

Le modèle du signal est décrit dans la figure A.1. Le canal qui est un filtre causal vu de l'antenne m est donné par

$$h_{k,m}(t) = \int_0^{\Delta T_c} p(t - \tau) \phi_{k,m}(\tau) d\tau \tag{A.2.5}$$

ou $p(t)$ est le filtre de transmission/réception combinés et $\phi_{k,m}(t)$ est la réponse impulsionnelle du canal de propagation en temps continu entre l'utilisateur k et l'antenne m. ΔT_c est la durée maximale

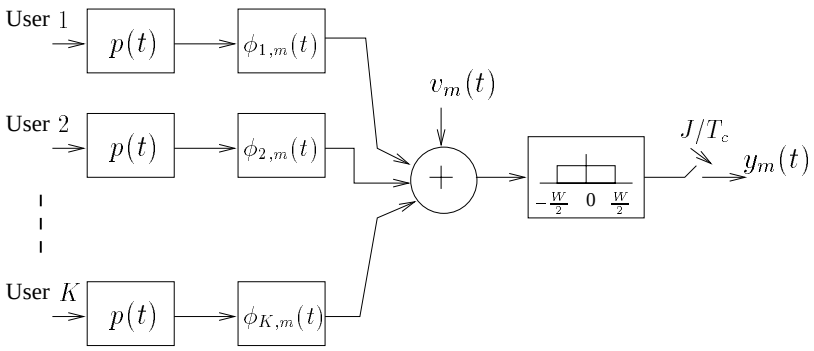

Figure A.1: Modèle du signal reçu en bande de base à la m-ième antenne.

de la réponse impulsionnelle $\phi_{k,m}(t)$, c'est-à-dire la durée maximale du canal à réponse impulsionnelle finie (RIF). Δ est un nombre entier positif. Le filtre de transmission est bande–limité avec un facteur d'accès de largeur de bande α montré dans la figure I.4. Quant au filtre de réception, il s'agit d'un filtre anti-repliement idéal, passe-bas avec une fréquence de coupure correspondant à la fréquence d'échantillonnage W. Donc, pour éviter le repliement du spectre, il suffit que la fréquence de coupure du filtre de réception se trouve au-dessous de la fréquence de Nyquist. Cette dernière correspond à l'échantillonnage critique du signal pour éviter le repliement du spectre.

Si on considère un échantillonnage au rythme W, on peut écrire le canal suréchantillonné total comme

$$h_{k,m}(t) = \sum_{l=0}^{L-1} p(t - \frac{l}{W})\phi_{k,m}(l) \tag{A.2.6}$$

Les $\phi_{k,m}(l)$ sont la représentation discrète de $\phi_{k,m}(t)$, correspondants à une version échantillonnée au taux W du canal filtré passe-bas. Comme détaillé dans la section § I.3.1.3, en fonction de la fréquence d'échantillonnage, les $\phi_{k,m}(l)$ peuvent avoir plusieurs valeurs rendant la représentation du canal filtré non unique. Au total, le canal en temps discret peut être écrit comme

$$\boldsymbol{h}_k = \underline{\widetilde{\boldsymbol{P}}}\boldsymbol{\phi}_k \tag{A.2.7}$$

où bien comme

$$\boldsymbol{h}_k = \underline{\widetilde{\boldsymbol{P}}}\,\underline{\boldsymbol{\Pi}}\widetilde{\boldsymbol{\phi}}_k, \tag{A.2.8}$$

le produit des matrices contenant les coefficients des filtres de transmission $\underline{\widetilde{\boldsymbol{P}}}$ et de reception $\underline{\boldsymbol{\Pi}}$ en fonction de la connaissance *a priori* de ces filtres. Cette représentation du canal présente comme avantage, la réduction du nombre de paramètres à estimer une fois les filtres, $\underline{\widetilde{\boldsymbol{P}}}$ et $\underline{\boldsymbol{\Pi}}$ sont connus.

A.2.3 Diversité de réception

Si les M antennes du récepteur sont placées suffisamment éloignées les uns des autres, on va recevoir M copies rétardées et déphasées du signal reçu. Cela correspond à la diversité spatiale. Le cas de $M = 2$ est représenté dans la figure I.5; on a ainsi deux canaux physiques. Inversement, un suréchantillonnage du signal reçu au rhythme $\frac{J}{T_c}$ crée aussi une diversité; cette fois artificielle. Ce mécanisme est illustré par la figure I.6 pour le cas $J = 2$. Les sous-canaux h_1 et h_2 se comportent comme

deux canaux virtuels transportant les composantes polyphases du signal. On peut ainsi écrire le signal vectoriel reçu par une m-ième antenne à l'instant n comme

$$\boldsymbol{y}_{k,m}(n) = \left[y_{k,m}(nT_c), y_{k,m}(nT_c + \frac{T_c}{J}), \ldots\ldots, y_{k,m}(nT_c + (J-1)\frac{T_c}{J}) \right]^T . \tag{A.2.9}$$

Empilant les signaux reçus sur les M antennes, on peut recevoir le signal vectoriel total comme

$$\boldsymbol{y}_k(n) = \left[\boldsymbol{y}_{k,1}^T(n), \boldsymbol{y}_{k,2}^T(n) \ldots\ldots, \boldsymbol{y}_{k,M}^T(n) \right]^T , \tag{A.2.10}$$

Dans la pratique, il existe des limitations sur le facteur J de suréchantillonnage, à cause des conséquences de l'excès de bande.

A.2.4 Modèle du signal asynchrone en temps discret

La figure I.7 montre le signal équivalent en bande de base. Le signal total reçu à la m-ième antenne peut être écrit comme

$$y_m(t) = \sum_{k=1}^{K} \sum_{n} a_k(n) g_{k,m}(t - nT) + v_m(t), \tag{A.2.11}$$

où les $a_k(n)$ sont les symboles transmis par le k-ième utilisateur. $g_{k,m}(t)$ est la réponse impulsionnelle du canal total (contenant l'effet de la séquence d'étalement et les filtres de transmission et de réception) pour le k-ième utilisateur et la m-ième antenne. On considère dans ce développement, les séquences d'étalement périodiques. $v_m(t)$ et le bruit blanc circulaire centré et gaussien, de densité spectrale de puissance unilatérale $\mathcal{N}_0$. On fait l'hypothèse de cyclostationarité conjointe au sens large (deuxième ordre) de $v_m(t)$ et les $a_k(n)$ avec la période symbole, T. Le canal total, $g_{k,m}(t)$, peut alors être écrit comme la convolution entre la séquence d'étalement et $h_{k,m}(t)$, ce dernier étant lui-même la convolution du canal de propagation et le filtre de mise en forme, et le filtre de réception. On peut exprimer cette convolution comme

$$g_{k,m}(t) = \sum_{p=0}^{P-1} c_k(p) h_{k,m}(t - pT_c); \tag{A.2.12}$$

Le signal vectoriel stocké peut être écrit comme

$$\boldsymbol{y}(n) = \sum_{k=1}^{K} \sum_{i=0}^{N_k-1} \boldsymbol{g}_k(i) a_k(n-i) + \boldsymbol{v}(n) = \sum_{k=1}^{K} \boldsymbol{G}_{k,N_k} A_{k,N_k}(n) + \boldsymbol{v}(n) = \boldsymbol{G}_N \boldsymbol{A}_N(n) + \boldsymbol{v}(n), \tag{A.2.13}$$

avec

$$\boldsymbol{y}(n) = \begin{bmatrix} \boldsymbol{y}_1(n) \\ \vdots \\ \boldsymbol{y}_P(n) \end{bmatrix}, \boldsymbol{y}_p(n) = \begin{bmatrix} \boldsymbol{y}_{p,1}(n) \\ \vdots \\ \boldsymbol{y}_{p,M}(n) \end{bmatrix}, \boldsymbol{y}_{p,m}(n) = \begin{bmatrix} y_{p,1m}(n) \\ \vdots \\ y_{p,Jm}(n) \end{bmatrix}$$

$$\begin{aligned} \boldsymbol{G}_{k,N_k} &= [\boldsymbol{g}_k(N_k-1) \ldots \boldsymbol{g}_k(0)] \ , \boldsymbol{G}_N = [\boldsymbol{G}_{1,N_1} \ldots \boldsymbol{G}_{K,N_K}] \\ A_{k,N_k}(n) &= [a_k(n-N_k+1) \ldots a_k(n)]^T \ , \boldsymbol{A}_N(n) = \left[A_{1,N_1}^T(n) \ldots A_{K,N_K}^T(n) \right]^T , \end{aligned} \tag{A.2.14}$$

Pour l'utilisateur désiré (utilisateur 1), $\boldsymbol{g}_1(i) = (\boldsymbol{C}_1(i) \otimes I_{MJ})\, \boldsymbol{h}_1$, où $\boldsymbol{h}_1$ est le vecteur du canal de propagation de longeur $MJ\Psi_1 \times 1$ donné par (I.3.14) (I.3.14) et peut être écrit comme

$$\boldsymbol{h}_1 = \begin{bmatrix} \boldsymbol{h}_{1,1} \\ \vdots \\ \boldsymbol{h}_{1,\Psi_1} \end{bmatrix}, \boldsymbol{h}_{1,i} = \begin{bmatrix} \boldsymbol{h}_{1,i1} \\ \vdots \\ \boldsymbol{h}_{1,iM} \end{bmatrix}, \boldsymbol{h}_{1,im} = \begin{bmatrix} h_{1,im}(1) \\ \vdots \\ h_{1,im}(J) \end{bmatrix},$$

$\otimes$ signifie le produit de Kronecker, et la matrice Toeplitz $\boldsymbol{C}_1(i)$ est montrée dans la fig. A.2, où la bande consiste en séquence d'étalement $[c_0 \ \ldots \ c_{P-1}]^T$ decalée successivement à droite et en bas d'une position. Pour les interféreurs, on à une même configuration sauf que la bande dans la figure I.8 est

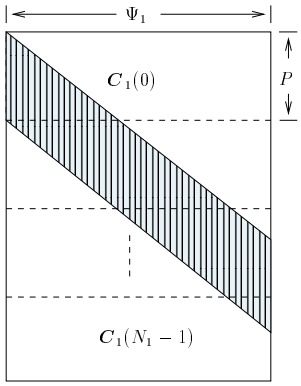

Figure A.2: La matrice de convolution de code C_1.

décalée par n_k périodes chips et ne coincide plus avec celui de l'utilisateur désiré. On désigne par $\boldsymbol{C}_1$, la concatenation des matrices de code pour l'utilisateur désiré 1: $\boldsymbol{C}_1 = [\boldsymbol{C}_1^T(0) \ \ldots \ \boldsymbol{C}_1^T(N_1-1)]^T$.

On peut voir dans les équations (I.3.14) et (I.3.15), que $\boldsymbol{h}_1$ peut être décomposé comme étant une cascade du filtre de mise-en-forme, du filtre de réception et du canal discret proprement dit. On peut ainsi écrire

$$\boldsymbol{g}_1(i) = \{\boldsymbol{C}_1(i) \otimes I_{MJ}\} \ \boldsymbol{h}_1 = \widetilde{\boldsymbol{C}}_1(i) \, \boldsymbol{\phi}_1 = \widetilde{\widetilde{\boldsymbol{C}}}_1(i) \, \widetilde{\boldsymbol{\phi}}_1, \tag{A.2.15}$$

où,

$$\widetilde{\boldsymbol{C}}_1(i) = \{\boldsymbol{C}_1(i) \otimes I_{MJ}\} \, \underline{\widetilde{\boldsymbol{P}}}, \quad \text{and,} \quad \widetilde{\widetilde{\boldsymbol{C}}}_1(i) = \{\boldsymbol{C}_1(i) \otimes I_{MJ}\} \, \underline{\widetilde{\boldsymbol{P}}} \, \underline{\boldsymbol{\Pi}}. \tag{A.2.16}$$

Dans tous les cas, on va considérer $PMJ > K$, une condition qui demeure correcte même si le facteur de chargement[1] est plus grand que 1.

A.2.5 L'interférence entre symboles (IES)

Un vecteur de longeur L du signal stationnaire reçu est écrit comme

$$\boldsymbol{Y}_L(n) = \mathcal{T}_L(\boldsymbol{G}_N) \boldsymbol{A}_{N+K(L-1)}(n) + \boldsymbol{V}_L(n). \tag{A.2.17}$$

où,

$$\mathcal{T}_L(\boldsymbol{G}_N) = [\mathcal{T}_L(\boldsymbol{G}_{1,N_1}), \ \ldots \ , \mathcal{T}_L(\boldsymbol{G}_{K,N_K})],$$

[1] le facteur de chargement est défini comme $\mathrm{LF} = \frac{K}{P}$

et $\mathcal{T}_L(\boldsymbol{x})$ est la matrice bande bloc Toeplitz matrix avec L lignes blocs et $\begin{bmatrix}\boldsymbol{x} & \mathbf{0}_{p\times(L-1)}\end{bmatrix}$ comme la première ligne bloc (p est le nombre de lignes en $\boldsymbol{x}$), et $\boldsymbol{A}_{N+K(L-1)}(n)$ signifie la concaténation des vecteurs de symboles des utilisateurs $[A^T_{1,N_1+L-1}(n), A^T_{2,N_2+L-1}(n), \ldots, A^T_{K,N_K+L-1}(n)]^T$. $\boldsymbol{V}_L(n)$ est le vecteur du bruit du canal considére spatialement et temporellement blanc. On nomme $\mathcal{T}_L(\boldsymbol{G}_{k,N_k})$ la *matrice de convolution du canal* pour le k-ième utilisateur.

Le signal non-bruité ($v(t) \equiv 0$) est illustré par la figure A.3 et montre la contribution de l'utilisateur

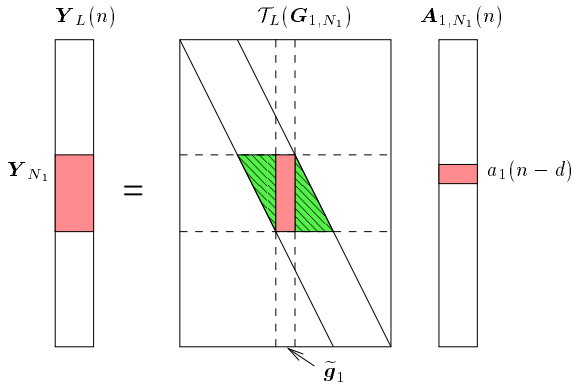

Figure A.3: L'interférence entre symboles pour l'utilisateur souhaité.

1 (considéré ici comme l'utilisateur de choix) au signal total $Y_L(n)$. Le symbole utile au n-ième instant, $a_1(n-d)$, multiplie la colonne $\widetilde{\boldsymbol{g}}_1$ de la matrice de convolution $\mathcal{T}_L(\boldsymbol{G}_{1,N_1})$. A cause de la durée limitée du canal de propagation, l'effet d'un certain symbole $a_1(n-d)$ influence N_1 symboles, rendant le canal un processus de moyenne ajustée (MA) d'ordre $N_1 - 1$. On est intéressé par l'estimation du symbole $a_1(n-d)$. On peut remarquer que le symbole $a_1(n-d)$ apparaît dans la portion Y_{N_1} du vecteur $Y_L(n)$. Les triangles hachurés constituent l'IES. Les contributions des autres utilisateurs au signal reçu ont une structure identique. Les méthodes d'annulation d'interférences sont destinées à enlever ces triangles hachurés du signal utile.

A.2.6 L'estimation du canal dans les systèmes AMRC

Afin de déterminer un récepteur, les paramètres comme le délai asynchrone et la réponse impulsionnelle du canal de l'utilisateur en question doivent d'abord être estimés. Les techniques mono-utilisateur pour l'estimation et l'égalisation sont basées sur la méthode de séquence d'apprentissage, où le signal envoyé contient une séquence d'apprentissage connue du récepteur. Cette dernière est utilisée par le récepteur pour estimer la réponse impulsionnelle du canal ou directement l'égaliseur. En GSM par exemple, le paquet transmis contient une séquence de symboles connus située au milieu de ce paquet. Les 26 symbôles suffisent pour estimer le canal par la méthode de moindres carrés dans la plupart des cas. Une version simplifiée de moindres-carrés, mise en place comme corrélation est utilisée plus souvent. Dans le cas d'un mono utilisateur en bruit blanc, la méthode de moindres-carrés correspond à la méthode du maximum de vraisemblance (ML). Néanmoins, l'intégration de séquences d'apprentissage entraîne une perte de 20% en termes d'efficacité spectrale, et constitue l'effet indésirable de cette méthode.

L'alternative consiste en l'estimation aveugle, c.-à-d. estimer les paramètres comme les coefficients du canal ou l'égaliseur sans aide de la séquence d'apprentissage. Les méthodes aveugles font appel aux

statistiques du signal reçu. Une branche des méthodes aveugles se fonde sur les statistiques de second ordre du signal reçu à travers plusieurs canaux de diversité (suréchantillonnage et/ou antennes multiples). Ces canaux de diversité donnent naissance à un modèle à entrée unique et à sorties multiples. Il a été démontré que le signal suréchantillonné contient les propriétés de la redondance spectrale et que l'amplitude et la phase du canal vectoriel pouvaient être récupérées en utilisant les statistiques de deuxième ordre. Cependant, dans le contexte multi- utilisateurs, les canaux de différents utilisateurs peuvent être identifiés à un mélange près. Les propriétés de ce mélange (instantané ou convolutif) dépendent de l'ordre relatif des canaux (considérés comme étant à RIF) des différents utilisateurs. En conséquence, il faut faire appel aux autres propriétés du signal comme les statistiques d'ordres supérieurs.

En général, le cas multi–utilisateurs n'a pas été intéressant pour le système pratique. Inversement, dans le cas multi–utilisateurs AMRC utilisant la méthode de séquence directe, on peut séparer les différents utilisateurs en exploitant les statistiques d'ordre deux. Ce fait, dû aux séquences d'étalement distinctes, souligne les avantages de la technique AMRC pour les réseaux mobiles ou sans fil.

A.3 Les récepteurs AMRC

Les récepteurs AMRC peuvent être répartis en deux catégories principales selon la classification traditionelle. Ces deux catégories s'appelle les récepteurs *conventionnels* et *multi-utilisateurs*. Les récepteurs de cette deuxième catégorie peuvent également être classées dans deux sous-branches : récepteurs *centralisés* et *décentralisés*.

A.3.1 Le récepteur AMRC conventionnel

Pour les communications sur le canal bruit-blanc gaussien centré (BBGC) et dans le cas d'un système synchrone ($\tau_k\,,\ \forall k$), la transmission des signaux orthogonaux pour K utilisateurs donne un système parfaitement orthogonal.

$$\int_{-\infty}^{+\infty} \psi_j(t)\psi_k^*(t)dt = \begin{cases} 1, & \text{for} \quad j = k \\ 0, & \text{for} \quad j \neq k \end{cases}\ , \tag{A.3.1}$$

Les $\psi_k(t)$ sont les filtres d'étalement de l'energie normalisée. Un récepteur conventionnel à filtre adapté au signal de l'utilisateur désiré permet l'annulation automatique d'interférences. Les puissances inégales (dûe à l'éffet *near-far*) des interférences n'ont pas d'effet sur la performance du récepteur du à l'orthogonalité de la modulation. Cependant, toute dérive par rapport au système idéal, par exemple le choix de codes non orthogonaux ou le phénomène de multi–trajets ou une combinaison de ces phénomènes, aboutit à un terme non nul dû aux interférences à la sortie du filtre adapté de l'utilisateur désiré.

A.3.1.1 Diversité des fréquences et le récepteur RAKE

La largeur de bande W d'un signal AMRC est en géneral beaucoup plus grand que la bande de cohérence du canal. Pour un tel rapport entre la bande de cohérence et la largeur de bande du signal utile le phénomène de multi–trajets se produit comme indiqué dans la section § I.2.1.1. Les différents trajets subissent des évanouissement indépendants. Si la résolution temporelle du récepteur est T_c, la période chip, $\frac{T_m}{T_c}$ trajets sont captés par le récepteur et donnent une diversité en fréquence de l'ordre de $\frac{T_m}{T_c}$. Le récepteur optimal pour ce signal est le RAKE, qui est un filtre adapté à la cascade "séquence

d'étalement" "canal de propagation". Ce récepteur combine les trajets de manière cohérente. Dans le contexte multi–canaux à temps discret abordé dans la section § I.3.2, le RAKE consiste en une étape de corrélation adaptée aux trajets décalés donnés par $\boldsymbol{T}_1^H = \boldsymbol{C}_1 \otimes \boldsymbol{I}_{MJ}$, et le canal de propagation, $\boldsymbol{h}_1$. Le recepteur RAKE est alors adapté au canal total, $\widetilde{\boldsymbol{g}}_1 = \boldsymbol{T}_1^H \boldsymbol{h}_1$ (fig. A.3).

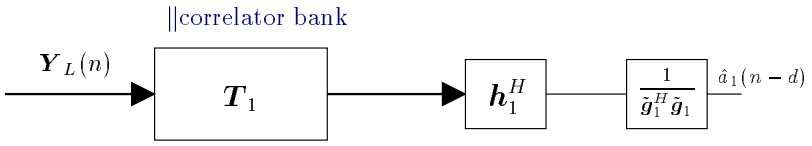

Figure A.4: Récepteur RAKE cohérent en temps discret.

Les puissances relatives des interférences ont un impact significatif à la sortie du filtre adapté (RAKE) entraînant ainsi le problème *near–far* tant redouté. Ce problème se manifeste par des puissances fortes reçues des interféreurs par rapport à la puissance du signal utile. L'interférence totale peut être assez élévée pour noyer le signal utile. Quand on peut exercer un contrôle de puissance, le filtre adapté reste le récepteur optimal du point de vue de la maximisation du rapport signal à interférence plus bruit, si les séquences d'étalement sont apériodiques et le canal BBGC. Ce comportement du filtre adapté peut être expliqué par la nature des interférences pseudo-aléatoire (PN) des autres utilisateurs qui se manifestent de la même façon que du bruit décorrelé. Alors, la performance du RAKE peut être raisonnable si le nombre d'utilisateurs est nettement inférieur au facteur d'étalement (rapport de chargement du système beaucoup plus petit qu'un système orthogonal). Cette nature d'interférences persiste à la sortie du RAKE dans les canaux à trajets multiples. Pourtant, le phénomène de saturation commence à intervenir, car le signal décalé de chaque utilisateur se manifeste comme un nouvel utilisateur. La plupart des études démontrent que le système devient très vite limité par l'interférence, et ce d'autant plus lorsque les codes sont périodiques.

A.3.2 Récepteurs multiutilisateurs centralisés

Aussi connu sous le nom de *détecteurs conjoints*, ces récepteurs sont destinés à détecter les symboles de tous les utilisateurs en même temps. Ainsi, une application se trouve sur la liaison ascendante d'un système cellulaire, où la station de base doit impérativement détecter tous les utilisateurs en service dans la cellule d'intérêt. Le premier des récepteurs et tout le domaine de détection multi–utilisateurs à été introduit par Verdu en 1986 [Ver86]. Cet ouvrage décrit le récepteur optimal de Viterbi, destiné à détecter tous les utilisateurs et s'appelle le détecteur optimal multi–utilisateur. Pourtant, il n'y à rien de magique à propos de ce récepteur. Il est, tout simplement, le détecteur de séquence à maximum de vraisemblance (DSMV) pour le cas mono-utlisateurs étendu au cas utilisateurs multiples. Dû à l'aspet multiutilisateur, malheureusement, ce récepteur à une complexité qui est exponentielle en nombre d'utilisateurs dans le cas d'un canal non-selectif en fréquence. En plus, pour les canaux à trajets multiples, une complexité liée à l'ordre du canal s'ajoute au système augmentant ainsi, le nombre d'états dans le treillis de l'algorithme de Viterbi. Ce fait rend l'application de cet utilisateur dans les systèmes chargés impossible et justifie la nécessité de trouver des récepteurs moins complexes. Parmi eux, les récepteurs linéaires comme le récepteur décorrelateur est une version multi–utilisateurs du récepteur forçant à zéro l'interférence entre symboles dans le cas mono–utilisateur. Un autre récepteur est celui minimisant l'erreur quadratique moyenne entre le symbole et son estimé.

Dans le cadre de récepteurs conjoints non linéaires, il existe des détecteurs annulant l'interférence

successivement (SIC) ou en parallèle (PIC). Un autre récepteur linéaire connu dans la littérature est le détecteur centralisé à retour de décision (DF) qui a comme homologue mono–utilisateur le récepteur non-causal à retour de décisions. Plusieurs stratégies impliquant ces récepteurs non linéaires à plusieurs étapes et retour de décision douce ont aussi été proposés.

A.3.3 Récepteurs multi-utilisateurs décentralisés

Dans le contexte de détection centralisée décrit auparavant, les récepteurs doivent impérativement connaître les paramètres comme le délai d'arrivée et les réponses impulsionnelles des canaux de tous les utilisateurs en communication avec la station de base en question. L'interférence issue des cellules voisines est ignorée. Cela entraîne une perte en termes de performance des récepteurs centralisés. Une innovation récente dans le domaine de détection multi–utilisateurs est le récepteur aveugle multi-utilisateurs [HMV95], où il a été démontré que le problème multi–utilisateurs pouvait être amené dans un cadre mono–utilisateur. Le système est ainsi transposé du problème de séparation de source à l'annulation d'interférences. Le récepteur aveugle travaille sur le signal reçu pour démoduler le signal de l'utilisateur utile.

Un des récepteurs linéaires récemment proposé est le récepteur optimal décentralisé minimisant l'erreur quadratique moyenne. Une mise en oeuvre relativement moins complexe a été décrite en utilisant la technique de prédiction linéaire. Un des grands avantages des récepteurs décentralisés provient du fait qu'ils ne font pas la distinction entre les utilisateurs sortant d'une cellule d'intérêt ou d'une cellule voisine. Dans le cadre de cette thèse, nous traiterons des techniques d'annulation d'interférences décentralisées.

A.4 Le récepteur EQMM-FZ / projection

Dans le problème multi–utilisateurs donné dans l'équation I.3.29, il existe une multitude de contraintes correspondant au forçage à zéro, dont le forçage à zéro de l'interférence d'accès multiple (IAM) seulement, le forçage à zéro de l'interférence entre symboles (IES) uniquement, ou les deux. On va considérer la dernière possibilité par la suite. La contrainte de distorsion nulle peut être écrite comme

$$\boldsymbol{f}^H \mathcal{T}(\boldsymbol{G}_N) = \boldsymbol{e}_d^T, \tag{A.4.1}$$

où, $\boldsymbol{e}_d^T = [0\cdots0|\overbrace{0\cdots0}^{d}\ 1\ 0\cdots0|0\cdots0]$, avec d le délai d'égalisation pour l'utilisateur désiré. Le récepteur minimisant l'erreur quadratique moyenne-forçage à zéro (EQMM-FZ) est le récepteur connu sous le nom de décorrelateur dans la littérature AMRC et correspond à la solution de forçage à zero qui entraîne le mimimum d'amplification du bruit.

Proposition 1: Le récepteur EQMM-FZ est équivalent à une transformation qui projette le signal reçu sur un sous-espace qui est le complément orthogonal du sous-espace engendré par l'IAM et l'IES; et ensuite projette le vecteur résultant sur un sous-espace unidimensionnel adapté au signal restant dans le vecteur reçu.

Démonstration: appendice IIA.

Le récepteur EQMM-FZ décrit ci-dessus ne peut être déterminé que si la matrice de convolution $\mathcal{T}_L(G_N)$ du canal (les délais d'arrivée et les réponses impulsionnelles des canaux de tous les utilisateurs) est connue. Comme on va le démontrer par la suite, ce récepteur peut être déterminé de manière

décentralisée en utilisant la connaissance a priori de l'utilisateur d'intérêt, comme solution du critère de réponse sans distorsion a variance minimale (LCMV).

A.4.1 Formation de voie minimisant la variance sous contrainte linéaire de distortion nulle

Il est utile de comparer le problème d'annulation d'interférences décrit par la figure A.3 à celui de la formation de voie et d'estimation de direction d'arrivée dans la littérature de traitement d'antennes [JD93]. Une source se trouvant à un angle θ_0 par rapport à un réseau d'antennes génère un signal $\boldsymbol{Y}(n)$ à l'instant n à la sortie du réseau d'antennes donné par

$$\boldsymbol{Y}(n) = \boldsymbol{S}(\theta_0)a(n) + \boldsymbol{V}(n), \tag{A.4.2}$$

où $\boldsymbol{S}(\theta_0)$ est la réponse du réseau d'antennes pour la direction θ_0 et $\boldsymbol{V}(n)$ est le vecteur du bruit additif circulaire qui est spatialement blanc. $a(n)$ est le signal de source avec variance σ_a^2. Il est évident que ce problème comporte deux inconnues; la direction d'arrivée θ_0 et le signal transmis de source $a(n)$. Dans un premier temps, on va considérer θ_0 et donc $\boldsymbol{S}(\theta_0)$ connu. Un formeur de voie linéaire $\boldsymbol{f}$ peut donner une estimation du signal $a(n)$ comme $\hat{a}(n) = \boldsymbol{f}^H\boldsymbol{Y}(n)$. Ce formeur de voie doit renforcer les signaux arrivant de la direction θ_0 tout en supprimant le bruit. On impose alors la contrainte de distorsion nulle $\boldsymbol{f}^H\boldsymbol{S}(\theta_0) = 1$ sur le formateur de voie et on minimise la variance, $E|\boldsymbol{f}^H\boldsymbol{Y}(n)|^2$, à sa sortie sous cette contrainte. La solution à ce problème donne le formeur de voie LCMV

$$\min_{\boldsymbol{f}:\boldsymbol{f}^H S(\theta_0)=1} E|\hat{a}_k|^2 \leftrightarrow \min_{\boldsymbol{f}:\boldsymbol{f}^H S(\theta_0)=1} \boldsymbol{f}^H\boldsymbol{R}_{YY}\boldsymbol{f} \;=\; \mathrm{MV}, \tag{A.4.3}$$

qui donne

$$\boldsymbol{f} = \frac{1}{\boldsymbol{S}^H(\theta_0)\boldsymbol{R}_{YY}^{-1}\boldsymbol{S}(\theta_0)}\boldsymbol{R}_{YY}^{-1}\boldsymbol{S}(\theta_0),\;\; \mathrm{MV} = \left(\boldsymbol{S}^H(\theta_0)\boldsymbol{R}_{YY}^{-1}\boldsymbol{S}(\theta_0)\right)^{-1}. \tag{A.4.4}$$

On peut trouver la direction d'arrivée, θ_0, encore inconnue comme solution à la méthode de Capon, qui correspond à la maximisation de la variance minimale sur toutes les directions d'arrivées possibles

$$\begin{aligned}\widehat{\theta} &= \arg\max_{\theta}\left(\boldsymbol{S}^H(\theta)\boldsymbol{R}_{YY}^{-1}\boldsymbol{S}(\theta)\right)^{-1} = \arg\min_{\theta}\boldsymbol{S}^H(\theta)\boldsymbol{R}_{YY}^{-1}\boldsymbol{S}(\theta)\\ &= \boldsymbol{S}^{-1}\left(V_{\max}(\boldsymbol{R}_{YY})\right) = \boldsymbol{S}^{-1}\left(\boldsymbol{S}(\theta_0)\right) = \theta_0,\end{aligned} \tag{A.4.5}$$

où $\boldsymbol{R}_{YY} = \sigma_a^2\boldsymbol{S}(\theta_0)\boldsymbol{S}^H(\theta_0) + \sigma_v^2\boldsymbol{I}$, est la matrice de covariance du signal reçu. $V_{\max}(\boldsymbol{R}_{YY})$ signifie la vecteur propre associée à la valeur propre maximale de la matrice, $\boldsymbol{R}_{YY}$.

On peut constater que la méthode de Capon peut être appliquée au problème multi-sources si ces dernières sont décorrélées et traitées conjointement. La motivation d'application de ces critères dans le cas d'annulation d'interférences en AMRC s'explique par la similarité frappante entre ce problème illustré par la figure A.3 et celui de la formation de voies. Plus précisément, on démontre qu'étant donné certaines conditions liées au nombre d'utilisateurs, la connaissance partielle des réponses impulsionnelles des canaux $\boldsymbol{T}_k^H$ des différents utilisateurs en termes de séquences d'étalement distincts $\boldsymbol{C}_k$ nous permet d'identifier leurs canaux sans ambiguité.

A.5 Relations entre les divers critères

Les différents critères linéaires sont liés entre eux comme indiqué par la proposition suivante :
Proposition 2: Les critères minimisant l'erreur quadratique moyenne (EQMM) et minimisant l'énergie à la sortie (EMS) peuvent se remplacer et sont équivalents à la maximisation du rapport signal à l'interférence et bruit (RSIB).
Démonstration: Cf. section II.5.

On peut donc identifier la relation entre le critère du EMS non-biaisé linéaire et celui de l'EQMM non-biaisé : les deux donnent le même filtre linéaire. En tout cas, les deux donnent le récepteur EQMM-FZ dans le cas sans bruit. Une observation aussi intéressante est que la contrainte de biais nul n'est pas même que celui du forçage à zéro. C'est cette dernière qui garantit la variance minimale (σ_a^2) avec une réponse fixe pour l'utilisateur utile; le but dans l'approche LCMV ou MVDR. On constate aussi, que la contrainte non-biaisée donne un FZ dans le cas sans bruit. Strictement parlant, pour arriver à satisfaire le contrainte de distortion nulle, il nous faut résoudre le problème de l'annulation d'interférences pour trouver un récepteur linéaire EQMM–ZF par la minimisation de l'énergie à la sortie (EMS) ou variance (MV) sous la contrainte de forçage à zéro. Dans le cas avec bruit, nous proposons donc de travailler avec le signal débruité ou les statistiques d'ordre deux débruitées.

A.6 Récepteur linéaire non-biaisé minimisant l'énergie à sa sortie

Le récepteur EMS peut ainsi être déterminé comme solution du critère EMS sous contrainte de bias nul. Le problème total est ainsi un problème max/min qúon résoud dans deux étapes suivantes
étape 1: *EMS non-biaisé*

$$\min_{f:f^H\tilde{g}_1=1} \boldsymbol{f}^H \boldsymbol{R}_{YY}^d \boldsymbol{f} \Rightarrow \boldsymbol{f} = \frac{1}{\widetilde{\boldsymbol{g}}_1^H \boldsymbol{R}_{YY}^{-d} \widetilde{\boldsymbol{g}}_1} \boldsymbol{R}_{YY}^{-d} \widetilde{\boldsymbol{g}}_1, \tag{A.6.1}$$

avec $\mathrm{MOE}(\hat{h}_1) = \frac{1}{\widetilde{\boldsymbol{g}}_1^H \boldsymbol{R}_{YY}^{-d} \widetilde{\boldsymbol{g}}_1}$, suivi par,

étape 2: *Méthode de Capon*

$$\max_{\hat{h}_1:\|\hat{h}_1\|=1} \mathrm{MOE}(\hat{\boldsymbol{h}}_1) \Rightarrow \min_{\hat{h}_1:\|\hat{h}_1\|=1} \hat{\boldsymbol{h}}_1^H \left(\boldsymbol{T}_1 \boldsymbol{R}_{YY}^{-d} \boldsymbol{T}_1^H \right) \hat{\boldsymbol{h}}_1, \tag{A.6.2}$$

d'où, $\hat{\boldsymbol{h}}_1 = V_{\min}(\boldsymbol{T}_1 \boldsymbol{R}_{YY}^{-d} \boldsymbol{T}_1^H)$, qui est l'estimation (à un facteur scalaire de phase près) du canal RIF de l'utilisateur désiré.

Ce récepteur peut aussi être formulé de la façon d'un formateur de voie généralisé pour annuler les lobes secondaires (GSC) comme décrit dans la section II.5.4. Une étude sur les conditions d'identifiabilité a aussi été faite dans le cadre de ce récepteur en fonction des longueurs des canaux. Il a été démontré qu'étant donné un certain nombre d'utilisateurs, il suffit de choisir une fenêtre de traitement, L, assez longue afin d'identifier la réponse impulsionnelle du canal et le récepteur aveugle.

A.7 Récepteurs semi-aveugles

Le récepteur EQMM–FZ aveugle proposé est un récepteur de mode paquets et se fonde sur une estimation de la matrice de covariance du signal reçu $\boldsymbol{R}_{YY}$, pour laquelle un grand nombre d'échantillons

du signal reçu est nécessaire. Pour améliorer la performance de ce récepteur on peut faire appel aux méthodes semi–aveugles qui utilisent la connaissance des séquences d'apprentissage en conjonction avec les statistiques d'ordre deux du signal. On a constaté dans le chapitre II, que l'estimation du vecteur de canal est suffisamment bonne pour un nombre faible d'échantillons du signal reçu. En conséquence, la séquence d'apprentissage peut être utilisée pour réestimer le filtre d'annulation d'interférences dans la branche inférieure du GSC II.1. En fait, c'est la présence du terme fort en énergie dans la branche supérieure à la sortie des corrélateurs pour l'utilisateur d'intérêt qui en quelque sorte perturbe l'estimation du terme contenant les interférences à partir de la sortie de $\boldsymbol{T}_2$. Cela entraîne une erreur d'estimation excessive qui est proportionnelle à l'erreur quadratique moyenne minimale (MMSE). Afin de diminuer l'erreur résiduelle, on propose d'enlever la contribution du signal utile pendant la période contenant les symboles d'apprentissage. Ainsi, on introduit la formulation moindres carrés pondérés donnant la fonction de coût suivante

$$\min_{\boldsymbol{Q}} \left\{ \frac{1}{\sigma_u^2} \sum_{n \in \Omega_u} \| \boldsymbol{Z}_n \|_2^2 + \frac{1}{\sigma_k^2} \sum_{n \in \Omega_k} \| \boldsymbol{Z}_n - \boldsymbol{T}_1^H \widehat{\boldsymbol{h}}_1 a_{1,n-d} \|_2^2 \right\}, \tag{A.7.1}$$

où, $a_{1,n-d}$ sont contraints de se trouver dans la séquence d'apprentissage. Les facteurs de pondération σ_u^2 et σ_k^2 peuvent être déterminés respectivement comme les moyennes d'ensemble de $\| \boldsymbol{Z}_n \|_2^2$ et $\| \boldsymbol{Z}_n - \boldsymbol{T}_1^H \widehat{\boldsymbol{h}}_1 a_{1,n-d} \|_2^2$ pour la partie aveugle et non aveugle du signal reçu.

L'algorithme est semi-aveugle pour l'estimation du filtre d'annulation d'interférence, mais reste aveugle pour l'estimation du canal. Une estimation récursive dans une mise-en-oeuvre itérative peut être envisagée pour le vecteur du canal. Les performances comparatives des versions aveugles et semi-aveugles du récepteur EQMM-FZ sont illustrées par la figure III.1.

A.7.1 Exploitation de la propriété d'alphabet fini

Une mise en oeuvre itérative de l'algorithme EQMM-FZ qui réutilise à chaque itération les symboles détectés pour réestimer le filtre d'annulation d'interférences $\boldsymbol{Q}$ peut aussi être envisagée. Dans cette configuration, on propose de prendre des décisions dures et de les retourner comme des symboles connus augmentant ainsi le nombre de symboles connus dans l'equation A.7.1. Si la longueur des séquences d'apprentissage est suffisamment élevée, on trouve des performances améliorées à chaque itération. Les performances de l'algorithme de décision dure sont aussi illustrées par la figure III.1. Dans cet exemple, on considère un facteur d'étalement de 16 et un paquet de 200 symboles transmis avec une séquence d'apprentissage de longueur 25.

A.8 Récepteur RAKE avec annulation des interférences

La branche supérieure du récepteur EQMM-FZ peut être le filtre adapté à la cascade de $\boldsymbol{T}_1$ et de $\boldsymbol{h}_1$ dans le cas où $\boldsymbol{h}_1$ est connu ou estimé *a priori*. Cela implique que la branche inférieure contient un filtre vectoriel d'annulation d'interférences au lieu d'une matrice comme cela était le cas pour le récepteur EQMM-FZ. La quantité à estimer devient ainsi un scalaire simplifiant l'estimation du filtre $\boldsymbol{W}$ (cf. figure III.2). Les mêmes considérations d'erreurs résiduelles de l'estimation indiquées dans le cas d'EQMM-FZ sont valables. La condition principale pour une bonne estimation du filtre $\boldsymbol{W}$ de l'annulation d'interférence est que la sortie du filtre adapté ne contienne aucune contribution du signal de l'utilisateur d'intérêt. Sinon, il y aura une tendance d'annulation du signal utile à la sortie du

filtre adapté. Contrairement à l'EQMM-FZ le ICRR correspond à l'annulation d'interférences après la combinaison cohérente du signal.

A.8.1 Algorithmes adaptatifs

La formulation GSC du critère EMS non-biaisé se prête bien aux applications adaptatives surtout dans le cas de canaux spéculaires (nombre de trajets limité). Dans ce cas, $\boldsymbol{T}_1$ défini par (II.5.27) contient un nombre faible de lignes non nulles soulignant le fait que l'énergie est captée par des corrélateurs dans ces directions. Le filtre d'annulation d'interférences $\boldsymbol{Q}$ peut ensuite être adapté par un algorithme de gradient comme LMS normalisé. Cette adaptation de $\boldsymbol{Q}$ est entièrement indépendante de l'estimation du canal qui peut aussi être adapté par un algorithme simple de poursuite des valeurs propres extrêmes. La convergence de ces algorithmes est garantie grâce aux fonctions de coût quadratique. Les figures III.4, III.5 et III.6 illustrent la convergence pour des valeurs différentes du pas de l'algorithme LMS normalisé. Il existe des possibilités d'adapter simultanément le délai des différents trajets. Une amélioration peut aussi être obtenue en utilisant les décisions à retour dans le mode doux ou dur.

A.9 La liaison descendante

Bien que les algorithmes complexes multi-utilisateurs aient été proposés pour la liaison ascendante dans les systèmes mobiles à accès multiples de troisième génération, la situation de la liaison descendante a toujours été considérée comme trop déficiente en terme d'information *a priori* et de puissance de traitement. Une raison supplémentaire étant l'inefficacité du récepteur RAKE pour combattre l'effet proche-loin (near-far) qui a été considéré plus important dans le cas de la liaison ascendante. Pourtant, la capacité nette des systèmes peut être augmentée si les deux liaisons sont capables de supporter les mêmes débits. Dans certaines applications comme la navigation sur l'internet, par exemple, la liaison descendante doit supporter les débits plus élevés que son homologue ascendante. Jusqu'à présent, la plupart des méthodes proposées pour l'augmentation de la capacité sur la liaison descendante sont fondées sur le traitement d'antenne à la station de base pour améliorer le mécanisme de transmission, pour ajouter en quelque sorte, la diversité au récepteur mobile. Ces techniques restent pourtant efficaces pour les canaux peu sélectifs en fréquence, ou la diversité des trajets multiples n'existe pratiquement pas.

Dans les situations d'un faible nombre d'utilisateurs, le récepteur RAKE peut marcher suffisamment bien, et tout traitement avancé reste inutile. Cela suggère un rapport de chargement d'approximativement 20% dans le cas de contrôle de puissance ou un rapport signal à interférence (RSI) d'environ 7dB. On peut constater qu'un système comme UMTS WCDMA peut héberger à peu près 50 utilisateurs pour un facteur d'étalement de 256. Un rapport de chargement plus élevé pourtant a un effet catastrophique sur la performance du récepteur RAKE. Cela résulte du traitement de l'IAM comme bruit décorrélé par ce récepteur.

Sur la liaison descendante, aux utilisateurs sont attribués des codes orthogonaux périodiques suivis par un brouilleur qui est unique pour une cellule ou un secteur de cellule. Une alternative au RAKE, dans le cas de codes périodiques est le récepteur linéaire décentralisé, traité dans le chapitre II. En termes de complexité d'information, ce récepteur se comporte comme le RAKE et la connaissance des paramètres des autres utilisateurs n'est pas nécessaire. Cependant, dans le cas des codes apériodiques, quand le brouilleur est activé, le traitement invariant dans le temps n'est plus possible à cause du

changement de canal total pour chaque symbole. Le brouilleur reste une partie intégrale du système pour les liaisons descendantes afin de distinguer entre les signaux issus de différentes cellules.

Dans le cadre de la liaison descendante pour une cellule isolée, le canal de propagation est un canal point-à-point entre la station de base et une station mobile. Pour identifier ce canal, un signal connu sous la forme d'un pilote est transmis en continuité dans la norme américaine IS-95. Ce pilote est généralement beaucoup plus puissant que les signaux utiles (environ 10 dB) et suffit pour estimer le canal de façon cohérente. Plusieurs travaux dirigés vers l'identification du canal en liaison descendante ont étés proposés dans [LZ97, MS98a, WLLZ98] mais ces méthodes fondées sur la moyenne statistique sur le brouilleur restent inéfficaces.

Nous proposons les récepteurs linéaires forçage à zéro (FZ) et maximisant le rapport signal à interférence plus bruit (RSIB) pour la liaison descendante d'un système ARMC. Le récepteur FZ égalise pour le canal une fois que ce dernier est estimé pour rendre les signaux de différents utilisateurs orthogonaux en supprimant l'effet de canal. Ensuite, un corrélateur pour l'utilisateur désiré suffit afin de supprimer l'IAM générée par les autres utilisateurs. Le récepteur maximisant le RSIB est un récepteur aveugle et évite le problème d'explosion du bruit du récepteur FZ. On considère que la station mobile reçoit le signal à travers plusieurs canaux de diversité venant de l'aspect multiples antennes ou suréchantillonnage.

A.9.1 Modèle de la liaison descendante

La figure A.5 décrit le modèle du canal sur la liaison descendante. Les K utilisateurs intra cellule

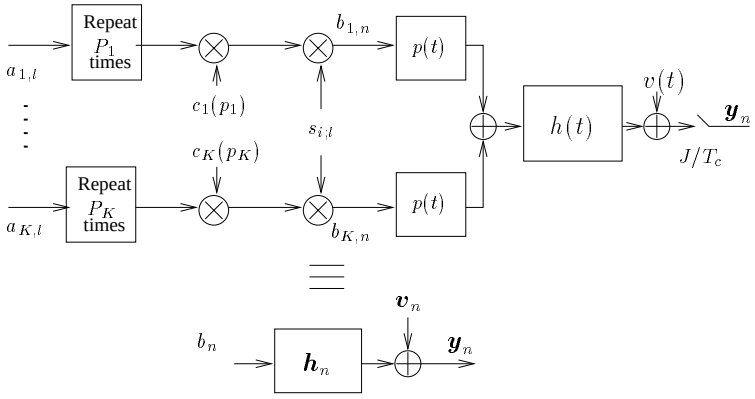

Figure A.5: Modèle du signal pour la liaison descendante.

transmettent des signaux modulés par une modulation linéaire sur un canal linéaire à trajets multiples avec du bruit additif gaussien. Le signal est reçu à travers M canaux multiples obtenus par suréchantillonnage du signal reçu plusieurs fois par chip ou à travers des antennes multiples. Le signal en bande de base équivalent peut être écrit comme

$$y_m(t) = \sum_{k=1}^{K} \sum_{n} b_{k,n} h_{km}(t - nT_c) + v_m(t). \tag{A.9.1}$$

$h_{km}(t)$ caractérise la réponse impulsionnelle du canal pour la m-ième antenne et le k-ième utilisateur et $\{v_m(t)\}$ est le bruit additif. Les $\boldsymbol{w}_k^l = [w_{k,P_k-1}^l, w_{k,P_k-2}^l, \ \ldots, \ w_{k,0}^l]^T$ sont les codes apériodiques

pour le symbole l du k-ième utilisateur. Les codes apériodiques sont formés par une séquence brouilleur $s_{i,l}$ qui multiplie les séquences périodiques $\boldsymbol{c}_k = [c_{k,P_k-1}, \ldots, c_{k,0}]$ de Walsh-Hadamard. On peut écrire les séquences chip correspondant au symbole $a_{k,l}$ comme

$$b_{k,n} = a_{k,l} w^l_{k,n \bmod P_k}. \tag{A.9.2}$$

Le facteur d'étalement peut être différent pour différents utilisateurs selon le débit de transmission exigé par les applications diverses dans les systèmes de troisième génération. Les séquences périodiques sont sélectionnées pour la cellule en question selon l'arbre indiqué dans la figure IV.2 et donc sont mutuellement orthogonales. La séquence de chips composite passe au travers d'un filtre de mise en forme et ensuite à travers le canal de propagation commun. Le signal reçu peut être écrit comme un signal vectoriel

$$\boldsymbol{y}_n = \sum_{k=1}^{K}\sum_{i=0}^{N-1} \boldsymbol{h}_i b_{k,n-i} + \boldsymbol{v}_n = \sum_{i=0}^{N-1} \boldsymbol{h}_i \left(\sum_{k=1}^{K} b_k\right)_{n-i} + \boldsymbol{v}_n = \boldsymbol{H}_N \boldsymbol{B}_n + \boldsymbol{v}_n, \tag{A.9.3}$$

où,

$$\boldsymbol{y}_n = \begin{bmatrix} y_{1,n} \\ \vdots \\ y_{M,n} \end{bmatrix}, \boldsymbol{h}_n = \begin{bmatrix} h_{1,n} \\ \vdots \\ h_{M,n} \end{bmatrix}, \boldsymbol{v}_n = \begin{bmatrix} v_{1,n} \\ \vdots \\ v_{M,n} \end{bmatrix},$$

$\boldsymbol{H}_N = [\boldsymbol{h}_0\ \boldsymbol{h}_1\ \ldots\ \boldsymbol{h}_{N-1}]$ est la matrice $M \times N$ du canal, qui inclut la contribution des filtres de transmission et de réception et $\boldsymbol{B}_n = \sum_{k=1}^{K} \boldsymbol{B}_{k,n}$, où $\boldsymbol{B}_{k,n} = [b_{k,n}\ \ldots\ b_{k,n-N+1}]^T$, est la séquence chips d'entrée au n-ième instant pour le k-ième utilisateur. On considère un bloc de $l_1P + l_2 + l_6$ vecteurs de données $\boldsymbol{y}_n$, que l'on note $\boldsymbol{Y}_n$

$$\boldsymbol{Y}_n = \mathcal{T}(\boldsymbol{h}) \widetilde{\boldsymbol{S}}_n \sum_{k=1}^{K} \widetilde{\boldsymbol{C}}_k \boldsymbol{A}_{k,n} + \boldsymbol{V}_n, \tag{A.9.4}$$

où,

$$\boldsymbol{Y}_n = \begin{bmatrix} \boldsymbol{y}_{n,l_6-1} \\ \vdots \\ \boldsymbol{y}_{n,0} \\ \boldsymbol{y}_{n-1,P-1} \\ \vdots \\ \boldsymbol{y}_{n-l_1,0} \\ \boldsymbol{y}_{n-l_1-1,P-1} \\ \vdots \\ \boldsymbol{y}_{n-l_1-1,P-l_2} \end{bmatrix}, \qquad \boldsymbol{h} = \left[\boldsymbol{h}^H_{N-1}, \cdots, \boldsymbol{h}^H_0\right]^H$$

$$\widetilde{\boldsymbol{C}}_k = \begin{bmatrix} \underline{\boldsymbol{c}}_k & \boldsymbol{0} & \cdots & & \boldsymbol{0} \\ \boldsymbol{0} & \boldsymbol{c}_k & \boldsymbol{0} & \cdots & \\ \vdots & & \ddots & & \vdots \\ & & & \boldsymbol{c}_k & \\ \boldsymbol{0} & \cdots & & & \overline{\boldsymbol{c}}_k \end{bmatrix}$$

$$\boldsymbol{c}_k = \begin{bmatrix} c_{k,P-1} \\ \vdots \\ c_{k,1} \\ c_{k,0} \end{bmatrix}, \overline{\boldsymbol{c}}_k = \begin{bmatrix} c_{k,P-1} \\ \vdots \\ c_{k,P-l_4} \end{bmatrix}, \underline{\boldsymbol{c}}_k = \begin{bmatrix} c_{k,l_6-1} \\ \vdots \\ c_{k,0} \end{bmatrix}.$$

$\mathcal{T}(\boldsymbol{h})$ est la matrice $M(L+P-1) \times \overline{N}$ bloc Toeplitz du canal remplie avec les coefficients de $\boldsymbol{h}$, et est, en général de rang plein. $\overline{N} = L + P + N - 2$ et la matrice de codes périodiques $\widetilde{\boldsymbol{C}}_k$ est de dimensions $(l_3P + l_4 + l_6) \times (l_3 + 2)$ tenant compte de la contribution de $l_3 + 2$ symboles dans le signal reçu $\boldsymbol{Y}_n$. $\underline{\boldsymbol{c}}_k$ et $\overline{\boldsymbol{c}}_k$ signifient la contribution partielle des symboles de bords du bloc de donées. $\boldsymbol{A}_{k,n} = [a_{k,n}, \ldots, a_{k,n-l_3-1}]^T$ est le vecteur de symboles, et $\widetilde{\boldsymbol{S}}_n$ signifie la matrice diagonale du brouilleur de dimension $L + P + N - 2 = l_3P + l_4 + l_6$ avec la diagonale donnée par

$$\left[s_{n,l_6-1}, \ldots, s_{n,0}, s_{n-1,P-1}, \cdots, s_{n-l_3,0}, s_{n-l_3-1,P-1}, \ldots, s_{n-l_3-1,P-l_4}\right].$$

Il est évident qu'on peut estimer la réponse du canal si les séquences de chips de tous les utilisateurs sont connues du récepteur comme décrit dans la section IV.3.

A.9.2 Récepteur à forçage à zéro (FZ)

Comme indiqué auparavant, dans le problème ARMC, il existe plusieurs sortes de récepteurs FZ. Comme le problème multi utilisateurs de la liaison descendante ressemble à un problème mono-utilisateur (mono-entrée / mono-sortie), on va considérer le forçage à zéro uniquement pour l'IES. Un récepteur $\mathbf{f}(z)$ est qualifié comme un récepteur de forçage à zéro pour le canal $\mathbf{h}(z)$ avec un délai d si $\mathbf{f}(z)\mathbf{h}(z) = z^{-d}$. La longueur minimale pour satisfaire les conditions de forçage à zero est indiquée par (IV.4.2). Il est utile de supprimer l'IAM et l'IES dans les systèmes AMRC, mais la structure particulière du problème de la liaison descendante nous permet de supprimer l'IAM par un simple corrélateur de séquence de l'utilisateur d'intérêt une fois le canal égalisé. Un des désavantages du récepteur à forçage à zéro est l'amplification du bruit dûe au fait que le rapport signal à bruit par chip reste relativement faible dans les systèmes avec un grand facteur d'étalement.

Les environnements multi–céllulaires peuvent également être traités si le nombre de canaux multiples (suréchantillonnage/antennes multiples) est suffisamment large. Le transfert de contrôle doux entre les stations de base[2] peut être géré de façon naturelle par la solution FZ en forçant à zéro l'IES de toutes les céllules en gardant une coefficient par station de base. Les canaux peuvent être estimés conjointement par le critère moindres carrés. Les dimensions de $\mathcal{T}(\boldsymbol{h})$ devront être de telle sorte que cette dernière reste rang plein. En général, dans le pire des cas, le nombre de cellules intervenant est de trois dans une géométrie hexagonale.

A.9.2.1 Interférences intercéllulaires

L'interférence intercéllulaire s'ajoute comme du bruit cyclostationnaire au taux chips. Cela est dû au fait que les brouilleurs mutuellement peu corrélés sont utilisés dans les différentes cellules. La matrice de covariance du bruit $\sigma_b^2 \sum_{u=2}^{U} \mathcal{T}(\boldsymbol{h}_u)\mathcal{T}^H(\boldsymbol{h}_u) \rightarrow \sigma_b^2 \boldsymbol{R}_{\boldsymbol{hh}}$ est une matrice Toeplitz bande avec une diagonale relativement forte. $\boldsymbol{R}_{\boldsymbol{hh}} \rightarrow \boldsymbol{I}$ comme la longueur du canal tend vers 1 (canal BBGC échantillonné au rythme chip). Si les interfereurs sont faibles, leur effet peut être ignoré grâce au terme faible des éléments hors diagonales de la matrice $\boldsymbol{R}_{\boldsymbol{hh}}$.

A.9.3 Récepteur maximisant le rapport signal à interférence plus bruit

Un récepteur quelconque $\boldsymbol{f}$ donne $\mathbf{f}(z)\mathbf{h}(z) = \sum_{i=0}^{L+N-2} \alpha_i z^{-i}$. On peut écrire ces équations dans le domaine temporel comme

$$\mathcal{T}(\boldsymbol{f})\mathcal{T}(\boldsymbol{h}) = \mathcal{T}(\underline{\boldsymbol{\alpha}}) = \mathcal{T}(\underline{\boldsymbol{\alpha}}_d) + \mathcal{T}(\overline{\underline{\boldsymbol{\alpha}}}_d), \tag{A.9.5}$$

où, $\mathcal{T}(\boldsymbol{f})$ is a $P \times M(L+P-1)$ est la matrice bloc Toeplitz remplie avec des coefficients de l'égaliseur. $\mathcal{T}(\underline{\boldsymbol{\alpha}})$ définit la matrice Toeplitz avec la première ligne $[\underline{\boldsymbol{\alpha}} \;\; \mathbf{0}_{P-1}]$; ce qui est vrai aussi pour $\mathcal{T}(\underline{\boldsymbol{\alpha}}_d)$ et $\mathcal{T}(\overline{\underline{\boldsymbol{\alpha}}}_d)$, où,

$$\begin{aligned} \underline{\boldsymbol{\alpha}} &= [\alpha_0 \; \alpha_1 \; \ldots \; \alpha_{L+N-2}], \;\; \underline{\boldsymbol{\alpha}}_d = [0 \ldots 0 \; \alpha_d \; 0 \ldots 0] \\ \overline{\underline{\boldsymbol{\alpha}}}_d &= [\alpha_0 \; \ldots \; \alpha_{d-1} \; 0 \; \alpha_{d+1} \; \ldots \; \alpha_{L+N-2}]. \end{aligned} \tag{A.9.6}$$

Le vecteur $P \times 1$ des sorties successives de l'égaliseur peut être écrit comme

$$\boldsymbol{Z}_n = \mathcal{T}(\boldsymbol{f})\boldsymbol{Y}_n = \mathcal{Y}_n \boldsymbol{f}^T, \tag{A.9.7}$$

[2] soft handoff

Le signal égalisé, $\boldsymbol{Z}_n$ doit maintenant être débrouillé comme $\boldsymbol{X}_n = \boldsymbol{S}_{n-l_5-1}^H \boldsymbol{Z}_n$, où

$$\boldsymbol{S}_n = \mathrm{diag}\left\{s_{n,P-1}, \ldots, s_{n,1}, s_{n,0}\right\}.$$

On remarque que si ce égaliseur est un FZ ($\underline{\boldsymbol{\alpha}}_d = \mathbf{0}$), dans le cas sans bruit ($v(t) \equiv 0$), le corrélateur lui-même suffit pour annuler l'interférence en $\boldsymbol{X}_n$ apportée par les autres utilisateurs grâce a l'orthogonalité des codes [GS98b]. On définit par

$$\underline{\underline{C}} = [\boldsymbol{c}_1 \ \ldots \boldsymbol{c}_K], \text{ and } \underline{\underline{C}}^{\perp} = [\boldsymbol{c}_{K+1} \ \ldots \boldsymbol{c}_P],$$

les matrices dont les colonnes constituent les codes de Walsh-Hadamard utlisés et non-utilisés pour le système en question ($\underline{\underline{C}}^{\perp H}\underline{\underline{C}} = \mathbf{0}$). Un égaliseur $\boldsymbol{f}$ peut être obtenu en imposant que la sortie débrouillé de l'égaliseur soit orthogonal aux codes contenus dans $\underline{\underline{C}}^{\perp}$ dans le cas sans bruit [LL99]. En outre, l'égaliseur peut être obtenu comme argument de la fonction de coût suivante:

$$\arg \min_{\boldsymbol{f}} \ E\|\underline{\underline{C}}^{\perp H}\boldsymbol{X}_n\|^2. \tag{A.9.8}$$

Une réponse fixe doit être imposée à la sortie nettoyée de brouilleur de l'égaliseur afin d'éviter l'annulation du signal de l'utilisateur d'intérêt, c.-à-d.,

$$E|\boldsymbol{c}_1^H \boldsymbol{X}_n|^2 = \mathrm{cnst}.. \tag{A.9.9}$$

La solution à ce problème d'optimisation quadratique sous contrainte également quadratique est donné par le vecteur propre généralisé minimal

$$\boldsymbol{f}^T = \arg \min_{\boldsymbol{f}} \ \frac{\boldsymbol{f}^* \widehat{\boldsymbol{R}}_0 \boldsymbol{f}^T}{\boldsymbol{f}^* \widehat{\boldsymbol{R}}_1 \boldsymbol{f}^T}, \tag{A.9.10}$$

où, $\widehat{\boldsymbol{R}}_0 = \mathrm{avg}\{\mathcal{Y}_n \boldsymbol{S}_n \underline{\underline{C}}^{\perp}\underline{\underline{C}}^{\perp H}\boldsymbol{S}_n^H \mathcal{Y}_n^H\}$, et $\widehat{\boldsymbol{R}}_1 = \mathrm{avg}\{\mathcal{Y}_n \boldsymbol{S}_n \boldsymbol{c}_1 \boldsymbol{c}_1^H \boldsymbol{S}_n^H \mathcal{Y}_n^H\}$, et avg signifie la moyenne temporelle et peut être remplacé par un opérateur d'espérance si le brouilleur est inactif, i.e., $\boldsymbol{S}_n \equiv \boldsymbol{I}_P$ et $\widetilde{\boldsymbol{S}}_n \equiv \boldsymbol{I}$.

A première vue, il est difficile de dire de quel problème d'optimisation $\boldsymbol{f}$ est une solution. Il a été démontré dans la section IV.5.1 que le récepteur donné par le critère (A.9.10) aboutit à un récepteur qui maximise le RSIB à sa sortie. Le RSIB à la sortie du récepteur peut être écrit comme

$$\Gamma_r = \frac{\sigma_1^2 |\alpha_d|^2}{\boldsymbol{f}\boldsymbol{R}_{VV}\boldsymbol{f}^H + \frac{1}{P}\left(\sum_{k=1}^K \sigma_k^2\right)\|\underline{\boldsymbol{\alpha}}_d\|^2 + \sum_{k=1}^K \sigma_k^2 \,\mathrm{tr}\left\{\boldsymbol{B}\boldsymbol{D}_k\boldsymbol{D}_1\boldsymbol{B}^*\boldsymbol{D}_k\boldsymbol{D}_1\right\}} \tag{A.9.11}$$

dans le cas de brouilleur réel et réduit à

$$\Gamma_c = \frac{\sigma_1^2 |\alpha_d|^2}{\boldsymbol{f}\boldsymbol{R}_{VV}\boldsymbol{f}^H + \frac{1}{P}\left(\sum_{k=1}^K \sigma_k^2\right)\|\underline{\boldsymbol{\alpha}}_d\|^2}, \tag{A.9.12}$$

dans le cas complexe. Il a été démontré dans la section IV.5.1, que si le brouilleur est inactif, plusieurs symboles contribuent à la sortie du récepteur. En conséquence, un égaliseur entrée simple / sortie simple (SISO) au rythme symbole est inévitable à la sortie de ce récepteur.

A.9.4 Récepteur RAKE

Le récepteur RAKE est convenablement inclus dans la dérivation du chapitre IV. Le RSIB à la sortie du RAKE pour le cas du brouilleur réel et complexe est respectivement donné par

$$\Gamma_{\mathrm{RAKE},r} = \frac{\sigma_1^2 \|\boldsymbol{h}\|^4}{\boldsymbol{h}^H \boldsymbol{R}_{VV} \boldsymbol{h} + \frac{1}{P}\left(\sum_{k=1}^{K} \sigma_k^2\right) \|\underline{\boldsymbol{\alpha}}_d^h\|^2 + \sum_{k=1}^{K} \sigma_k^2 \,\mathrm{tr}\left\{\boldsymbol{B}_h \boldsymbol{D}_k \boldsymbol{D}_1 \boldsymbol{B}_h^* \boldsymbol{D}_k \boldsymbol{D}_1\right\}}, \quad \text{(A.9.13)}$$

et

$$\Gamma_{\mathrm{RAKE},c} = \frac{\sigma_1^2 \|\boldsymbol{h}\|^4}{\boldsymbol{h}^H \boldsymbol{R}_{VV} \boldsymbol{h} + \frac{1}{P}\left(\sum_{k=1}^{K} \sigma_k^2\right) \|\underline{\boldsymbol{\alpha}}_d^h\|^2} \quad \text{(A.9.14)}$$

A.9.5 Comparaisons des différents récepteurs

Le traitement précédent est extrêmement utile pour la comparaison des différentes techniques de réception pour la liaison descendante dans les systèmes AMRC tel que le UMTS WCDMA. Pour débuter, on constate que le brouilleur complexe donne le récepteur maximisant le RSIB. Il y a un terme perturbateur qui reste en dénominateur pour le brouilleur réel. Une autre observation est que l'allocation de codes orthogonaux est la meilleure stratégie pour la liaison descendante. Si les codes aléatoirement choisis sont attribués, le RSIB diminue, car un terme correspondant à l'intercorrélation de codes est ajouté au dénominateur.

Le facteur d'étalement P, en relation avec la longeur du canal N, et le nombre d'utilisateurs actifs K, est décisif pour le choix du récepteur à employer. Si le rapport N/P et K sont petits, un RAKE suffit comme technique de réception. Sinon, il faut impliquer les récepteurs plus avancés pour obtenir une performance acceptable. Plusieurs exemples numériques sont montrés sur les figures IV.6 á IV.10 pour illustrer cet argument.

A.10 Traitement d'antenne pour la transmission liaison descendante

Le traitement d'antenne à la réception est connu pour améliorer la performance des systèmes grâce à la diversité de réception. La possibilité d'employer les antennes multiples sur la liaison descendante reste pourtant difficile à cause des contraintes d'espace et de la puissance de traitement. Il est aussi connu que la pluralité des antennes à la transmission n'ajoute pas les mêmes gains que celle à la réception. Cela semble intuitivement évident car les antennes tentent de distribuer l'énergie dans l'espace sans tenir compte de la façon dont sont couplés les canaux des différents utilisateurs mobiles. Un des problèmes traité dans cette thèse consiste en l'utilisation de la connaissance totale ou partielle des canaux de la liaison descendante pour la conception des filtres de transmission afin de les découpler. Naturellement, la performance de la liaison descendante peut être nettement améliorée en utilisant la technique de la transmission par des antennes multiples.

A.10.1 Transmission en mode DDT et DDF

Plusieurs systèmes cellulaires de troisième génération envisagent aussi d'utiliser les techniques de diversité de transmission pour augmenter la capacité des systèmes. Le mode duplex de division en

temps (DDT) semble plus adapté pour ces techniques de transmission car le canal peut être considéré invariant dans le temps si la vitesse du mobile est faible et si le transmetteur et le récepteur sont calibrés de manière appropriée. L'estimation du canal à la liaison ascendante pour tous les utilisateurs peut être considéré valable pour la liaison descendante. Nous proposons de restaurer l'orthogonalité des séquences par le traitement approprié à la station de base. Cela correspond au forçage à zéro de l'interférence inter-utilisateurs (IIU). Le modèle du canal et le schéma du système sont illustrés sur la figure V.1. Chacun des utilisateurs mobiles est considéré muni d'une seule antenne et est supposé avoir un récepteur corrélateur. Le signal discret reçu par l'i-ème utilisateur peut être écrit comme

$$y_i(n) = \mathbf{c}_i^H(q)\mathbf{H}_i^T(q)\sum_{j=1}^{K}\mathbf{F}_j(q)a_j(n) + v_i(n) \tag{A.10.1}$$

où, $a_j(n)$ sont les symboles destinés au i-ème mobile, $\mathbf{H}_i^T(z)$ est le canal de la liaison descendante, et $\mathbf{F}_j(z) = \mathbf{F}'_j(z)\mathbf{c}_j$ sont les filtres spatio-temporels incluant les codes d'étalements supposés périodiques pour le signal du i-ème utilisateur. L'optimisation se fait donc en deux étapes: on conçoit d'abord les filtres de transmission $\boldsymbol{F}_j^{'}, \forall j = 1 \ldots K$ pour découpler les canaux des différents utilisateurs, et puis on alloue les puissance pour assurer un RSIB minimal pour tous.

Cependant, pour le mode duplex de division en fréquence (DDF), les canaux ne peuvent pas être traités de la même manière pour les deux liaisons. Certains paramètres comme les angles d'arrivée et de départ, les délais d'arrivée des différents trajets peuvent cependant être les même si l'écart des fréquences porteuses pour les deux liaisons est faible (généralement le cas). Autres paramètres, par exemple les amplitudes et les phases des trajets sont dépendantes des fréquences porteuses. On peut néanmoins supposer que la matrice de covariance du canal moyenne sur les phases et les amplitudes des trajets est connu. On peut aussi supposer que les différents trajets sont séparables spatio- temporellement. Ainsi chaque trajet venant du signal d'un mobile se comporte comme un utilisateur corrélé. Contrairement au cas DDT, le nombre d'utilisateurs virtuels devient égal au nombre total de trajets. Les délais pour les trajets qui ne sont que séparables en espace peuvent être ajustés a la transmission pour être distincts en temps. On suppose que le canal du i-ème utilisateur possède Q_i trajets spéculaires. La q-ième composant du i-ème utilisateur vu à la station de base peut être modélisé en temps continu comme

$$\boldsymbol{h}_{iq}^T(\tau,\, t) = \alpha_{iq}(t)\mathbf{a}^T(\theta_{iq})\delta(\tau - \tau_{iq}) \tag{A.10.2}$$

où τ_{iq}, θ_{iq}, et α_{iq} correspondent aux délais, à l'angle d'arrivée et au coefficient d'évanouissement respectivement pour le q-ième trajet du i-ème utilisateur. $\boldsymbol{a}(\theta)$ est la réponse du réseau d'antenne.

A.10.2 DDT: critères d'optimisation

La borne du filtre adapté (BFA) est une bonne mesure pour la performance. Pour le i-ème utilisateur cela peut être écrit comme

$$\mathrm{MFB}_i = \frac{1}{2\pi \mathrm{j}}\oint \frac{\sigma_a^2\mathbf{T}_{ii}^{\dagger}(z)\mathbf{T}_{ii}(z)}{\sigma_a^2\sum_{j\neq i}\mathbf{T}_{ji}(z)\mathbf{T}_{ji}^{\dagger}(z) + \sigma_{v_i}^2}\frac{\mathrm{d}z}{z} \tag{A.10.3}$$

où $\mathbf{T}_{ji}(z) = \mathbf{G}_i^T(z)\mathbf{F}_j(z)$, $\sigma_a^2 = \mathrm{E}\{|a_i(n)|^2\}$, et $\sigma_{v_i}^2$ est la variance du bruit $v_i(n)$, considéré spatialement et temporellement blanc par la suite. La fonction de coût peut alors être écrite comme

$$\max_{\{\mathbf{F}_j(z)\}}\min_i\{\mathrm{MFB}_i\} \tag{A.10.4}$$

ce qui signifie la maximisation du minimum de BFA entre les utilisateurs. On peut écrire le problème dans le domaine temporel par les équations (V.2.4). La BFA pour le mode paquet peut ainsi être écrite comme

$$\mathrm{MFB}_i^{(M)} = \frac{1}{M}\,\mathrm{tr}\{\boldsymbol{R}_{ii}^{(M)}[\sum_{j\neq i}\boldsymbol{R}_{ji}^{(M)} + \sigma_{v_i}^2\mathbf{I}_M]^{-1}\} \tag{A.10.5}$$

où $\sum_{j\neq i}\boldsymbol{R}_{ji}^{(M)}$ represente la matrice de covariance en mode paquet de l'IIU au i-ème récepteur. Remarquons que si M tend vers l'infini, $\mathrm{MFB}_i^{(M)} \to \mathrm{MFB}_i$. On peut donc réécrire la BFA comme

$$\max_{\{F_j\}} \min_i \{\mathrm{MFB}_i^{(M)}\}. \tag{A.10.6}$$

Les problèmes (A.10.4) et (A.10.6) sont tous deux trop complexes pour trouver une solution analytique. Cependant, on peut trouver les solutions analytiques en supposant que la solution optimale correspond au rapport interférence à bruit (RIB) faible pour tous les utilisateurs,

$$\mathrm{RIB}_i = \frac{\sigma_a^2}{2\pi\mathrm{j}\sigma_{v_i}^2}\sum_{j\neq i}\oint \mathbf{T}_{ji}^{\dagger}(z)\mathbf{T}_{ji}(z)\frac{\mathrm{d}z}{z} \ll 1, \qquad \forall i. \tag{A.10.7}$$

On peut ainsi considérer que la maximisation de la BFA est équivalente à celle de RSIB. Dans le mode paquet, le RSIB peut être écrit comme

$$\mathrm{RSIB}_i = \frac{\mathrm{tr}\{\boldsymbol{R}_{ii}^{(M)}\}}{\mathrm{tr}\{\sum_{j\neq i}\boldsymbol{R}_{ji}^{(M)} + \sigma_{v_i}^2\mathbf{I}_M\}} \tag{A.10.8}$$

En substituant $\boldsymbol{F}_i^t = [\boldsymbol{f}_i^T(L-1)\ \ldots\ \boldsymbol{f}_i^T(0)]$, cela s'écrit comme

$$\mathrm{RSIB}_i = \frac{\sigma_a^2\boldsymbol{F}_i^t\boldsymbol{R}_i\boldsymbol{F}_i^{tH}}{\sigma_a^2\sum_{j\neq i}\boldsymbol{F}_j^t\boldsymbol{R}_i\boldsymbol{F}_j^{tH} + \sigma_{v_i}^2} \tag{A.10.9}$$

où $\boldsymbol{R}_i$ est une matrice de covariance structurée de manière appropriée et liée au canal $\boldsymbol{G}_i^t$. On définit $\mathrm{RSIB}_i = \gamma_i$, et $\boldsymbol{F}_i^t = \sqrt{p_i}\boldsymbol{U}_i^t$, où $\boldsymbol{U}_i^t$ est un vecteur à norme unité (e.g., $\|\boldsymbol{U}_i^t\|_2 = 1$ ou $\boldsymbol{U}_i^t\boldsymbol{R}_i\boldsymbol{U}_i^{tH} = 1$). Le vecteur des RSIB inverse est $\boldsymbol{\gamma}^{-1} = [\gamma_1^{-1}\ \ldots\ \gamma_K^{-1}]^T$, et $\boldsymbol{p} = [p_1, \ldots, p_K]^T$ est le vecteur des puissances allouées. La puissance totale est donnée par $p_{\max}$ à la station de base. Le critère peut être écrit comme

$$\min_{\boldsymbol{p},\{\boldsymbol{U}_i\}} \|\boldsymbol{\gamma}^{-1}\|_\infty \quad \text{s.t.} \quad \boldsymbol{\zeta}^T\boldsymbol{p} \leq p_{\max} \tag{A.10.10}$$

où $\boldsymbol{\zeta} = [\|\boldsymbol{U}_1^t\|_2^2\ \ldots\ \|\boldsymbol{U}_K^t\|_2^2]^T$. Dans la suite, on considère le problème d'optimisation de RSIB (A.10.10), sans considération de sa relation avec le BFA (A.10.4). Dans ce cas $\sigma_{v_i}^2$ peut également tenir compte de la variance de l'interférence inter-cellulaire. On définit alors la puissance normalisée issue du j-ème filtre de transmission $\boldsymbol{F}_j$ et reçue par le i-ème utilisateur comme $c_{ji} = \boldsymbol{U}_j^t\boldsymbol{R}_i\boldsymbol{U}_j^{tH}$. Pour un i quelconque, on a

$$\gamma_i^{-1}p_ic_{ii} = \sum_{j\neq i}p_jc_{ji} + \nu_i \tag{A.10.11}$$

où on a intoduit $\nu_i = \sigma_{v_i}^2/\sigma_a^2$ pour tous les i. Afin de tenir compte de tous les utlisateurs, on introduit la matrice $\boldsymbol{C}^T$ définie comme

$$\left[\boldsymbol{C}^T\right]_{ij} = \begin{cases} c_{ji} & \text{for} j \neq i \\ 0 & \text{for} j = i \end{cases} \tag{A.10.12}$$

la matrice $\boldsymbol{D}_c = \mathrm{diag}\{[c_{11} \ \ldots \ c_{KK}]\}$, le vecteur $\boldsymbol{\nu} = [\nu_1 \ \ldots \ \nu_K]^T$ et la matrice $\boldsymbol{P} = \mathrm{diag}(\boldsymbol{p})$. On a donc la rélation suivante pour le RSIB inverse

$$\boldsymbol{\gamma}^{-1} = \boldsymbol{D}_c^{-1}\boldsymbol{P}^{-1}(\boldsymbol{C}^T\boldsymbol{p} + \boldsymbol{\nu}) \quad . \tag{A.10.13}$$

En conclusion, le critère ((A.10.10) donne un ensemble de problèmes couplés et la solution analytique n'est pas possible. On suppose cependant que le critère donne le même RSIB pour tous les utilisateurs. Si γ_i ne sont pas les mêmes, on peut toujours ajuster $\{p_i\}$ pour ameliorer $\gamma_{\min}$.

A.10.3 La solution forçage à zéro

Dans le cas sans bruit, une solution au problème d'optimisation de la BFA devient

$$\max_{\|\boldsymbol{U}_i^t\|_2=1} \{\boldsymbol{U}_i^t \boldsymbol{R}_i \boldsymbol{U}_i^{tH}\} \qquad \text{s.t.} \qquad \sum_{j\neq i} p_j \boldsymbol{U}_j^t \boldsymbol{R}_i \boldsymbol{U}_j^{tH} = 0 \tag{A.10.14}$$

Remarquons que la condition $\sum_{j\neq i} p_j \boldsymbol{U}_j^{tH} \boldsymbol{R}_i \boldsymbol{U}_j^t = 0$ est équivalente à l'ensemble des conditions FZ dans la forme $\boldsymbol{U}_i^t \boldsymbol{R}_j \boldsymbol{U}_i^{tH} = 0$, pour $j \neq i$. Cela réduit le problème d'optimisation à

$$\max_{\|\boldsymbol{U}_i^t\|_2=1} \|\boldsymbol{U}_i^t \mathcal{T}_L(\boldsymbol{G}_i)\|_2^2 \quad \text{s.t. } \boldsymbol{U}_i^t \mathcal{T}_L(\boldsymbol{G}_j) = \boldsymbol{0} \text{ for } j \neq i. \tag{A.10.15}$$

Définissons par $\boldsymbol{B}_i = [\mathcal{T}_L(\boldsymbol{G}_j)]_{j\neq i}$ la matrice bloc Toeplitz tenant compte de tous les canaux sauf $\boldsymbol{G}_i$. La solution à (A.10.15) est donnée par $\boldsymbol{U}_i^{tH} = V_{\max}(\mathbf{P}_{\mathbf{B}_i}^{\perp} \boldsymbol{R}_i \mathbf{P}_{\mathbf{B}_i}^{\perp})$. Pour une solution non triviale, on exige $m > K-1$, qui est valable quand on utilise les antennes multiples où le suréchantillonnage et les contraintes ne doivent pas fixer tous les degrés de liberté disponibles qui donnent comme longeur de filtres de transmission

$$L > \frac{\sum_{j\neq i} N_j - (K-1)}{m_{\text{eff}} - (K-1)}. \tag{A.10.16}$$

où $m_{\text{eff}} = \mathrm{rank}\{\boldsymbol{G}_N\}$ est le nombre effectif des sous-canaux. Les contraintes données par (A.10.15) mènent à l'annulation parfaite de l'IIU. Cela est pourtant obtenu au prix de l'IES surajouté au récepteur. Pour annuler l'IES, il faudrait des contraintes supplémentaires qu'on appelle les contraintes de pré-égalisation.

Le but de cette optimisation est de maximiser la BFA qui correspond, en absence de l'IIU à l'énergie dans la cascade du pré-filtre et le canal. Alors, la BFA est minimisée si l'énergie est concentrée en un seul coefficient. Un équilibre entre la performance et la complexité détermine le choix de la longueur L du filtre. Dans le cas ou les contraintes annulent seulement l'IIU, le récepteur mobile devra égaliser pour l'IES résiduelle. Finalement, on peut remarquer que les filtres FZ correspondent à la conception d'un transmultiplexeur bi-orthogonal ayant la propriété de construction parfaite où les $\boldsymbol{F}_i$ and $\boldsymbol{G}_i$ sont respectivement les bancs de filtres de synthèse et d'analyse.

La transmission sur la liaison descendante peut être organisée de façon synchrone ou asynchrone. En tout cas, comme les canaux des utilisateurs sont connus à la station de base, on peut compenser les délais asynchrones en fabriquant la matrice de covariance des canaux descendants manuellement.

Autres solutions, EQMM et EMS par exemple, sont également proposées pour ce problème et correspondent à la solution FZ. Une solution ad hoc connue sous le nom de pré-RAKE, consiste en une pré-distorsion du signal transmis sur la liaison descendante pour chaque utilisateur en sélectionnant $\boldsymbol{U}_i^{tH} = \boldsymbol{G}_i^t / \|\boldsymbol{G}_i^t\|_2^2$ comme le filtre normalisé de transmission. Le récepteur mobile n'a qu'à s'adapter au trajet significatif du signal pré-distordu. Bien que ce soit une solution a complexité réduite, le pré-RAKE reste une solution sous optimale du problème de la liaison descendante.

A.10.3.1 Optimisation de la puissance allouée

Etant donné un ensemble $\{\boldsymbol{U}_i\}$, la solution optimale signifie les mêmes valeurs de RSIB γ_i pour tous les utilisateurs. La solution optimale pour le vecteur des puissances donné dans l'équation (A.10.13) est le vecteur propre correspondant à la valeur propre maximale de la matrice $\boldsymbol{E}$ donnée par

$$\boldsymbol{E}\tilde{\boldsymbol{p}} = \gamma^{-1}\tilde{\boldsymbol{p}}, \qquad \boldsymbol{E} = \begin{bmatrix} \boldsymbol{A}^T & \boldsymbol{\mu} \\ \frac{\boldsymbol{\zeta}^T \boldsymbol{A}^T}{p_{\max}} & \frac{\boldsymbol{\zeta}^T \boldsymbol{\mu}}{p_{\max}} \end{bmatrix}, \tag{A.10.17}$$

où $\tilde{\boldsymbol{p}} = [\boldsymbol{p}^T \; 1]^T$, $\boldsymbol{\mu} = \boldsymbol{D}_c^{-1}\boldsymbol{\nu}$, $\boldsymbol{A}^T = \boldsymbol{D}_c^{-1}\boldsymbol{C}^T$, et $\boldsymbol{\zeta}^T\boldsymbol{p} = p_{\max}$. Cette solution est unique pour un $\boldsymbol{E}$ donné sous la contrainte de la puissance maximale à la station de base. La performance de la solution FZ et le pré-RAKE sont comparés sur les figures V.2 à V.4 pour différentes valeurs de L.

A.10.4 DDF : Les critères d'optimisation

Comme indiqué auparavant, les Q_i trajets correspondants à un utilisateur i peuvent être considérés comme Q_i utilisateurs virtuels pour le problème DDF. Les critères d'optimisation correspondent à l'annulation de l'interférence entre utilisateurs, à l'annulation de l'interférence entre symboles et à la pré-décorrélation sont données par les équations (VI.4.1) (VI.4.2) (VI.4.3) et (VI.4.4). Naturellement, le problème de FZ exige des longueurs de filtre L plus importantes que dans le cas de DDT. On suppose que les délais τ_{iq}, $\forall i = \{1, \ldots, K\}$, $q = \{1, \ldots, Q_i\}$, pour tous les utilisateurs sont connus des transmetteurs. Cela signifie que la position du corrélateur à la réception est aussi supposée fixe et connue dans le temps. On considère *a priori* que les délais fixés d'avance vont maximiser le rapport signal-à-bruit (RSB) à la sortie. Cette supposition a comme conséquence que les délais des corrélateurs fixés d'avance ne soient pas les optimaux globals. Cela rend le problème d'optimisation couplé et l'algorithme devra chercher la solution optimale sur tous les délais de tous les utilisateurs testés un par un; ce qui complique énormément la tâche. Une alternative découplée et de complexité réduite consiste en sélectionnant le trajet dominant avant la conception des filtres $\boldsymbol{U}_{iq}$ et en supposant que les positions du corrélateur sont alignées à ce même trajet.

A.10.4.1 Diversité de transmission et allocation de puissance en DDF

On a supposé que chaque récepteur est un corrélateur par composante multi- trajet. On suppose aussi que les sorties des corrélateur seront combinées en rapport maximal (MRC). Les trajets multiples sont

supposés tels que les sorties du corrélateur sont décorrélées. Le RSB à la sortie du i-ème utilisateur est donné par

$$\mathrm{SNR}_i = \frac{\mathrm{E}[|\sum_{q=1}^{Q_i} |\alpha_{iq}|^2 p_{iq} a_i(n)|^2]}{\sigma_{v_i}^2 \sum_{q=1}^{Q_i} \mathrm{E}|\alpha_{iq}|^2 p_{iq}} = \frac{\sigma_a^2}{\sigma_{v_i}^2} \sum_{q=1}^{Q_i} \mathrm{E}[|\alpha_{iq}|^2] p_{iq} \tag{A.10.18}$$

où $\sigma_a^2 = \mathrm{E}[|a_i(n)|^2]$ pour tout i et $\sigma_{v_i}^2$ est la variance de bruit à la sortie de chaque corrélateur. L'allocation de puissance parmi les différents trajets qui maximisent le RSB est déterminée comme solution du problème

$$\max_{p_{iq}} \{\sum_{q=1}^{Q_i} (\mathrm{E}|\alpha_{iq}|^2) p_{iq}\} \qquad \text{s.t. } \sum_{q=1}^{Q_i} p_{iq} = p_i. \tag{A.10.19}$$

La solution de ce critère correspond à la diversité de sélection et suggère l'excitation d'un seul trajet portant la plus grande puissance moyenne. Le récepteur optimal est donc un filtre adapté au filtre de mis-en-forme suivi par un simple corrélateur de séquence d'étalement de l'utilisateur en question. On remarque que le trajet le plus puissant est celui portant l'énergie maximale dans la cascade du canal et du pré-filtre. Donc, dans le sens strict ce trajet doit être sélectionné après les conceptions du filtre de transmission.

En général, le phénomène d'explosion du bruit va influencer la performance de cette stratégie dont l'effet sera minimal si un grand nombre de degrés de liberté sont ajoutés en utilisant un nombre conséquent d'antennes. Plusieurs exemples de cette manipulation dans le cas DDF sont illustrés dans les figures VI.3 et VI.4.

A.10.5 Traitement d'antenne pour les systèmes à séquence apériodique

Si les séquences d'étalement sont apériodiques, la conception des filtres invariants dans le temps n'est plus possible. Le traitement spatio-temporel dégénère alors en un traitement purement spatial. Le canal spéculaire à trajets multiples peut être écrit en temps continu comme indiqué par VII.2.1. Les trajets peuvent être collectionnés dans les paquets comme montré dans VII.2.2. Le canal total peut être modélisé comme la superposition de ces paquets comme montré dans l'équation VII.2.3. On va supposer que la transmission sur la liaison descendante se fait par les mêmes faisceaux que son homologue ascendant. Le problème devient alors celui de la maximisation du minimum de RSIB parmi K utilisateurs. Le RSIB pour le i-ème utilisateur est donne par VII.5.1. Cela est encore un problème découplé et suggère comme auparavant de concevoir les formateurs de voies et ensuite d'optimiser pour les puissances allouées. On démontre qu'une fois les formateurs de voies conçus, il existe une solution unique pour le vecteur d'allocation de puissance. Cette allocation est étroitement liée aux mesures de congestion dans les systèmes AMRC qui constituent une direction active de recherche dirigée vers le rapprochement des opérations de la couche physique et celui de contrôle dans ces systèmes. Les performances des méthodes de formation de voie sont illustré dans les figures VII.2 à VII.4. Les cas de séquences d'étalement réelles et complexes sont aussi traités dans le cours de ce développement.

En conclusion, le traitement purement spatial reste moins performant par rapport au traitement spatio-temporel où l'on arrive a annuler l'interférence avant la transmission. Pourtant, des gains relativement importants sont obtenus par rapport au cas ordinaire (antenne unique). De plus, le traitement invariant dans le temps n'est en tout cas pas approprié quand des codes apériodiques sont employés.

Bibliography

[AFFM98] T. Asté, P. Forster, L. Féty, and S. Mayrargue. Downlink beamforming avoiding DOA estimation for cellular mobile communications. In *Proc. ICASSP'98*, Seattle, WA, May 1998.

[AS97] Jaouhar Ayadi and Dirk T. M. Slock. Crámer-Rao bounds for knowledge based estimation of multiple FIR channels. In *Proc. 1st IEEE Conf. on Signal Processing Advances in Wireless Communications*, pages 353–356, Paris, France, April 1997.

[Bap96] J. L. Bapat. *Partially Blind Identification of FIR Channels for QAM Signals*. PhD thesis, Pennsylvania State University, Aug. 1996.

[Bel99] Jean-Claude Belfiore. Space-Time Diversity, June 1999. Presentation at GdR meeting, ENST, Paris.

[BJU+99] C. Brunner, M. Joham, W. Utschick, M. Haardt, and J. A. Nossek. Downlink beamforming for WCDMA based on uplink channel parameters. In *Proc. 3rd. Euro. Pers. & Mob. Comm. Conf*, pages 375–380, Paris, France, March 1999.

[Cai99] Giuseppe Caire. Adaptive linear receivers for DS/CDMA - part II: Improved non-data aided schemes. Submitted to IEEE Trans. Commun., Feb. 1999.

[Car75] A. B. Carleial. A case where interference does not reduce capacity. *IEEE Trans. Info. Theory*, IT-21:569–70, Sept. 1975.

[CDEF95] J. M. Cioffi, G. P. Dudevoir, M. V. Eyuboglu, and G. D. Forney. MMSE Decision-Feedback Equalizers and Coding. Part 1: Equalization Results. *IEEE Trans. Communications*, 43(10), Oct. 1995.

[CGKS92] M. V. Clark, L. J. Greenstein, W. K. Kennedy, and M. Shafi. Matched Filter Performance Bounds for Diversity Combining Receivers in Digital Mobile Radio. *IEEE Trans. Vehicular Technology*, 41(4), Nov. 1992.

[CM99] Giuseppe Caire and Urbashi Mitra. Structured multiuser channel estimation for block-synchronous DS/CDMA. Submitted to IEEE Trans. Commun. (pre-print), 1999.

[COS89] 207 COST. Digital Land Mobile Radio Communications. Technical report, Office for Official Publications of the European Communities, 1989. Luxembourg, final report.

[CR94] D.S. Chen and S. Roy. An adaptive multiuser receiver for CDMA systems. *IEEE Journal on Selected Areas in Communications*, 12:808–816, 1994.

[CTK94] I. Chiba, T. Takahashi, and K. Karasava. Transmitting null beamforming with beamspace adaptive array antennas. In *Proc. VTC'94*, pages 1498–1502, 1994.

[dC99] Elisabeth de Carvalho. *Blind and Semi-blind Multichannel Identification and Equalization for Wireless Communications*. PhD thesis, Ecole Nationale Supérieure des Télécommunications, 1999.

[dCDS98] Elisabeth de Carvalho, Luc Deneire, and Dirk Slock. "Blind and Semi-Blind Maximum Likelihood Techniques for Multiuser Multichannel Identification". In *European Association for Signal Processing EUSIPCO 98*, Island of Rhodes, Greece, September 1998.

[dCS96] E. de Carvalho and D. T. M. Slock. "Maximum-Likelihood Blind Equalization of Multiple FIR Channels". In *Proc. ICASSP 96 Conf.*, Atlanta, USA, May 1996.

[dCS97] Elisabeth de Carvalho and Dirk T. M. Slock. Crámer-Rao bounds for semi-blind, blind and training sequence based channel estimation. In *Proc. 1st IEEE Conf. on Signal Processing Advances in Wireless Communications*, pages 129–132, Paris, France, April 1997.

[DH93] A. Duel-Hallen. Decorrelating decision-feedback multiuser detector for synchronous code-division multiple-access channels. *IEEE Transactions of Communications*, 41(2):285–290, Feb. 1993.

[DHZ95] A. Duel-Hallen, Jack Holtzman, and Zoran Zvonar. Multi-user detection for CDMA systems. *IEEE Personal Communications Magazine*, 2(2):46–58, April 1995.

[ETS95] ETSI. European digital cellular telecommunications system (phase 2): Radio transmission and reception (GSM 05.05). Technical report, ETSI, Dec. 1995. Sophia Antipolis, France.

[ETS97a] ETSI. Concept Group Alpha-Wideband DS-CDMA. Technical report, European Telecommunications Standards Institute, December 1997. Madrid (Spain).

[ETS97b] ETSI. WB-TDMA/CDMA System Description Performance Evaluation. Technical report, European Telecommunications Standards Institute SMG2#24, December 1997. Madrid (Spain).

[For72] G. D Forney. Maximum-Likelihood Sequence Estimation of Digital Sequences in the Presence of Intersymbol Interference. *IEEE Trans. Information Theory*, 18(3), May 1972.

[For73] G. D Forney. The Viterbi Algorithm. *Proceedings of the IEEE*, 61(3), Mar. 1973.

[FV98] Colin D. Frank and Eugene Visotsky. Adaptive interference suppression for direct-sequence CDMA systems with long spreading codes. In *Proc. 36th Annual Allerton Conference on Communication, Control, and Computing*, Urbana-Champaign, IL, September 1998.

[Gar91] W.A. Gardner. "A New Method of Channel Identification". *IEEE Transactions on Communications*, 39:813–817, June 1991.

[GF97] J. Goldberg and J. Fonollosa. Downlink beamforming for cellular mobile communications. In *Proc. VTC'97*, volume 2, pages 632–636, May 1997.

[GJ+91] Klein S. Gilhousen, Irwin M. Jacobs, et al. On the capacity of a cellular CDMA system. *IEEE Transaction on Vehicular Technology*, 40 No. 2, May 1991.

[GL89] G. H. Golub and C. F. Van Loan. *Matrix Computations*. The Johns Hopkins University Press, 1989.

[Gor97] A. Gorokhov. *Séparation autodidacte des mélanges convolutifs: méthodes du second ordre*. PhD thesis, Ecole Nationale Supérieure des Télécommunications, 1997.

[GRS98] J. Scott Goldstein, Irving S. Reed, and Louis L. Scharf. A multistage representation of the wiener filter based on orthogonal projections. *IEEE Transactions on Information Theory*, 44(7):2943–2959, November 1998.

[GS97] Irfan Ghauri and Dirk T. M. Slock. Blind optimal MMSE receiver for asynchronous CDMA in the presence of multipath. In *Proc. 31st Asilomar Conf. on Signals, Systems & Computers*, Pacific Grove, CA, November 1997.

[GS98a] Irfan Ghauri and Dirk T. M. Slock. Blind and semi-blind single user receiver techniques for asynchronous CDMA in multipath channels. In *Proc. Globecom*, Sydney, Australia, November 1998.

[GS98b] Irfan Ghauri and Dirk T. M. Slock. Linear receivers for the DS-CDMA downlink exploiting orthogonality of spreading sequences. In *Proc. 32nd Asilomar Conf. on Signals, Systems & Computers*, volume 1, pages 650–654, Pacific Grove, CA, November 1998.

[GS99a] Irfan Ghauri and Dirk T. M. Slock. Adaptive interference suppression for DS-CDMA in multipath channels. In *Proc. 33rd Asilomar Conf. on Signals, Systems & Computers*, Pacific Grove, CA, October 1999.

[GS99b] Irfan Ghauri and Dirk T. M. Slock. Blind channel and linear MMSE receiver determination in DS-CDMA systems. In *Proc. ICASSP'99*, volume 5, pages 2699–2702, Phoenix, AZ, March 1999.

[GS99c] Irfan Ghauri and Dirk T. M. Slock. Blind decentralized projection receiver for asynchonous CDMA in multipath channels. *Annals of Telecommunications*, pages 379–391, Jul./Aug. 1999.

[GSP98] David Gesbert, Joakim Sorelius, and A. Paulraj. Blind multi-user MMSE detection of CDMA signals. In *Proc. ICASSP*, Seattle, WA, May 1998.

[Hat80] M. Hata. Emperical formulae for propagation loss in land mobile radio services. *IEEE Transactions on Vehicular Technology*, VT-29(3):317–25, 1980.

[HG98] Michael L. Honig and J. Scott Goldstein. Adaptive reduced-rank residual correlation algorithms for DS-CDMA interference suppression. In *Proc. 32nd Asilomar Conf. on Signals, Systems & Computers*, Pacific Grove, CA, November 1998.

[HJ85] R. A. Horn and C.R. Johnson. *Matrix analysis*. Cambridge University Press, 1985.

[HM98] Anders H⌀st-Madsen. Semi-blind decorrelating multi-user detectors for CDMA: Subspace methods. In *Proc. PIMRC*, Boston, MA, September 1998.

[HMV95] M. Honig, U. Madhow, and S. Verdú. Blind adaptive multiuser detection. *IEEE Trans. on Info. Theory*, 41(4):944–960, July 1995.

[Hua96] Y. Hua. "Fast Maximum Likelihood for Blind Identification of Multiple FIR Channels". *IEEE Transactions on Signal Processing*, 44(3):661–672, March 1996.

[HX99] Michael L. Honig and Weimin Xiao. Large system performance of reduced-rank linear filters. In *Proc. 36th Annual Allerton Conference on Communication, Control, and Computing*, Urbana-Champaign, IL, September 1999.

[Jak74] William C. Jakes. *Microwave Mobile Communications*. Wiley, New York, 1974.

[JBS93] Peter Jung, Paul Walter Baier, and Andreas Steil. Advantages of CDMA and spread spectrum techniques over FDMA and TDMA in cellular radio applications. *IEEE Transaction on Vehicular Technology*, 42 No. 3, Aug. 1993.

[JD93] Don H. Johnson and Dan E. Dudgeon. *Array Signal Processing - Concepts and Techniques*. Prentice Hall, Englewood Cliffs, NJ, 1993.

[JS88] Peter M. Janssen and Petre Stoica. On the expectation of the product of four matrix-valued Gaussian random variables. *IEEE Transactions on Automatic Control*, 33(9):867–870, Sep. 1988.

[Kay93] S. M. Kay. *Fundamentals of Statistical Signal Processing, Estimation Theory*. Prentice Hall, Englewood Cliffs, NJ, 1993.

[KBP98] Amit Kansal, Stella N. Batalama, and Dimitris A. Pados. Adaptive maximum SINR RAKE filtering for DS-CDMA multipath fading channels. *IEEE J. Select. Areas in Comm.*, 16(9):1765–1773, September 1998.

[KIHP90a] R. Kohno, H. Imai, M. Hatori, and S. Pasupathy. An adaptive canceller of cochannel interference for spread-spectrum multiple-access communication networks in a power line. *IEEE JSAC*, 8(4):691–99, May 1990.

[KIHP90b] R. Kohno, H. Imai, M. Hatori, and S. Pasupathy. Combination of an adaptive array antenna and a canceller of interference for direct sequence spread-spectrum multiple-access system. *IEEE JSAC*, 8(4):675–82, May 1990.

[Kle97] Anja Klein. Data detection algorithms specially designed for the downlink of CDMA mobile radio systems. In *Proc. VTC*, pages 203–207, Phoenix, AZ, May 1997.

[KZ99] Thomas P. Krauss and Michael D. Zoltowski. Two-channel zero forcing equalization on CDMA forward link: Trade-offs between multi-user access interference and diversity gains. In *Proc. 33rd Asilomar Conf. on Signals, Systems & Computers*, Pacific Grove, CA, October 1999.

[LA98] Matti Latva-Aho. *Advanced Receivers for Wideband CDMA Systems*. PhD thesis, University of Oulu, Oulu, Finland, 1998. Department of Electrical Engineering.

[Lee89] W. C. Y. Lee. *Mobile Cellular Communications*. New York: McGraw-Hill, 1989.

[LL99] Kemin Li and Hui Liu. A new blind receiver for downlink DS-CDMA communications. *IEEE Communication Letters*, 3(7):193–195, July 1999.

[LV89] R. Lupas and S. Verdú. Linear multiuser detectors for synchronous code-division multiple access channels. *IEEE Transactions on Information Theory*, 35:123–136, Jan. 1989.

[LV90] R. Lupas and S. Verdú. Near-far resistance of multiuser detectors in asynchronous channels. *IEEE Transactions on Communications*, 38:496–508, April 1990.

[LZ97] Hua Liu and Michael D Zoltowsky. Blind equalization in antenna array CDMA systems. *IEEE Trans. on Signal Processing*, 45(1):161–172, January 1997.

[Mad98] U. Madhow. Blind adaptive interference suppression for direct-sequence CDMA. *Proc. of the IEEE*, pages 2049–2069, October 1998.

[Mar87] F. A. Marvasti. *A Unified Approach to Zero-Crossings and Nonuniform Sampling of Single and Multidimensional Signals and Systems*. Nonuniform Publications, Oak Park. IL, 1987.

[MH94] U. Madhow and M.L. Honig. MMSE interference suppression for direct-sequence spread-spectrum CDMA. *IEEE Transactions on Communications*, 42:3178–3188, Dec. 1994.

[Mil95] Scott L. Miller. An adaptive direct-sequence code division multiple-access receiver for multiuser interference rejection. *IEEE Transactions on Communications*, 43:1746–1755, Feb.-April 1995.

[Mos96] Shimon Moshavi. Multi-user detection for DS-CDMA communications. *IEEE Communications Magazine*, pages 124–136, October 1996.

[MS98a] Urbashi Mitra and Dirk T. M. Slock. On blind channel identification for DS-CDMA communications. In *Proc. IEEE DSP Workshop*, Bryce Canyon, UH, August 1998.

[MS98b] Giuseppe Montalbano and Dirk T. M. Slock. Spatio-temporal array processing for matched filter bound optimization in SDMA downlink transmission. In *Proc. ISSSE*, Pisa, Italy, September 1998.

[NCP] B.C. Ng, M. Cedervall, and A. Paulraj. A structured channel estimator for maximum likelihood sequence detection in multipath fading channels. submitted to IEEE Transactions on Vehicular Technology, Jan. 1997.

[NCP97] B.C. Ng, M. Cedervall, and A.J. Paulraj. A structured channel estimation for maximum-likelihood sequence detection. *IEEE Communications Letters*, 1(2), March 1997.

[NP94] Ayman F. Naguib and Arogyaswami Paulraj. Effect of multipath and base-station antenna arrays on uplink capacity of cellular CDMA. In *Proc. GLOBECOM'94*, volume I, pages 395–399, San Fransisco, November 1994.

[OSV99] Eko N. Onggosanusi, Akbar M. Sayeed, and Barry D. Van Veen. Canonical space-time processing in CDMA systems. In *Proc. ICASSP*, Phoenix, AZ, March 1999.

[OVSN93] B. Ottersen, M. Viberg, P. Stoica, and A. Nehorai. "Exact and Large Sample ML Techniques for Parameter Estimation and Detection in Array Processing". In T.J. Shepherd S. Haykin, J. Litva, editor, *Radar Array Processing*. Springer-Verlag, 1993.

[Pap91] Athanasios Papoulis. *Probability, Random Variables, and Stochastic Processes*. McGraw-Hill, New York, 3rd. edition, 1991.

[PD98] E. Pitié and P. Duhamel. "Bilinear Methods for Blind Channel Equalization: (No) Local Minimum Issue". In *Proc. ICASSP 98 Conf.*, Seattle, USA, May 1998.

[PG58] R. Price and P. E. Green Jr. A communication technique for multipath channels. *Proc. of the IRE*, 46:555–570, March 1958.

[PH94] P. Patel and Jack Holtzman. Analysis of a simple successive interference cancellation scheme in ds/cdma systems. *IEEE JSAC*, 12(5):796–807, June 1994.

[PMS82] Raymond L. Pickholtz, Laurence B. Milstein, and Donald L. Schilling. Spread spectrum for mobile communications. *IEEE Transactions on Communications*, 40 No. 2:313–321, May 1982.

[PO98] Ramjee Prasad and Tero Ojanperä. An overview of CDMA evolution toward wideband CDMA. *IEEE Transactions Communication Surveys*, 1(1):2–29, Fourth Quarter 1998.

[PP97] A. J. Paulraj and C. B. Papadias. Space-time processing for wireless communications. *IEEE Signal Processing Magazine*, pages 49–83, November 1997.

[Pro95] J. G. Proakis. *Digital Communications*. McGraw-Hill, New York, NY, 3rd. edition, 1995.

[PRS97] A. Paulraj, V. Roychowdhury, and C. Schaper, editors. *Communications, Computation, Control, and Signal Processing - A Tribute to Thomas Kailath*. Kluwer Academic Publishers, Boston, Mass., 1997. Chapter: From sinusoids in noise to blind deconvolution in communications by D.T.M. Slock).

[PV97] H. V. Poor and Sergio Verdù. Probability of error in mmse multiuser detection. *IEEE Trans. Info. Theory*, 43:858–871, May 1997.

[PZE+95] Roger L. Peterson, Ziemer, Rodger E., Borth, and David E. *Introduction to spread-spectrum communications*. Prentice Hall, Englewood Cliffs, NJ, 1995.

[Rap96] T. S. Rappaport. *Wireless Communications - Principles & Practice*. Prentice Hall, Upper Saddle River, NJ, 1996.

[RFT98] F. Rashid-Farrokhi and L. Tassiulas. Power control and space-time diversity for CDMA systems. In *Proc. Globecom*, Sydney, Australia, November 1998.

[RZ97] Javier Ramos and Michael D. Zoltowski. Blind 2D rake receivers for CDMA incorporating code synchronization and multipath time delay estimation. In *Proc. ICASSP'97*, pages 4025–4029, Munich, April 1997.

[SA99] Akbar M. Sayeed and Behnaam Aazhang. Joint multipath-doppler diversity in mobile wireless communications. *IEEE Transactions on Communications*, 46, January 1999.

[Sat75] Y. Sato. A Method of Self–Recovering Equalization for Multilevel Amplitude Modulation Systems. *IEEE Transactions on Communications*, 23:679–682, June 1975.

[Skl97] Bernard Sklar. Rayleigh fading channels in mobile digital communication systems - characterization & mitigation. *IEEE Communications Magazine*, 35(7):90–109, July 1997.

[Slo93] D. T. M. Slock. Blind Fractionally-Spaced Equalization and Channel Identification from Second-Order Statistics or Data. Technical report, EURECOM, Sophia Antipolis, 1993. Research Report No 93-002, Eurecom, France.

[Slo94a] D. T. M. Slock. Blind Fractionally-Spaced Equalization, Perfect-Reconstruction Filter Banks and Multichannel Linear Prediction. In *Proc. ICASSP'94 Conference*, Apr. 1994. Adelaide, Australia.

[Slo94b] Dirk T. M. Slock. Blind joint equalization of multiple synchronous mobile users using oversampling and/or multiple antennas. In *Proc. 28th Asilomar Conf. on Signals, Systems & Computers*, Pacific Grove, CA, November 1994.

[Slo94c] Dirk T. M. Slock. Subspace techniques in blind mobile radio channel identification and equalization using fractional spacing and/or multiple antennas. In *3rd. International Workshop on SVD and Signal Processing*, Leuven, Belgium, August 1994.

[Slo96] Dirk T. M. Slock. Spatio-temporal training-sequence-based channel equalization and adaptive interference cancellation. In *Proc. ICASSP'96*, Atlanta, GA, May 1996.

[Slo99] Dirk T. M. Slock. Multiuser Detection for DS-CDMA, June 1999. Presentation at Texas Instruments, Villeneuve Loubet.

[SM97] Petre Stoica and Randolph L. Moses. *Introduction to Spectral Analysis*. Prentice Hall, Upper Saddle River, NJ, 1997.

[SNXP93] Bruno Suard, A. F. Naguib, Guanghan Xu, and Arogyaswami Paulraj. Performance of CDMA mobile communication systems using antenna arrays. In *Proc. ICASSP'93*, volume VI, Minneapolis, MN, April 1993.

[SOSL94] Marvin K. Simon, J. K. Omura, R. A. Scholtz, and B. K. Levitt. *Spread Spectrum Communications Handbook*. McGraw-Hill, New York, NY, 1994.

[SP95] D.T.M. Slock and C.B. Papadias. "Further Results on Blind Identification and Equalization of Multiple FIR Channels". In *Proc. ICASSP 95 Conf.*, Detroit, Michigan, May 1995.

[SRAX96] C. Schlegel, S. Roy, P. Alexander, and Z. Xiang. Multiuser projection receivers. *IEEE J. on Selected Areas in Communications*, 14(8):1610–1618, October 1996.

[Ste92] Raymond Steele. *Mobile Radio Communications*. Pentech Press Limited, 1992.

[TIA93] TIA/EIA/IS-95. Mobile Station Base-Station Compatibility Standard for Dual-Mode Wideband Spread Spectrum Cellular System. Technical report, Telecommunication Industry Association, 1993.

[Tri99] H. Trigui. *Annulation d'Interférences et Égalisation pour les systèmes Mobiles Utilisant L'AMRT - Application aux Système GSM*. PhD thesis, Ecole Nationale Supérieure des Télécommunications, 1999.

[Tsa97] Michail K. Tsatsanis. Inverse filtering criteria for CDMA systems. *IEEE Transactions on Signal Processing*, 45:102–112, Jan. 1997.

[TX97a] Murat Torlak and Guanghan Xu. Blind multiuser channel estimation in asynchronous CDMA systems. *IEEE Trans. on Communications*, 45(1):137–147, January 1997.

[TX97b] Michail K. Tsatsanis and Zhengyuan Xu. On minimum output energy CDMA receivers in the presence of multipath. In *Proc. Conf. on Information Sciences and Systems*, pages 102–112, Johns Hopkins University, MD, March 1997.

[TX98] Michail K. Tsatsanis and Zhengyuan Xu. Performance analysis of minimum variance CDMA receivers. *IEEE Transactions on Signal Processing*, 46(11):3014–3022, November 1998.

[TXK91] L. Tong, G. Xu, and T. Kailath. "A New Approach to Blind Identification and Equalization of Multipath Channels". In *Proc. of the 25th Asilomar Conference on Signals, Systems & Computers*, pages 856–860, Pacific Grove, CA, Nov. 1991.

[TXK93] L. Tong, G. Xu, and T. Kailath. "Fast Blind Equalization Via Antenna Arrays". In *Proc. ICASSP*, volume IV, pages 272–275, Minneapolis, MN, April 27-30 1993.

[TZ98] Lang Tong and Qing Zhao. Blind channel estimation by least squares smoothing. In *Proc. ICASSP*, Seattle, WA, May 1998.

[Ung76] G. Ungerboeck. Fractional Tap-Spacing Equalizer and Consequences for Clock Recovery in Data Modems. *IEEE Trans. Communications*, 24, Aug. 1976.

[VA90] M.K. Varanasi and B. Aazhang. Multistage detection in asynchronous code-division multiple-access communications. *IEEE Transactions on Communications*, 38(4):509–519, April 1990.

[VA91] M.K. Varanasi and B. Aazhang. Optimally near-far resistant multiuser detection in differentially coherent synchronous channels. *IEEE Transactions on Information Theory*, pages 1006–1018, July 1991.

[Vai93] P. P. Vaidyanathan. *Multirate Systems and Filter Banks*. Prentice Hall, Englewood Cliffs, NJ, 1993.

[Ver86] S. Verdú. Minimum probability of error for asynchronous Gaussian multiple access channels. *IEEE Transactions on Information Theory*, IT-32:85–96, Jan. 1986.

[Ver98] Sergio Verdú. *Multiuser Detection*. Cambridge University Press, 1998.

[Vit90] Andrew J. Viterbi. Very low rate convolutional codes for maximum theoretical performance of spread-spectrum multiple-access channels. *IEEE JSAC*, 8(4):641–49, May 1990.

[Vit95] Andrew J. Viterbi. *CDMA - Principles of Spread Spectrum Communications*. Addison-Wesley, Reading, Mass., 1995.

[VON95] M. Viberg, B. Ottersten, and A. Nehorai. Performance Analysis of Direction Finding with Large Arrays and Finite Data. *IEEE Trans. Signal Processing*, Feb. 1995.

[WF97] Anthony J. Weiss and Benjamin Friedlander. CDMA downlink channel estimation with aperiodic spreading. In *Proc. 31st Asilomar Conf. on Signals, Systems & Computers*, Pacific Grove, CA, November 1997.

[Win98] J. H. Winters. The Diversity Gain of Transmit Diversity in Wireless Systems with Rayleigh Fading. *IEEE Trans. Vehicular Technology*, 47, Feb. 1998.

[WLLZ98] Tan F. Wong, Tat M. Lok, James S. Lehnert, and Michael D. Zoltowsky. A linear receiver for direct-sequence spread-spectrum multiple-access systems with antenna arrays and blind adaptation. *IEEE Transactions on Information Theory*, 44:659–676, March 1998.

[WMN93] S. S. H. Wijayasuriya, J. P. McGeehan, and G. H. Norton. RAKE decorrelating receiver for DS-CDMA mobile radio networks. *Electronics Letters*, 29(4):395–396, Feb. 1993.

[WP98a] Xiaodong Wang and Vincent Poor. Blind equalization and multiuser detection in dispersive CDMA channels. *IEEE Transactions on Communications*, 46(1):91–103, January 1998.

[WP98b] Xiaodong Wang and Vincent Poor. Blind multiuser detection: A subspace approach. *IEEE Transactions on Information Theory*, 44(2):677–690, March 1998.

[WS85] Bernard Widrow and S. D. Stearns. *Adaptive Signal Processing*. Prentice Hall, Englewood Cliffs, NJ, 1985.

[XLTK95] G. Xu, H. Liu, L. Tong, and T. Kailath. "A Least Squares Approach to Blind Channel Identification". *IEEE Transactions on Signal Processing*, 43(12):2982–2993, Dec. 1995.

[XRS90] Z. Xie, C. Rushforth, and R. Short. Multiuser signal detection using sequential decoding. *IEEE Transactions on Communications*, 38, No. 5:578–583, May 1990.

[XT98] Zhengyuan Xu and M. K. Tsatsanis. Blind stochastic gradient methods for optimal minimum variance CDMA receivers. In *Proc. 32nd Asilomar Conf. on Signals, Systems & SComputers*, Pacific Grove, CA, November 1998.

[YX98] Weidong Yang and Guanghan Xu. Optimal downlink power assignment for smart antenna systems. In *Proc. ICASSP'98*, pages 3337–3340, Seattle, WA, May 1998.

[ZB92] Zoran Zvonar and David Brady. Coherent and differentially coherent multiuser detectors for asynchronous CDMA frequency-selective channels. In *Proc. of Milcom*, San Diego, CA, Oct. 1992.

[Zet97] P. Zetterberg. *Mobile cellular communications with base station antenna arrays: Spectrum efficiency, algorithms and propagation models*. PhD thesis, Royal Inst. of Technology, Stockholm, Sweden,, 1997. Department of signals sensors and systems.

[ZT98] Qing Zhao and Lang Tong. Semi-blind equalization by least squares smoothing. In *Proc. 32nd Asilomar Conf. on Signals, Systems & Computers*, Pacific Grove, CA, November 1998.